Shape Switchable Azo Macrocycles

Inauguraldissertation

zur

Erlangung der Würde eines Doktors der Philosophie

vorgelegt der

Philosophisch - Naturwissenschaftlichen Fakultät

der Universität Basel

von

Marcel Müri

aus

Schinznach-Dorf (AG), Schweiz

Basel 2011

Originaldokument gespeichert auf dem Dokumentenserver der Universität Basel
edoc.unibas.ch

Dieses Werk ist unter dem Vertrag „Creative Commons Namensnennung-Keine kommerzielle Nutzung-Keine Bearbeitung 2.5 Schweiz“ lizenziert. Die vollständige Lizenz kann unter
creativecommons.org/licences/by-nc-nd/2.5/ch
eingesehen werden.

Genehmigt von der Philosophisch-Naturwissenschaftlichen Fakultät der Universität Basel auf Antrag von:

Prof. Dr. Marcel Mayor

Prof. Dr. Edwin Constable

Basel, den 21.06.2011

Prof. Dr. Martin Spiess

creative commons

Namensnennung-Keine kommerzielle Nutzung-Keine Bearbeitung 2.5 Schweiz

---

Sie dürfen:

das Werk vervielfältigen, verbreiten und öffentlich zugänglich machen

Zu den folgenden Bedingungen:

Namensnennung. Sie müssen den Namen des Autors/Rechteinhabers in der von ihm festgelegten Weise nennen (wodurch aber nicht der Eindruck entstehen darf, Sie oder die Nutzung des Werkes durch Sie würden entlohnt).

Keine kommerzielle Nutzung. Dieses Werk darf nicht für kommerzielle Zwecke verwendet werden.

Keine Bearbeitung. Dieses Werk darf nicht bearbeitet oder in anderer Weise verändert werden.

- Im Falle einer Verbreitung müssen Sie anderen die Lizenzbedingungen, unter welche dieses Werk fällt, mitteilen. Am Einfachsten ist es, einen Link auf diese Seite einzubinden.
- Jede der vorgenannten Bedingungen kann aufgehoben werden, sofern Sie die Einwilligung des Rechteinhabers dazu erhalten.
- Diese Lizenz lässt die Urheberpersönlichkeitsrechte unberührt.

Die gesetzlichen Schranken des Urheberrechts bleiben hiervon unberührt.

Die Commons Deed ist eine Zusammenfassung des Lizenzvertrags in allgemeinverständlicher Sprache: http://creativecommons.org/licenses/by-nc-nd/2.5/ch/legalcode.de

Haftungsausschluss:
Die Commons Deed ist kein Lizenzvertrag. Sie ist lediglich ein Referenztext, der den zugrundeliegenden Lizenzvertrag übersichtlich und in allgemeinverständlicher Sprache wiedergibt. Die Deed selbst entfaltet keine juristische Wirkung und erscheint im eigentlichen Lizenzvertrag nicht. Creative Commons ist keine Rechtsanwaltsgesellschaft und leistet keine Rechtsberatung. Die Weitergabe und Verlinkung des Commons Deeds führt zu keinem Mandatsverhältnis.

Quelle: http://creativecommons.org/licenses/by-nc-nd/2.5/ch/ Datum: 3.4.2009

Dedicated to:

Esther and Hans-Jörg

Acknowledgements

First of all I would like to thank Prof. Dr. Marcel Mayor. It was a great honor and a real pleasure to work in your group. I really enjoyed the cooperative working atmosphere with the great intellectual curiosity. Moreover I would like to thank Dr. Heike Riel from the IBM Research Center in Rüschlikon for being my second supervisor. I also would like to thank Prof. Dr. Edwin Constable for being co-referee.

Many thanks go to all members of the Mayor group. I am especially grateful to Torsten Peterle, Jens Tüxen, Federica Reinders, Jens Hermes, Fabian Sander, David Vonlanthen and Thomas Eaton for all the fruitful discussions and for being great friends. A special thank goes to my lab mate for many years Sergio Grunder.

A great thank goes to my collaborators: Dr. Heike Riel, Dr. Bernd Gotsmann and Dr. Emanuel Lörtscher from the IBM Research Center in Rüschlikon for the great collaboration within my thesis; Dr. Klaus C. Schuermann and Prof. Dr. Luisa De Cola from the Westfälische Wilhelmsuniversität in Münster; and Dr. Yann Leroux.

I would like to thank Dr. Daniel Häusinger for helpful discussion concerning the NMR investigations and Markus Neuburger for measuring the X-ray solid state structures. I am also thankful to Dr. Heinz Nadig, who recorded the EI and FAB mass spectra, Werner Kirsch, who recorded the elemental analyses, the complete “Werkstatt” and “Materialausgabe” team and the secretaries of the department. These are the people who keep the Department of Chemistry running.

A special thank goes to Dr. Stefan Husi from the SNF for the scholarship co-founded by NRP 47 and CTI.

I also acknowledge Thomas Eaton, Federica Reinders and Jens Tüxen for proof reading this thesis and Roger Müri for the cover design.

A very big thanks go to my family, for all their support in any situation of my life. Sandra, thank you so much for your love, your support and your appreciation.

1 Introduction

Movement is one of life's central attributes. Nature provides living systems with complex molecules called "motor proteins", which work inside cells like molecular machines built for everyday needs. Because of such motor proteins, we can walk, talk and even think. At the root of existence lies movement at the molecular level.[1][2] Today, continuous miniaturization raises the question of investigating the possibility of designing machines on the nanometer scale at the molecular level. The fundamental condition for molecular machines is the mechanical movement in the molecule itself or in supramolecular assemblies.

Molecular level machines operate as the result of atomic movements caused by chemical reactions.[3][4] Any kind of chemical reactions involves, of course, some atomic displacement. The term "molecular machine", is however used only for chemical systems performing reactions that can cause motions of large amplitude, leading to real translocation of some component parts of the system. Molecular machines must contain a "motor", which in principal consists of a mobile and a stationary part. An external operator should be able, by means of a given input, to induce the displacement of the movable component from the stationary part. When the system is investigated in solution, in which both components are in motion, the larger is considered to be static and the other is said to move relative to it.

For artificial molecular machines of particular interest are atomic motions related to: 1. Isomerization reactions involving ─N=N─, ─C=N─ and ─C=C─ double bonds in molecular structures. 2. Acid – base or redox reactions causing intermolecular bonds interactions (including hydrogen bonds). 3. Metal – ligand reactions causing the formation or disruption of coordination bonds.

Like macroscopic machines, molecular – level machines are characterized by energy, motion and control.[3][5] In particular the kind of energy which is supplied to make them work. There are different possibly ways to trigger molecular – level machines: Either by chemical energy, by electrochemical energy or by light. The last being of particular interest, as this is the system investigated here. In the

following we focus exclusively on the light triggered isomerization reaction of azo compounds (R─N=N─R', *trans* ↔ *cis*), in particular of macrocyclic azo structures.

1.1 Azo Compounds

Azo compounds are a pair of symmetrically or asymmetrically substituted nitrogen atoms that are connected by a double bond.[6] The synthesis of the simplest aromatic azo compound, the azobenzene, was first described by Mitscherlich in 1834 when he mixed nitrobenzene in an alcoholic potassium hydroxide solution.[7] The obtained red crystals were analyzed to be azobenzene. In the following years the synthesis was described in detail and the potential of azo compounds as dyes for textiles was discovered.[8][9]

In modern times azo compounds are common dyes as colorants for inkjet printers, as pigments in paint and furthermore they are used as indicators and as titrates in analytical chemistry.[10] The research of azo compounds has now been expanded to evaluate the potential as functional components in catalysis,[11][12] as optical storage media,[13]-[15] in supramolecular chemistry[16]-[18] and in polymer chemistry.[19]-[21]

The name "azo compound" is not the officially IUPAC[22] name for this compounds, but the historic term "azo" is still generally used and understood. Officially it has been replaced by the systematic term of "diazene", azobenzene is therefore named as "diphenyldiazene" and the *cis* compound are called "*Z*" form and the *trans* "*E*" forms. However in the following the historic terms azo, *cis* and *trans* are used.

1.1.1 Synthetic Procedures

1.1.1.1 Azo Coupling Reaction (Electrophilic Aromatic Substitution)

The azo coupling is the best known and most widely used method to build azo compounds.[23] In principle it is an electrophilic aromatic substitution between a diazonium salt **A5** and an electron rich aromatic compound **A6** (**Scheme 1**).[24] Since the reaction mechanism follows the pathway of an electrophilic aromatic substitution reaction, due to electronic reasons and steric hindrance, the substitution mainly occurs in the *para* position to the activating group and only if the *para* position is blocked *ortho* substitution is observed.[24][25]

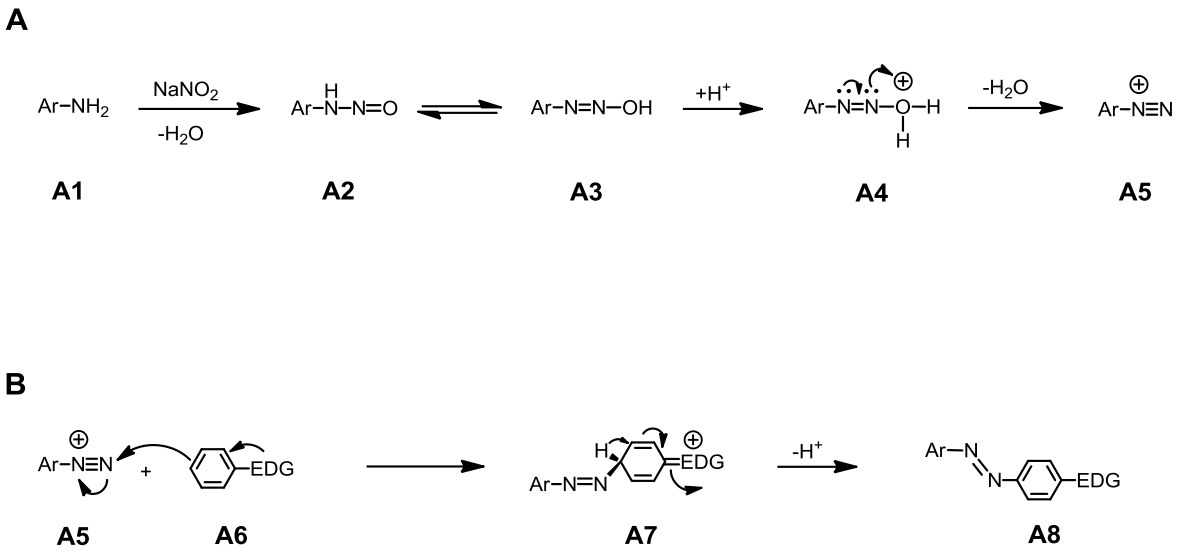

Scheme 1 Mechanism of the azo coupling.[24] (A) The formation of the diazonium salt **A5**. (B) The electrophilic aromatic substitution to the azo compound **A8**.

In a first step (**Scheme 1A**) an aromatic amine is reacted with sodium nitrite in hydrochloric acid at low temperatures. After addition of NO under the elimination of water the nitrosamine **A2** is formed, which tautomerised to the diazohydroxide **A3**. The diazonium salt **A5** is formed after repeated water elimination. In a second step, the diazonium salt **A5** can attack the electron rich coupling component **A6** following the mechanism of an electrophilic aromatic substitution reaction (**Scheme 1A**) to form the desired azo compound **A8**. Unfortunately diazonium salts are rather weak electrophiles and therefore only arenes bearing electron donating groups (EDG)

can be employed. Due to this limiting factor of the azo coupling other procedures to build up azo compounds are important and will be discussed in the following.

1.1.1.2 Oxidative and Reductive Coupling

To build up azo compounds several oxidative methods[26]-[28] starting form primary amines and several reductive methods[29][30] starting from nitro compounds are known. In **Scheme 2** the most important pathways with their corresponding reducing- or oxidizing agents are summarized. These dimerization methods are in particular used for the formation of symmetric azo compounds. It is rather complicated to prepare asymmetrically substituted azo compounds using these protocols, but it is not impossible. By the use of two different nitro **A9** or amines compounds **A10** respectively, a statistical mixture of the products of 25%:50%:25% is expected, in which at most 50% of the asymmetrical azo compound is formed. With suitable separation methods it is possible to isolate all three variably substituted products.

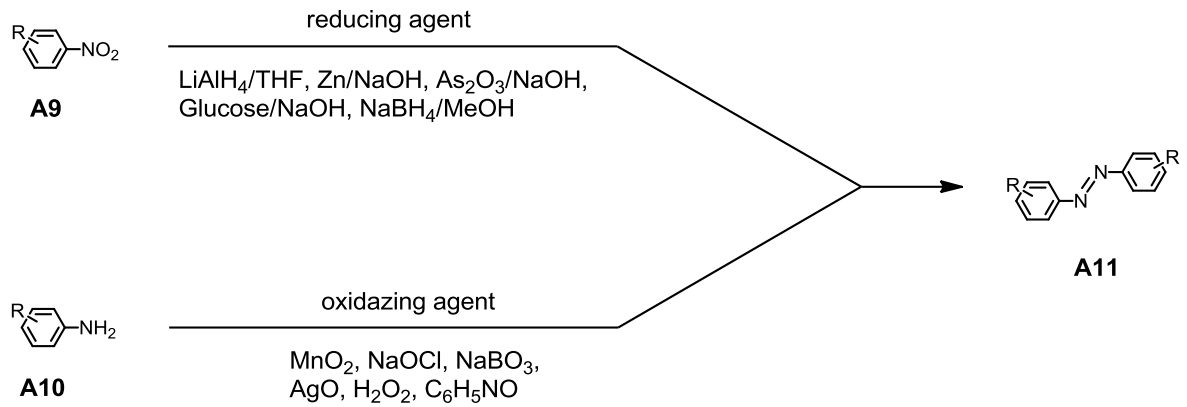

Scheme 2 Reductive and oxidative methods (dimerization) to prepare azo compounds **A11**, starting for amines **A9** and nitro compounds **A10** respectively.[25]

Mechanistically these dimerization methods are equivalent to the Mills reaction (see below). By selective oxidation or reduction respectively, a nitroso compound is

formed in situ which reacts immediately with the corresponding amine to form the desired azo compound. The reaction mechanism is shown in detail in **Scheme 3**.

1.1.1.3 The Mills Reaction

In comparison to the dimerization methods described above, the reaction of primary amines **A13** with aromatic nitroso compounds **A12** under acidic conditions is particularly suitable for the synthesis of asymmetric azo compounds.[31]-[33] This reaction sequence, where the nitroso compound **A12** and the amine **A13** were isolated before the coupling reaction is called the "Mills reaction." The mechanism of this coupling reaction is shown in **Scheme 3** and has been verified by kinetic studies.[34] In the first rate determining step the amine **A13** is added by a nucleophilic attack to the aromatic nitroso coupling partner **A12**. In a second step water is eliminated via the intermediates **A14** and **A15**, providing the desired azo functionality in **A16**. The actual reaction mechanism differ not from the mechanism in the dimerization reaction described above, but here the nitroso compound **A12** and the amine **A13** were first isolated and can be supplied to the coupling conditions in the desired composition.

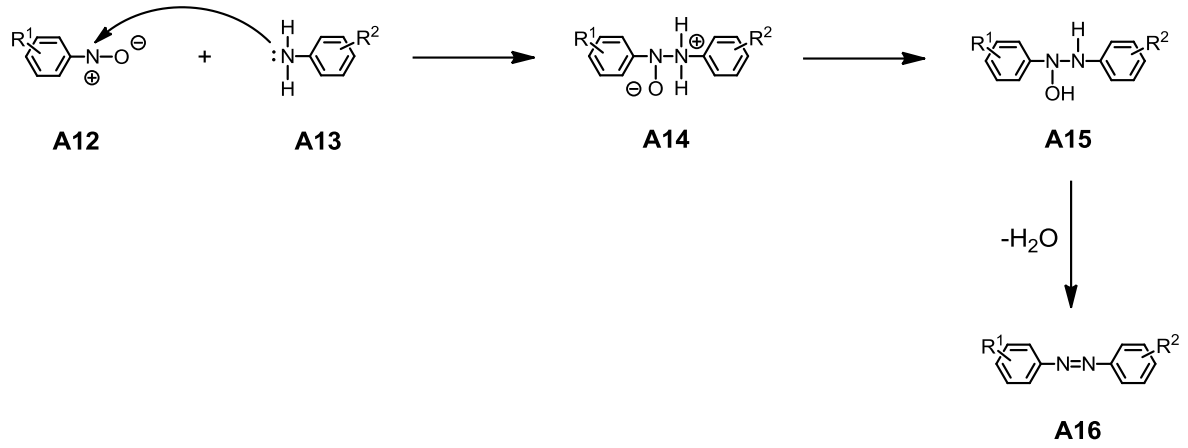

Scheme 3 Mechanism of the Mills reaction with nitroso compound **A12** and amine **A13** to form asymmetric azo compound **A16**.[30]

In correlation with the mechanism, donating substituents (R^2) in the amine **A13** accelerate the reaction, whereas electron withdrawing groups (R^2) in the amine **A13** decelerate the reaction. According to the reaction mechanism, for the nitroso compound **A12**, the opposite effect is observed for R^1. The Mills reaction tolerates a number of different functionalities including, nitro groups, protected amines, alkyloxy groups, halides, acids and esters as the coupling partners.[32] Even so the Mills reaction has a huge potential for building up asymmetric azo compounds in industrial application the azo coupling is favored due to the instability of many nitroso compounds **A12**.[6][10]

1.1.1.4 Palladium Catalyzed Azo Formation

Recently, a novel route to asymmetric azobenzenes via palladium catalyzed coupling reaction has been published.[35] The reaction sequence of this coupling protocol is shown in **Scheme 4**. In a palladium catalyzed Hartwig – Buchwald type reaction[36][37] an aryl halide **A17** is coupled with Boc protected hydrazine **A18** to provide a N-Boc aryl hydrazine **A19** as one of the coupling partner. The hydrazine **A19** then undergoes a palladium catalyzed coupling reaction with the other coupling partner, an aryl halide, to provide an asymmetric N-Boc diaryl hydrazines **A20**. The resulting diaryl hydrazines **A20** are directly oxidized to the corresponding azobenzenes **A21**. The reaction sequence is tolerant to a huge range of functional groups, since electron withdrawing (EWG) and electron donating groups (EDG) are possible. Substituents in *ortho* and *meta* positions decrease the yield noticeably, if the substituents are sterically to demanding.[38][39]

Despite the three reaction steps involved this novel reaction sequence is a suitable alternative to build up asymmetric azo compounds, even if the yields are not always remarkable. However, this method has already been applied for successful azo macrocyclization reaction and is not only suitable for linear azo compounds.[38]

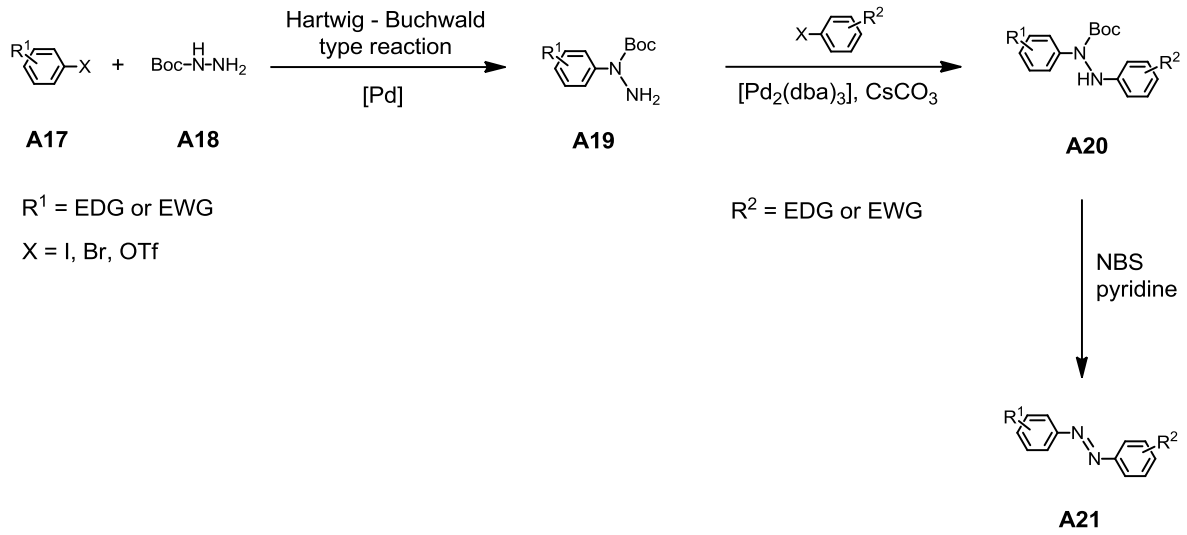

Scheme 4 Reaction mechanism of palladium catalyzed azo formation via the introduction of a Boc protected hydrazine followed by oxidation to an asymmetric azo compound **A21**.[35]

1.1.2 Photophysical Properties of Azo Compounds

Azo compounds are photochromic compounds and the azo function is isosteric with ethylene groups.[40] Thus two stable configurations can be expected which have been called *trans*- and *cis* isomers. In 1937 Hartley discovered the influence of light on the configuration of the nitrogen ─ nitrogen double bond and he was able to isolate and characterize *cis* azobenzene.[41] Since then a lot of studies have been done dealing with the particular photochromic and isomerization properties of azo compounds. Wyman has covered the literature up to 1955[42][43] and Ross and Blanc up to 1970.[44] The spectroscopy was reviewed by Rau in 1973[45]-[48] and the chemistry and characteristics of azo compounds were studied extensively by Zollinger.[6][10]

Hence, today it is well known that azobenzene derivatives exhibit photochemical *trans* → *cis* and *cis* → *trans* isomerization upon irradiation of UV- and visible light, respectively. Usually the *cis* isomer is thermally less stable, so *cis* → *trans* thermal isomerization takes place at room temperature in the dark.[49]-[51]

Thus, two different distinct configurations of azo compounds are possible (**Figure 1A**). These two configurations can be inter-converted by irradiating light on the sample. The *cis* isomer is stable in the solid state, but isomerizes in solution to the thermodynamically more favored *trans* isomer. The C–N bond length in the *trans* isomer was determined to be 1.41 Å and is slightly shorter than in the *cis* isomer with 1.46 Å. The overall expansion of two isomers is significantly different depending on the present configuration. While the *trans* isomer has a length of 1.0 nm, in the *cis* form, where the phenyl rings are rotated by 56° with respect to each other, the distance is only 0.59 nm (**Figure 1A**).[48][52]

1.1.2.1 Absorption Spectra of Azo Compounds

A major feature of the azo group is its capability to isomerize, in **Figure 1B** the absorption spectra of *trans* azobenzene and *cis* azobenzene respectively, are shown.

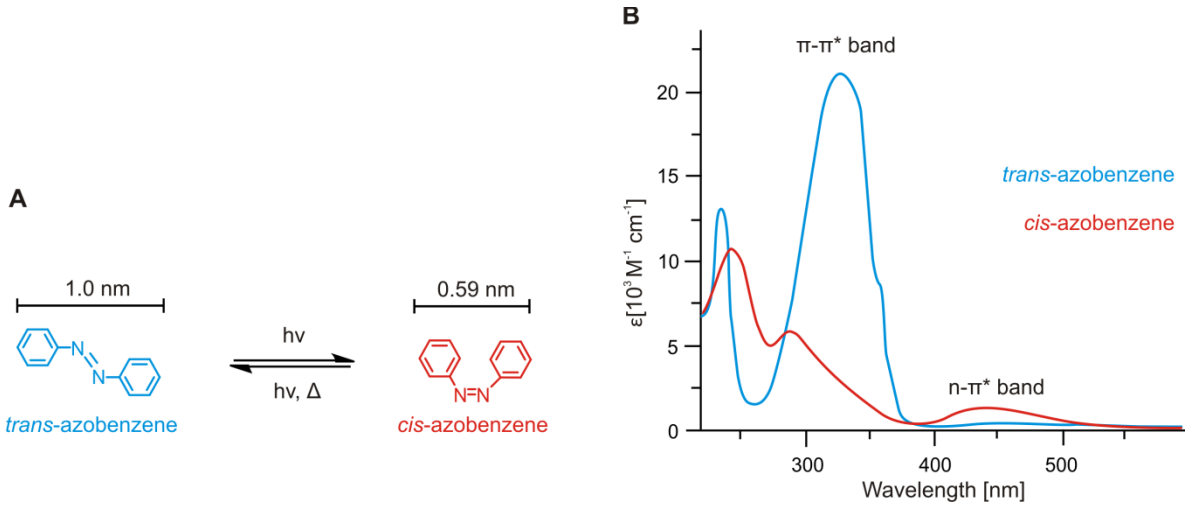

Figure 1 (A) The *trans* ↔ *cis* isomerization system of azobenzene, with the diameter of each configuration. (B) Absorption spectra of *cis*- and *trans* azobenzene in an ethanol solution.[48]

The parent *trans* isomer is about 50 kJ mol^{-1} more thermodynamically stable in solution then the corresponding *cis* isomer.[53] Isomerization is the main photoreaction of most aromatic azo compounds, the photo isomerization barrier is

approximately 200 kJ mol^{-1}. In the absorption spectrum of trans azobenzene (blue curve in **Figure 1B**) an intense π-π* transition band at around 330 nm and a weaker n-π* transition band around 440 nm is observed.[30][45][46][54] This excitation is symmetry forbidden for *trans* azobenzene. In contrast, the n-π* transition in the *cis* isomer is allowed and thus shows a higher intensity compared to the *trans* isomer (see red curve in **Figure 1B**). Based on the well separated transition bands at 330 nm and 440 nm, respectively, azo compounds can be isomerized from *trans* to *cis* by irradiating at the π-π* transition band and switched back from *cis* to *trans* by irradiating at the n-π* transition band. However, there is a photostationary equilibrium containing a maximum of about 85% of the *cis* form, since there will be reached a steady state upon irradiation light at 330 nm. The isomerization mechanism of azo benzene is discussed in section 1.1.2.2.

The above described behavior with well separated π-π* transition (330 nm) and n-π* transition (440 nm) is true for azobenzene derivatives **A22** with balanced electronic properties. The energy gap between the π-π* transition and the n-π* transition is very sensitive to substitution of the aryl rings, which influences the spectroscopic and photochemical features of different azo compounds. Therefore Rau[45][46][48] has distinguished three different classed of azobenzenes. In **Figure 2** the three classes are summarized with their corresponding spectra.

Type 1 contains “normal” azobenzene **A22**, with well separated transition bands, while type 2 comprises azobenzenes substituted with electron donors **A23** and type 3 includes azobenzenes bearing an electron donor on one side and an electron acceptor on the other side **A24** (push-pull system, pseudo-stilbene). In type 2 compounds **A23** the π-π*- and the n-π* transition band nearly overlap and just a shoulder at about 460 nm can be observed (green curve in **Figure 2**). In contrast, in type 3 compounds **A24** the energy of the two transitions is exchanged compared to type 1. The n-π* transition band is observed slightly lower than the π-π* transition band, which is red shifted to 460 nm. The two bands effectively overlap and thus a single wavelength of light in the visible region will induce both

cis → *trans* and *trans* → *cis* isomerization at the same time. Therefore, the substituents need to be careful chosen in order to obtain the desired switching properties of azo compounds.

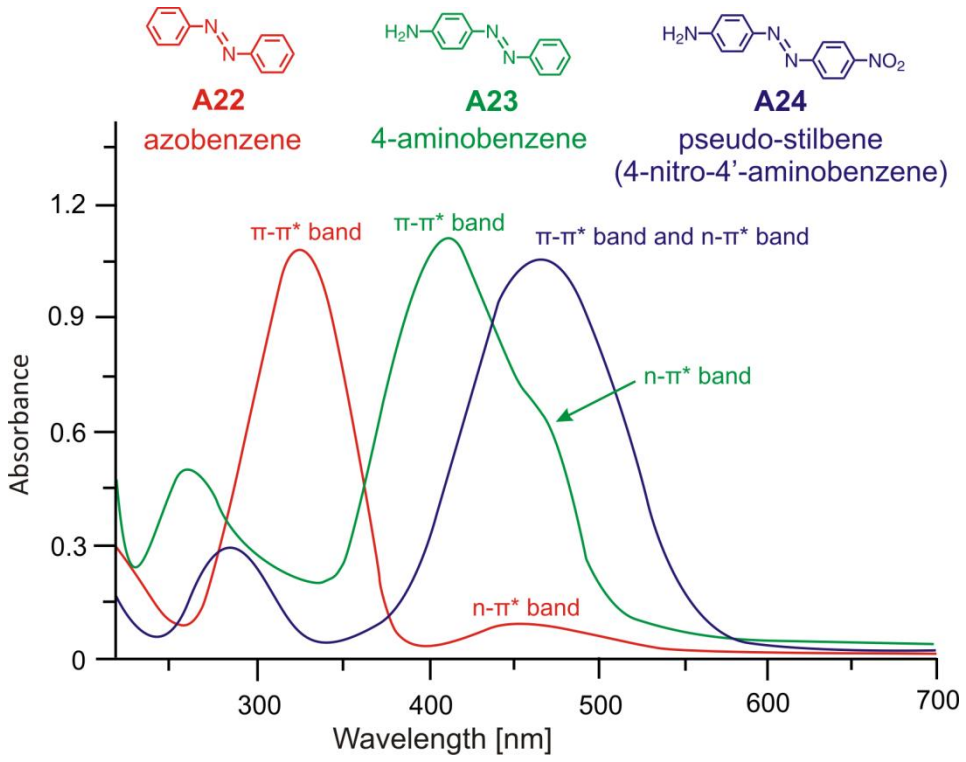

Figure 2 Absorption spectra of azobenzene, 4-aminoazobenzene and 4-nitro-4'-amino-azobenzene (pseudo-stilbene type) molecules in an ethanol solution.[48]

1.1.2.2 The Isomerization Mechanism of Azo Compounds

The close similarity between azobenzene and stilbene suggested that their isomerization mechanism might be the same. In stilbene the isomerization occurs by rotation around the central double bond which was predicted to be the same for azobenzene. In 1966 a second, different isomerization mechanism was proposed, a rehybridization of the azo group should create a planar transition state that can isomerize.[55] The two different mechanism for the *cis* → *trans* isomerization of azo compounds are shown in **Scheme 5**.[56]-[58]

In the upper pathway in **Scheme 5** a rotation around N─N single bond takes place. When the azobenzene is substituted in 4- and 4'-position a dipolar transition state was found, since the isomerization rate of 4-(dimethylamino)-4'-nitroazobenzene was strongly influenced by the solvent polarity. However, the second, the inversion mechanism (lower pathway in **Scheme 5**) seems to be favored for the same compound in apolar solvents such as *n*-hexane. In this mechanism one of the nitrogen atoms is sp-hybridized in the linear transition state and subsequently interconverts to the corresponding isomer. This pathway is also dominant in azobenzenes that lack electron donating substituents in the 4-position.[59] A direct proof of the inversion mechanism has been given by Rau and Lüddecke[60] and by Tamaoki,[61]-[63] who found that azobenzenophanes that cannot rotate still isomerize.

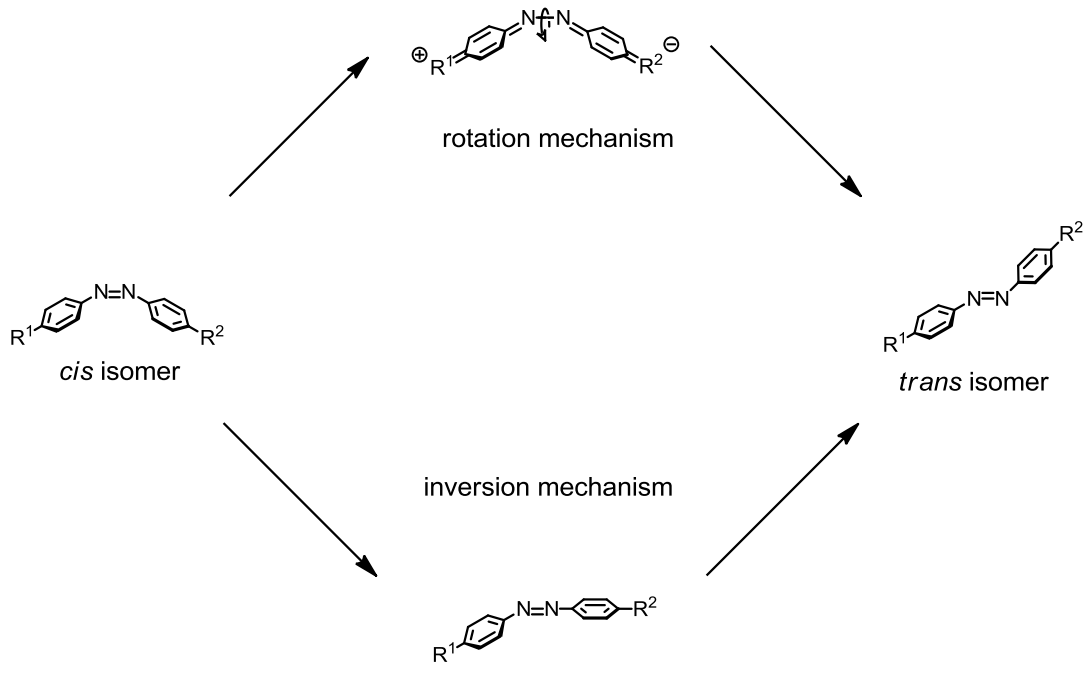

Scheme 5 Possible mechanism for the isomerization reaction from the *cis* isomer to the *trans* isomer. Either via a rotation mechanism (upper pathway) or via an inversion mechanism (lower pathway).[10]

The mechanism of the isomerization is still the subject of some debate. However it is commonly accepted that the *trans* → *cis* conversion occurs via rotation, whereas

inversion gives rise to the *cis* → *trans* conversion, but none of the mechanisms can be excluded and they may occur in parallel. It is still under discussion which excited state plays a direct role in the series of the photoisomerization behavior. Recently a new isomerization pathway was proposed by Diau,[64] the "concerted inversion" pathway in which both C─N=N bond angles bend at the same time.

The photoisomerization of azobenzenes is a very fast reaction. The exited molecules either isomerize or return to their ground state with high efficiency upon irradiation with light. Hence the photo isomerization is the predominant reactive route and azobenzenes are photochemically stable. Thus azo compounds have the potential to survive many isomerization cycles. Therefore they are preferred in photo responsive devices where stability is necessary.[15][48][65]-[67] If a complex substitution pattern is considered for such devices, care should be taken to find compounds with a distinct and characteristic n-π* band in the absorption spectrum.

1.1.3 Macrocyclic Azo Compounds

The development of photo sensitive functional systems which change their chemical and physical properties in response to optical stimuli is a topic of current interest.[68] Chemical substances exhibiting photo induced structural changes are not only suitable candidates for the storage of light energy but also for the conversion of light into mechanical motion.[3][4][49][51][69] As described above the photo induced reversible trans ↔ cis isomerization of azobenzene derivatives provides structural change to a considerable extent.[43][70]-[73] The azobenzene motif is thus an ideal building block to integrate light induced conformational changes in molecular structures.[16][74]-[76] A certain drawback of the structural change of such molecular structures was the relatively short life time of the thermodynamically less favored *cis* isomer. This drawback can be solved by interconnecting two azo functionalities in one macrocyclic compound and was first investigated in 1994 by Rau.[77] The first synthesized and characterized macrocycles **A25**-**A27** with two interconnected azo units are shown is **Figure 3**. With such a macrocyclic design

the half-life time in the dark of the thermodynamically less favored (*cis,cis*) isomer was increased from 2.5 days for simple azobenzene to 5 days for **A25** and up to one year for the sterically more hindered **A26** and **A27**.[77][78]

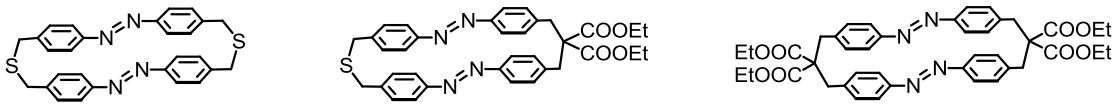

A25 **A26** **A27**

Figure 3 First synthesized and characterized azo macrocycles **A25**-**A27** by Rau.[77]

Thus macrocyclic azo compounds are ideal building block for integrating light induced conformational changes into molecular structures and for creating patterns and nanostructures in polymeric and glass substrates.[65][79]-[82] Not only the cyclic structure but also bulky substituents cause steric hindrance and thus may influence the isomerization behavior of azo-functionalized systems. Of particular interest are rigid macrocycles comprised of several azo groups as their structural rearrangement upon isomerization becomes interdependent due to mechanical interlinkage, as described above.

Some years ago Grützmacher synthesized macrocyclic azo compounds (**A28**-**A30** in **Figure 4**) in which the 4- and 4'-positions were connected by a covalent chain.[83] Thermally stable *cis* isomers were isolated when the chain contains four, six and seven atoms, but these compounds photo chemically decomposed upon irradiation with UV light. A thermal equilibrium was observed, when the connecting chain was elongated to eight and nine atoms.

Recently, Tamaoki reported the synthesis of a (3,3)-azobenzophane (**A31** in **Figure 4**) displaying inverted thermodynamic stabilities.[84] Owing to steric strain, the *cis* isomer of this azobenzophane was more stable, whereas steric repulsion usually favors the *trans* isomers of azo derivatives. Thus, the thermal back reaction

of (3,3)-azobenzophane **A31** was the opposite way from the *trans* to the *cis* isomer, and under irradiation the amount of *trans* isomer was increased.

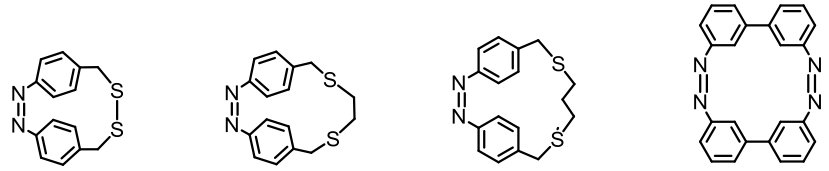

A28 **A29** **A30** **A31**

Figure 4 Azo macrocycles **A28**-**A31** with thermally stable *cis* isomers.

1.1.4 Immobilization of Organic Molecules

The self assembly of organic molecules on surfaces has gained considerable attention in the last few years and will be briefly discussed. In particular the molecular scale, structural resolution and optical control over functional groups is expected to provide wide application potential. This requires an accurate control of the molecular arrangements over a wide range of length scales, from micrometers down to the molecular level. Covalent, but more often non covalent intermolecular forces have been used to engineer highly ordered three dimensional supramolecular architectures where the single building blocks are held together by specific interactions, such as metal – ligand bonding,[85]-[87] hydrogen bonding[88]-[91] and π – π stacking.[92] On the other hand, self assembly at the solid – liquid interface has been successfully used to control the molecular arrangement in two dimensions.[91][93]

1.1.4.1 Adsorption on Graphite

Since the invention of Scanning Tunneling Microscopy (STM),[94] increasing interest has been directed towards real space imaging of single molecules and supramolecular assemblies on surfaces. STM is a technique which allows the investigation of absorbed layers of macro molecules, both at the graphite – solution

interface[95]-[98] and in dry thin films on conductive substrates with molecular resolution.[99] Numerous further investigations have been reported in the field of self assembled monolayers.[100]-[102] Shape persistent two dimensional oligomers such as spoked wheels[103] as well as shape persistent macrocycles based on a phenyl ethynyl backbone have been immobilized on graphite.[104]-[106] In **Figure 5** the deposition from solution to the surface of highly oriented pyrolytic graphite (HOPG) is shown. The shape persistent macrocycle (A in **Figure 5**) forms a highly ordered and stable monolayer at the solution – HOPG surface interface. High resolution STM images show the two dimensional structures of the macrocycles (B in **Figure 5**).

Alkyl chains are equally important as the aromatic units for the self assembly features on graphite. Generally the longer the alkyl chains the better the adsorption properties, since with an increasing number of carbon atoms the van der Waals (vdW) forces are also increased which promotes the deposition. See also section 2.1 Alkyl Functionalized Azo Macrocycles.

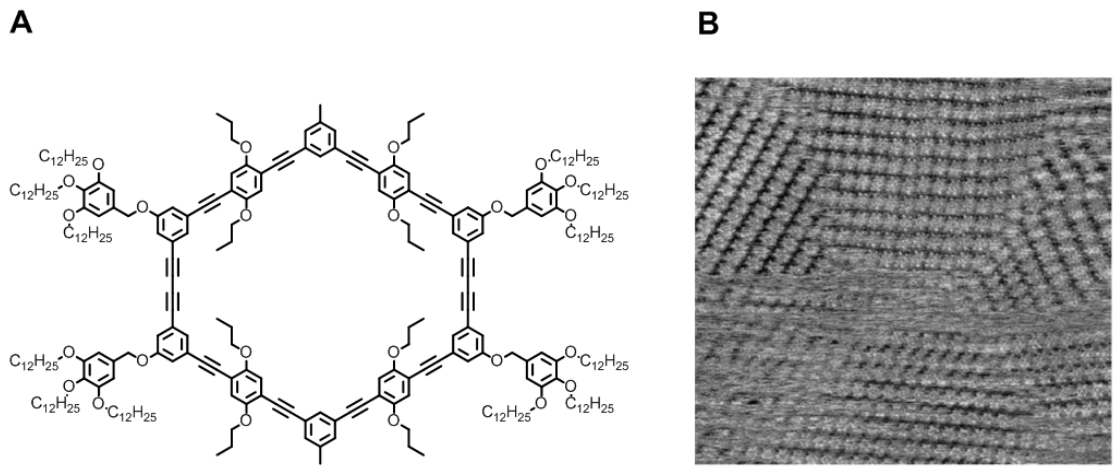

Figure 5 (A) Molecular structure of a shape persistent macrocycle based on a phenyl-ethynyl backbone with extra annular alkyl chains for surface adsorption on graphite. (B) STM picture of the adsorbed molecule from solution onto graphite. Image size: 90 nm × 90 nm.[105]

1.1.4.2 Covalent Linkage to Gold

For a covalent linkage of an organic molecule to a metal surface a suitable anchor group is required. In the last few years the role of different anchor groups has become one of the most important issues in molecular electronics.[107] The type of the interconnecting bond between anchor group and metal surface is very important for the overall characteristic of the device.[108]

The investigations of various metal ─ molecule bond interactions including S, O, Se and NC connections to metal surfaces on a theoretical level have been made in the last ten years. These investigations manifested thiols and isocyanides (NC) as the best anchoring molecules to metal contacts (in particular gold) due to a strong metal ─ molecule coupling.[109]-[111]

In **Figure 6** different types of interactions between possible anchor groups and metal surfaces which are used to immobilize organic molecules are shown. The binding energy of the anchoring bond and the substrate determines the degree of electronic coupling between each other. For a strong interaction, especially for covalent bonds, an increased orbital overlap was observed and therefore also the binding energy was higher.[108]

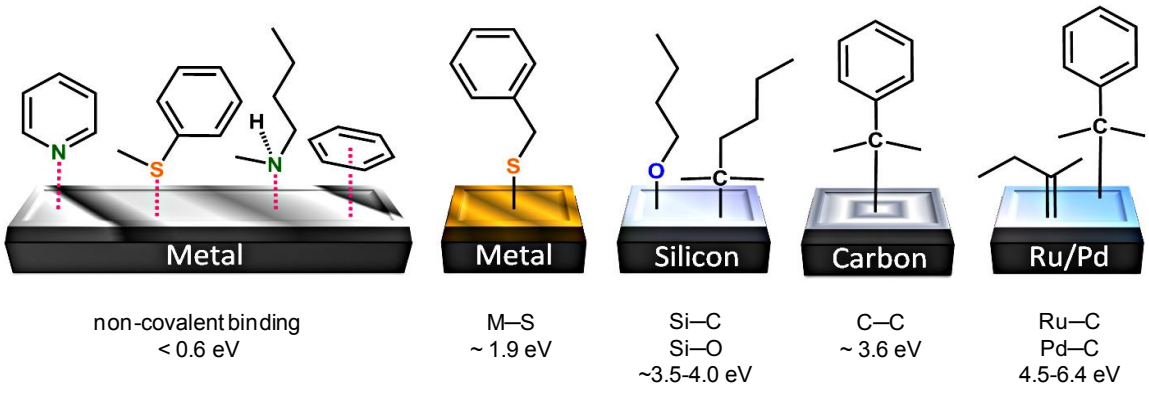

Figure 6 Bonding energies of various types of molecule ─ substrate interactions. The different anchoring groups determine the stability of the organic molecules attached to the corresponding surfaces.[112]

The binding energy between the organic molecule and the substrate does not only influence the force between the deposited layer it also has a significant influence on the conductance. Tao has determined the effect of different anchor groups on

the single molecule conductance of thiol-, amine-, and carboxylic acid. The conductance was found to be highly sensitive to the type of anchoring group, which varied in the order of Au─S > Au─NH_2 > Au─COOH. This large dependence was attributed to different electronic coupling efficiencies provided by the different anchoring groups.[113]

Hence noble metals such as gold in connection with sulfur as anchor group are ideal candidates for the immobilization of organic molecules to a metal. Based on the formed covalent bond a high stability of the molecular layer with the substrate is guaranteed.

In section 2 and section 4, different azo compounds, integrated as functional units in macrocyclic structures will be discussed.

1.2 Surface Modification

Chemically modified surfaces were already the subject of many studies in the last decades since they find application in numerous areas including electro-catalysis,[114][115] corrosion protection,[116] molecular electronics,[117][118] integrated circuits,[119][120] information storage,[120]-[122] sensing[123][124] and many others.

Subsequently a few examples are stated, to show the wide variety of functionalization possible with different types of surfaces. For example, thiol-ene click chemistry was used for the attachment of a variety of functional molecules onto oxide-free silicium (111) surfaces using very mild conditions at room temperature.[125] Ferrocene containing molecules have been grafted to silicium (100) surfaces to form mono- and multi-layers via triazene derivatives and their subsequent diazonium chemistry,[126] and a broad variety of differently linked ferrocenes were introduced by click chemistry.[120] A multistep route for the covalent anchoring of a Europium(III) complex on silicium (100) has also been reported.[127] The silicon was first functionalized with activated carboxylic acid, followed by nucleophilic substitution at the carboxylic sites.

Even more interesting than silicon are metal substrates as potential electrode materials. A platinum microelectrode was modified by electrochemically grafted nitrophenyl groups and was used as electrode for scanning electrochemical microscopy (SEM).[128] More recently, nitrophenyl groups have been deposited on a platinum surface and have been reduced subsequently to the corresponding amine. In a last step an enzyme was covalently linked to the exposed amino groups on the surface.[129]

In the following the focus is held to the electrochemical reduction of diazonium salts in order to functionalize different types of substrates.

1.2.1 Surface Functionalization by Electrochemical Reduction of Diazonium salts

Surface modification of a material, by grafting organic molecules is one of the most used techniques to introduce specific properties to a surface.[130] Functional molecular materials are playing an ever increasing role in the fabrication of smart integrated devices and molecular electronics. The attachment of functional self assembled monolayers onto insulating, semiconducting, metallic or carbon based substrates constitutes an attractive approach for building novel interfaces.[131] The modification of conducting surfaces at the molecular level with functional active building blocks represents a potential approach to the fabrication of novel types of electrodes.[132]

In order to build high quality layers to control the surface properties of electrodes, organic molecules need to be chemically attached. A very interesting approach was proposed in 1992 by Pinson[133] who showed that the reduction of aryl diazonium salt at carbon surfaces resulted in a strongly attached surface layer (electrochemical grafting) and suggested covalent bond formation between an aryl radical and the carbon surface. Five years later XPS and Raman spectroscopy provides evidence for the formation of covalent bonds between the modifier and the carbon surface.[134][135] The direct covalent linking avoids the tunnel barriers in contrast to a linking via hetero atoms, such as gold ─ sulfur linked molecules. Thus, the primary advantage of electrochemical grafting is the formation of such a covalent bond between the surface and the aryl group, resulting in a tightly bound organic layer and provides good conducting properties.[136]

The electrochemical grafting of specific organic molecules has become a method of choice since the deposition conditions can be easily controlled and adapted to the substrate. The surface immobilization proceeds via the electrochemical formation of highly reactive aryl radical species by the loss of N_2 (a in **Scheme 6**). These radicals form bonds not only to the electrode materials but also to the aryl groups already attached to the surface (b in **Scheme 6**), frequently resulting in multilayer films.[137][138] Furthermore a diazonium cation can also attack an aryl radical already attached to the surface (c in **Scheme 6**).

Scheme 6 Schematic reaction sequence for the radical growth of an organic layer on the substrate **S** (metal, carbon, semiconductor or polymer). (a) Attack of an aryl radical, generated by electro chemical reduction of the corresponding diazonium salt, on the substrate. (b) Attack of an aryl radical on an already attached aryl group. (c) Attack of a diazonium cation on an aryl radical.

The radical forming electroreduction occurs preferentially at freely available electrode surfaces quickly covering remaining uncoated surface areas. This intrinsic "self-sealing" feature of the method results in dendritic growth of an organic film and avoids the formation of pin holes or exposed domain boundaries. The diazonium salt can be reduced by controlled potential electrolysis or cyclic voltammetry (CV). The latter has the advantage of its easy use and broad applicability. With appropriate experimental conditions homogenous monolayers can be grafted, which is rather difficult to achieve by traditional chemical methods only.[20][139]-[141]

Recently, Pinson[137] studied the steric effects in the reaction of aryl radicals on surfaces. They have shown that it is possible to prevent multilayer formation by hindering different positions of the diazonium ions. A schematic overview of different steric substituents is shown in **Figure 7**. However, substitution of one or two *ortho* position prevented any reaction with the surface. The other investigated

sterically less demanding substituents at 3-, 4- and 5-position respectively lead to formation of multilayers. Blocking the growth of multilayers is much more difficult, but it could be obtained by bulky *tert*-butyl substituents in *meta* position to the diazonium functionality.

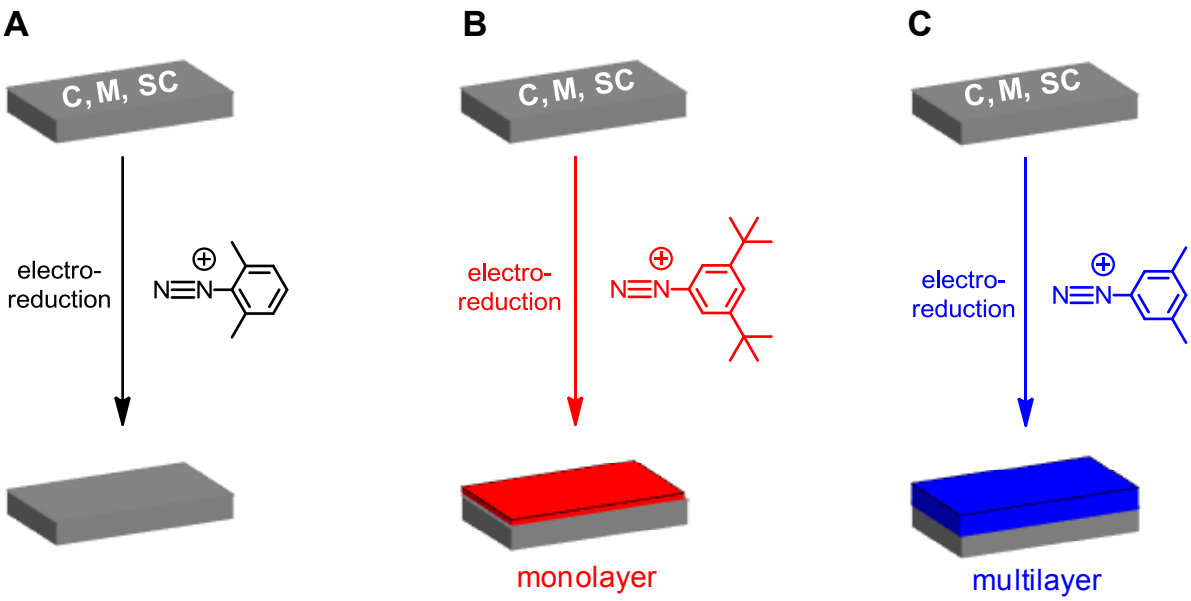

Figure 7 Schematic of electrochemical reduction of diazonium salts with different substituents to different surfaces (C = carbon, M = metal, SC = semiconductor).[137] (A) Sterical demanding substituents in 2,6-position hinder the grafting to the surface. (B) Sterical demanding substituents in 3,5-positions limited the growth of the organic layer by sterical effects and a monolayer is formed. (C) Sterical less demanding diazonium salts formed multilayer.

1.2.2 The Sonogashira Reaction

Nowadays, there are some predominant methods that are in use to chemically modify surfaces, due to the smooth chemically conditions needed and the wide range of functional groups that can be introduced: the click chemistry[142][143] and the peptide coupling.[119] More recently, some new techniques were proposed to enhance and diversify the number of method that can be used to chemically modify surfaces. For example, the introduction of functional groups via Grignard reaction on chlorinated or brominated carbon surfaces,[144] or via photochemical functionalization of acyl chloride modified surfaces. [145]

In this thesis (see section: 3 Platinum Electrode Modification) a different strategy using the Sonogashira cross coupling reaction, which is a cross coupling reaction of terminal alkynes with aryl or vinyl halides is discussed. The Sonogashira cross coupling reaction is well known as being one of the most important and utilized reactions for the construction of carbon ─ carbon bonds.[146] This type of reaction is widely applied to introduce divers functional group in organic chemistry, material science and molecular electronics.[136][146][147]

The Sonogashira reaction is a palladium catalyzed coupling reaction with a copper(I) salt as co-catalyst.[148][149] The catalytic cycle of the reaction is displayed in **Scheme 7**.

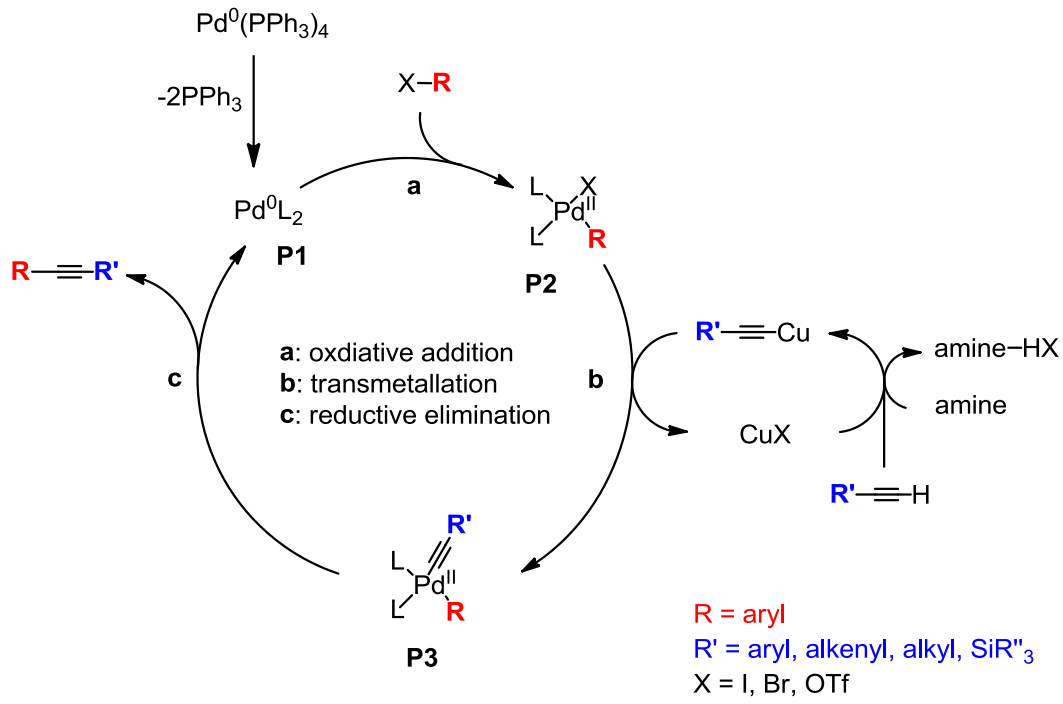

Scheme 7 Catalytic cycle of the palladium catalyzed Sonogashira cross coupling reaction. (a) Oxidative addition. (b) Transmetallation. (c) Reductive elimination. R = aryl. R′ = aryl, alkenyl, alkyl or SiR''$_3$. X = I, OTf, Br.

The acetylene is coordinated to the cooper, causing a significant reduction of the pk$_A$, followed by a deprotonation by the amine base forming an acetylide and an

amine salt as side product. To stabilize the acetylide and increase its nucleophicility, the copper(I) salt is required as co-catalyst. Rarely the reaction is also performed without co-catalyst, since the copper can support the unwanted acetylene homo-coupling.[146] The first step in the main catalytic cycle is an oxidative addition (a in **Scheme 7**). The active catalyst is an electron deficient palladium(0) complex **P1** to which the halide bearing reagent is introduced and the palladium is oxidized to a palladium(II) complex **P2**. The oxidative addition is the rate determining step of the reaction. In a subsequent transmetallation step (b in **Scheme 7**) the palladium complex **P3** is formed with the introduced acetylene. Followed by the reductive elimination the cross coupling product is relieved and the active palladium(0) catalyst is regenerated.

The most often used catalysts are $[Pd(PPh_3)_2Cl_2]$ and $[Pd(PPh_3)_4]$. As co-catalyst copper(I) iodide is used. As base, amine bases are employed either as solvent or as reagents in a huge excess. There are many parameters that dictate the overall efficiency of the catalytic cycle such as, catalyst, amine base, solvent and the electronic and steric characteristics of the aryl halide and the alkyne. Electron deficient organic halides are more reactive to cross coupling conditions then electron rich, for the alkynes the opposite is true.[149]-[151] The general reactivity order for the aryl halides are: iodines > triflates ≥ bromines >> chlorines.[149]

The mild and well explored Sonogashira cross coupling reaction is suitable for a wide variety of functional groups. Thanks to its high reactivity under mild conditions it is also a suitable reaction for surface functionalization.[146][152] This approach will be discussed in section 3.

1.3 Biphenylic Compounds

Since organic structures have been considered as the active elements in electronic nanoscale devices, the electron transport properties through molecules have received great attention.[136][153]-[157] Single molecules in electronic circuits can be integrated in various experimental setups to measure their conductance. Such measurements enable basic investigations of the correlation between the molecular structure and transport properties.[158]-[160]

1.3.1 Biphenyls in Molecular Electronics

For this purpose biphenylic compounds, which consist of two aromatic rings connected by a single carbon ─ carbon bond, have attracted considerable attention because of their size and ready availability.[161][162] Biphenyl derivatives have been considered as potential conductance switches as the two π systems of the phenyl rings can be either in the same plane or perpendicular to each other representing an “ON” and an “OFF” state, respectively.[163]-[165] In **Figure 8** the two different states are shown depending on the conformation of the two phenyl rings.

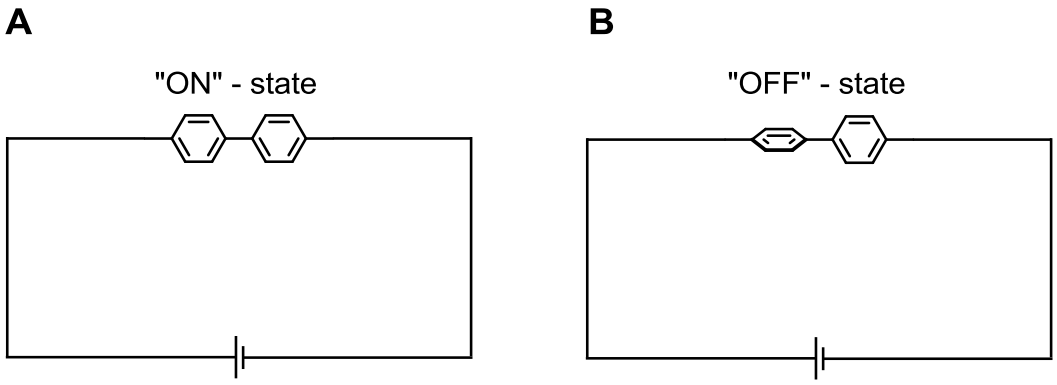

Figure 8 (A) “ON” – state of a biphenyl in an electronic circuit, where the two phenyl rings are in the same plane. (B) “OFF” – state of a biphenyl, where the two phenyl rings are perpendicular to each other, reduces the electrical conductance.

The torsion angel between the two phenyl rings of a biphenylic system is not at all fixed, it is very sensitive to its chemical environment and the substitution

pattern.[166]-[169] In **Figure 9** the rotational barriers of differently substituted biphenyls are shown. The required free rotation energy for an unsubstituted biphenyl is only 8-12 kJ mol^{-1}. Attaching of methyl groups in the *ortho* position of the biphenyl increases the rotational barrier to about 30-40 kJ mol^{-1} for mono substitution, and to 80 kJ mol^{-1} for a substitution on both positions.[170][171] For bridged biphenyls the required energy is even higher.[172]

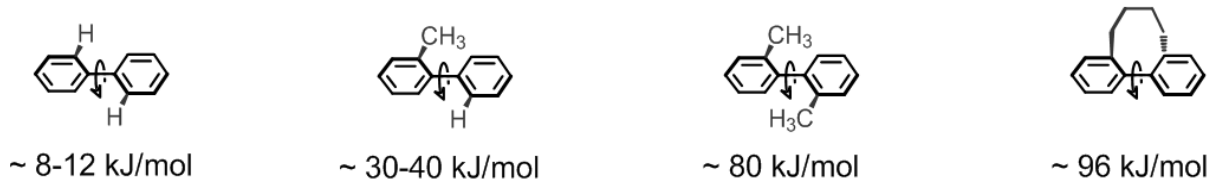

Figure 9 Rotational barriers of sterically different *ortho* substituted biphenyls. All values were obtained by dynamic NMR investigations.

1.3.2 Correlation between Conformation and Conductance in Biphenyls

Biphenyls are interesting model compounds to investigate electronic transport properties, since it is the smallest building block with two neighboring benzene rings as individual π-systems.[161][173] From a chemical point of view biphenyls are also interesting due to their easy synthetic accessibility via various cross coupling reactions.[149]

The degree of π-electron delocalization between the two phenyl units is expected to vary with the interplanar torsion angle Φ. If the two phenyl rings are in one plane a high conducting state is expected for a biphenylic system (A in **Figure 10**), while a reduced conductance is expected for systems with twisted phenyl rings (B in **Figure 10**). And for phenyl rings perpendicular to each other, the two π systems are decoupled and no π overlap is observed, therefore almost no conductance is expected.

Theoretical calculation showed that σ—σ, and σ—π interactions are also involved as conducting channels, but the π—π coupling is by far the most important.[174] If the two phenyl rings are nearly perpendicular to each other, the π—π coupling is

significantly reduced and the other coupling (σ—σ and σ—π) become more important and will dominate the transport properties.[165][174][175]

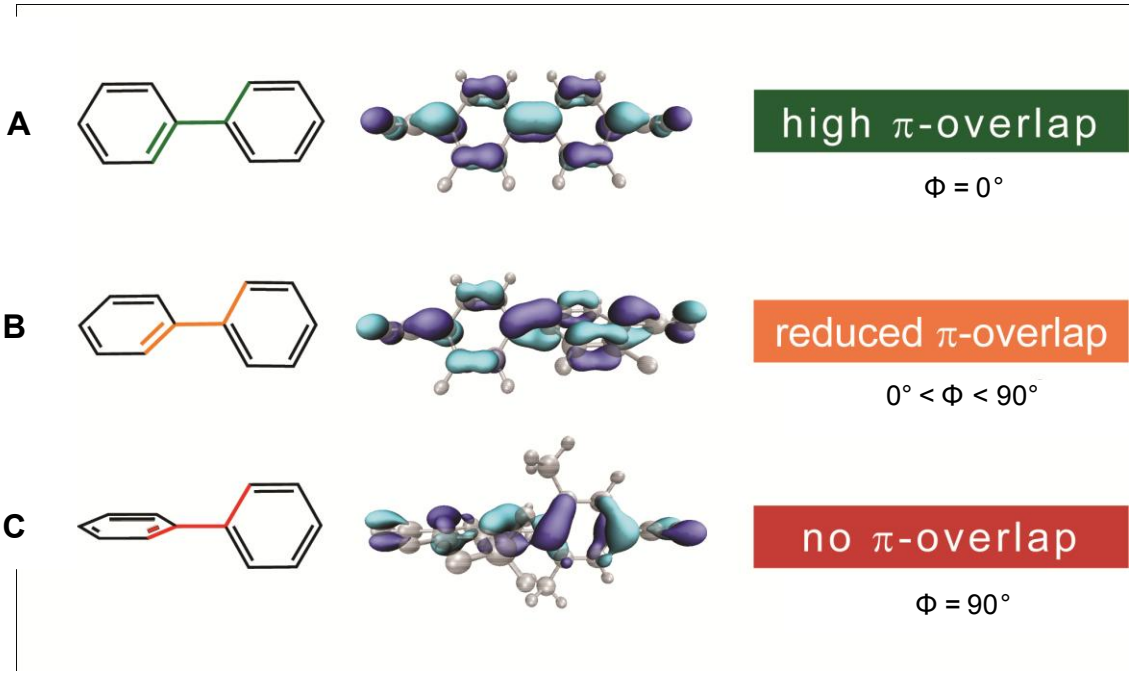

Figure 10 Schematic of three biphenyl conformation and the degree of π-conjugation, represented by the LUMO orbitals.[112] (A) The neighboring π orbitals connecting the two phenyl rings most efficiently. (B) The overlap is reduced by a certain twist. (C) The neighboring phenyl rings are perpendicular to each other. The two π systems are decoupled.

The interdependence between single molecule conductance and the molecular conformation of biphenyls was first investigated by Venkataraman in 2006.[176] The single molecular conductance of a number of biphenylic compounds comprising various donor and acceptor substituents was measured. The obtained results are summarized in **Figure 11**.

It was hypothesized that a linear correlation between the $\cos^2$ of the interplanar torsion angle θ and the molecular conductance (C in **Figure 11**). The results have to be handled with a certain skepticism, due to the different attached donor and acceptor substituents on the biphenyls. As anchor group amines were used to link the biphenyl to the electrodes of the STM break junction, where the conductance was measured.

This study nicely demonstrated the correlation between the conductance and the degree of π-conjugation in the biphenyl backbone, but it did not address the influence of the donor and acceptor substituents and the torsion angle were obtained from theory and not from single crystal structures.

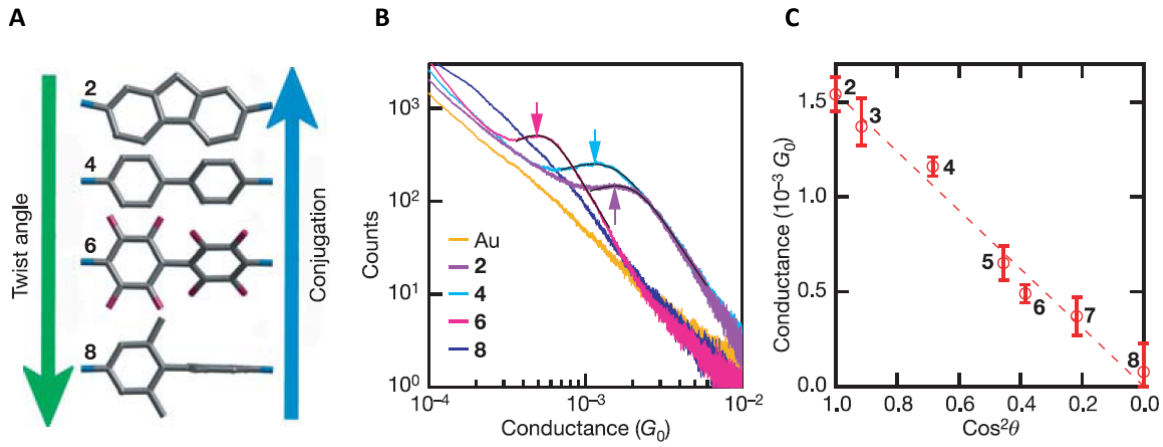

Figure 11 (A) Structures of a subset of the biphenyl series studied, shown in order of increasing twist angle and decreasing conjugation. (B) Conductance histograms obtained from measurements of the corresponding biphenyl structures. (C) Position of the peaks for all the molecules studied plotted against $\cos^2\theta$, where θ is the calculated interplanar twist angle for each molecule.[176]

Recently the correlation between conductance of the biphenylic backbone and the torsion angle was systematically investigated with biphenyls, where two phenyl rings were interconnected by alkyl chains of various length in order to obtain different twist angles (**Figure 12A**).[112][157][177][178] The torsion angles φ were determined from single crystals and the conductance was measured in a STM break junction.

Investigation of the single molecule conductance of this series **M1**-**M8** displayed a linear correlation with the $\cos^2\varphi$ of the inter-ring torsion angle φ for the biphenyls with sulfur anchor groups with a divided π-system.

A similar trend at increased conductance values has been reported for amine terminated biphenyls comprising various substituents.[176] In contrast to their findings, the planar fluorene derivative **M2** displayed a reduced conductivity,

pointing at additional and equally important parameters governing the transport efficiency in addition to the planarity of the π-system.[112]

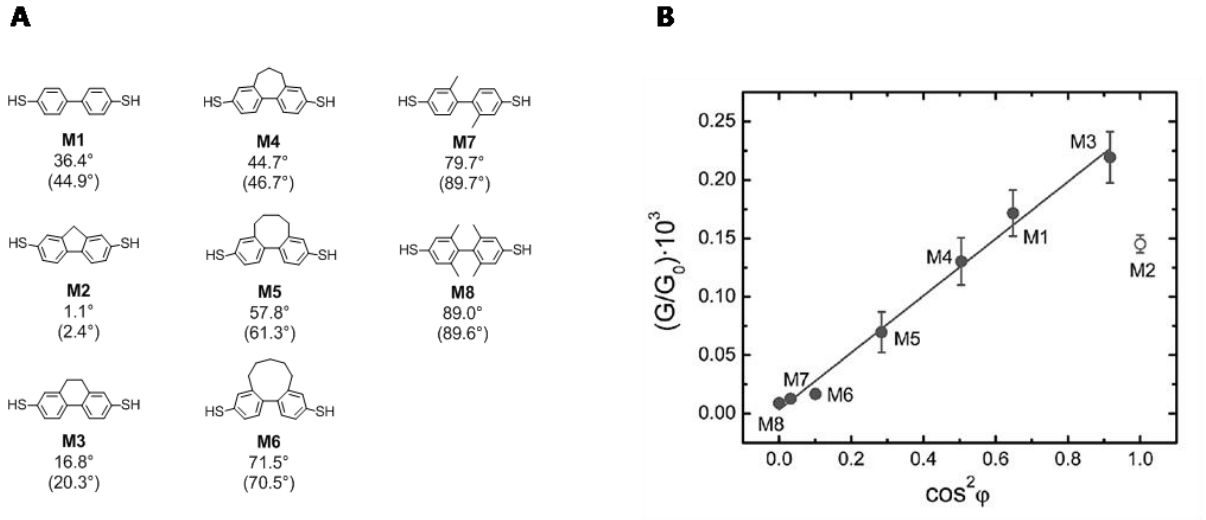

Figure 12 (A) Investigated biphenylic structures with the corresponding interplanar torsion angles φ from X-ray structures and the calculated values (in bracket). (B) Experimentally determined conductance of thiol terminated biphenyl molecules **M1**-**M8** versus $\cos^2\varphi$, where φ is the torsion angle of the molecules as given by the X-ray data.[179]

The integration of an azo bridge in a biphenylic system, in order to adjust the twist angle by light, will be discussed in section 4 Switchable Conducting Azo Biphenyls.

1.4 Aim of the Work

The present thesis is organized as follows: In a first research project the integration of azobenzene motives as functional unit in molecular structures is discussed. In a second project the modification of platinum electrodes with different functional molecules, in order to obtain tailor made surfaces is investigated. In a last project a switchable conduction biphenyl is synthesized as a potential conductance switch.

The aim of the present work is the synthesis and characterization of different azo macrocycles. The spatial arrangement of shape switchable macrocycles with two azo functionalities will depend strongly on the conformation of the optically addressable joint of the azobenzene subunit. These optically addressable switches should give access to two conformations with large differences in exterior form, namely a flat cycle (like an open trap) in the (*trans,trans)* form and a bent cycle (like a close trap) in the (*cis,cis)* form. Due to the rigid design with a *m*-terphenyl backbone and the integration of two azo units a considerable stabilization of the thermodynamically less favored (*cis,cis*) form is expected.

The aim of the platinum electrode modification is to find ways to chemically deposit suitable molecular films onto surfaces. A modular approach to chemically modify surfaces, more precisely platinum electrodes, will be discussed. By electrochemically grafting the electrodes with a suitable diazonium salt, an organic coated platinum electrode exposing iodoaryls is obtained. Subsequent Sonogashira cross coupling chemistry with tailor made acetylene molecules allows substituting the exposed iodines with various functional groups. The new technique is improved in order to introduce a wide range of functional groups onto electrode surfaces with a high surface coverage of the functional subunit.

The aim of the last project is the synthesis and characterization of a biphenyl with switchable conductance as a novel molecular switche and memory device based on “mechanical” motion in molecular biphenylic structures. In order to alter the transport properties by an external stimulus, such as light, we planned to integrate bistable molecular sub units with state dependent length as bridging systems. Potential candidates as bridging sub units are azo compounds due to their optically addressable *cis*/*trans* isomerization. Other possible switching units are:

diarylethene based switches, redox switches or voltage triggered hysteretic switches.

Surface modification and switching concepts in molecular electronics is a very interdisciplinary field and requires a close collaboration of researchers from different backgrounds in science such as physics and chemistry. However this thesis is written from a chemist's point of view and focus on the design and synthesis of molecules.

2 Azo Macrocycles

Shape switchable azo macrocycles with a rigid backbone are paving the way towards photo switchable macrocycles, of which the isomers have improved thermodynamic stability features[84][180] as well as considerably different spatial appearances. However, the combination of efficient photochemical switching with large difference in appearance requires a subtle balance between the rigidity and flexibility of the macrocycle subunits.

In this section the synthesis and shape switching behavior of azo macrocycles **1**-**7** (**Figure 13**) is described. First (section 2.1) the alkyl functionalized azo macrocycles **1**-**4** are described and then (section 2.2) the sulfur functionalized azo macrocycles **5**-**7**, with a anchor group for a covalent linking to gold surfaces are described.

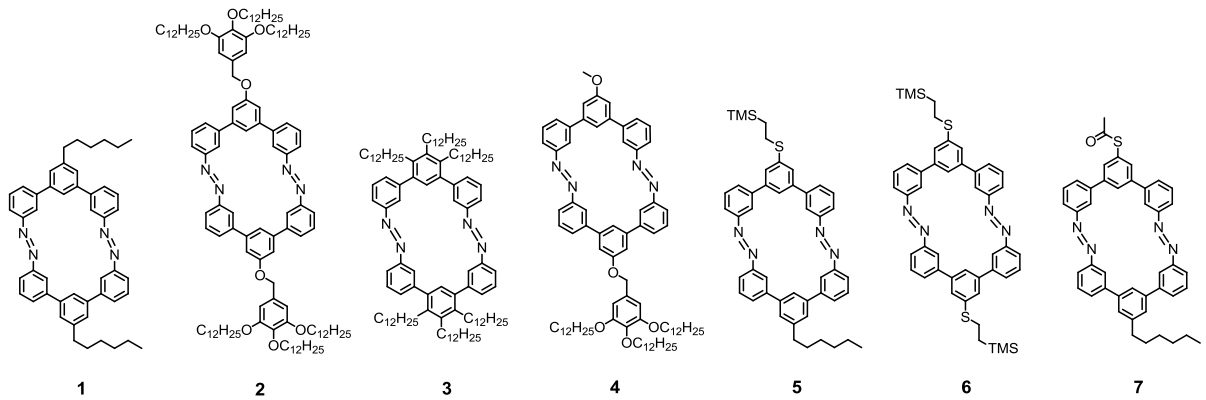

Figure 13 Overview of all shape switchable azo macrocycles **1**-**7**. Macrocycles **1**-**4** functionalized with long alkyl chains and macrocycles **5**-**7** functionalized with sulfur anchor groups.

The common parts of all macrocycles **1**-**7** are two rigid *m*-terphenyl semicircles interlinked by two azo groups. Although the central photochemically active macrocycle is in common, they differ considerably in the substituents on the central ring of their terphenyl subunits. This variation of substituents not only leads to changes in chemical properties including solubility, processability and adhesion features as well as physical properties of size and shape. Whereas the target structures **1**-**3** and **6** are symmetric azobenzene macrocycles consisting of two

identical semicircles, the central substituents on both semicircles are different in the asymmetric macrocycles **4**, **5** and **7**.

The spatial arrangement of shape switchable monodisperse azo macrocycles with two azo functionalities on opposed sides of the cycle will depend strongly on the conformation of the optically addressable joint of the azobenzene. In **Figure 14** the working principal of macrocycles **1**-**7** is schematically shown. These optically addressable switches should give access to two conformations with large differences in exterior form, namely a flat cycle (like an open trap) in the (*trans,trans)* form and a bent cycle (like a close trap) in the (*cis,cis)* form, as it is shown schematically in **Figure 14**. Due to the rigid design with a *m*-terphenyl backbone the (*trans,cis*) intermediate is supposed to be a short lived isomer, if one azo function is switched to its *cis* form the other is forced to switch as well, since a (*cis,trans*) mixed state is higher in energy.[181]

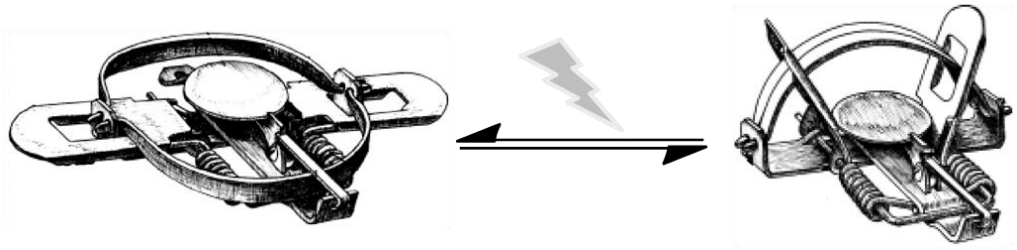

Figure 14 Schematic of the working principal of optical switchable azo macrocycles in analogy to an open and closed bear trap. In contrast to a bear trap, the optical switching of azo macrocycles is fully reversible.

2.1 Alkyl Functionalized Azo Macrocycles

2.1.1 Design of Alkyl Functionalized Azo Macrocycles

Macrocyclic model compounds consisting of two azobenzene subunits interlinked by alkyl chains have already been synthesized to investigate the influence of steric restrictions on the photochemical properties of these photoactive subunits (**Figure 15B**).[80][182] Recently, the synthesis of an azobenzophane displaying inverted thermodynamic stabilities has been reported (**Figure 15A**).[84] Owing to steric strain, the *cis* isomer of this azobenophane was more stable, whereas steric repulsion usually favors the *trans* isomers of azo derivatives. While the more flexible alkyl linked structure **B** displayed some probability for a (*cis,trans*) intermediate, the more rigid azobenzophane structure **A** did not show any (*cis,trans*) intermediates.[84][181]

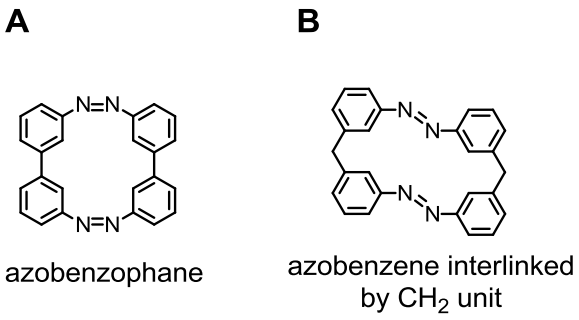

Figure 15 Already synthesized azo macrocycles with two azo functions. (A) Azobenzophane with a thermodynamically stable *cis* isomer. (B) Two azobenzenes interlinked by a CH_2 unit.

Based on this considerable stabilization of thermodynamically less favored isomers, some interesting investigations of *cis* conformations can be performed, like e.g. investigation of the difference of surface covering and packing features of *cis* and *trans* isomers respectively. Therefore macrocyclic azo compounds for surface investigations are designed.

The macrocycle present in its thermodynamically more stable *trans* form covers a large surface area and is occupying space mainly in two dimensions (**Figure 16**). After light induced switching to its *cis* form the macrocycle is bent at the azo joint

and covers only half of the surface area than in its *trans* arrangement. It should be possible to investigate this interesting surface covering and packing features by scanning tunneling microscopy (STM) at the liquid│solid interface. STM allows the investigation of absorbed layers of molecules, both at the graphite – solution interface[96]-[98] and in dry films on conductive substrates with molecular resolution.[183]

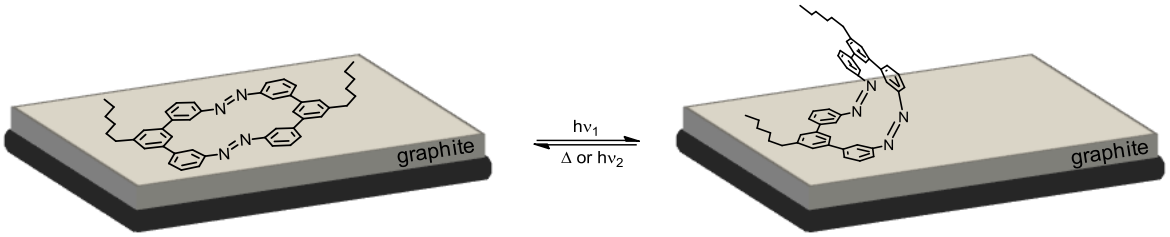

trans form of adsorbed macrocycle **1** *cis* form of adsorbed macrocycle **1**

Figure 16 Expected surface adsorption of the macrocycles **1** on a graphite surface. After photo isomerization to its *cis* form, the macrocycles are expected to cover only half of the surface area than when in the *trans* state.

Two rigid semicircles which are interconnected by two azo groups as joints, which are switchable by light, are envisaged. To provide the required rigidity for an optimal and complete switching behavior, *m*-terphenyl was chosen for the semicircles. To combine efficient photochemical switching properties with large differences in surface covering features, a subtle balance between rigidity and flexibility of the macrocycle subunit has to be found. While subunits of the macrocycle which are too rigid may handicap the isomerization reaction, subunits which are too flexible may result in indistinguishable (*cis,trans*) intermediates. Hence, rigid macrocycles comprised of several azo groups, as their switching unit upon isomerization, are of particular interest, due to the possible stabilization of the thermodynamically less favored *cis* isomers. Because of the increased rigidity in the macrocyclic systems the two azo functions are no longer independent and therefore a simultaneously switching of both azo joints is predicted. As a consequence of such a switching behavior a stable *trans* but also a stable *cis* conformation can be expected.

Interestingly, alkyl chains are as important as the aromatic core for the adsorption features. For example hexa-*peri*-hexabenzocoronene has different self assembly characteristics at the solid – liquid interface depending on the length of the alkyl side chains.[101] While relatively short C6 alkyl chains show some weak adsorption features with a slight freedom of movement on the surface, longer C12 alkyl chains showed much better adsorption properties and tend to stick on the surface.[93][104][105][184] Depending on the force of the van der Waals (vdW) interaction between the molecule and the surface it will be easier or harder to switch the macrocycles on the surface in order to obtain a three dimensional arrangement in which one semicircle is still fixed at the surface. As this adsorption properties of alkyl chains with an aromatic core are hardly predictable three different type of alkyl functionalization on the central core have been envisaged (macrocycles **1**-**3** in **Figure 13**).

In macrocycle **1** the central ring of the *m*-terphenyl semicircle was functionalized with one hexyl chain. The van der Waals (vdW) forces of the alkyl chains and of the core should be a subtle balance between the adsorption tendency to the graphite and the possibility of lifting up one part of the macrocycle while switching to its *cis* form, as it is shown schematically in **Figure 16**.

To increase the possibility of a self assembling tendency of the macrocycle on the graphite surface, macrocycle **2** and **3** were also envisaged. These macrocycles consist of more and significant longer alkyl chains, which should increase the interaction between the organic molecule and the graphite surface. It has been shown that the trialkyloxybenzyl auxiliary synthesized by Höger et al. supported the adsorption at the liquid│solid interface for STM investigations.[106] Beside the similarity in the length of the alkyl chains, macrocycle **2** and **4** differ considerably in their electronic properties. Macrocycle **3** is electronically poorer in contrast to macrocycle **2**, since the trialkyloxybenzyl auxiliary of macrocycle **2** increases the electronic density of the aromatic core considerably.

With the asymmetric macrocycle **4** we would have a building block in hand for further functionalization at one semicircle to build more complex macrocycles with specific features. A functionalization of one side with hydrophilic acid groups would give access to changeable surface properties by light. In a flat *trans* conformation

the surface properties would be dominated by the hydrophobic core of the macrocycle while in the switched *cis* conformation with the acid groups perpendicular to the surface, the hydrophilic properties would dominate.

Based on all these structural considerations, such as photo isomerization, considerable stabilization of the thermodynamically less favored *cis* isomer and adsorption features on graphite surface; the alkyl macrocycles **1**-**4** have been envisaged.

2.1.2 Retro Synthesis of Alkyl Functionalized Azo Macrocycles

Two rigid semicircles are interconnected by two azo groups as joints, which are switchable by light. To provide the required rigidity for an optimal and complete switching behavior, *m*-terphenyl was chosen for the semicircles. Since all target structures **1**-**4** are macrocycles consisting of two *m*-terphenyl semicircle subunits and two azo groups on opposite sides, similar synthetic strategies were considered in all four cases. The synthetic strategy of macrocycle **1** will be discussed in detail, in particular the cyclization reaction. An overview of the retro synthesis of macrocycle **1** is shown in **Scheme 8**.

The key step of all synthetic pathways will be the formation of both azo groups as the macrocyclization. As already described in the introduction, different synthetic strategies are available for the formation of azo groups, depending on their precursors. Thanks to the symmetry of macrocycle **1**-**3** it allows a dimerization strategy (pathway **b** and **c** in **Scheme 8**) but also an asymmetric build up via a Mills reaction[32] (pathway **a**) or via palladium catalyzed formation of Boc protected hydrazines followed by oxidation[38][39][185][186] (pathway **d**) can be envisaged. For the dimerization either the buildup of both azo functions by reductive methods[29][180] by coupling two nitro semicircles in the presence of a reducing agent or by oxidative methods[26]-[28] by coupling two amino precursors in the presence of an oxidizing agent, have been envisaged. Mechanistically the reductive dimerization and the Mills reaction are the same, while in the Mills reaction the nitroso- and the amino precursor are separated and subsequently

coupled, in the reductive dimerization they are formed in situ and directly coupled to form an azo group. This is also the reason why the Mills reaction is better for an asymmetric target compound. The nitroso precursor[187]-[189] for the Mills reaction can either by synthesized by a selective reduction (pathway **g**) from the nitro compound or by a selective oxidation starting from an amine. In contrast to this one step synthesis, the precursor for the palladium catalyzed hydrazines coupling needs a three step reaction. First the reduction to the amine (pathway **h**), then a Sandmayer reaction to introduce a suitable leaving group for cross coupling reactions (pathway **i**) and finally the palladium catalyzed Hartwig – Buchwald type reaction[38] (pathway **j**) to introduce the Boc protected hydrazine.

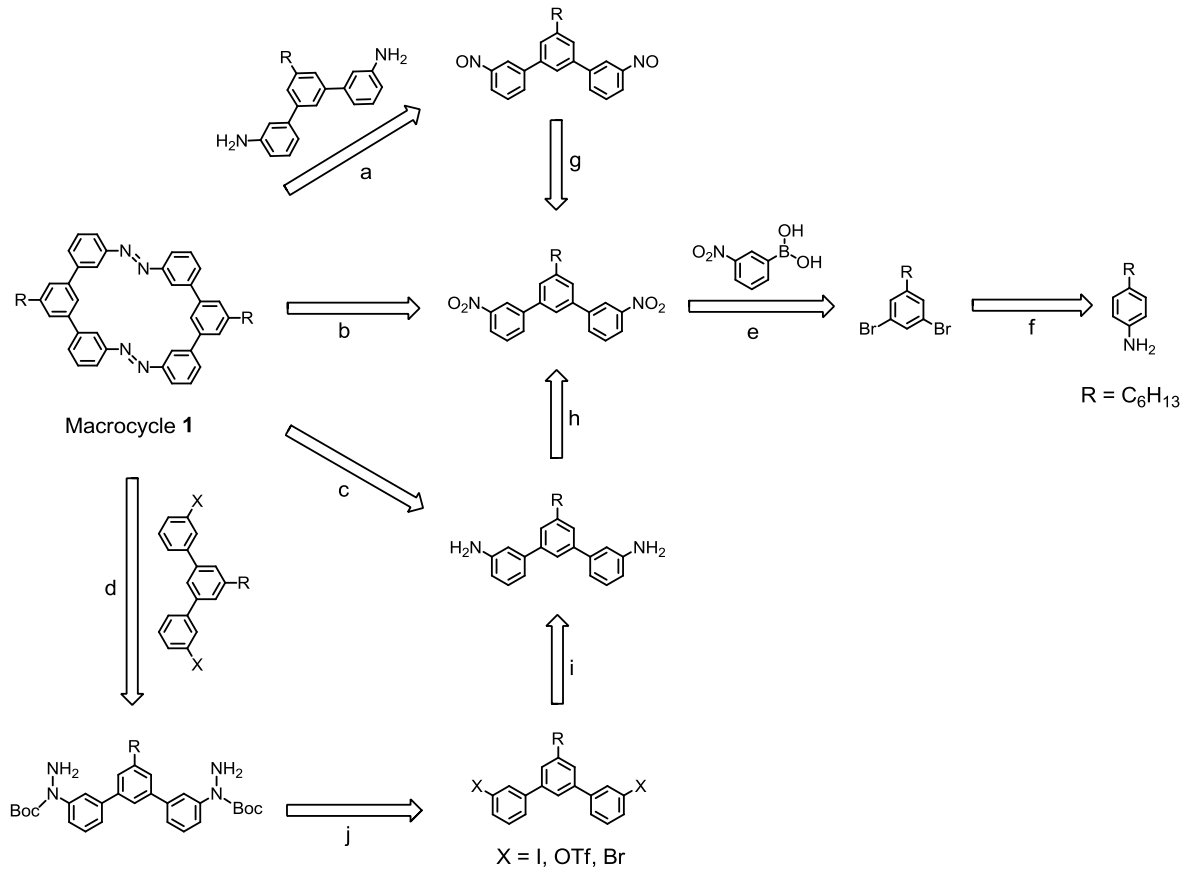

Scheme 8 Retrosynthetic scheme for the synthesis of the symmetric macrocycle **1**. (a) Mills reaction. (b) Reductive dimerization. (c) Oxidative dimerization. (d) Palladium catalyzed hydrazine formation followed by oxidation. (e) Suzuki cross-coupling reaction. (f) Bromination and deamination. (g) Selective reduction. (h) Reduction. (i) Sandmayer reaction. (j) Palladium catalyzed Hartwig-Buchwald type reaction.

Owing to the synthetic availability of its precursors, the reductive dimerization between nitro functionalized *m*-terphenyl semicircles was favored as the ring-closing reaction and was envisaged first. A Suzuki cross coupling reaction should provide the *m*-terphenyl semicircle as a key intermediate of the synthesis. The dibromo precursor for the Suzuki reaction can be provided from commercially available 4-hexylaniline by bromination and subsequent deamination under acidic conditions.

The assembly of macrocycle **2** consists of the same key steps as the assembly of macrocycle **1** and is shown in **Scheme 9**. Due to the short synthetic pathway the key macrocyclization and the formation of the azo joints will be provided through the same reductive dimerization (pathway **a** in **Scheme 9**) as described above. 1,3,5-Tribromobenzene is singly substituted to 3,5-dibromoanisole (pathway **d**) which is a suitable starting material for the Suzuki reaction (pathway **c**). It will provide a phenolic hydroxyl group on the *m*-terphenyl semicircle after dealkylation, which would enable its further functionalization by a nucleophilic substitution reactions with tris(dodecyloxy) functionalized chloromethylbenzene (pathway **b**). The chloromethyl benzene derivative can be synthesized following a literature known protocol.[105]

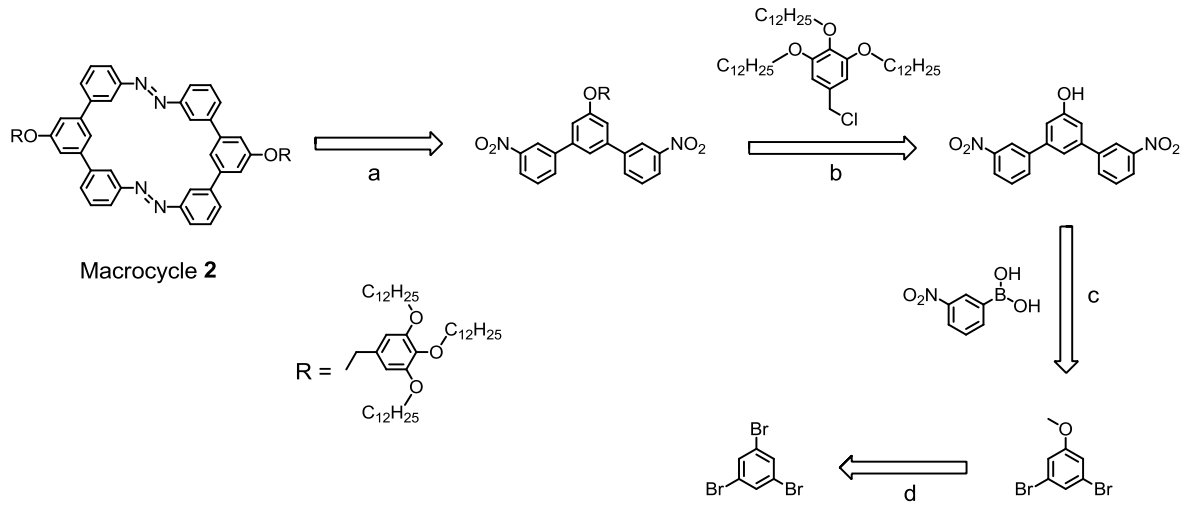

Scheme 9 Retrosynthetic scheme for the synthesis of symmetric macrocycles **2**. (a) Reductive dimerization. (b) Nucleophilic substitution. (c) Suzuki cross-coupling reaction. (d) Nucleophilic aromatic substitution reaction.

Also macrocycle **3** can be assembled through a reductive dimerization (pathway **a** in **Scheme 10**). To obtain a suitable 2,3,4-trialkyl-1,5-dibromobenzene precursor for the Suzuki reaction, 2,6-diiodo-4-nitroaniline was considered as a starting material. A Sandmayer reaction will provide 3,4,5-triiodo-1-nitrobenzene (pathway **f**) and subsequent substitution of the iodine atoms by alkynyl chains in a Sonogashira - Hagihara reaction (pathway **e**) should yield the required alkyl chains. Hydrogenation should reduce both the triple bonds and the nitro group to provide 3,4,5-trialkylaniline (pathway **d**), a suitable precursor for introducing bromine atoms at the 2- and 6-positions. Subsequent deamination should give the desired 2,3,4-trialkyl-1,5-dibromobenzene precursor for the Suzuki reaction (pathway **b**).

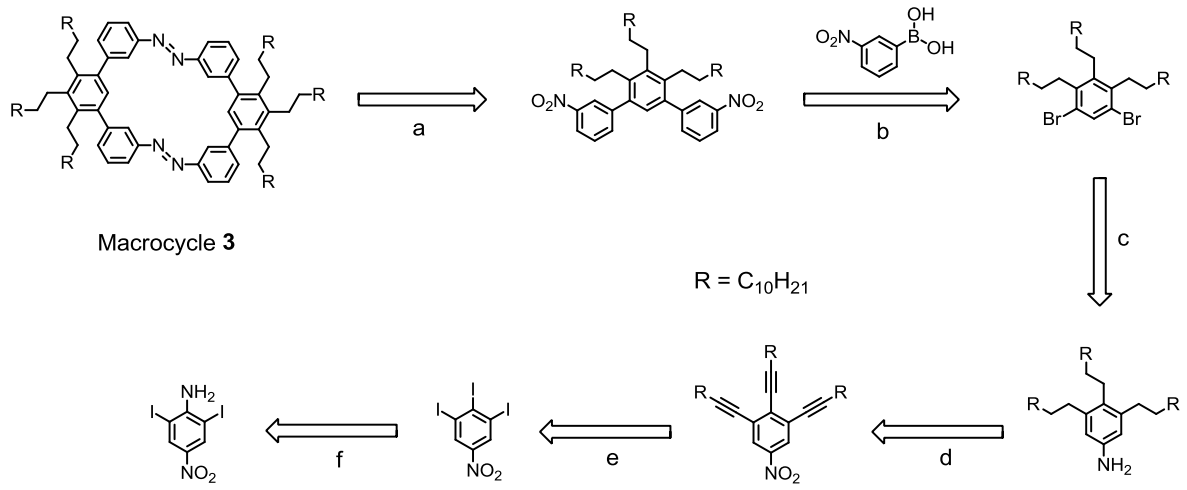

Scheme 10 Retrosynthetic scheme for the synthesis of symmetric macrocycles **3**. (a) Reductive dimerization. (b) Suzuki cross-coupling reaction. (c) Bromination and deamination. (d) Hydrogenation. (e) Sonogashira-Hagihara cross-coupling reaction. (f) Sandmayer reaction.

In the case of the asymmetric macrocycle **4**, the coupling between a nitroso- and an amino-functionalized semicircle (Mills reaction)[32] might be more favorable in order to enable the coupling of two different precursors (pathway **a** in **Scheme 11**). This consideration was even more supporting of the general strategy, as the nitroso precursors for the Mills reaction should be available by selective reduction of the original starting materials, namely the corresponding nitro functionalized

semicircles (pathway **c** in **Scheme 11**). For the other semicircle a reduction to the corresponding amine (pathway **b**) was envisaged.

As an alternative for the macrocyclization reaction the palladium catalyzed formation of Boc protected hydrazines followed by oxidation, as described above, would also be possible, as well as a statistical dimerization reaction of both nitro functionalized semicircles. Due to the large differences of all three possible dimerization products, a separation with size exclusion chromatography should be possible.

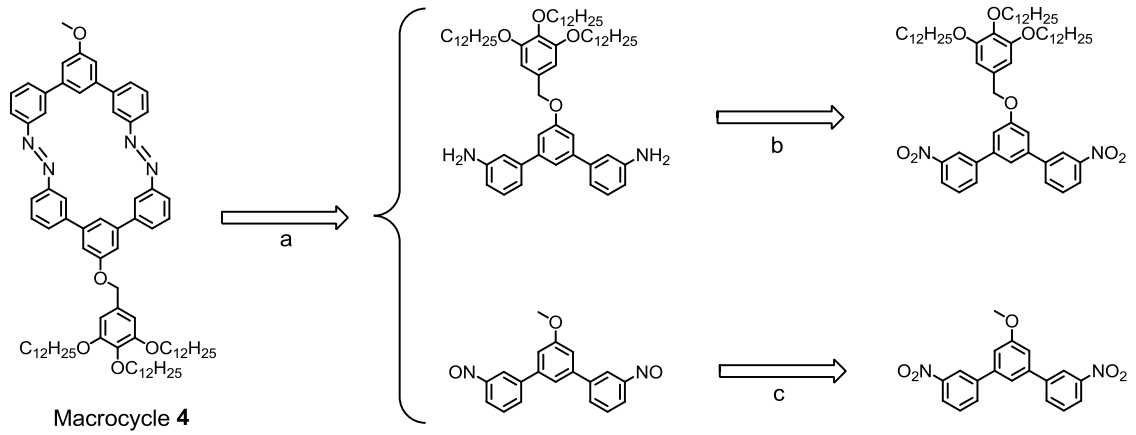

Scheme 11 Retrosynthetic scheme for the synthesis of asymmetric macrocycles **4**. (a) Mills reaction. (b) Reduction. (c) Reduction and selective oxidation.

2.1.3 Synthesis of Alkyl Functionalized Azo Macrocycles

First the simplest symmetric azo macrocycle **1** with one hexyl chain on the middle ring of the *m*-terphenyl semicircle was synthesized. In **Scheme 12** the four step synthesis to the target macrocycle **1** is shown.

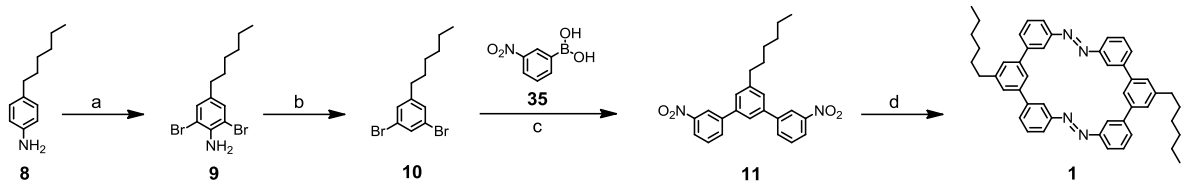

Scheme 12 Synthetic route to the symmetric hexyl functionalized macrocycle **1**. Reagents and conditions: (a) NBS, DMF, 0°C → RT, 3 h, 86%. (b) $NaNO_2$, H_2SO_4, EtOH, 75°C, 2 h, 60%. (c) $[Pd(PPh_3)_4]$, K_2CO_3, $C_6H_5CH_3$, EtOH, 85°C, 3 h, 95% or $[Pd(PPh_3)_4]$, K_2CO_3, $C_6H_5CH_3$, EtOH, 120°C, 10 min in MW, 98%. (d) $LiAlH_4$, THF, RT, 5 h, 50%.

The dibromo intermediate **10** was obtained from commercially available 4-hexylaniline (**8**). Treatment of 4-hexylaniline (**8**) with *N*-bromosuccinimide (NBS) in *N,N*-dimethylformamide (DMF) gave the doubly brominated product **9** as dark red crystals in a good yield of 86%.[190] Deamination with concentrated sulfuric acid and sodium nitrite in ethanol at 75°C after 3 hours provided the desired dibromo compound **10** which was isolated by column chromatography on silica gel in 52% yield over both steps.

The subsequent Suzuki cross coupling reaction was slightly modified compared to the literature known conditions.[191]-[194] The solvent was changed from the reported toluene to a more polar and protic solvent mixture of toluene with ethanol. This solvent mixture resulted in a significant 20% increase in the yield. Treatment of 2.6 equivalents of the commercially available 3-nitrophenyl-boronic acid (**35**) and the dibromoaryl compound **10** with 8 mol-% of tetrakis(triphenylphosphine)-palladium $[Pd(PPh_3)_4]$ as catalyst and potassium carbonate as base in toluene:ethanol (3:1) at 85°C for 3 hours in an inert atmosphere provided the desired *m*-terphenyl semicircle **11** as a light green solid in a good yield of 95% after column chromatography on silica gel.[195] The same reaction with the same palladium catalyst could be performed in the microwave in an inert atmosphere at

120°C for 10 minutes and gives an increased yield of 98% for the Suzuki reaction. A comparison and discussion of Suzuki reactions under conventional conditions and microwave conditions will be provided in section 2.2.3.2.

For the subsequent reductive dimerization to the target azo macrocycle **1** several different reaction conditions were investigated. It was found, that three parameters are important for a successful macrocyclization and that the conditions are adaptable to all cyclization reactions with these similar nitro functionalized semicircles. The temperature, the addition time of the reducing agent and the overall reaction time played an important role and will be discussed in detail. As reducing agent lithium aluminum hydride ($LiAlH_4$) in a 1 molar THF solution was chosen, as it is known to be a suitable reducing agent for the stepwise reduction of a nitro compound via the nitroso intermediate to the amine.[29] To favor the dimerization over polymer formation high dilution conditions of 2.0×10^{-4} molar were applied. The use of lithium aluminium hydride necessitated the use of absolutely water free conditions; therefore THF was used as solvent, which was dried by distillation over sodium and potassium prior use. The role of the solvent was not further investigated in the subsequent studies. In **Table 1** the systematic variation of the three key parameters are shown.

First the influence of the reaction temperature was investigated in some test reactions. Is the reaction temperature too low (<RT, entry 1 and entry 2 in **Table 1**) the complete reduction to the amine is favored over the selective reduction to the nitroso compound which can further react and form the azo joint. But is the temperature too high (>40°C, entry 3) it seems that the formation of larger oligomers and polymers is favored. The crude reaction mixtures were investigated by MALDI-TOF spectrometry and by TLC in order to roughly determine the formed products and the conversion and it turned out, that at 40°C the major product is the desired macrocycle **1**.

Further the addition time of the reducing agent was analyzed and it has been shown that a slow addition of the $LiAlH_4$ solution is necessary. But in contrast to that, a too slow addition (entry 6) slightly decreased the yield and a increased

polymer formation was observed. Overall a slow addition between 1 hour and 2 hours gave the best conversion and the macrocycle **1** could be isolated in yields up to 45%.

Table 1 Investigation of the three key parameters (reaction temperature, addition time of $LiAlH_4$ and reaction time) in the reductive dimerization reaction in order to form macrocycle **1**. All reaction were performed in 250 mL dry THF under an inert argon atmosphere with 0.05 mmol of **11** and 0.4 mmol of a 1 molar $LiAlH_4$ in THF solution.

entry	reaction temperature [°C]	addition duration of $LiAlH_4$ [min]	reaction time [h]	remarks and yield
1	0°C	15 min	4 h	mainly reduction to amine[a]
2	RT	15 min	4 h	product **1** but mainly polymer formation[a]
3	50°C	15 min	4 h	product **1** and polymer[a]
4	40°C	15 min	4 h	mainly product **1**[a], ~30%[b]
5	40°C	60 min	4 h	~45%[b]
6	40°C	360 min	10 h	product **1** but also polymer[a]
7	40°C	120 min	4 h	~45%[b]
8	40°C	60 min	18 h	~40%[b]
9	40°C	60 min	6 h	50%

[a] MALDI-TOF mass spectrometry and TLC investigations
[b] calculated from ^{1}H-NMR spectrum, after prep. GPC

The third parameter the reaction time plays a minor role. It turned out that an overall reaction time of at least 4-6 hours is required (entry 7 and 9), while longer reaction times of 18 hours (entry 8) resulted in a slightly decreased yield. However, with these optimizations a yield of 50% for the hexyl functionalized macrocycle **1** was obtained (see below).

To assemble macrocycle **1**, the nitro semicircle **11** was treated with lithium aluminum hydride under high dilution conditions (0.49 mM) in dry THF at 40°C for 6 hours. The nitro compound **11** is reduced step wise to the nitroso- and amino

compound, respectively; which immediately react together and form the azo joint. Subsequent extraction with dichloromethane and purification by size exclusion chromatography (SEC) resulted in an almost pure product. Dissolution of the pre cleaned product in hot toluene:ethanol (6:5) and collection of the oily residue after storage at -20°C for ten days gave the desired macrocycle **1** in 50% yield and in a pure form according to analytical GPC.

To further clarify the surprising efficiency of the cyclization reaction, the crude mixture was also investigated by analytical GPC (**Figure 17**). And indeed, besides the dominant main peak (71% intensity) corresponding to the macrocycle **1** with a retention time of 11.84 min, only a few rather weak peaks at shorter retention times, probably arising from larger oligomers, and a single small peak at 21.05 min retention time, probably due to the fully reduced diamino semicircle, were observed. However, these side products were not further investigated.

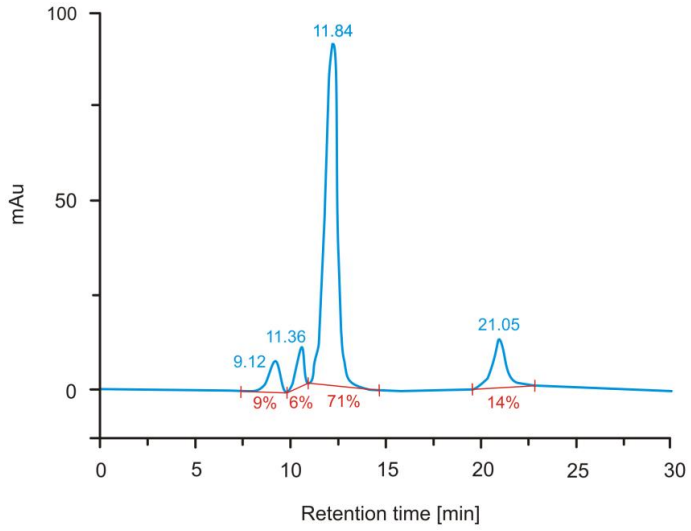

Figure 17 GPC chart of the crude reaction mixture of macrocycle **1**. Analyzed in toluene at λ = 220 nm with a flow rate of 0.5 mL/min. The main peak with an intensity of 71% at 11.84 min corresponds to compound **1**. The integrations are shown in red and the retention times in blue.

Macrocycle **1** was fully analyzed by TLC, MALDI-TOF and EI mass spectrometry, UV/Vis, IR, VPO and by NMR-spectroscopy (^{1}H-NMR, ^{13}C-NMR, HMBC, HMQC,

and COSY). The absorption spectroscopic analysis will be discussed in section 2.1.5.

Later, while assembling the sulfur functionalized azo macrocycle **5** an alternative purification procedure was found, but with a significant decrease of the yield from 50% to 15%. After extraction with dichloromethane the orange crude was chromatographed with silica gel. The pre cleaned product was chromatographed again by preparative TLC to obtain the macrocycle **1** as orange crystals. After this purification method it was possible to obtain single crystals suitable for X-ray structural analysis (**Figure 19** in section 2.1.4).

To increase the molecular weights of the subunits of the two semicircles moving relative to each other and thus to increase the spatial difference of the two isomers and the adsorption features on a graphite surface, the macrocycles **2** and **3** were envisaged. Shape persistent macrocycles comprising similar polyalkyl substituents have already been reported by Höger et al..[104][106][184][196]-[198] Increased adsorption properties of these macrocycles with an increasing number of alkyl chains were observed. The driving force for the adsorption of the macrocycles at the surface is the nonspecific attractive van der Waals (vdW) interaction of the rigid and the flexible ring parts, including the alkyl chains, with the graphite surface. This difference in adsorption properties could be an interesting aspect in view of future scanning probe investigations of switching macrocycles.

The synthetic route to the desired hydroxy *m*-terphenyl intermediate is shown in **Scheme 13**. The commercially available 1,3,5-tribromobenzene (**14**) was converted into **15** with a nucleophilic aromatic substitution reaction[199] with 1.4 equivalent of sodium methoxide in DMF at 80°C. After column chromatography, the desired monosubstituted product **15** was isolated in a good yield of 70% considering the statistical nature of the reaction. Subsequent Suzuki cross coupling reaction turned out to be challenging under conventional conditions.[149][192]

With $[Pd(PPh_3)_4]$ as catalyst and potassium carbonate as base, the dibromo compound **15** was treated under an inert atmosphere with 2.6 equivalents of (3-nitrophenyl)boronic acid (**35**) in toluene:ethanol (8:3) at 85°C for 2 hours. The

doubly arylated product **16** was obtained as white powder in moderate yield of 33% after recrystallization from hot toluene. Neither increased amounts of boronic acid **35**, nor increased temperature and reaction time yielded in a better conversion. In addition, shorter reaction times provided the monocoupled compound as the main product.

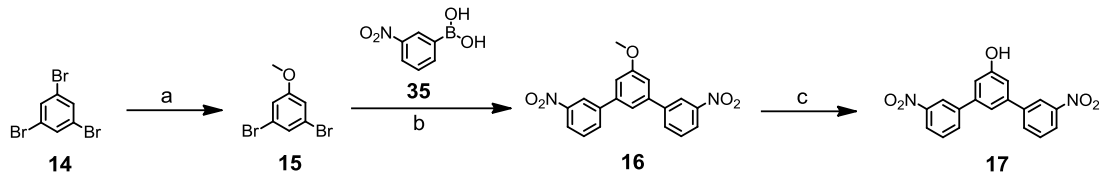

Scheme 13 Synthetic route to the hydroxy *m*-terphenyl intermediate **17**. Reagents and conditions: (a) NaOMe, DMF, 80°C, 8 h, 70%. (b) $[Pd(PPh_3)_4]$, K_2CO_3, $C_6H_5CH_3$, EtOH, 85°C, 2 h, 33% or $[Pd(PPh_3)_4]$, K_2CO_3, $C_6H_5CH_3$, EtOH, 120°C, 10 min in MW, 90%. (c) BBr_3, CH_2Cl_2, -78°C → RT, 2.5 h, 95%.

Applying microwave conditions to the Suzuki cross coupling reaction offered significantly better yields than the applied conventional conditions.[200][201] The same reagents, the same catalyst and the same purification steps were applied but the temperature was increased from 85°C to 120°C for the microwave reaction. After ten minutes at 120°C in the microwave the desired product **16** was isolated as white powder after recrystallization from hot toluene in an excellent yield of 90%. A detailed analysis of the Suzuki cross coupling reaction and the advantages of microwave condition is given in section 2.2.3.2. The methoxy *m*-terphenyl semicircle **16** was almost quantitatively deprotected to the free alcohol **17** with boron tribromide in dichloromethane at -78°C.

The oligoalkylated chloromethylbenzene intermediate **21** was synthesized according to a literature procedure[105][202] in an excellent overall yield of 85%, as shown in **Scheme 14**. The commercially available methyl-3,4,5-trihydroxybenzoate (**18**) was alkylated with 1-bromododecane in a standard S_N2 reaction[203][204] in DMF with potassium iodide as a nucleophilic catalyst at 70°C. The product **19** was isolated as a yellow solid in a yield of 90% after purification by column chromatography on silica gel. In a reduction with lithium aluminum hydride in ethyl

ether the benzoate **19** was converted to the benzylic alcohol **20**. After a simple extraction the product **20** was isolated as a white resin in 96% yield. Subsequently, the alcohol **20** was substituted by a chlorine with thionyl chloride and a few drops of DMF in dichloromethane to give the desired intermediate **21** as a pale yellow solid, in an almost quantitative yield of 98%.

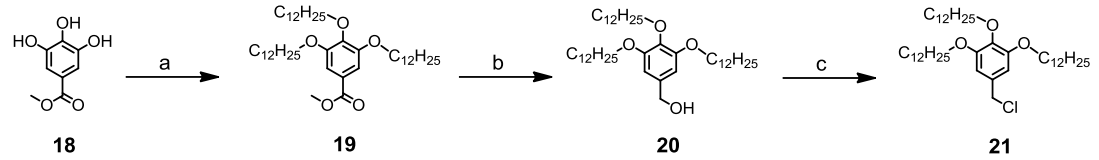

18 **19** **20** **21**

Scheme 14 Synthetic route to the oligoalkylated chloromethylbenzene intermediate **21**. Reagents and conditions: (a) 1-bromododecane, K_2CO_3, KI, DMF, 70°C, 30 h, 90%. (b) 1.) $LiAlH_4$, Et_2O, RT, 1.5 h. 2.) NaOH, H_2O, RT, 15 min, 96%. (c) $SOCl_2$, CH_2Cl_2, DMF, RT, 45 min, 98%.

The deprotected semicircle **17** was reacted with the electrophile **21** in a S_N2 reaction to the trialkyloxybenzyl functionalized semicircle **22** (**Scheme 15**). The S_N2 reaction was performed with potassium carbonate in DMF at 65°C. After column chromatography the semicircle **22** was isolated as white powder in a good yield of 89%.

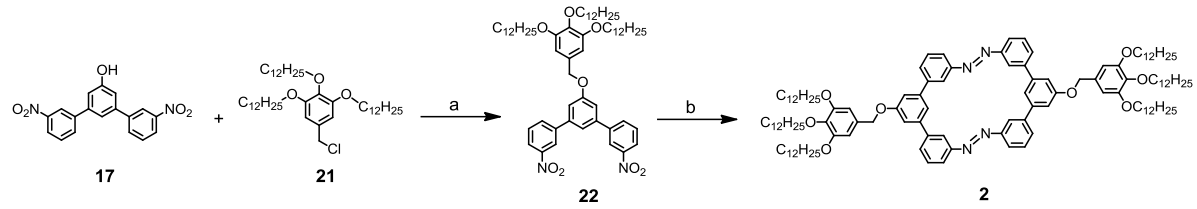

17 **21** **22** **2**

Scheme 15 Synthetic route to the key intermediate **22** and to alkyloxybenzene functionalized azo macrocycle **2**. Reagents and conditions: (a) K_2CO_3, DMF, 65°C, 22 h, 89%. (b) $LiAlH_4$, THF, RT, 2.5 h, 34%.

For the macrocyclization reaction similar conditions to those described above for the macrocycle **1** were applied. Thus, after treating **22** in THF (0.06 mM) with lithium aluminum hydride, the macrocycle **2** was isolated in a yield of 34% as an intensely orange colored resin. Thanks to the large difference in molecular weights

of semicircle **22** and macrocycle **2**, of more than 850 amu it was possible to purify the product by gel permeation chromatography. Despite the easier purification method compared to macrocycle **1**, the yield slightly decreased. However, a single peak in the analytical GPC at a retention time of 10.8 min further confirmed the purity of the isolated compound.

As a more compact macrocycle consisting of trialkyl functionalized semicircles, target structure **3** was envisaged with three long alkyl chains directly connected to the central ring of the *m*-terphenyl subunit (**Scheme 16**). With three alkyl chains per semicircle the solubility and the adsorption properties on surfaces as well as the absorption properties of the macrocycle **2** should be maintained, but the floppiness and the electron density of the semicircle subunits should be reduced due to the absence of the ─O─CH_2 linker.

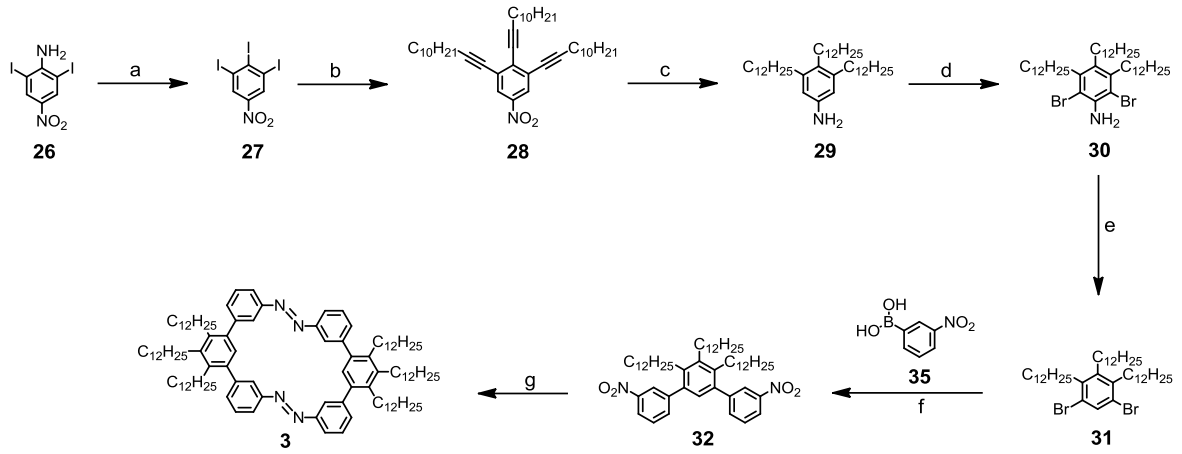

Scheme 16 Synthetic route to target macrocycle **3**. Reagents and conditions: (a) 1.) AcOH, $NaNO_2$, H_2SO_4, 15°C → RT, 1.5 h. 2.) KI, H_2O, CH_3COOH, H_2SO_4, 95°C, 2 h, 80%. (b) $HCCC_{10}H_{21}$, $[Pd(PPh_3)_2Cl_2]$, CuI, NEt_3, 85°C, 3 h, 89%. (c) H_2, Pd/C, EtOH, AcOEt, RT, 28 h, 59%. (d) NBS, DMF, 0°C → RT, 2 h, 70%. (e) H_2SO_4, $NaNO_2$, EtOH, 85°C, 4 h, 95%. (f) $[Pd(Ph_3)_4]$, K_2CO_3, $C_6H_5CH_3$, EtOH, 85°C, 3 h, 85% or $[Pd(PPh_3)_4]$, K_2CO_3, $C_6H_5CH_3$, EtOH, 120°C, 10 min in MW, 96%. (g) $LiAlH_4$, THF, 40°C, 3 h, 49%.

The commercially available 2,6-diiodo-4-nitroaniline (**26**) was first converted through a Sandmayer reaction[205] into triiodobenzene **27** in 80% yield. According to

the literature,[206] intermediate **29** was synthesized by a Sonogashira-Hagihara cross coupling reaction in triethylamine followed by a palladium catalyzed hydrogenation in ethanol and ethyl acetate in 53% yield over both steps. The moderate yield of the hydrogenation reaction was due to incomplete hydrogenation of the double bond in *para* position to the nitro group, probably as a result of the sterically hindered formation of the π complex in the catalytic cycle.[204][207] However, neither increased hydrogen pressure nor an increased concentration of the catalyst provided a better yield.

The subsequent assembly of macrocycle **3** was similar to the synthesis described above for macrocycle **1**. The reaction of amine **29** with NBS in DMF gave the doubly brominated product **30** as a yellowish oil in 70% yield after purification by column chromatography on silica gel.[190] Deamination with concentrated sulfuric acid and sodium nitrite provided the desired dibromo compound **31**, which was isolated by column chromatography on silica gel in pure hexane in a good yield of 95%. A Suzuki cross coupling reaction with commercially available 3-nitrophenylboronic acid (**35**) allowed the triply alkylated semicircle **32** to be prepared in 81% yield. The desired azo macrocycle **3** was obtained by reductive dimerization with lithium aluminum hydride, highly diluted in THF (0.06 mM) at room temperature. After purification with size exclusion chromatography (SEC) by using toluene as eluent, the pure product was isolated in 49% yield as an intensely orange colored resin. Analytical GPC confirmed the purity of the compound with a single peak with a retention time of 10.9 min.

To differentiate between the semicircles which sticks to the surface and the one which protrude upon switching by light, an asymmetric azo macrocycle **4** was envisaged (**Figure 13**). In contrast to a symmetric assembly an asymmetric macrocycle is more difficult to build up, since two different precursors need to be coupled. Whereas in the reductive dimerization the two required precursors (R–NO and R'–NH_2) were formed in situ, in the Mills reaction[32] these two precursors has to be isolated first in order to couple one with the other. This reaction sequence previously turned out to be very efficient for constructing asymmetric azo compounds.[16][30][208] Because of the different functionalities required as

precursors, it is ideally suited for the assembly of two different building blocks as shown in **Scheme 17**. However, the synthesis of nitroso functionalized *m*-terphenyl semicircles turned out to be troublesome.

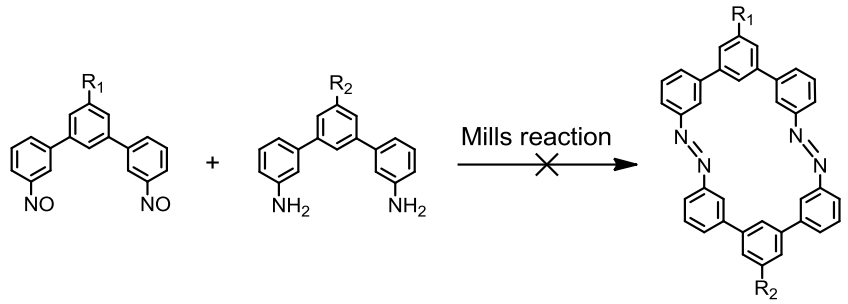

Scheme 17 Assembly of an asymmetric azo macrocycle via Mills reaction.

There are in principle two possible strategies for the synthesis of nitroso compounds.[188] Either, the reduction from the nitro group to the nitroso (which is in fact an insitu reduction of the nitro group to the amine followed by an oxidation to the nitroso),[209] or a stepwise procedure including the reduction to the amine and subsequent oxidation to the nitroso.[189][210] Both strategies had in common the problem of the delicate oxidation, in order not to over oxidizing to the nitro group. In **Scheme 18** an overview of the possible synthetic strategies towards the nitroso *m*-terphenyl intermediates is shown.

The shortest and most convenient procedure is the straight forward pathway **g**. It consists of a reduction with zinc in a solvent mixture of methoxyethanol and water containing ammonium chloride at elevated temperature, followed by subsequent selective oxidation with iron(III)chloride in a mixture of water and ethanol at -5°C.[30][211] After the first reduction step with zinc an black oily suspension was observed, despite this it was possible to further convert it in a slightly greenish crude, which is typical for nitroso compounds. According to ^{1}H-NMR and MALDI-TOF mass spectrometry investigations of the crude, the desired products were formed in the case of **13**, **25** and **34**. However, in the case of the semicircle **24** no conversion was observed as it seemed to be even more delicate than the other semicircle and therefore no further investigations were made. All attempts to purify the nitroso products have not yet come to fruition, since it decomposed directly.

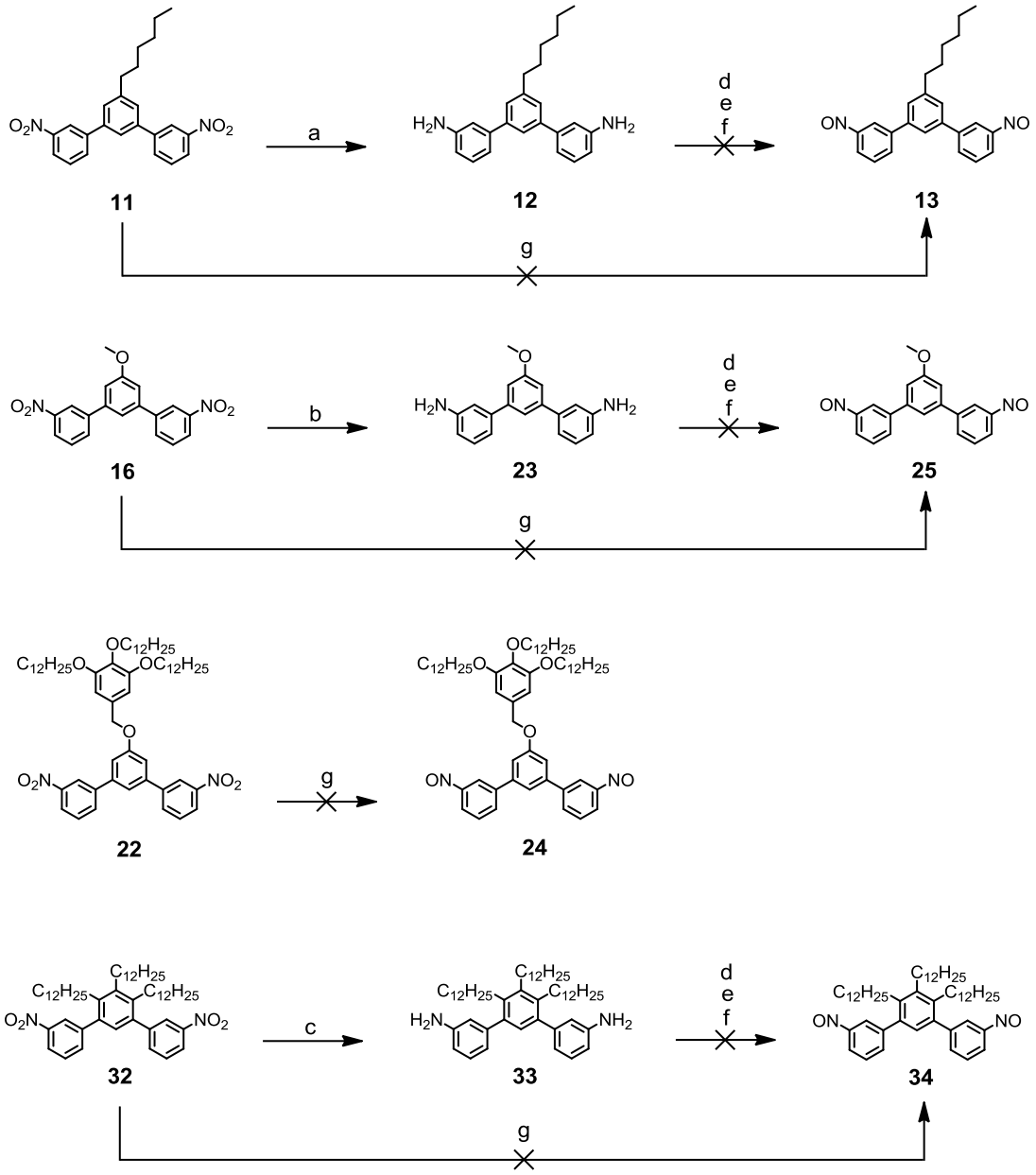

Scheme 18 Synthesis towards nitroso functionalized *m*-terphenyl semicircles. Successful reduction to amino functionalized semicircles **12**, **23** and **33** but unsuccessful oxidation to nitroso functionalized semicircles **13**, **24**, **25** and **34**. Reagents and conditions: (a) 20 bar H_2, Pd/C, CH_2Cl_2, RT, 16 h, 87%. (b) conc. HCl, Sn, THF, RT, 4h, 98%. (c) conc. HCl, Sn, THF, RT, 5h, 73%. (d) *Oxone*® potassium peroxomonosulfate, CH_2Cl_2, H_2O, RT. (e) $FeCl_3$, EtOH, 0°C. (f) PhSeSePh, aq. H_2O_2, $CHCl_3$, RT. (g) 1. Zn, NH_4Cl, H_2O, 2-methoxy-methanol, 33°C. 2. $FeCl_3$, EtOH, -5°C.

An alternative route to prepare the nitroso compounds was the reduction and isolation of the corresponding amines followed by a selective oxidation. Amino

functionalized semicircles **12**, **23** and **33** were readily available by reducing the corresponding dinitro semicircles. The amine functionalized semicircle **12** was obtained using palladium on activated carbon as catalyst in the hydrogenation of the dinitro compound **11**.[212] The reduction in an autoclave with Pd/C in dichloromethane under a hydrogen pressure of 20 bars at room temperature afforded the diamino **12** as a yellowish solid in a good yield of 87%. The dinitro semicircle **16** was reduced with tin powder and concentrated hydrochloric acid at room temperature to afford the diamino compound **23** in a slightly better yield of 98% compare to the hydrogenation reduction.[25] Appling the same conditions afforded the trialkyl functionalized amino semicircle **33** as a colorless solid in a yield of 73%.

These synthesized amino semicircles **12**, **23** and **33** are precursor for the Mills reaction as well as for the selective oxidation to the corresponding nitroso compounds. However, a dinitroso functionalized semicircle as the second precursor for the Mills reaction could not be obtained in reasonable yields, not by selective oxidation with iron(III)chloride and not with diphenyl diselenide and hydrogen peroxide. Following a second strategy, the amino semicircles were treated with potassium peroxomonosulfate (*Oxone®)* in a dichloromethane:water solvent mixture.[210] Both ^{1}H-NMR and MALDI-TOF mass spectrometry investigations revealed the presence of the desired compound in the crude reaction mixture. However, all attempts to isolate these labile nitroso semicircles **13**, **25** and **34** by column chromatography or by crystallization failed. As an alternative, an in situ preparation of the dinitroso semicircle was envisaged. However, treatment of the reaction mixture comprising the dinitroso semicircle with a diamino semicircle only provided poor amounts of an inseparable mixture, probably of various oligomers.

An alternative strategy towards an asymmetric azo macrocycle consists of the statistical assembly of two different dinitro or diamino semicircles. It is possible to close the ring with a reductive dimerization[29] or with an oxidative dimerization[26]-[28] starting from the nitro compound or from the amino compound, respectively. In

consideration of the fact that the dinitro semicircle is easier to obtain, a reductive dimerization was preferred (**Scheme 19**).

Thus, the two semicircles **16** and **22** with the largest possible difference in molecular weight to that of the semicircles already synthesized were subjected to the macrocyclization conditions described above.

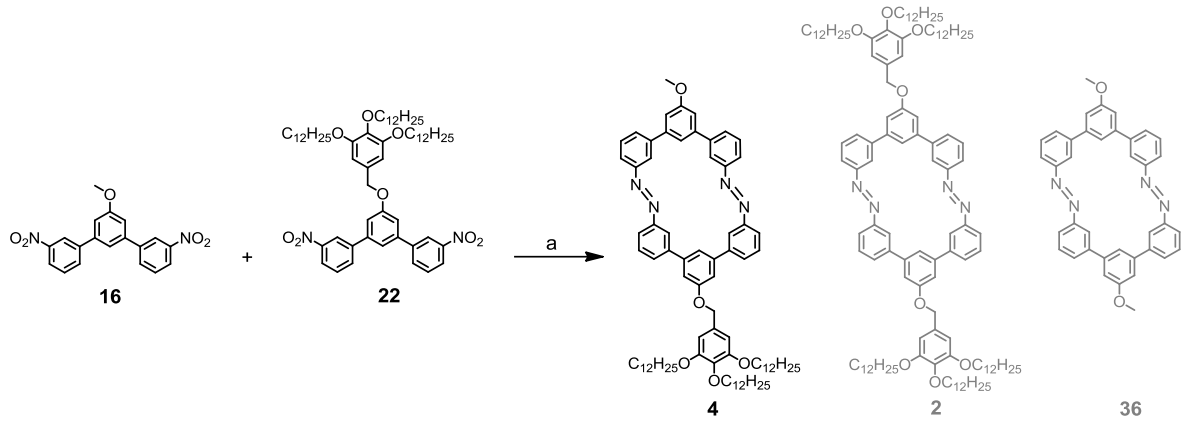

Scheme 19 Synthesis to asymmetric target macrocycle **4** via reductive dimerization. Reagents and conditions. (a) $LiAlH_4$, THF, 40°C, 5 h, 34%.

Equimolar amounts of the two different semicircles **16** and **22** were dissolved in THF. A 1 M lithium aluminum hydride solution in THF was slowly added at room temperature. After keeping the reaction mixture at 40°C for 5 hours, it was poured onto water and extracted with dichloromethane. Owing to the statistical nature of the reaction, not only the desired macrocycle **4** but most probably also the symmetric macrocycles **2** and **36** were formed. Fortunately, the molecular weights of the three macrocycles **2**, **4** and **36** are sufficiently different to allow their separation by size exclusion chromatography (SEC). Although with analytical GPC it was not possible to separate the crude reaction mixture properly. Whereas preparative SEC divided the sample into three well defined bands, of which the most intense central one was isolated. Owing to the limited amounts formed, the two accompanying bands were not further analyzed. The analytical data (^{1}H-NMR, GPC, VPO and IR) of the isolated central band indicated a pure chemical compound with the structure of macrocycle **4**. The isolated intensely orange

colored resin corresponded to a yield of 34% of the non symmetrical compound **4** and displayed a single symmetric peak with a retention time of 11.0 min in analytical GPC. Despite of many attempts it was not possible to grow a crystal suitable for X-ray scattering. The efficiency of the formation of the symmetric macrocycle **4** remains to some extent inexplicable. It might be related to the restricted formation of the symmetric macrocycle **2** comprising two sterically more demanding semicircles.

2.1.4 Characterization of Alkyl Functionalized Azo Macrocycles

The precursors **9**-**13**, **15**-**17**, **19**-**23**, **27**-**32** and **33** were fully characterized by ^{1}H and ^{13}C-NMR spectroscopy, mass spectrometry and elemental analysis, the characterization of the macrocycles **1**-**4** turned out to be more challenging.

Although the ^{1}H-NMR spectra corroborated the suggested structures of all macrocycles **1**-**4**, one dimensional ^{13}C-NMR spectra could only be obtained for the macrocycles **1** and **4**. The size and the relatively high inertia of each of the larger macrocycle **2** and **3** cause long rotational correlation times (τ). Because τ is proportional to the linewidths of the resonance in the NMR spectra, the signal-to-noise ratio for the relatively insensitive ^{13}C-NMR spectra turned out to be too small to obtain meaningful one dimensional ^{13}C{^{1}H} NMR spectra.[213] However, the more sensitive ^{1}H detected HMBC and HMQC spectra allowed full characterization of the carbon resonances of both macrocycles **2** and **3**.

Of particular importance is the determination of the purity and the molecular weight of each of the isolated macrocycles, as the synthetic strategy based on the dimerization of two bifunctional building blocks allows the formation of larger cyclic oligomers with comparable NMR spectra. Analytical gel permeation chromatograms were recorded to document the purity of macrocycles **1**-**4** (**Figure 18**). All four compounds displayed well defined single peaks at λ = 220 nm with retention times R_t (**1**) = 11.85 min, R_t (**2**) = 10.80 min, R_t (**3**) = 10.87 min and R_t (**4**) = 11.01 min in the expected order of decreasing molecular weight.

However, owing to the particular shape and thus hydrodynamic volume of the macrocycles **1**-**4**, GPC is not suited to determining their molecular weights. Similar GPC conditions applied to polystyrene standards displayed systematically shorter retention times than the more compact macrocycles.

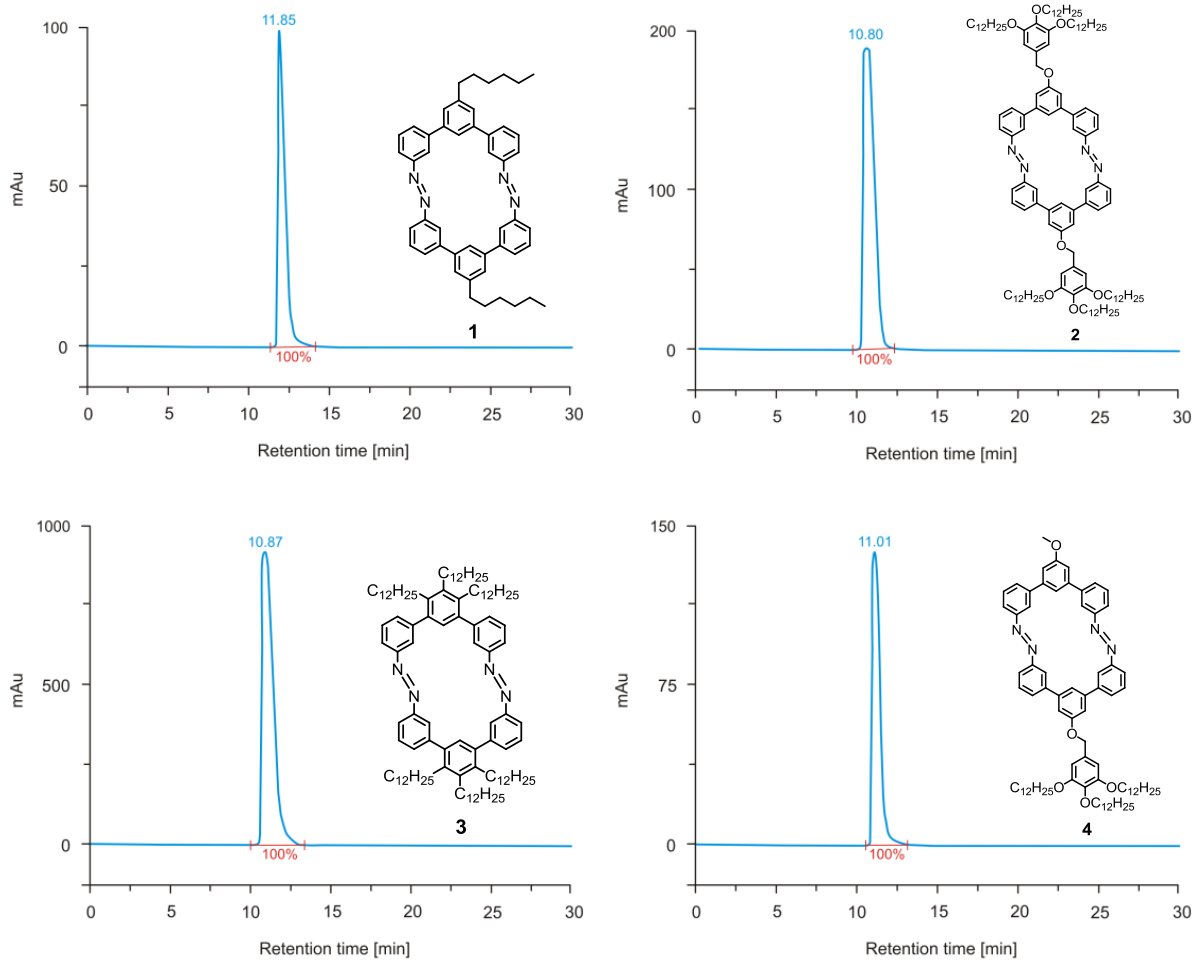

Figure 18 GPC charts of all synthesized macrocycles **1**-**4** with well defined single peaks. Analyzed in toluene with a flow rate of 0.5 mL/min at λ = 220 nm. The integrations are shown in red numbers and the retention times in blue numbers.

Fortunately, the molecular signals of the macrocycles **1** and **3** were also detected in mass spectrometry by electron impact ionization for **1** and by matrix-assisted laser desorption ionization in the case of **3** which enabled the peaks detected by analytical GPC to be calibrated. All attempts to ionize macrocycles **2** and **4** for subsequent detection by mass spectrometry failed. Neither the molecular ions nor characteristic decomposition fragments were observed. As a complementary method for determining the molecular weights of macrocycles **1**-**4** vapor pressure osmometry (VPO) was considered. Thus, the molecular weights of the macrocycles **1**-**4** were determined by VPO and are displayed in **Table 2**. The VPO apparatus was calibrated with a benzyl standard. Each pure compound was

separately dissolved in chloroform and measured at 42°C at least three times and the average value was calculated. All concentrations were higher than the critical lower concentration of about 0.005 mol/kg indicated for the VPO apparatus. Within the limits of experimental accuracy, the expected molecular weights were recorded for all macrocycles **1**-**4**, further corroborating their structures.

Table 2 Molecular weights of macrocycles **1**-**4** measured by vapor pressure osmometry. All measurements were performed in $CHCl_3$ at 42°C.

macrocycle	measured molecular weight [g/mol]	calculated molecular weight [g/mol]	concentration [mg/g]	standard deviation[a]
1	709.1	680.4	3.93	0.06
2	1739.7	1830.8	5.22	0.05
3	1500.7	1522.5	4.69	0.07
4	1174.4	1201.7	1.44	0.09

[a] Standard deviation of the measured samples derived from at least three independent measurements.

Further proof for the successful assembly of these azo macrocycles **1**-**4** was given by the obtained crystal structure of macrocycle **1**. As mentioned above thanks to a different purification method it was possible to get the compound suitable for crystal growing. The pure compound was dissolved in chloroform and placed in a crystallization tube and the crystals were grown by slowly evaporating chloroform at ambient conditions. In **Figure 19** there are two pictures of the obtained crystals. Picture **A** represents the crystal growth at ambient light and picture **B** represents the crystal growth under permanent irradiation of UV light (366 nm). With the irradiation of UV light we would like to obtain crystals suitable for X-ray scattering in the thermodynamically less favored *cis* conformation. The significant optical difference of the crystals could arise from a different crystallization pattern, such as crystal growth in *cis* form.

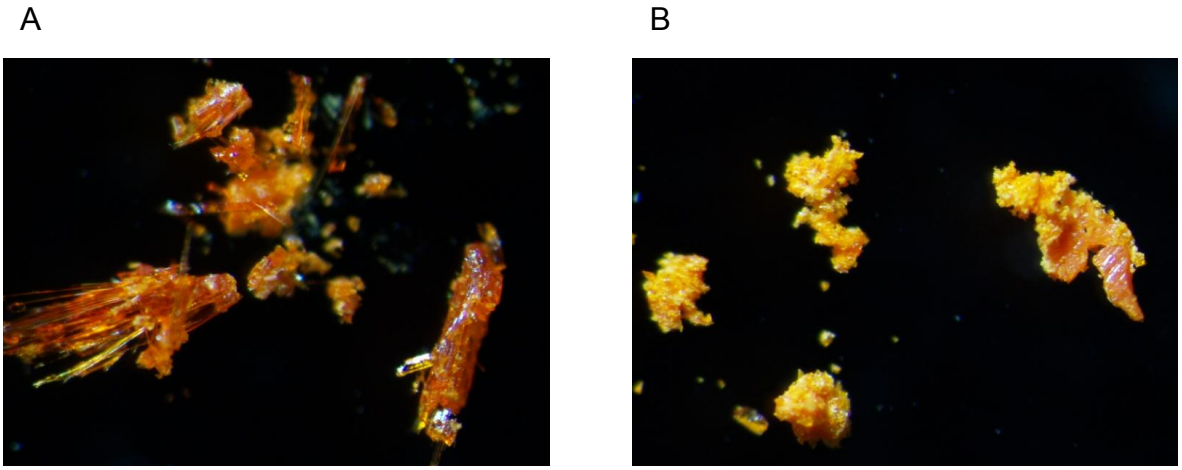

Figure 19 Macroscopic picture of the obtained crystals. (A) Crystals were grown in chloroform at ambient conditions under visible light. (B) Crystals were grown in chloroform at ambient conditions exclusively under UV light (366 nm) during the whole crystallization process.

To further prove this hypothesis, solid state structures from both crystals were measured by X-ray scattering (**Figure 20**). In crystal structure **A** (visible light) we obtained in principle a flat and shape persistent macrocycle but with a marginal tilt of the middle ring of the *m*-terphenyl subunit. Interestingly these middle rings are mirror inverted to each other, the one hydrogen of the middle ring points down and the opposite one points up, allowing a denser packing of the crystals. Regrettably it was not possible to get a proper X-ray structure of the grained part of the second crystals (366 nm). Only the flat and plane part of the crystal was suitable for X-ray scattering. Since the photo isomerization process is an equilibration-process, and the photo stationary state of macrocycle **1** consists of all-*cis* isomers (85%) and all-*trans* isomers (15%), it was most likely that only the all-*trans* isomer formed nice crystals, suitable for X-ray analysis. The major part of the crystal, which would probably be the interesting all-*cis* isomer, was too grained and not suitable for X-ray investigations. **Figure 20B** therefore shows an almost identical crystal structure, with the only difference being in the alignment of the middle phenyl ring of the *m*-terphenyl subunit. The middle phenyl ring is mirrored but no longer inverted. This phenomenon probably does not have its origin in the irradiation of UV light (366 nm) during the crystallization process, it is probably more the different possibilities in the crystallization process.

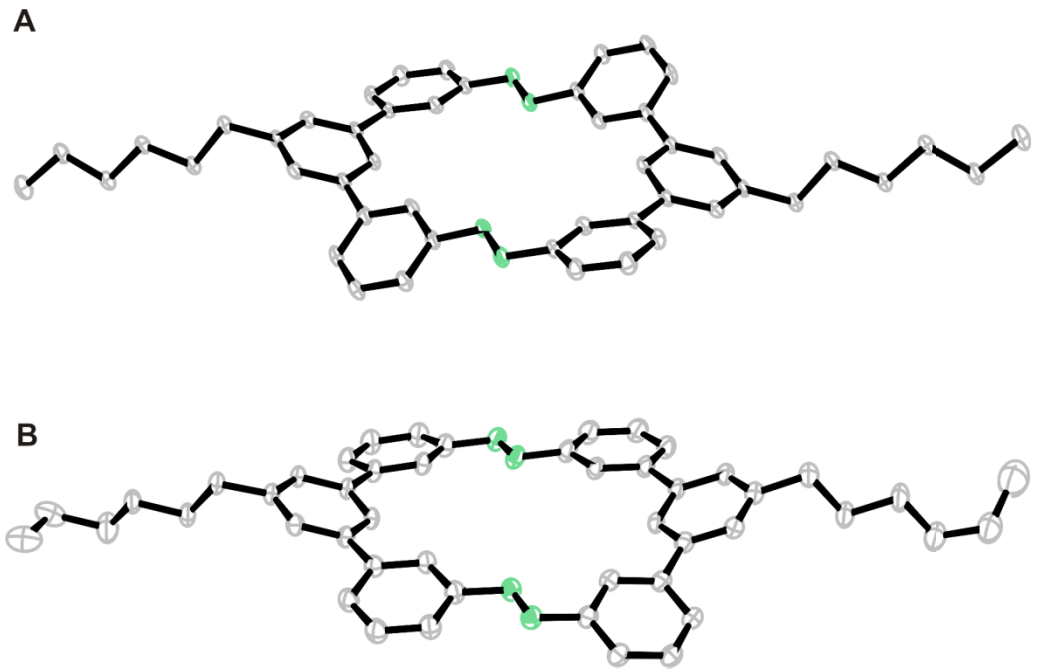

Figure 20 Solid state structure of azo macrocycle **1**. The structure is persistent, aligned flat and the middle phenyl ring of the *m*-terphenyl semicircle is slightly twisted. Figure A represents the crystal obtained by ambient light. The middle phenyl rings are mirror inverted to each other. In contrast figure B shows the crystal structure, obtained from the sample grown when irradiating with UV light (366 nm). The only difference is the middle phenyl ring which is mirrored but no longer inverted.

The chemical structures of all four macrocycles **1**-**4** were fully confirmed by the analytical investigations described above. Additional supporting evidence was obtained from their UV/Vis and IR spectra. For example, the UV absorbance in the region of 320 nm and the visible band at about 450 nm, responsible for the bright orange color of the compounds, are characteristic features of the azo derivatives.[47][48] The cyclization reaction was further monitored by comparison of the IR spectra of the macrocycles **1**-**4** and their precursors. The disappearance of the characteristic aromatic nitro band in the region of 1520 cm^{-1} together with the appearance of the signals at 1450 and 1240 cm^{-1}, which were assigned to an azo subunit, further document the transformation of the nitro groups of the semicircles into the azo groups of the macrocycles. Furthermore, even linear oligomers could be excluded by IR spectroscopy, as neither signals expected for aromatic nitro functions (1660-1440 cm^{-1}) nor those expected for aromatic amines (3500-3300 cm^{-1}) were observed. [214]

2.1.5 Photochemical Switching Investigations, UV/Vis Measurements

In this section the photochemical behavior of the macrocycles **1**-**4** will be discussed in detail. Furthermore, the stability of the thermodynamically less favored *cis* isomers will be analyzed as well as their switching behavior. All four macrocycles **1**-**4** showed absorption bands at about 450 nm as well as at about 320 nm and 285 nm. In particular, the high energy bands were attributed to π → π* transition and the broad low energy absorption was attributed to n → π* transitions.[76][77]

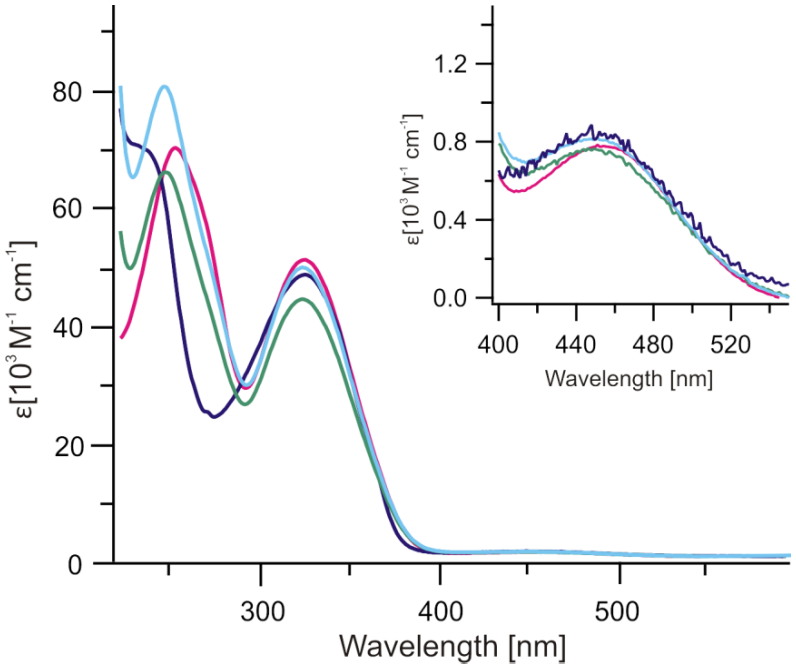

Figure 21 Absorption spectra of the macrocycles **1**-**4** in 1.7 × 10^{-5} molar THF solution. Marcrocycle **1**: red line. Macrocycle **2**: light blue line. Macrocycle **3**: dark blue line. Macrocycle **4**: green line.

All the macrocycles **1**-**4** displayed similar spectra that differ mainly in the UV region, that is, at about 250 nm (**Figure 21**). This has been attributed to the different substituents on the central ring of the *m*-terphenyl subunit, which cause a twisting of the phenylene units resulting in electronic decoupling of the aromatic moieties. Thus, a blueshift of this band was observed for the sterically more

hindered compound **2** and **3**. Emission was not detected for any of these macrocycles, neither at room temperature nor at 77 K.

Upon exposure to UV light, considerable changes in the UV/Vis spectra were observed, as expected for azo derivatives.[48] Photoisomerization reactions were investigated for all compounds **1**-**4** in THF by observing the changes in their absorption spectra.

In order to investigate the *trans* → *cis* isomerization mechanism, all the macrocycles **1**-**4** were irradiated at 313 nm. For the irradiation a 200 W mercury lamp with a dichromic filter (280-400 nm) and a 320 nm band-pass filter to select only the peak at 313 nm were used. All four macrocycles **1**-**4** displayed very similar spectral changes. As a typical example, the behavior of macrocycle **1** in THF at a concentration of 1.7×10^{-5} mol/L is shown in **Figure 22**.

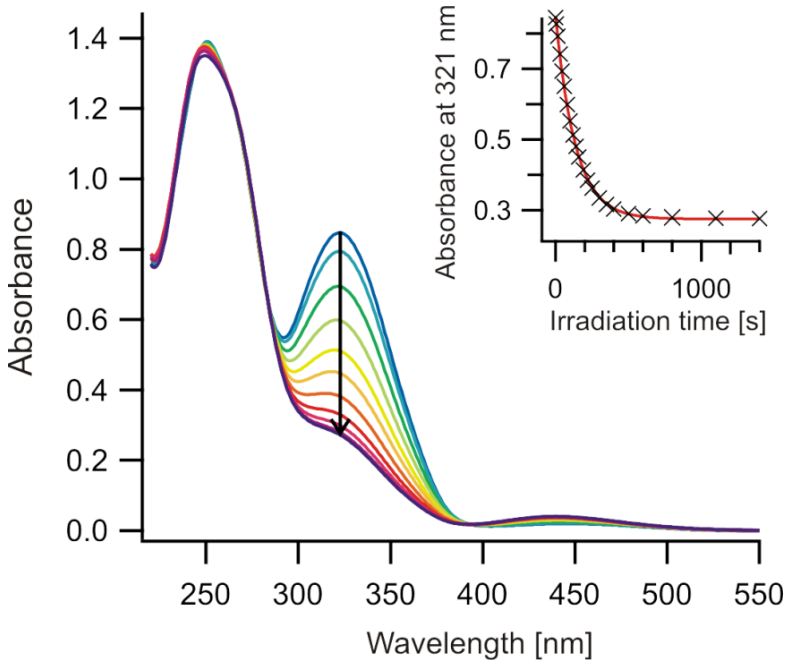

Figure 22 Changes in the absorption spectra of macrocycle **1** in THF upon irradiation at 313 nm. Inset: absorbance change versus irradiation time.

The decrease in the absorbance of the π → π* band and the increase in the n → π* absorbance upon irradiation over time was attributed to the formation of the *cis* isomer. The photoisomerization reaction presented two isosbestic points at

285 nm and 395 nm and reached the photostationary state within 8 min of irradiation under the experimental conditions applied.

The inset in **Figure 22** displays the absorbance at 321 nm plotted against the irradiation time. The evaluation of the 321 nm signal (see inset) followed an exponential trend. This suggests a switching dynamic for the pair of azo chromophores in the macrocycle **1**, which should involve, at least within the temporal resolution of the optical investigation, the switching of both azo groups.

The photoisomerization reaction at 313 nm was monitored by ^{1}H-NMR spectroscopy in order to determine the ratio of *cis* and *trans* isomers and to calculate the molar extinction coefficient (ε) of the *cis* isomer. The isomerization was performed in a deuterated THF solution, and measurements were taken at different irradiation times. The ^{1}H-NMR spectra and the corresponding UV/Vis absorption of macrocycle **1** are displayed in **Figure 23**. Since the other compounds **2**-**4** behave similarly, their results are summarized in **Table 3**.

Table 3 Quantum yields (Φ) of photoisomerization and molar extinction (ε) coefficients at 321 nm of macrocycles **1**-**4**.

macrocycle	$\Phi_{trans\text{-}cis}$	$\Phi_{cis\text{-}trans}$	ε_{trans} [dm^3/mol cm]	ε_{cis} [dm^3/mol cm]
1	0.29	0.43	50’800	7100
2	0.33	0.56	49’300	15’900
3	0.28	0.45	48’300	8600
4	0.26	0.51	44’000	14’500

The *cis* isomers displayed signals in the ^{1}H-NMR spectra at different chemical shifts to those of the *trans* isomers. Both the UV/Vis and ^{1}H-NMR spectra were used to calculate the concentration of the *cis* isomer formed. On the timescale of the ^{1}H-NMR measurements no detectable thermal back isomerization was observed, as shown by measuring the absorbance spectra before and after the ^{1}H-NMR experiment.

By integration of the corresponding ^{1}H-NMR signals, the amount of *trans* isomer in the photostationary sate at 313 nm was determined to be 15%. Furthermore, the ε values of the *cis* isomers of the macrocycles **1**-**4** were determined and are listed in **Table 3**. By using the acquired data, the photoisomerization quantum yields (Φ) for the *trans* → *cis* reactions were calculated (see **Table 3** according to the procedure reported by Zimmermann et al.[215]

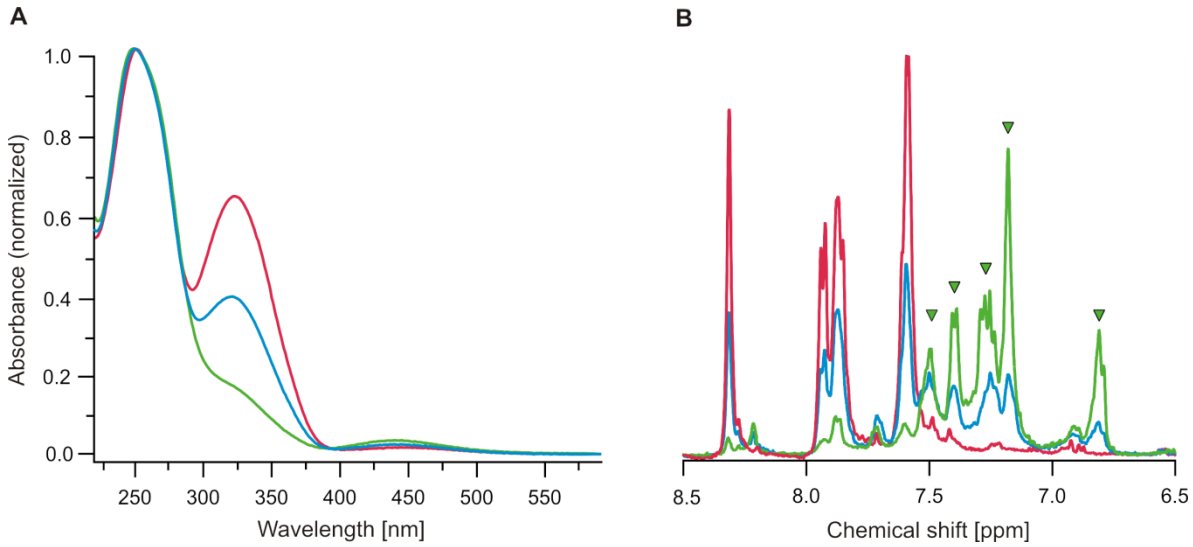

Figure 23 (A) UV/Vis spectra of macrocycle **1** of the corresponding cis/trans ratio (Red: thermally stable state. Blue: 50% isomerized. Green: photostationary state at 313 nm). (B) Corresponding HH-NMR spectra. Markers (▾) indicate the peaks corresponding to the *cis* isomer.

The ε values differed considerably for the different macrocycles **1**-**4** and were slightly higher than those found in comparable systems.[182] However, the calculated quantum yields (Φ) were comparable considering that both azo moieties underwent photoisomerization. Despite the fact that the two azobenzene groups are linked together, the formation of an intermediate *trans*/*cis* isomer upon irradiation with UV light was not observed. The UV/Vis and ^{1}H-NMR spectra gave no evidence of a *trans*/*cis* intermediate, as all spectra can be expressed as the sum of the absorbance of the *cis* and *trans* isomers. The macrocycles are extremely rigid, and therefore a small motion of half of the macrocycle forces the other half to switch accordingly. This explains the absence of *trans,cis*

intermediates, which have been observed in comparable, but less rigid azo systems.[76][182]

The *cis* → *trans* back isomerization was either triggered by light or was observed as a thermal back reaction. For the light induced back reaction, the sample was irradiated at the maximum of the peak of the *cis* isomer at 450 nm. To monitor the thermal back reaction with time, the sample was kept in the dark until the azo macrocycle **1** had switched back to its thermodynamically more stable *trans* form. The dynamics of the thermal back reaction were investigated by monitoring the increasing absorbance at 321 nm (**Figure 24**).

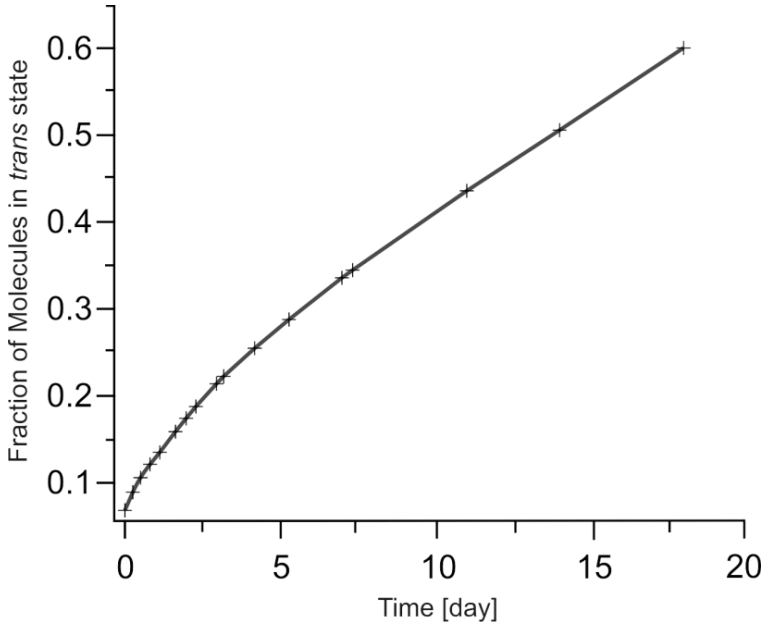

Figure 24 Thermal back reaction in the dark *cis* → *trans* of macrocycle **1** monitored over time.

The thermal back isomerization turned out to be a very slow reaction, which indicates a very stable *cis* isomer. The re-equilibration of the *cis*-enriched solution back to a solution comprising exclusively the thermodynamically favored *trans* form took almost three weeks. The rate constant for the thermal back isomerization was 1.15×10^{-6} s^{-1}, which is of a magnitude comparable to those of similar systems with multiple azobenzene moieties.[77]

To obtain a faster *cis* → *trans* isomerization and to monitor the reversibility of the photoisomerization reaction, the n → π* band at 450 nm was irradiated by using a xenon lamp and an appropriate set of filters (water filter and 450 nm BP). After the thermal back reaction, the macrocycle **1** was completely switched back to the *trans* isomer, whereas in the photochemical back reaction in the photostationary state 15% of the macrocycle still remained in its *cis* form. To gain information on the stability and fatigue resistance of the system, macrocycle **1** was cycled five times. Reversible switching between the two photostationary states was observed and is shown in **Figure 25**. The data were obtained by irradiating the macrocycle **1** at 313 nm for the *trans* → *cis* isomerization and at 450 nm for the *cis* → *trans* conversion. The data for macrocycle **1** is representative for all the target compounds **1**-**4**, since they have very comparable spectra. Even the analogousness to the sulfur functionalized azo macrocycles **5**-**7** is substantial (see section 2.2.5).

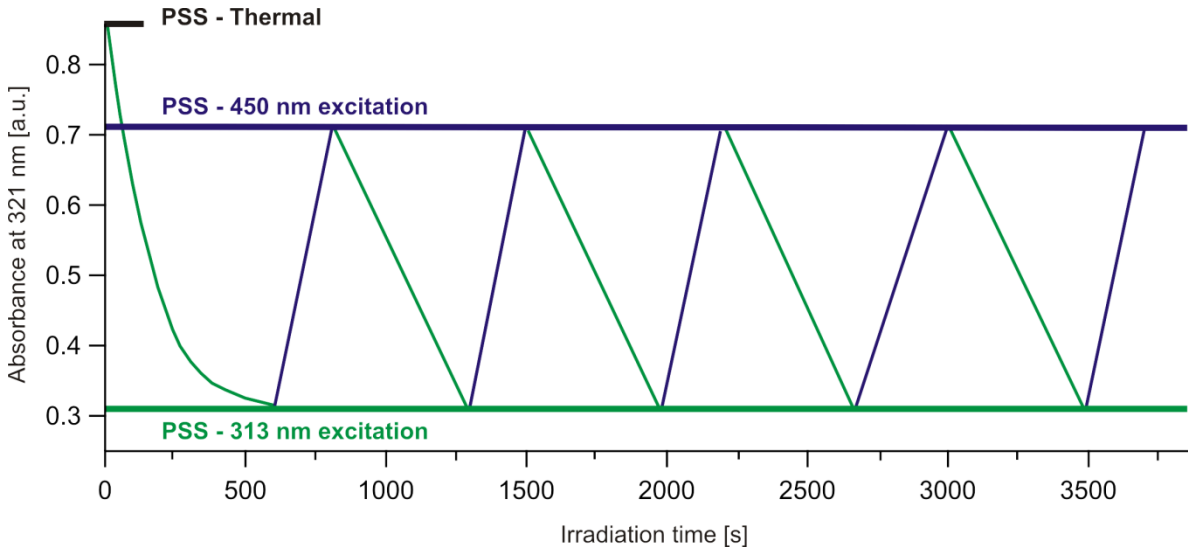

Figure 25 Photoinduced back reaction of macrocycle **1**, alternating irradiation with UV light (313 nm) and blue light (450 nm) to switch between the two photostationary states (PSS).

2.1.6 Conclusion and Outlook

Four shape switchable macrocycles **1**-**4** consisting of *m*-terphenyl semicircles interlinked by two azo joints have been synthesized and characterized. All four macrocycles were obtained by reductive dimerization of the corresponding dinitro semicircles. Although a synthetic strategy for asymmetric azo coupling (Mills reaction) is known it was not possible to synthesize and isolate the corresponding dinitroso semicircle which is essential for the Mills reaction. Hence, the asymmetric macrocycle **4** had to be synthesized trough a statistical dimerization. Considering the polymerization potential of the synthetic strategy, all four azo macrocycles **1**-**4** were isolated in surprisingly good yields, ranging from 34% for **2**, to 44% and 49% for **4** and **3**, respectively, up to 50% for macrocycle **1**. These macrocycles were characterized by ^{1}H and ^{13}C-NMR spectra, profiting from the more sensitive ^{1}H-dedected HMBC and HMQC techniques in the case of macrocycle **2** and **3**. Although the purity of **1**-**4** was shown by analytical GPC, the determination of their molecular weights turned out to be more troublesome in the case of **2** and **4**, but finally the molecular weights were determined by VPO. Mass spectra were also obtained for macrocycle **1** and **3**.

All four macrocycles **1**-**4** displayed comparable absorbance spectra, and showed almost similar *trans* → *cis* photoisomerization upon irradiation at 313 nm. A *trans*/*cis* ratio of 15:85 of the isomers was determined in their photostationary states. The full thermal back reaction required several weeks. Hence, the thermodynamically less favored *cis* isomer showed substantial stabilization by the rigid macrocyclic structure. Despite having two azo groups in the macrocyclic periphery, an intermediate mixed *trans*/*cis* isomer was not observed, the stiff *m*-terphenyl semicircles probably disfavor a strained mixed state.

These shape switchable macrocycles **1**-**4** were designed to investigate their spatial transformations by scanning probe methods. At the moment scanning probe investigations are ongoing.

2.2 Sulfur Functionalized Azo Macrocycles

In this section the further improved azo macrocycles **5**-**7** will be discussed (**Figure 26**). These macrocycles comprise a sulfur anchor group in contrast to the previously discussed alkyl functionalized azo macrocycles **1**-**4**.

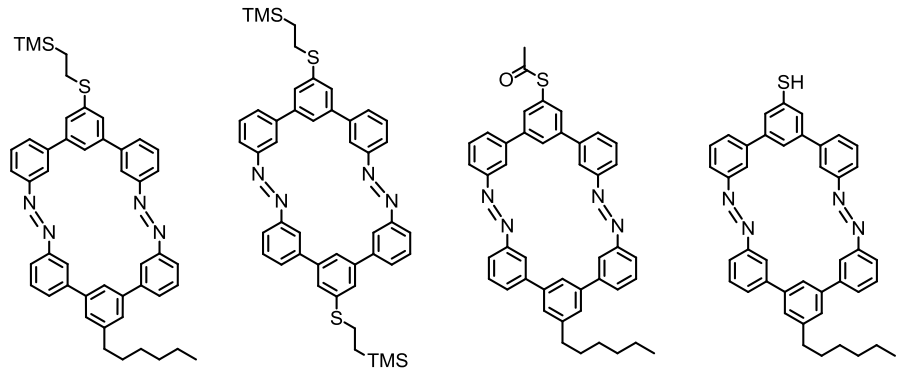

5 **6** **7** **37**

Figure 26 Overview of shape switchable azo macrocycles **5**-**7** (protected) and **37** (deprotected). Macrocycles **5**-**7** are functionalized with sulfur anchor groups, for a covalent linking to a gold surface.

2.2.1 Design of Sulfur Functionalized Azo Macrocycles

The problem of the immobilization of the alkyl functionalized azo macrocycles **1**-**4** on graphite necessitated the design of slightly modified compounds. A possibility to overcome this problem is a more stable covalent linking of the azo macrocycles with the surface. This could be facilitated by using sulfur, which forms a stable covalent bond to gold.[17][208][216] We therefore provided azo macrocycles with an sulfur anchor group at the end. For surface functionalization the compound need to bare a suitable protecting group which is easy to cleave in situ. Previous studies showed that acetyl protected sulfur are suitable protecting group for immobilization on gold.[217][218]

Recently, it has been shown that a properly designed azobenzene molecule can undergo *cis* → *trans* photoisomerization in large domains at surfaces. This switch, which occurs in densely packed single component SAMs without perturbing the molecular lattice, is complete over hundreds of molecules, and it exhibits a cooperative character.[208]

The sulfur functionalized macrocycles **5**-**7**, similar to those described above in section 2.1, should combine the properties of a stable thermodynamically less favored *cis* isomer and a sulfur anchor group for a covalently linking to a gold surface. The macrocycle present in its thermodynamically more stable *trans* form is supposed to stand upright on the surface covalently linked trough a gold – sulfur bond, as shown in **Figure 27** (left). After light induced switching to its *cis* form the macrocycle is bent at the azo joint and has a ducked conformation (right).

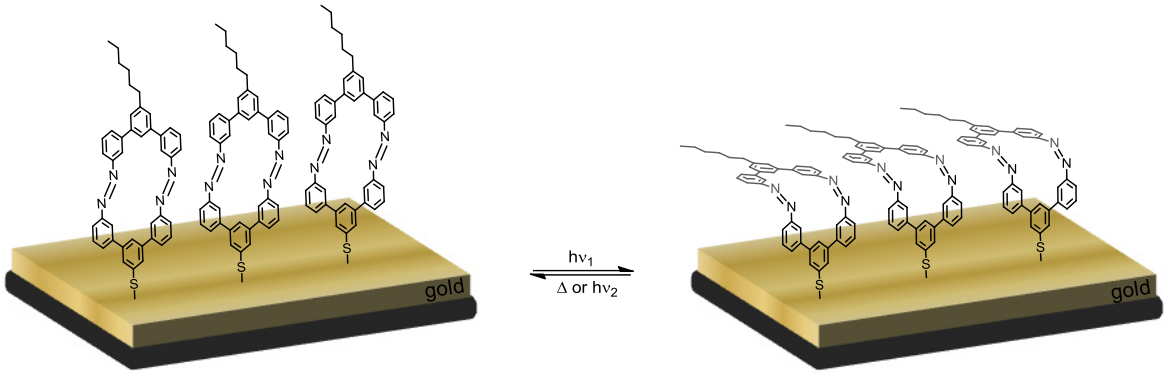

trans form of immobilized sulfur functionalized macrocycle **37**

cis form of immobilized sulfur functionalized macrocycle **37**

Figure 27 Expected self assembly of the sulfur functionalized azo macrocycles **5**-**7** on a gold surface. After photoisomerization to its *cis* form, the macrocycle should bend at the azo joints and be considerably lower than in its *trans* form.

Intermolecular interactions between adjacent molecules should stabilize the packing of domains consisting exclusively of *trans* isomers, as well as the packing of domains consisting exclusively of *cis* isomers. These interesting surface packing features are expected to be detectable by scanning tunneling microscopy (STM).

The requirements for the chemical design of the macrocyclic core are in fact the same as for the designed macrocycles **1**-**4**. For the described packing features on a gold surface an asymmetric macrocycle like compound **7** seems to be the best solution, but a symmetric macrocycle **6** could have similar packing features with an increased change of immobilization to the surface, therefore the symmetric macrocycle **6** was envisaged as well. For an optimal balance between efficient photochemical isomerization properties and a large difference in the exterior form, a subtle compromise between rigidity and flexibility of the subunits must be found.

In order to gain the required rigidity for an optimal and complete switching behavior, as well as to retain the observed stabilization of the thermodynamically less favored *cis* isomer, rigid *m*-terphenyl units have been chosen as semicircles. In contrast to the previously synthesized macrocycles **1**-**4**, the long alkyl chains were substituted with a suitable anchor group for gold, namely sulfur.

2.2.2 Retro Synthesis of Sulfur Functionalized Azo Macrocycles

The synthetic strategy of the sulfur functionalized azo macrocycles **5**-**7** is similar to the one described above in section 2.1.2. All target structures **5**-**7** are macrocycles consisting of two *m*-terphenyl semicircle subunits and two azo groups on opposite sides. Based on the macrocyclization via a statistical dimerization the target structures **5** and **6** can be obtained through one synthetic strategy (**Scheme 20**), target structure **7** results after trans-protection of compound **5**.

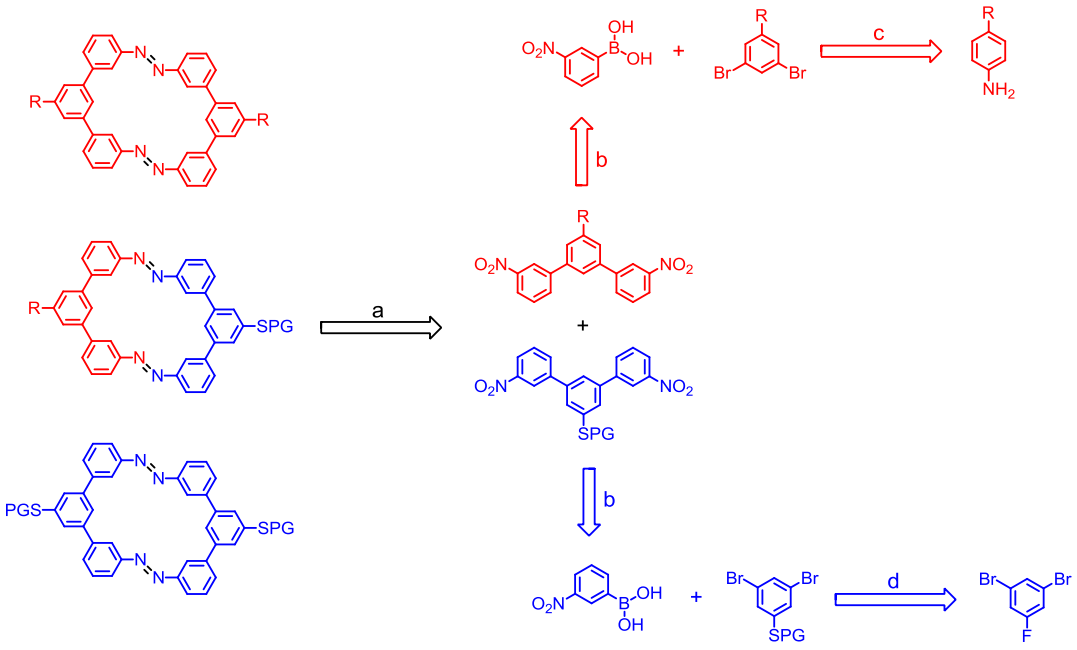

Scheme 20 Retrosynthetic scheme for the synthesis of sulfur functionalized macrocycle **5**-**7**. (a) Statistical reductive dimerization. (b) Suzuki cross-coupling reaction. (c) Bromination and deamination. (d) Nucleophilic insertion of sulfur, employing protecting group chemistry.

According to the previously discussed macrocycles the same key step, the formation of the azo functionality together with macrocyclization is required. Since the formation of a nitroso semicircle as key intermediate for an asymmetric Mills reaction could not be obtained (see section 2.1.3), again the same reductive dimerization, has been envisaged.[180] Owing to the synthetic availability of the precursors a reductive coupling between two nitro functionalized *m*-terphenyl semicircles was favored for the ring-closing reaction.

The hexyl functionalized semicircle was used in the synthesis of macrocycle **1**. For the second subunit, the sulfur functionalized semicircle, a Suzuki cross-coupling reaction was employed. Protected 3,5-dibromobenzenethiol as starting material for the Suzuki reaction will provide a sulfur group on the middle phenyl of the *m*-terphenyl semicircle after deprotection, which would enable its further linking to a gold surface. The sulfur can be inserted to 1,3-dibromo-5-fluorobenzene through an aromatic nucleophilic substitution reaction, followed by several trans-protection steps. The sulfur protecting group has several requirements: first it needs to be stable under basic Suzuki conditions, second it should be easy to cleave at the end of the reaction sequence and third it has to be suitable (polar enough or bulky enough) for a chromatographic separation due to the expected statistical mixture in the final macrocyclization step.

2.2.3 Synthesis and Characterization of Sulfur Functionalized Azo Macrocycles

In a first step the second nitro functionalized semicircle **43** with a protected sulfur anchor group on the middle phenyl ring of the *m*-terphenyl subunit was synthesized. The synthetic route to this target intermediate is shown in **Scheme 21**.

This sulfur functionalized semicircle **43** is needed for the second part of the macrocycle. With the sulfur functionalized semicircle **43** in hand all the different combination with the previously synthesized hexyl functionalized semicircle **11** are possible to form asymmetric macrocycles.

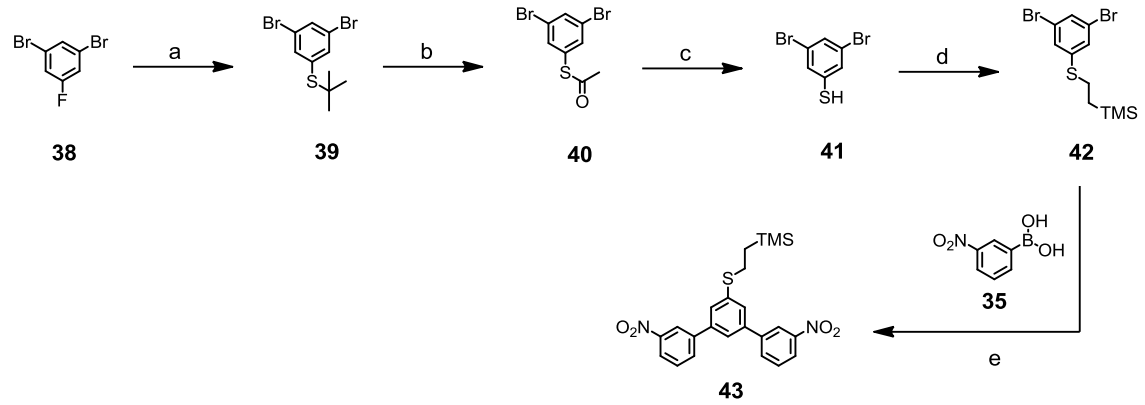

Scheme 21 Synthetic route to the sulfur functionalized key intermediate semicircle **43**. Reagents and conditions. (a) NaS-*tert*-butyl, DMF, RT, 2.5 h, 97%. (b) BBr_3, AcCl, $C_6H_5CH_3$, CH_2Cl_2, RT, 2 h, 87%. (c) AcCl, MeOH, CH_2Cl_2, 0°C → RT, 5 h, 100%. (d) CH_2CH-TMS, di-*tert*-butyl peroxide, neat, 65°C, 1.5 h, 91%. (e) $[Pd(PPh_3)_4]$, K_2CO_3, $C_6H_5CH_3$, EtOH, 85°C, 20 h, 47% or $[Pd(PPh_3)_4]$, K_2CO_3, $C_6H_5CH_3$, EtOH, 120°C, 10 min in MW, 93%.

The sulfur functionalized dibromo intermediate **41** was obtained from commercially available 1,3-dibromo-5-fluorobenzene (**38**). Treatment of 1,3-dibromo-5-fluoro-benzene (**38**) with sodium 2-methyl-2-propanethiolate in *N,N*-dimethylformamide (DMF) for 2.5 hours inserted the sulfur functionality at the desired 5-position of compound **39**, in 97% yield.[219] Thanks to the stable *tert*-butyl protection group on the sulfur, the insertion of the sulfur through an aromatic nucleophilic substitution

was easy and worked in excellent yield. But because of its stability the *tert*-butyl protection group had to be replaced to a protecting group which is easy to cleave at the end of the reaction sequence and was suitable for the Suzuki cross coupling reaction. The obtained *tert*-butyl protected compound **39** was successfully trans-protected to compound **40** with an acetyl protecting group, in a yield of 87%. An in situ deprotection and reprotection procedure was chosen to avoid disulfide formation.[220][221] Since an acetyl protection group is not stable under basic condition it was not suitable for the following Suzuki reaction and another trans-protection step was done. The acetyl protecting group of **40** was deprotected to the free thiole **41** by hydrochloric acid which was generated in situ with methanol and acetyl chloride in dichloromethane.[222] The big advantage of this method was the easy purification, by simply evaporating the solvent with all reagents and byproducts. A careful handling under an inert argon atmosphere was necessary to avoid disulfide formation; even so it was not possible to get an elemental analysis of the free thiole **41**. Therefore the subsequent protection with vinyltrimetylsilane to the ethane-TMS protected compound **42** was also delicate. Applying the literature known procedure[223] for this type of thiole protection yielded in just 33% of the desired product **41** but in over 40% of the unwanted disulfide. However, with slightly modified conditions, by replacing the toluene with an excess of vinyltrimetylsilane the ethyl-TMS protected dibromo compound **42** was obtained after 1.5 hours at 65°C without any solvent in a good yield of 91%.

With the ethyl-TMS protected dibromo compound **42** in hand the Suzuki cross coupling reaction was performed, applying a solvent mixture of toluene and ethanol compare to the reported standard conditions.[191] Treatment of 2.6 equivalents of the commercially available 3-nitrophenyl-boronic acid (**35**) and the dibromo compound **42** with 8 mol-% of tetrakis(triphenylphosphine)palladium [$Pd(PPh_3)_4$] in a solvent mixture of toluene:ethanol (3:1) at 85°C for 20 hours in an inert atmosphere provided the desired semicircle **43** as a light yellow solid in just 47% after column chromatography. As byproduct the mono coupled product was isolated in a yield of 41%, this fact explained the relatively low yield. Since, neither increased amounts of boronic acid, nor higher temperature and longer reaction times resulted in significantly better yields an alternative needed to be found. The

same reaction with the same palladium catalyst could be performed in the microwave in an inert atmosphere at 120°C for 10 minutes. The yield of the Suzuki reaction significantly increased to an excellent 93%. The difference between conventional and microwave conditions for Suzuki reactions is discussed in section 2.2.3.2. Overall, the target semicircle **43** was synthesized in a good yield of 71% over five steps.

With the semicircle **43** in hand, the symmetric sulfur functionalized azo macrocycle **6** was first assembled (**Scheme 22**). The nitro semicircle **43** was treated with lithium aluminum hydride (slow addition) in high dilution conditions (0.20 mM) in dry tetrahydrofuran at 40°C for 2 hours. The nitro compound **11** is reduced step wise to the nitroso- and amino compound, respectively; which will react immediately together and form the azo joint. Subsequent extraction with dichloromethane and time consuming purification with different chromatography steps resulted in the desired macrocycle **6**.

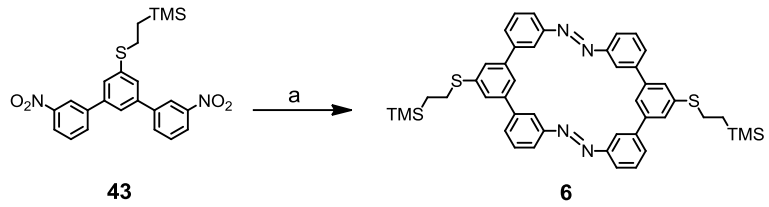

43 **6**

Scheme 22 Synthetic route to symmetric sulfur functionalized macrocycle **6**. Reagents and conditions: (a) $LiAlH_4$, THF (0.2 mM), RT → 40°C, 2 h, 5%.

The first purification step was a column chromatography with silica gel and dichloromethane, the obtained crude product was further purified by different preparative thin layer chromatography techniques, the use of *n*-hexane instead of cyclohexane and the use of 0.5 mm prep TLC plates instead of 2.0 mm prep TLC plates, respectively, turned out to be crucial for the purification. The separated bands of the chromatography were analyzed be MALDI-TOF mass spectrometry to determine the molecular weight; this purification procedure was repeated until the pure macrocyclic compound was isolated. After three purification steps

macrocycle **6** was isolated as a bright orange solid in a yield of 5%. The more difficult and time consuming purification method resulted in a significantly lower yield compared to the alkyl functionalized azo macrocycles **1**-**4**, especially the purification via three prep TLC is responsible for the loss of product. On every TLC plate a surprisingly strong start band was observed, probably due to a certain decomposition of the product on the TLC plate. The structure was analyzed by (^{1}H-NMR, HMBC, HMQC, MALDI-TOF and analytical GPC) furthermore crystals were obtained allowing the imaging of a barley resolved X-ray structure.

For the assembly of the asymmetric azo macrocycle **5**, a statistical assembly of two different dinitro semicircles **11** and **43** was envisaged (**Scheme 23**). By the statistical reductive dimerization method, macrocycles **1** and **6** were formed as byproducts as well. This less elegant method, compare to an asymmetric Mills reaction, was chosen, since it was not possible to obtain nitroso semicircles neither of the sulfur functionalized semicircle nor of the hexyl functionalized semicircle.

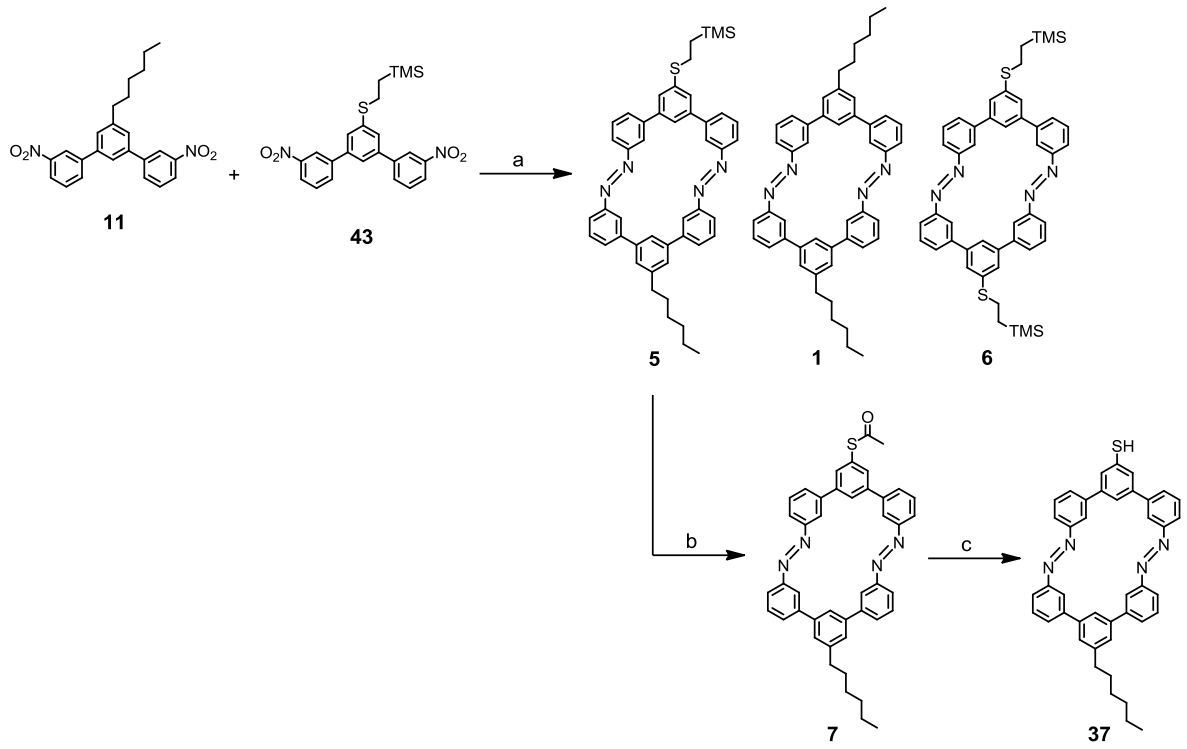

Scheme 23 Synthetic route to the asymmetric sulfur functionalized macrocycle **5**, and trans-protection to **7**. Reagents and conditions. (a) $LiAlH_4$, THF (0.16 mM), RT → 40°C, 2 h, macrocycle **5**: 6%, macrocycle **1**: 5%, macrocycle **6**: 4%. (b) 1. TBAF, THF, RT, 1 h. 2. AcCl, THF, 0°C, 1.5 h, 45%. (c) TBAOH, THF, RT, 2.5 h quant.

Thus, the two semicircles **11** and **43** were subjected to the macrocyclization conditions described above. Equimolar amounts of the two different semicircles **11** and **43** were dissolved in dry tetrahydrofuran. Drying the THF with elemental sodium and potassium was crucial for the reaction. A 1 M lithium aluminum hydride solution in THF was added slowly at room temperature. After keeping the reaction mixture at 40°C for 5 hours, it was quenched with water and extracted with dichloromethane. Owing to the statistical nature of the reaction, all possible macrocycles, namely **1**, **5** and **6** were formed (**Figure 28**). Unfortunately, the molecular weights of the three macrocycles **1**, **5** and **6** were not sufficiently different to allow their separation by size exclusion chromatography (SEC). In **Figure 28A** the analytical GPC chart of the crude reaction mixture is displayed. In the main peak at a retention time of 10.09 min all three target compounds **1**, **5** and **6** were detected by MALDI-TOF mass spectrometry. Fortunately the silica gel TLC showed three clearly separated spots (**Figure 28B**), allowing a separation by chromatography. Despite the well separated spots in the TLC (R_f = 0.49 for macrocycle **1**, R_f = 0.42 for macrocycle **2** and R_f = 0.35 for macrocycle **6**), it was not possibly to separate the compounds by column chromatography on silica gel.

However with an identical procedure as described above, the three macrocycles **1**, **5** and **6** were successfully separated by three consecutive prep TLCs, as bright orange solids in yield of 4%, 5% and 6%, respectively. The different spots of the prep TLC were first assigned with MALDI-TOF mass spectrometry and then further characterized by (^{1}H-NMR, HMBC, HMQC and analytical GPC) to fully confirm the structure.

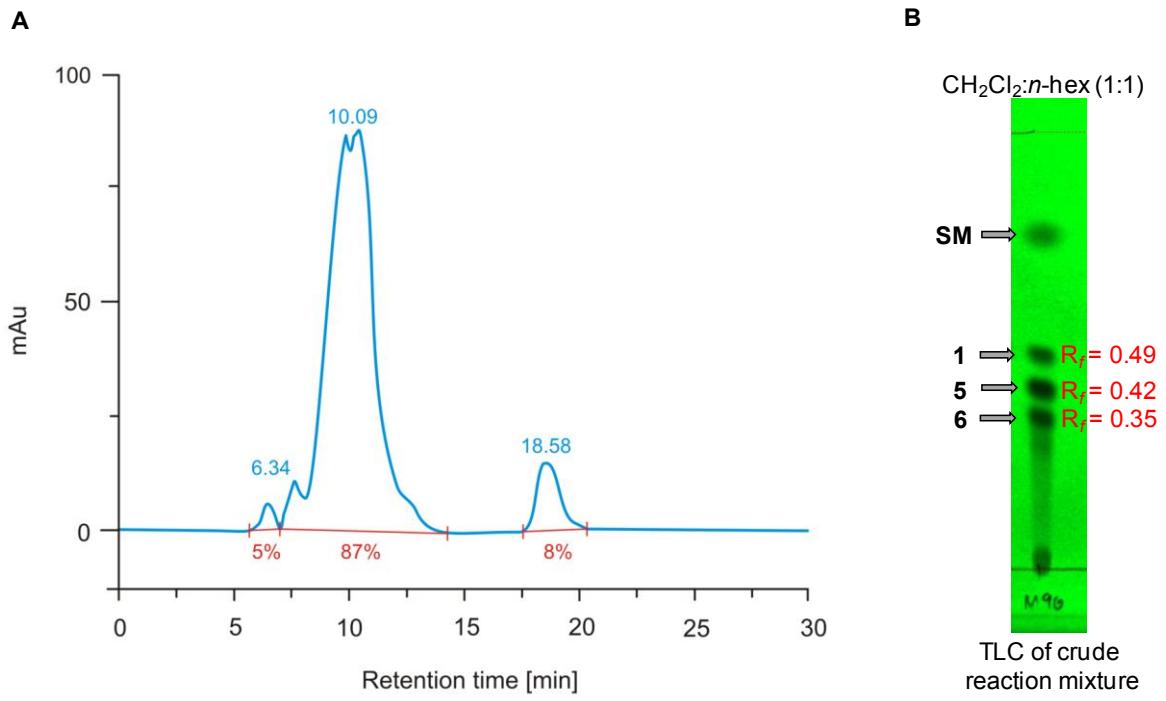

Figure 28 (A) GPC chart of the crude reaction mixture of macrocycle **1**, **5** and **6**. Measured in toluene with a flow rate of 1.0 mL/min at λ = 330 nm. Displaying all target structures in the main peak. The integrations are shown in red numbers and the retention times in blue numbers. (B) TLC of the crude reaction mixture in CH_2Cl_2:*n*-hexane (1:1), displaying well separated spots corresponding to the three formed macrocycles **1**, **5** and **6**.

To obtain the desired acetyl protected macrocycle **7** the ethyl-TMS protected macrocycle **5** was first deprotected in dry tetrahydrofuran with tetrabutylammonium fluoride at room temperature and subsequently protected with acetyl chloride at 0°C. After column chromatography on silica gel the acetyl protected macrocycle **7** was isolated as orange solid in a yield of 45%.

The necessary subsequent deprotection to the free thiol was performed with tetrabutylammonium hydroxide in tetrahydrofuran at room temperature. The reaction was monitored by TLC and showed full conversion after 2.5 hours, nevertheless the high disulfide formation tendency of this sulfur functionalized macrocycles made it impossible to isolate the free thiol **37**. However, thanks to the acetyl protecting group, acetyl protected macrocycle **7** can be deprotected in situ when immobilizing onto the gold surface.

2.2.3.1 Mechanism of Suzuki cross coupling reaction

The Suzuki reaction is a transition metal catalyzed cross coupling reaction, and is an efficient method to build up oligophenylic structures.[191][192][194][224] As it was a key reaction in the assembly of all target semicircles **11**, **16**, **32** and **43**, the mechanism including the catalytic cycle is shown in **Scheme 24** and will be briefly discussed.[24][207] The coupling takes place between an organoboronic acid and aryl halides. Recent catalyst and methods developments have broadened the possible applications enormously, so that the scope of the reaction partners is not restricted to aryls, but includes alkyls, alkenyls and alkynyls. Potassium trifluoroborates and organoboranes or boronate esters may be used in place of boronic acids. For the second coupling partner some pseudo halides (for example triflates) may also be used.

The boronic acid must be activated, for example with potassium carbonate as base, before it can undergo the transmetallation of the catalytic cycle. This activation of the boron atom enhances the polarization of the organic ligand, and facilitates the transmetallation. If starting materials are substituted with base labile functional groups, powdered potassium fluoride effects this activation while leaving base labile groups unaffected. The first step in the main catalytic cycle is an oxidative addition (**a** in **Scheme 24**). The active catalyst is a palladium(0) species **Pd1** to which the halide bearing reagent is introduced and the palladium is oxidized by +2 to **Pd2**. The oxidative addition is the rate limiting step of the reaction. In a transmetallation step (**b** in **Scheme 24**) the palladium complex **Pd3** is formed, where the second reagent is introduced to the metal. Followed by the reductive elimination (**c** in **Scheme 24**), the cross coupled product is formed and the active palladium catalyst is regenerated.

The most widely used catalysts are $[Pd(PPh_3)_4]$ and $[Pd(PPh_3)_2Cl_2]$. As base, inorganic acids are employed like, carbonates or hydroxides. There are many variables that dictate the overall efficiency of the catalytic cycle, including catalysts, inorganic base, solvent and the electronic and steric characteristics of the organic electrophile and organoboronic acid. Electron deficient organic halides are more reactive to cross coupling than electron rich. The general reactivity order of the sp^2 species is aryl iodide > aryl triflate > aryl bromide >> aryl chloride.[149][225]

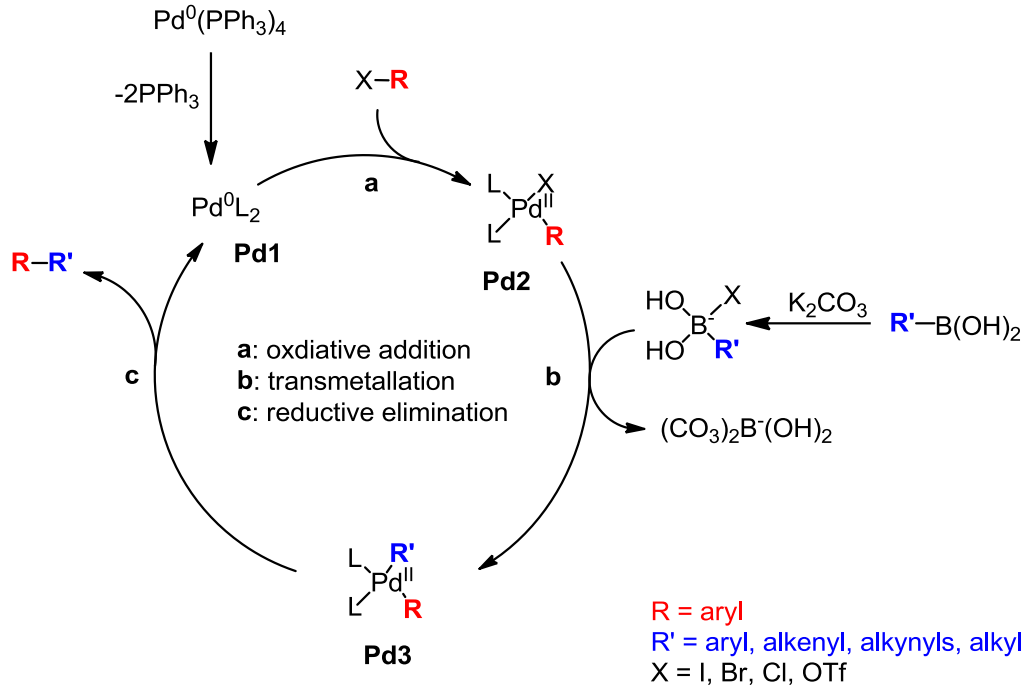

Scheme 24 Catalytic cycle of a palladium catalyzed Suzuki cross coupling reaction. (a) Oxidative addition. (b) Transmetallation. (c) Reductive elimination. R = aryl. R′ = aryl, alkenyl, alkynyls, alkyl. X = I, OTf, Br, Cl

2.2.3.2 Microwave and conventional conditions for Suzuki reaction

The Suzuki cross coupling reaction was a key step in the synthesis of all target semicircles **11**, **16**, **32** and **43**; therefore particular attention was paid to the Suzuki conditions.

The conventional Suzuki reaction conditions[194] had to be adapted to reach acceptable yields of at least 50%. This was achieved by changing the solvent to a solvent mixture of toluene and ethanol and increasing the equivalents of boronic acid. As expected the electron rich dibromides, like semicircles **16** and **43**, provided significantly lower yields then the electron poor semicircles **11** and **32** (see **Table 4**). It turned out that the second coupling was the limiting factor, as the electron density slightly increased after the first coupling. Because of the poor yield in case of **16** and **43** the reaction time was increased from 3 hours to 16 hours and 20 hours, respectively. Hence the yield could be slightly increased by about 10%. However, the same reaction under almost identical conditions with the same

palladium catalyst could be performed in the microwave in an inert atmosphere at 120°C for 10 minutes. The yield of the target semicircles **11**, **16**, **32** and **43** could be increased in all cases by applying microwave conditions. Interestingly, the difference of electron density observed before in the dibromides was no longer detected. As a nice side effect the reaction time was shortened from up to one day to 10 min. Not only that but also the catalyst loading could be reduced from 8.0 mol-% to 5.0 mol-% without effecting the overall yield at all.

Table 4 Overview of reaction conditions in conventional and microwave assisted Suzuki cross coupling reactions. All reactions were performed in a solvent mixture of toluene:ethanol, 8.0 eq. of K_2CO_3 as base, and 8.0 mol-% of $[Pd(PPh_3)_4]$ as catalyst. All yields are after at least one column chromatography and are elemental analysis pure. Always the best observed yields are presented for the particular conditions.

	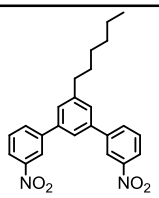 **11**	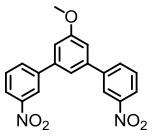 **16**	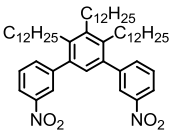 **32**	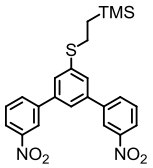 **43**
conventional conditions	3 h 85°C	16 h 85°C	2.5 h 85°C	20 h 85°C
yield	**95%**	**33%**	**85%**	**47%**[a]
microwave conditions	10 min 120°C	10 min 120°C	10 min 120°C	10 min 120 °C
yield	**98%**	**90%**[b]	**96%**[b]	**93%**[b]

[a] 41% of mono coupled product was isolated.

[b] Reaction performed with 5.0 mol-% without affecting the yield.

As a potential precursor for the Mills reaction, amino functionalized semicircles **12**, **23** and **33** (**Scheme 18**) were envisaged. The direct synthesis via the Suzuki reaction of dibromides and the corresponding 3-aminoboronic acid failed. Only the mono coupled product could be observed in moderate yields of up to 37%. It seems that the electron rich 3-aminobornonic acid lowers the reactivity too much, in particular due to the already deactivated dibromides. However, the amino

functionalized semicircles **12**, **23** and **33** were obtained in an alternative heterogeneous catalyzed route using a palladium on activated carbon catalyzed hydrogenation of the dinitro compound or by standard reduction with tin powder in concentrated hydrochloric acid (**Scheme 18**).

2.2.4 Characterization of Sulfur Functionalized Azo Macrocycles

The precursors **38**-**43** were fully characterized by ^{1}H and ^{13}C-NMR spectroscopy, mass spectrometry and elemental analysis, the characterization of the macrocycles **5**-**7** was a little more challenging and will be discussed in this section.

The ^{1}H-NMR spectra corroborated the suggested structures of all macrocycles **5**-**7**, representative for all sulfur functionalized azo macrocycles **5**-**7**, the most complex ^{1}H-NMR is shown in **Figure 29**. All peaks were assigned by HMBC, HMQC and COSY methods. The displayed ^{1}H-NMR spectrum of macrocycle **5** was recorded in deuterated chloroform at room temperature in a 500 MHz spectrometer with 256 scans. The color code shows the assignment of the protons in structure **5** to the observed ^{1}H-NMR peaks.

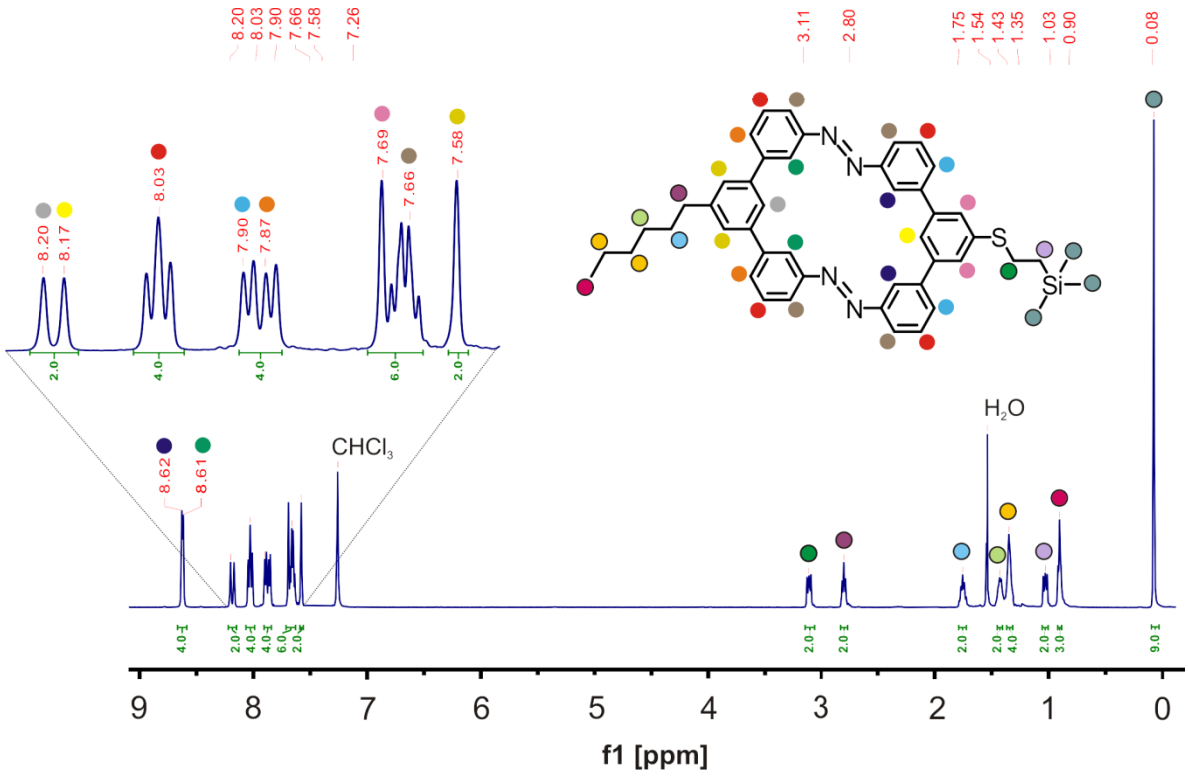

Figure 29 ^{1}H-NMR spectrum of the asymmetric macrocycle **5** in $CDCl_3$ at room temperature, recorded with 256 scans on a 500 MHz spectrometer. The signals were assigned by supporting HMBC, HMQC and COSY investigations to the different protons depicted by the color code.

One dimensional ^{13}C-NMR spectra could not be obtained. The size and the relatively high inertia of each of the sulfur functionalized macrocycle **5**-**7** cause long rotational correlation times τ. Because τ is proportional to the linewidths of the resonance in the NMR spectra, the signal-to-noise ratio for the relatively insensitive ^{13}C-NMR spectra turned out to be too small to obtain meaningful one dimensional ^{13}C{^{1}H} NMR spectra.[213] However, the more sensitive ^{1}H detected HMBC and HMQC spectra allowed full characterization of the carbon resonances of macrocycles **5**-**7**.

The same importance as full characterization of the target structures by NMR techniques is the determination of the purity and the molecular weight of each of the isolated macrocycles. Since the synthetic strategy was based on a reductive dimerization of two bifunctional building blocks allowing for the formation of larger cyclic oligomers with comparable NMR spectra. In the case of the statistical dimerization with different bifunctional semicircles **11** and **43**, even the formation of different possible macrocycles **1**, **5** and **6** was possible and needed to be differentiated. Analytical gel permeation chromatograms were recorded to document the purity of the macrocycles **1** and **5**-**7** (**Figure 30**).

All four compounds displayed well defined single peaks at λ = 220 nm with retention times R_t (**1**) = 10.85 min, R_t (**5**) = 9.04 min, R_t (**6**) = 8.04 min and R_t (**7**) = 9.95 min in the expected order of decreasing molecular weight. Owing to the particular shape and thus hydrodynamic volume of the macrocycles **1** and **5**-**4**, GPC is not suited to determining their molecular weights; there is just qualitative information about the order of these macrocycles as suitable standards for this macrocycles are unavailable. Tailing was observed for all compounds, even with further purification steps this tailing did not fully disappear and were always in the range of up to 1%. As all the other analytical data confirmed the purity of these compounds, this tailing could be an artifact of the chromatograms. However, the impurity of all synthesized macrocycles **5**-**7** was maximal 1%, the minor impurities were not further analyzed, in particular since the NMR spectra and MALDI-TOF spectra gave no evidence of impurities.

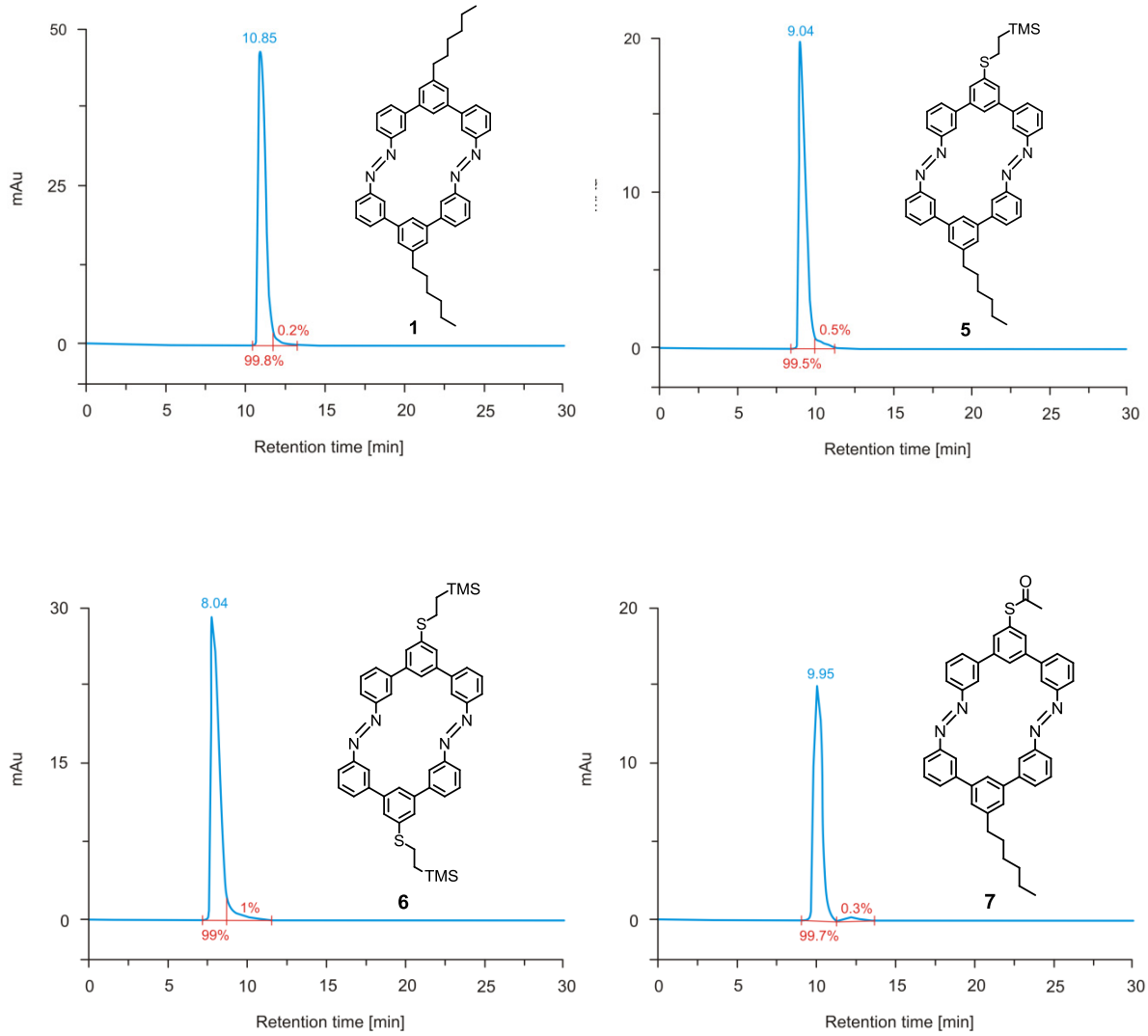

Figure 30 GPC charts of macrocycles **1** and **5**-**7**. Analyzed on an analytical GPC column in toluene with a flow rate of 1.0 mL/min at λ = 220 nm. The integrations are shown in red numbers and the retention times in blue numbers.

To fully characterize the synthesized macrocycles **5**-**7** mass spectra are essential, to exclude the formation of larger cyclic oligomers with comparable NMR spectra. In **Figure 31** the obtained MALDI-TOF mass spectra are shown with the corresponding chemical structure and the calculated exact molecular mass. The molecules **1** and **5**-**4** could not be ionized, neither by electron spray ionization (ESI) nor by electron ionization (EI) mass spectrometry methods. However, matrix assisted laser desorption ionization time of flight (MALDI-TOF) mass spectrometry was found to be suitable to measure mass spectra of this macrocyclic compounds

1 and **5**-**4**. 1,8,9-antthracentriol was used as matrix. The molecular mass of **1** was found by MALDI-TOF to be 681.3997 which fits well with 681.3957 calculated for $C_{48}H_{49}N_4$. The spectrum is nicely resolved, displayed in the zoomed in peak (inset of **Figure 31**). The calculated isotopic distribution is overlaid in red and matches very well with the isotopic distribution found with MALDI-TOF mass spectrometry.

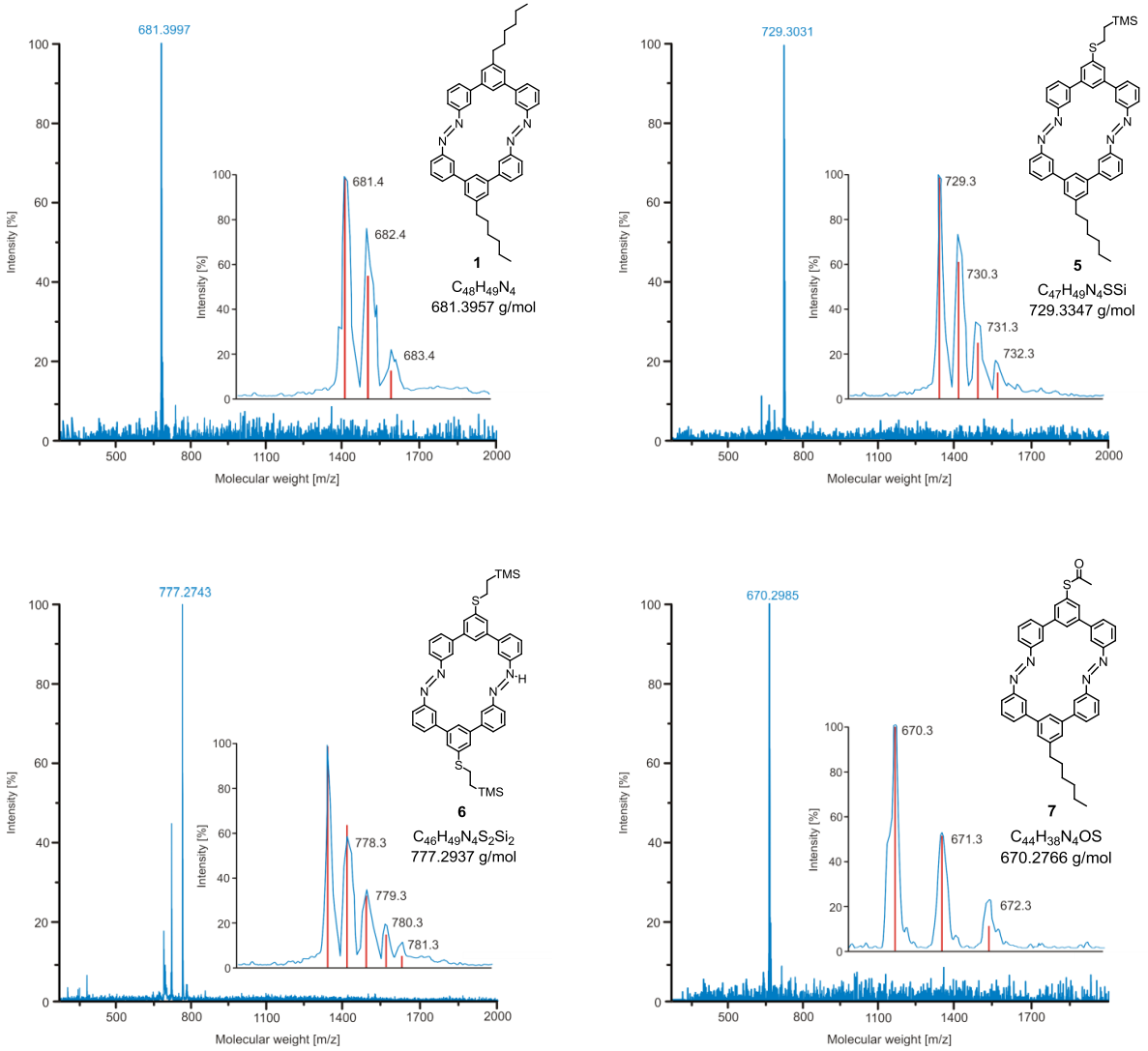

Figure 31 MALDI-TOF spectra of the synthesized azo macrocycles **1** and **5**-**7**. The corresponding chemical structure with the calculated exact mass is displayed beside the inset. The inset shows the enlarged molecular ion peak and the calculated isotopic distribution is overlaid in red.

Nearly the same accurate results were obtained for the sulfur functionalized macrocycles. The molecular mass of **5** was found by MALDI-TOF to be 729.3031

which fits well with 729.3347 calculated for $C_{47}H_{49}N_4SSi$, the measured and the calculated isotopic distribution matched nicely as well. For **6** the molecular mass was found by MALDI-TOF to be 777.2743 which matched with 777.2937 calculated for $C_{46}H_{49}N_4S_2Si_2$. And finally, the molecular mass of **7** was found by MALDI-TOF to be 670.2985 which fits well with 670.2766 calculated for $C_{44}H_{38}N_4OS$, the isotopic distribution correlated nicely as well.

As already discussed in section 2.1.4 the alkyl functionalized macrocycle **1** crystallized in chloroform and a crystal structure was obtained. The same crystallization procedure was applied to the sulfur functionalized macrocycles **5**-**7** as well. In the case of the symmetric macrocycle **6** some small crystals were obtained, allowing the visualization of the compound, but not a fully resolved X-ray structure. Due to the low resolution of the obtained X-ray picture no further detail statements on the structure can be made, but it clearly shows the desired macrocyclic structure **6** with two ethyl-TMS protected sulfur functionalities on opposite sides. The solid state structure of **6** is shown in **Figure 32** and displayed the same shape as the solid state structure of **1**. It is a flat a persistent macrocyclic structure with a marginal twist of the middle ring of the *m*-terphenyl subunit. The sulfur-ethane-TMS units are distorted and therefore the crystal structure could not be perfectly solved. However, the crystal structure shows that the molecule is macrocyclic with two azo joints on opposite sides, with a shape persistent and flat arrangement in the thermodynamically more stable *trans* conformation, as it was designed.

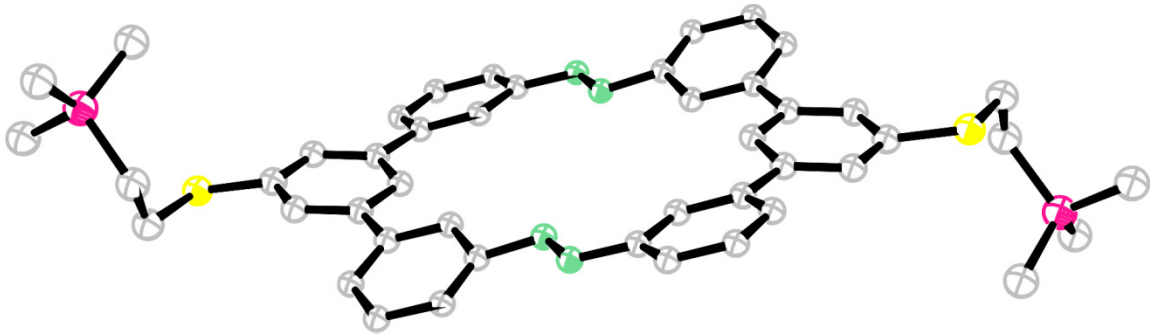

Figure 32 Solid state structure of the symmetric macrocycle **6**. The structure is flat and the phenyl rings are slightly twisted to each other.

2.2.5 Photochemical Switching Investigations, UV/Vis Measurements

In this section the photochemical behavior of the macrocycles **5**-**7** will be discussed in comparison to the already discussed macrocycle **1** (see section 2.1.5). Furthermore, the switching properties after irradiation at 313 nm and 450 nm will also be analyzed. All three macrocycles **5**-**7** showed absorption bands at about 450 nm as well as at about 320 and 285 nm and are very similar to those observed for macrocycle **1**. A comparison between these macrocycles is shown in **Figure 33**.

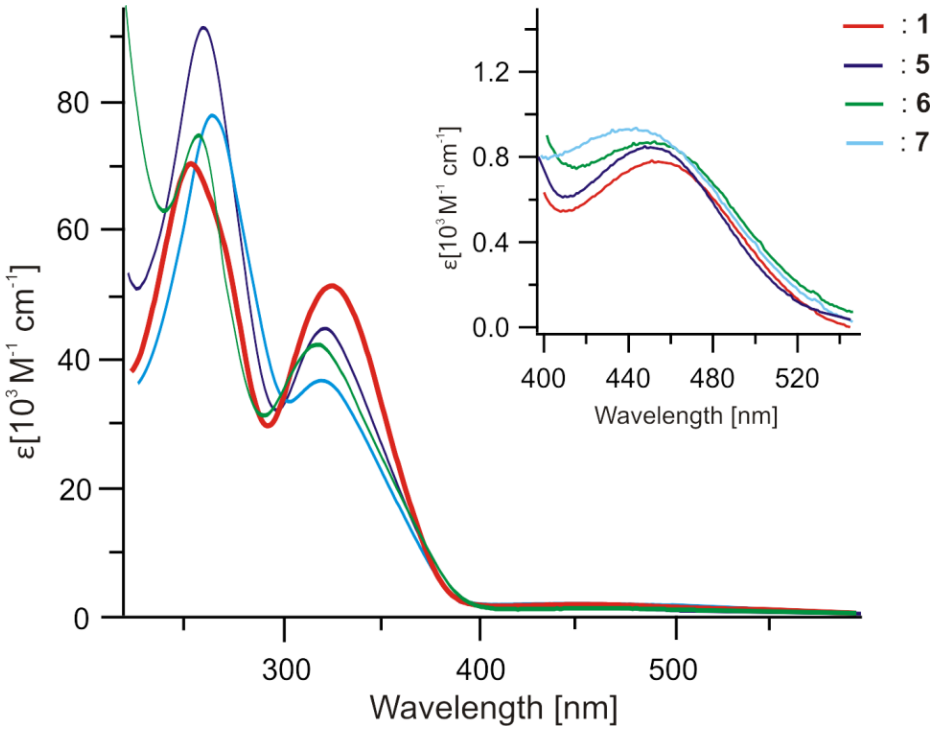

Figure 33 Absorption spectra of macrocycles **1** and **5**-**7** in 10^{-5} molar THF solution. Macrocycle **1** is marked with a bold red line. Macrocycle **5**: violet. Macrocycle **6**: green. Macrocycle **7**: blue.

In particular, the high energy bands were attributed to π → π* transition and the broad low energy absorption were attributed to n → π* transitions.[76][77] All displayed macrocycles **1** and **5**-**7** were analyzed in a 1×10^{-5} molar tetrahydrofuran solution and showed similar spectra that differ mainly in the UV region, that is, at about 250 nm. This has been attributed to the different substituents on the central ring of the *m*-terphenyl subunit. In the case of the sulfur functionalized macrocycles **5**-**7** a red shift of this band was observed compare to the alkyl functionalized macrocycles **1**-**4**, which could be caused by a less twisted structure

with even more planar phenylene units, resulting in less electron decoupling of the aromatic moieties. The intensity of the band at 320 nm is lower than in the compacter and less functionalized macrocycle **1**. Emission was not observed for any of these macrocycles **5**-**7**, identical to the macrocycles **1**-**4**.

The photoisomerization reactions were investigated for all sulfur functionalized compounds **5**-**7** in tetrahydrofuran by observing the changes in their absorption spectra.

To investigate the *trans* → *cis* isomerization mechanism, the macrocycles **5**-**7** were irradiated at 313 nm. The experimental setup was the same as used for macrocycle **1**-**4** in section 2.1.5. For the irradiation a 200 W mercury lamp with a dichromic filter (280-400 nm) and a 320 nm band-pass filter to select only the peak at 313 nm were used.

All three macrocycles **5**-**7** displayed very similar spectral changes. As a typical example, the behavior of macrocycle **7** in THF at a concentration of 1.0×10^{-5} mol/L is shown in **Figure 34** and discussed in detail, since this macrocycle with its acetyl protecting group at the sulfur is the closest possible approximation to the free thiole. The free thiole **37** will later be the molecule immobilized on the surface, but photoisomerization investigation in solution with the free thiole is not possible, because of instant disulfide formation. The UV/Vis spectra and the corresponding switching behavior of macrocycles **5** and **6**, are shown in **Figure 36** and **Figure 37**, respectively.

The decrease in the absorbance of the $\pi \rightarrow \pi^*$ band at 319 nm and the increase in the $n \rightarrow \pi^*$ absorbance at 447 nm upon irradiation over time was attributed to the formation of the *cis* isomer. The photoisomerization reaction presented two isosbestic points at 245 nm and 390 nm and reached the photostationary state within 30 min of irradiation under the experimental conditions applied. This is somewhat longer then the observed 8 min for macrocycle **1**, which is probably due to the slightly higher degree of functionalization of the middle ring of the *m*-terphenyl subunit, but it can also be attributed to a slight difference on the intensity of the lamp.

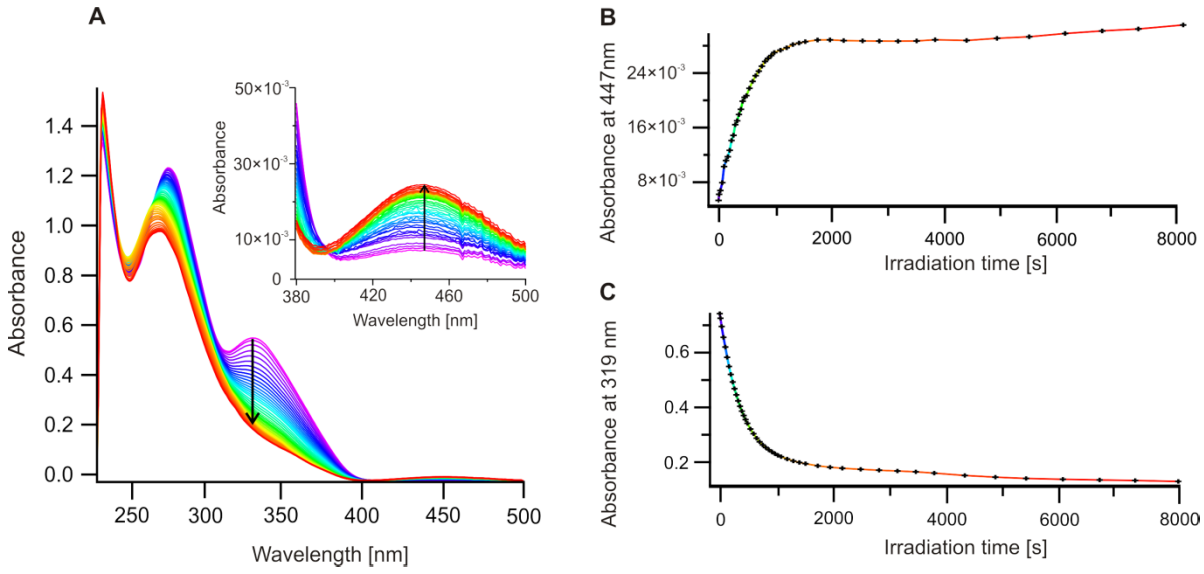

Figure 34 (A) Change in the absorbance spectra of macrocycle **7** in 1.0 × 10^{-5} molar THF solution upon irradiation at 313 nm. (B) Absorbance change at 447 nm versus irradiation time. (C) Absorbance change at 313 nm versus irradiation time.

Figure 34B and **C** displays the absorbance at 319 and 447 nm, respectively, plotted against the irradiation time. The evaluation of both signals followed an exponential trend. This suggests a switching dynamic for the pair of azo chromophores in the macrocycle **7**, which should involve, at least within the temporal resolution of the optical investigation, the switching of both azo groups. The same behavior was already found for the alkyl functionalized macrocycle **1**. Noticeable is also the peak shift of the band around 260 nm that did not occur in the absorbance spectrum of macrocycle **1**. This could be attributed to a slight bending of the *m*-terphenyl part in the *cis* conformation. Unfortunately it was not possible until now to obtain a solid state structure of the thermodynamically less favored *cis* isomer to further prove this hypothesis.

The *cis* → *trans* back isomerization was either triggered by light or was observed as a thermal back reaction. For the light induced back reaction the sample was irradiated at the maximum of the peak of the *cis* isomer at 450 nm. In order to monitor the thermal back reaction with time the sample was kept in the dark until the azo macrocycle **7** had switched back to its thermodynamically more stable *trans* form. The dynamics of the thermal back isomerization turned out to be the same as for macrocycle **1**. The re-equilibration of the *cis*-enriched solution back to

a solution comprising exclusively the thermodynamically favored *trans* form also took almost three weeks. This indicates that the rigid and stiff dimeric *m*-terphenyl core is responsible for this considerable stabilization of the *cis* conformation.

To investigate the switching behavior and to monitor the reversibility of the photoisomerization reaction of several switching cycles a faster *cis* → *trans* isomerization was needed. Therefore the n → π* band at 450 nm was irradiated by using a xenon lamp and an appropriate set of filters (water filter and 450 nm BP). After the thermal back reaction, the macrocycle **7** was completely switched back to the *trans* isomer, whereas in the photochemical back reaction in the photostationary state some of the macrocycle still remained in its *cis* form, which is comparable to the previously investigated macrocycle **1**. To gain information on the stability and fatigue resistance of the system, macrocycle **7** was cycled four times. Reversible switching between the two photostationary states was observed and is shown in **Figure 35**. The data were obtained by irradiating the macrocycle **7** at 313 nm for the *trans* → *cis* isomerization and at 450 nm for the *cis* → *trans* conversion. The investigated systems seemed to be very stable and fatigue resistant, no difference or fatigue was observed during the switching process.

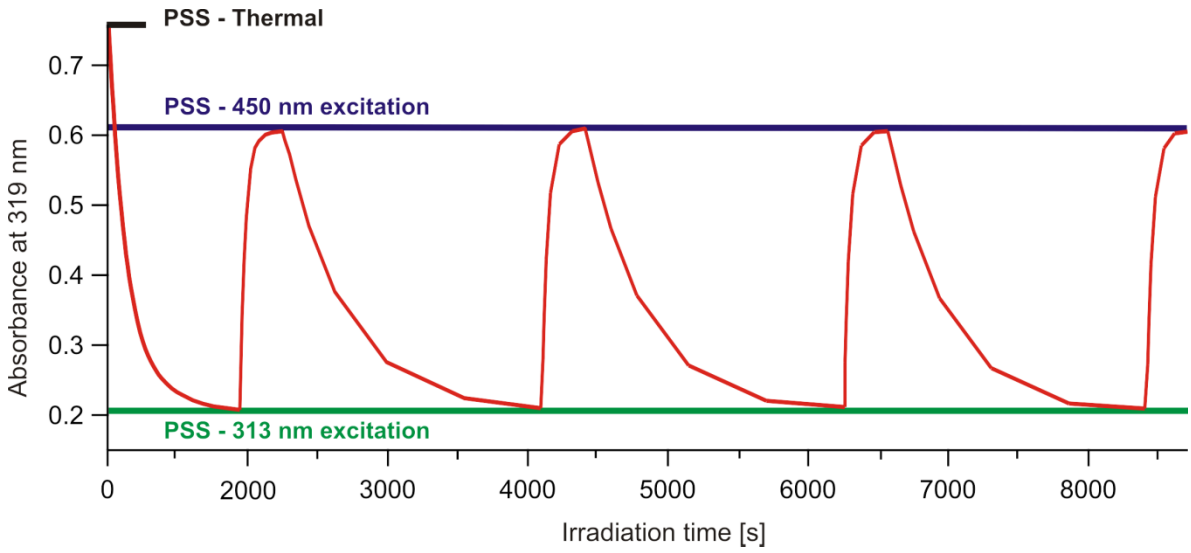

Figure 35 Photoinduced back reaction of macrocycle **7** in a THF solution, alternating irradiation with UV light (313 nm) and blue light (450 nm) to switch between the two photostationary states (PSS).

To investigate the *trans* → *cis* isomerization mechanism of the asymmetric macrocycle **5** and the symmetric macrocycle **6**, they were irradiated at 313 nm as well. Under the same conditions as described above, very similar spectra were obtained. The spectrum of macrocycle **5** with its corresponding switching between the two photostationary states (PSS) is shown in **Figure 36** and the one of macrocycle **6** is shown in **Figure 37**.

During the photoisomerization reaction (**Figure 36A** and **Figure 37A**) a significant decrease in the absorbance of the π → π* band at 320 nm and the increase in the n → π* absorbance at 450 nm upon irradiation over time was observed and attributed to the formation of the *cis* isomer. Two isosbestic points at 245 nm and 390 nm were found at nearly the same wavelength as for macrocycle **7**. The same noticeable peak shift of the band at about 260 nm occurred in the absorbance spectrum of macrocycle **5** and **6** and can be attributed to the same slight bending of the *m*-terphenyl part in the *cis* conformation.

Reversible switching between the two photostationary states was observed for both macrocycles **5** and **6** and is shown in **Figure 36B** and **Figure 37B**.

The data were obtained by irradiating the macrocycle **5**-**7** at 313 nm for the *trans* → *cis* isomerization and at 450 nm for the *cis* → *trans* conversion. The investigated systems seemed to be very sable and fatigue resistant, no difference or fatigue was observed during the switching process. The similarity of the structure with macrocycle **1** was also represented by the similarity of the photoisomerization investigations.

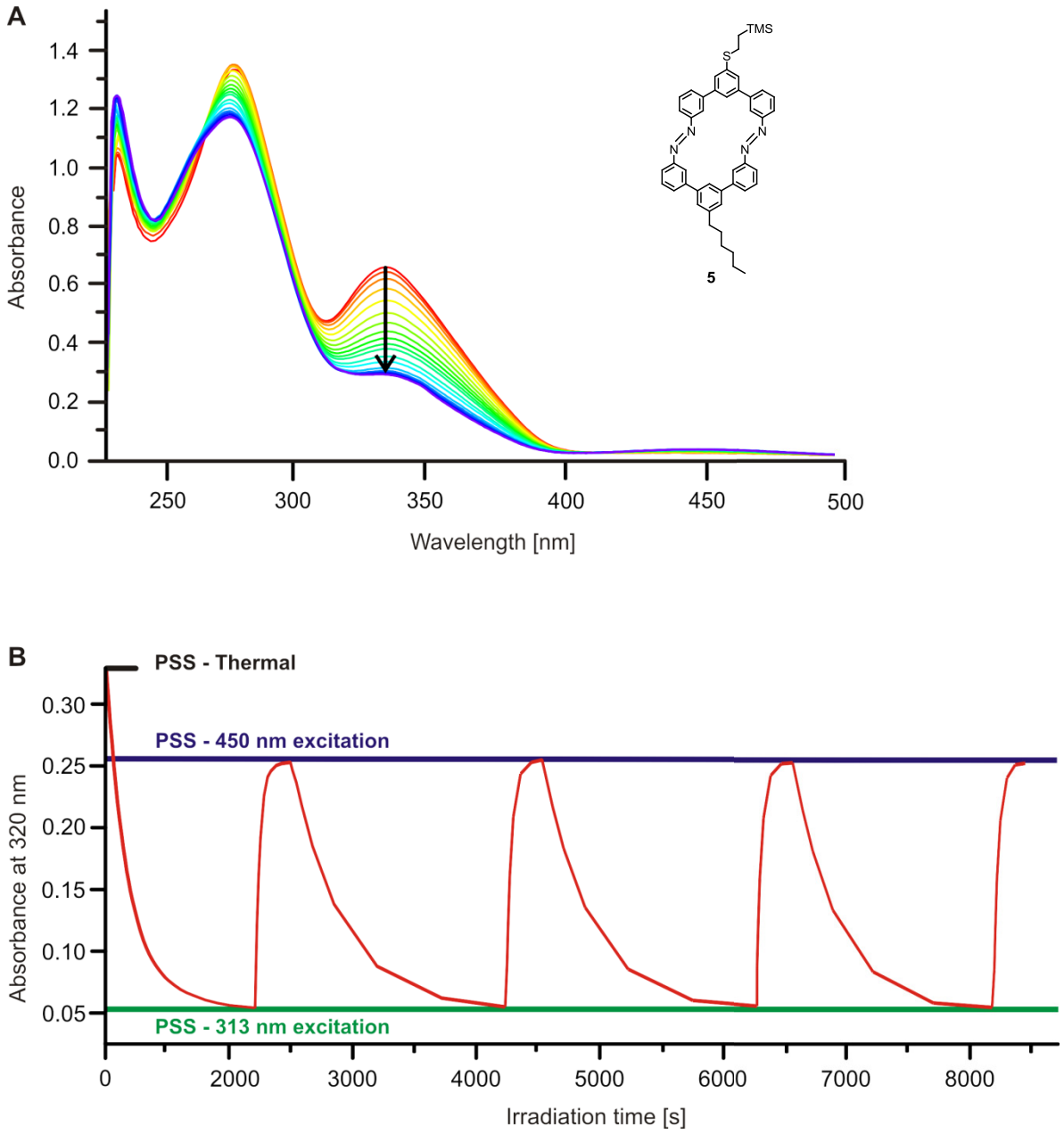

Figure 36 (A) Change of the absorbance spectra of the asymmetric macrocycle **5** in 1.0×10^{-5} molar THF solution upon irradiation at 313 nm. (B) Photoinduced back reaction of macrocycle **5** in a THF solution, alternating irradiation with UV light (313 nm) and blue light (450 nm) to switch between the two photostationary states (PSS).

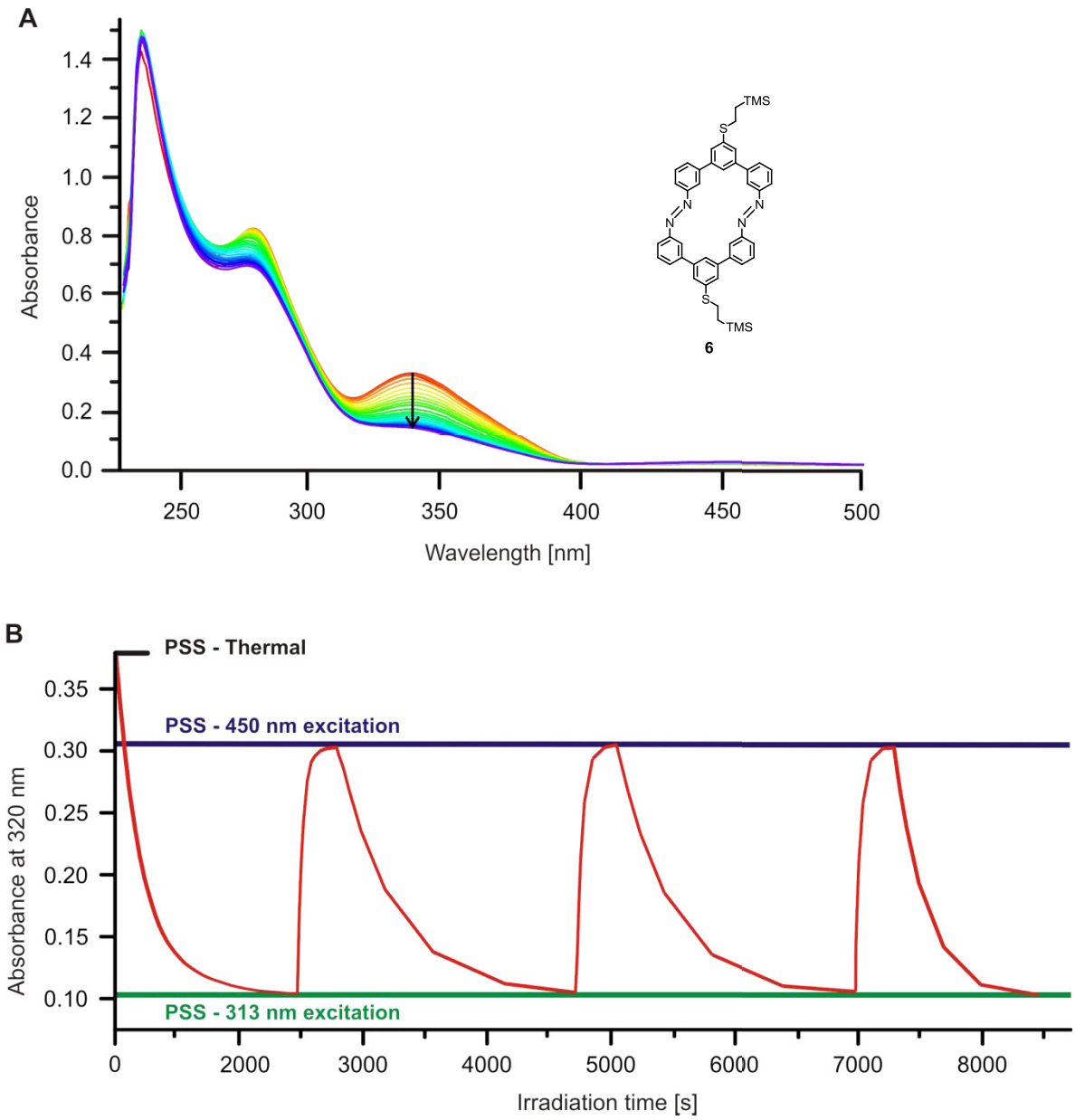

Figure 37 (A) Change of the absorbance spectra of the asymmetric macrocycle **6** in 1.0×10^{-5} molar THF solution upon irradiation at 313 nm. (B) Photoinduced back reaction of macrocycle **6** in a THF solution, alternating irradiation with UV light (313 nm) and blue light (450 nm) to switch between the two photostationary states (PSS).

2.2.6 Conclusion and Outlook

Three new sulfur functionalized shape switchable azo macrocycles **5**-**7** consisting of *m*-terphenyl semicircles interlinked by two azo joints have been synthesized and characterized. The three new macrocycles **5**-**7** were obtained with a similar protocol as the alkyl functionalized macrocycles **1**-**4** were synthesized, by a reductive dimerization of the corresponding dinitro semicircles. The asymmetric macrocycles **5** and **7** had to be synthesized by a statistical dimerization. Considering the minor difference in molecular weight of the two different semicircles **11** and **43**, a separation with size exclusion chromatography was not possible. Despite the potential for polymerization in the synthetic strategy and the separation difficulties, the asymmetric macrocycle **5** was isolated analytically pure in a rather low yield of 6%. The symmetric macrocycle **6** was also isolated by preparative TLC, in yield of 5%. These macrocycles were characterized by ^{1}H and ^{13}C-NMR spectra, profiting from the more sensitive ^{1}H-dedected HMBC and HMQC techniques. Although the purity of **5**-**7** was shown by analytical GPC, the determination of their molecular weights was, due to the presence of more functional groups and hetero atoms, less challenging compared to macrocycles **1**-**4**. All molecular weights were determined by MALDI-TOF mass spectroscopy with a very good correlation of the calculated and measured isotopic distribution.

All macrocycles **1**-**7** displayed comparable absorbance spectra, and showed very similar *trans* → *cis* photoisomerization upon irradiation at 313 nm. The time to reach the photostationary state at 313 nm increased from macrocycle **1** (8 min) to macrocycle **7** (30 min). The full thermal back reaction required several weeks, as well and was found to be at least as long as for macrocycle **1**, the thermodynamically less favored *cis* isomer showed substantial stabilization by the rigid macrocyclic structure. Despite having two azo groups in the macrocyclic periphery, an intermediate mixed *trans*/*cis* isomer was not observed, neither for macrocycle **1** nor for macrocycle **7**. The stiff *m*-terphenyl semicircles probably disfavor a strained mixed state.

These shape switchable macrocycles **5**-**7** were designed to investigate their spatial transformations by scanning probe methods. So far, all attempts to immobilize a self assembled monolayer (SAM) of these macrocycles on a gold surface have

failed in spite of the sulfur anchor group, which is known to have a high affinity to a gold surface.

3 Platinum Electrode Modification

Due to the increasing importance of modified electrodes for numerous applications including molecular electronics,[117][118] bioelectronics and sensors,[114][115][123][124] there is a need to find ways to chemically deposit suitable molecular films onto electrodes.

The grafting of molecular structures on surfaces in order to modify the exposed functionality of the materials or to introduce specific properties is a common strategy.[226]-[229] It has been successfully applied in numerous areas ranging from corrosion protection of bulk surfaces[116] to the integration of selective functionalities in nano sensing devices.[119][122][120] For electronic applications the modification of conducting surfaces at the molecular level with functional active building blocks represents a promising approach to new electrodes with tailor made surface chemistry.[128]

Strategies based on the stepwise functionalization of surfaces have already been reported.[143] Often, the first step is the introduction of a functional group via a suitable organic molecule as self assembled monolayer (SAM) on a noble metal substrate, [230][231] silicon or silicon oxide surfaces[125][127] or as coating ligand for nanoparicles.[152] After the introduction of a chemically addressable surface layer, efficient chemical conditions such as click chemistry[142][228][232] or peptide coupling[119] have been applied to further diversify the exposed surface functionality.

The variety of chemistry used to further modify pre-coated surfaces was further enlarged by the introduction of functional groups via Grignard reaction on chlorinated or brominated carbon surfaces[145] or by photochemical functionalization of acyl chloride modified surfaces.[145][233] Recently, the scope of chemical methods was further expanded by a microwave assisted surface Sonogashira cross coupling reaction to assemble extended conjugated organic structures on Si (111) surfaces.[234]

A general strategy for the coating of conducting substrates is the electrochemical grafting of aryl diazonium salts onto conducting surfaces.[133] Upon reduction of a

diazonium salt a covalently attached organic coating was observed, as corroborated by X-ray photoelectron spectroscopy (XPS) and Raman spectroscopy.[134][135] In principle, electrochemical grafting of aryl diazonium salts can be performed on any conducting or semi-conducting electrode material, resulting in a broad scope of starting surfaces potentially functionalizable by this method.[140]

In this section a modular approach to chemically modify surfaces, more precisely platinum electrodes, will be discussed. The general sketch is shown in **Figure 38**. By electrochemically grafting the electrodes with a suitable diazonium salt an organic coated platinum electrode exposing iodoaryls is obtained. Subsequent Sonogashira cross coupling chemistry with tailor made acetylene molecules (such as ferrocene acetylene) allows substituting the exposed iodines with various functional groups.

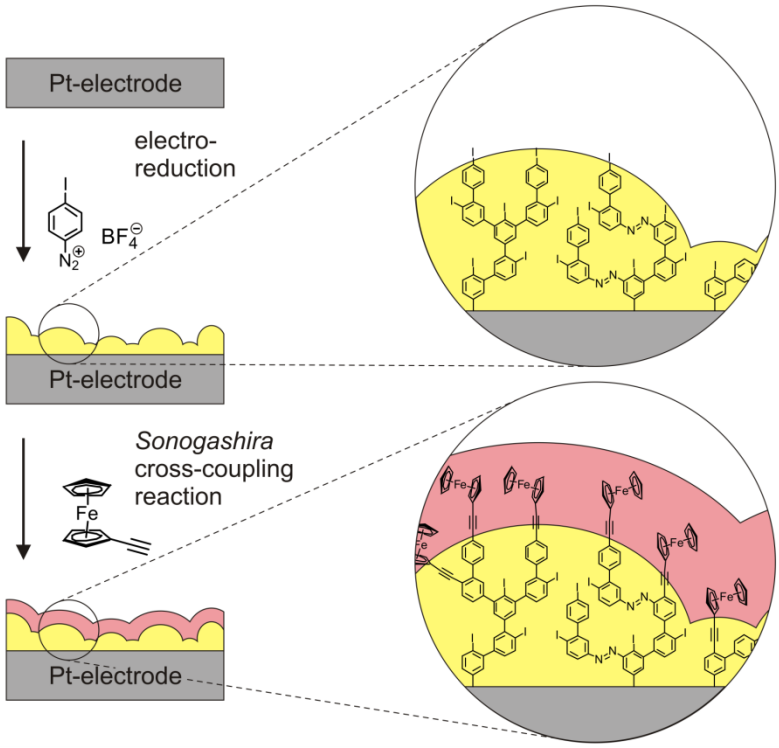

Figure 38 Stepwise functionalization of platinum electrodes. Electrochemical reduction of an iodoaryl diazonium salt in a first step and Sonogashira cross coupling reaction in the solid state as a second step to introduce a wide range of functional groups onto surfaces, with high surface coverage of the functional subunit.

3.1 Strategy to Chemically Modify Platinum Electrodes

For the functionalization of the platinum electrode **E0** a two step procedure was applied. The experimental strategy is sketched in **Scheme 25**. The bare platinum electrode **E0** is first coated by electrochemical reduction of 4-iodo-phenyldiazonium salt tetrafluoroborate (**48**) (**Scheme 25A**). In a second step, the coated electrode **E5** is subsequently exposed to a copper free Sonogashira cross coupling protocol in order to introduce peripheral functional groups by substitution of the exposed iodines with functionalized acetylenes (**Scheme 25B**).

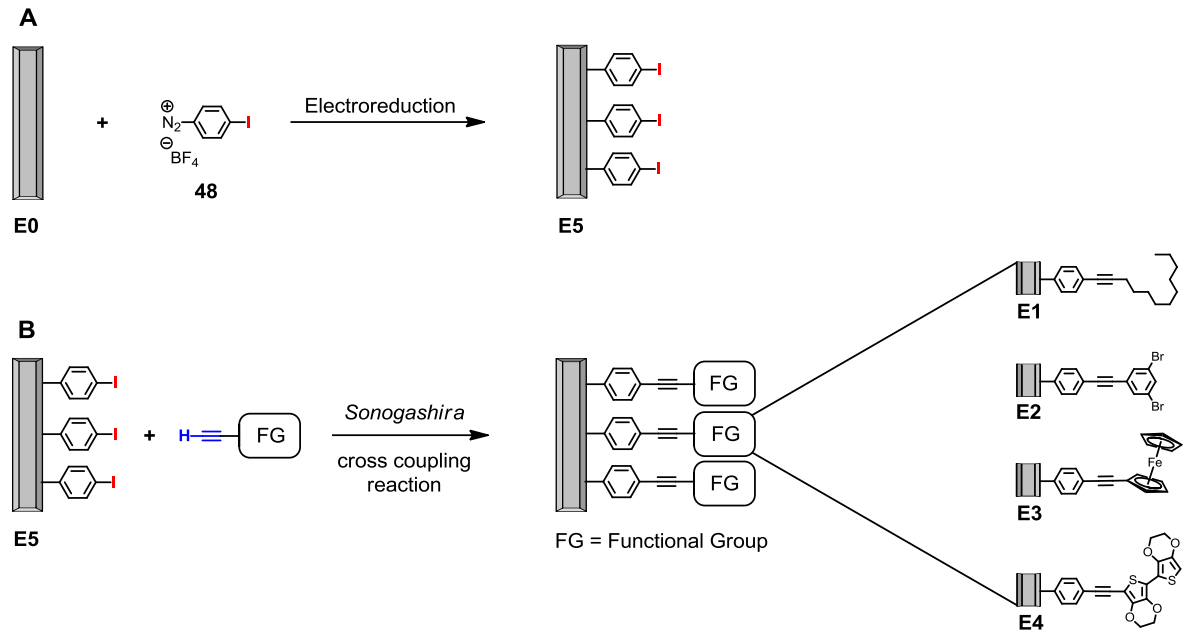

Scheme 25 Sketch of the strategy to modify surfaces. In the first step (A) the electrode **E0** is coated by electroreduction of 4-iodobenzene diazonium salt **48**. In a subsequent step (B), a variety of exposed functional groups are introduced by cross coupling reactions at the electrode surface.

As a first step the platinum surface of the electrode was modified by electro grafting of a diazonium salt. In an electrochemical reduction diazonium salts can be covalently attached to metal, carbon or silicon surfaces.[133][235][139][236] For a successful subsequent modification by cross coupling reactions a good leaving group for the palladium catalyzed reaction is needed, therefore 4-iodobenzene diazonium salt was chosen for the electroreduction.

It has been reported that sterically demanding diazonium salt hindered multilayer formation during the electroreduction step, while simple aryl diazonium slats tended to form multilayers.[137][138] Covalently grafting of a compact organic layer bearing aryl iodine moieties is important, especially for the subsequent modification by wet chemistry substituting iodine atoms attached to phenyl rings. Furthermore a sterically demanding group *ortho* to the iodide, in order to reduce multilayer formation, would hinder the subsequent cross coupling reaction. Therefore 4-iodobenzene diazonium tetrafluoroborate (**48**) is an ideal precursor to form a compact organic layer with easily accessible iodines for subsequent modifications.

To demonstrate the modularity and broad applicability of the modification method, four different functionalized platinum electrodes **E1**-**E4** were assembled. First a simple alkyl chain is immobilized to yield in the surface functionalized electrode **E1** which is expected to have a very hydrophobic surface. As next, electrode **E2** is modified using 3,5-dibromoethynylbenzene. With the two bromines as potential (but less reactive than iodine) leaving groups in cross coupling reactions, this surface is geared towards a dendritic branching unit after further functionalization. At the surface of electrode **E3** a redox active ferrocene unit is immobilized. And finally, 2,2'-bis(3,4-ethylenedioxythiophene) (BiEDOT) is immobilized at the surface of electrode **E4**. In this case BiEDOT is not only interesting as a redox active subunit, it might also be considered as a potential anchor group for an electrochemically grown EDOT polymer.[237]

Redox active subunits are of particular interest for an electrode surface. Suitably functionalized surfaces might find applications in information storage, sensing and switching devices. Furthermore, the presence of a redox chromophore can easily be investigated by cyclic voltammetry.

3.2 Modification of Platinum Electrode with Diazonium salt

In this section the coating of the electrode by electrochemical grafting is described and the analyses of the obtained surfaces are discussed. Section 3.3 deals with the further functionalization of the pre-coated electrodes by wet chemistry using Sonogashira cross coupling protocols. The analytical data obtained with these chemically modified substrates are discussed in section 3.4.

3.2.1 Synthesis of Diazonium salt and Electrochemical Reduction on Platinum Electrode

In **Scheme 26** the synthetic procedures for the preparation of the diazonium salts **48** and **49** as well as for the electrochemical reduction (electro grafting) to the platinum electrode **E0** are shown.

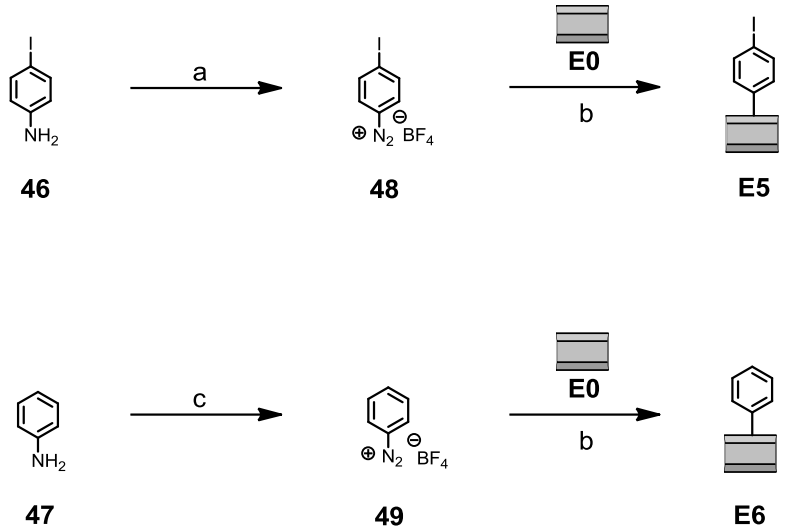

Scheme 26 Synthesis of the diazonium salts **48** and **49** and subsequent electrochemical grafting to the platinum electrode **E0**. Reagents and conditions: (a) $NaNO_2$, HBF_4, 0°C → RT, 3 h, 98%. (b) Electrochemical reduction (scan rate: 0.05 mVs^{-1} with a Ag/AgCl reference electrode) in acetonitrile with 10 mM of diazonium salts **48** or **49** and 100 mM $TBABF_4$ as supporting electrolyte. (c) $NaNO_2$, HBF_4, 0°C → RT, 3 h, 98%.

The key precursor **48** for the electroreduction was synthesized from commercially available 4-iodoanilin (**46**). The amine **46** was treated with 2 equivalents of sodium

nitrite and 20 equivalents of fluoroboric acid in water for 3 hours. After recrystallization form hot *n*-hexane with a few drops of TBME the desired diazonium salt **48** was isolated as violet crystals in 98% yield. For some test reactions (see section 3.4.3) the benzenediazonium salt **49**, bearing no iodine functionality was also synthesized applying the same protocol as described above. The product **49** was isolated as a light brown solid in 98% yield.

As starting surface for the electroreduction a cleaned and flat platinum electrode **E0** was used. This platinum electrode was fabricated by depositing a 5-nm-thick titanium film and a 25-nm-thick platinum film onto a silicon wafer using electron beam evaporation. 4-Iodobenzene diazonium tetrafluoroborate **48** was electro-reduced onto the platinum electrode **E0** following a literature procedure.[133] Potential cycling (cyclic voltammetry) in an acetonitrile solution containing 1 mM of the diazonium salt **48** and 100 mM of tetrabutylammonium tetrafluoroborate ($TBABF_4$) as supporting electrolyte was performed between +0.15 V and -0.90 V vs Ag/AgCl at 50 mVs^{-1} over five cycles. The electrode was rinsed with copious amount of acetonitrile, acetone and dichloromethane and then sonicated for 5 minutes in acetone and dried under a stream of argon. The phenyl modified electrode **E6** was synthesized with benzene diazonium tetrafluoroborate **49** by applying the same conditions and was used for some control experiments (see section 3.4.3).

3.2.2 Characterization of the Coated Platinum Electrode E5

In this section the characterization of the 4-iodobenzene modified platinum electrode **E5** is discussed. In the cyclic voltammogram (CV) during the electro grafting step a reduction peak at -92 mV vs. Ag/AgCl with no associated oxidation peak was observed for the first scan (a in **Figure 39A**). This is characteristic for the loss of N_2 and the formation of a 4-iodobenzene radical at the electrode surface.[134] In subsequent scans (b and c in **Figure 39A**) no further reduction

peaks in this voltage range were observed indicating the complete coating of the electrode by a closed organic film.

To investigate the completeness of the coating by the immobilized 4-iodophenyl molecules, the access of ferrocene to the platinum electrodes was investigated in a CV experiment (**Figure 39B**). As displayed in **Figure 39B**, the reversible oxidation of the ferrocene molecule was observed using the bare platinum electrode **E0**. After immobilization of the 4-iodobenzene diazonium salt **48**, the coated platinum electrode **E5** no longer displays the ferrocene oxidation signal under similar conditions. The access of ferrocene to the electrode is prohibited, indicating a compact organic layer covering the electrode.

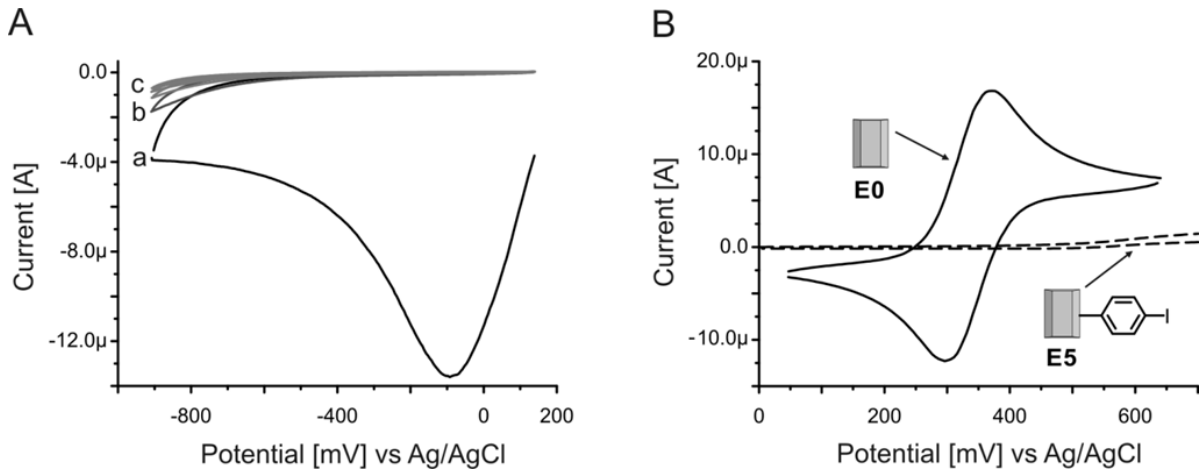

Figure 39 (A) Cyclic voltammetry (CV) of 4-iodobenzene diazonium tetrafluoroborate **48** in 1 mM solution in acetonitrile / 100 mM $TBABF_4$ on a platinum electrode **E0**. a) First scan displaying the reduction peak, b) second and c) further scans of the coated electrode. Scan rate: 0.05 mVs^{-1} with an Ag/AgCl reference electrode. (B) Cyclic voltammograms of a 1 mM ferrocene solution in acetonitrile / 100 mM $TBABF_4$ using as working electrode the electrode **E0** before (black solid line) and **E5** after the modification by electrochemical grafting of the diazonium salt (dashed line). Scan rate: 100 mVs^{-1} with an Ag/AgCl reference electrode.

The morphology of the coating film was also of particular interest. The nature of the formed organic surface is reported to depend on several different parameters of the preparation, such as applied voltage, concentration of the diazonium salt, exposed time and the substrate itself.[137] The obtained film was thus characterized by CV,

atomic force microscopy (AFM), contact angle (CA) measurements and X-ray photoelectron spectroscopy (XPS).

The area of the reduction peak in the CV during the modification of the electrode surface with diazonium salts (a in **Figure 39A**) allows calculation of the number of reduced molecules **48** per electrode surface to be (2.0 ± 0.9) × 10^{-8} mol cm^{-2} (see experimental section 6.1). McCreery et al. calculated the theoretical maximum surface coverage value for a monolayer of nitrophenyl groups on a glassy carbon electrode to be 1.2 × 10^{-9} mol cm^{-2}.[238] Assuming a comparable surface packing for nitrophenyl on carbon and iodophenyl on platinum, the comparison of both values clearly favors the formation of multilayers rather than a monolayer surface coverage.

To determine the surface roughness and film thickness AFM measurements were performed. In **Figure 40** the line scans of all different electrodes **E0**-**E6** are shown, displaying the roughness of the surface.

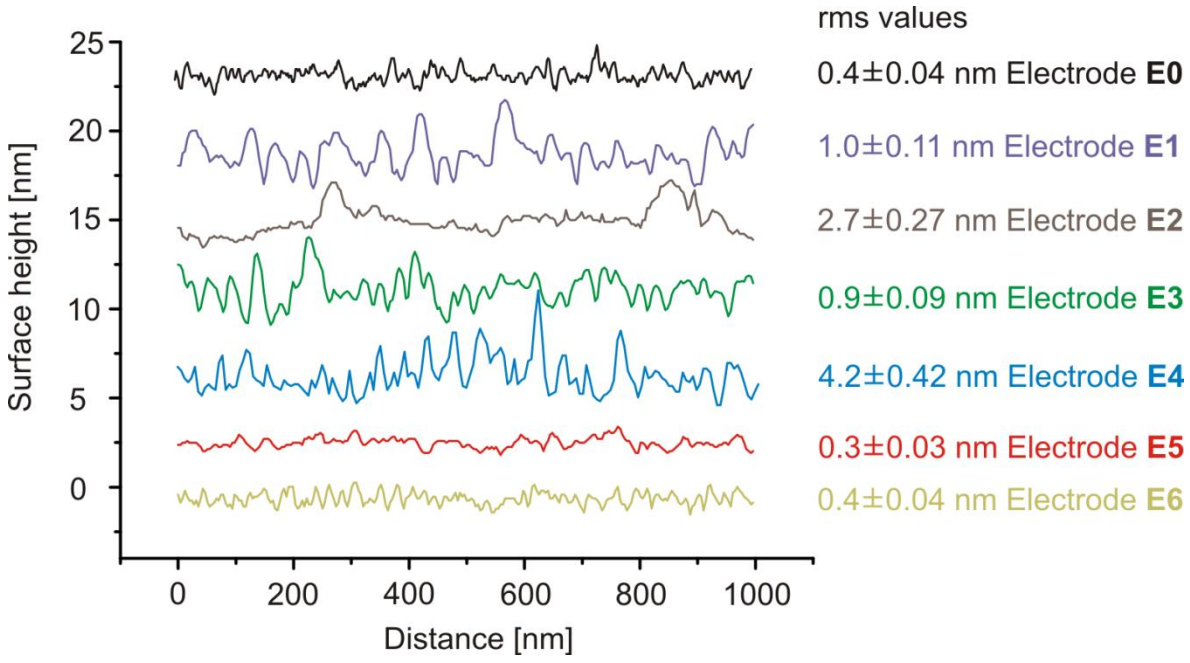

Figure 40 Line scans of the electrode surface of each electrode **E0**-**E6**. The line scans show the different roughness of the surface depending on the different functionalization. The rms values are given including the highest unevenness.

The graininess is largely given by the topography of the naked platinum electrode **E0**. However, distinct changes in the topography can be observed in images and line scans. For example, whereas the layer of electrode **E6** apparently covers the surface uniformly, the iodophenyl functionalized electrode **E5** leads to some smoothening attributed to the dendritic nature of the growth. Electrode **E5** has some slightly higher nodules, but overall the surface is still uniform. However, after the Sonogashira cross coupling reactions the surface of the electrodes **E1**-**E4** becomes more uneven due to the immobilized molecules. Some of the larger features on electrodes **E2**, **E4** and **E0** could be due to surface contamination.

The film thickness was determined by a scratching experiment.[239] First a clean and homogenous area of the electrode **E5** was imaged using the tapping mode (dynamic operation mode). Within that area a square of 500 nm × 500 nm was scratched off with the AFM tip operating at 2 Hz line frequency in the static operation mode (contact mode). During this scratching step a load force was chosen high enough to induce complete removal of the organic film, but yet low enough to leave the underlying platinum substrate intact (**Figure 41A**). In a subsequent imaging step using the dynamic mode, a larger area was scanned, allowing determination of the thickness of the removed layer thickness (**Figure 41B**).

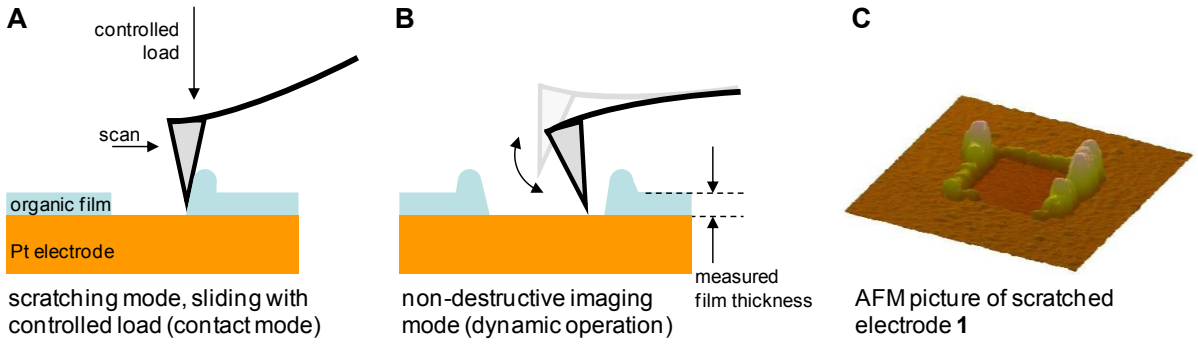

Figure 41 Sketch of the AFM scratching experiment. (A) Scratching of 500 nm × 500 nm square with the AFM tip at 2 Hz line frequency in the contact mode. (B) Imaging step using the dynamic mode to display the scratched square in order to determine the layer thickness. (C) Typical scratching image of electrode **E1** from which the line scans were extracted.

In **Figure 42** the line scan from the AFM scratching experiment of the electrodes **E5** is shown as a lateral cut. Applying this method a film thickness of 3.4 nm was determined for electrode **E5**. An alteration of the surface roughness of the platinum electrode upon coating with 4-iodobenzene moieties was not observed.

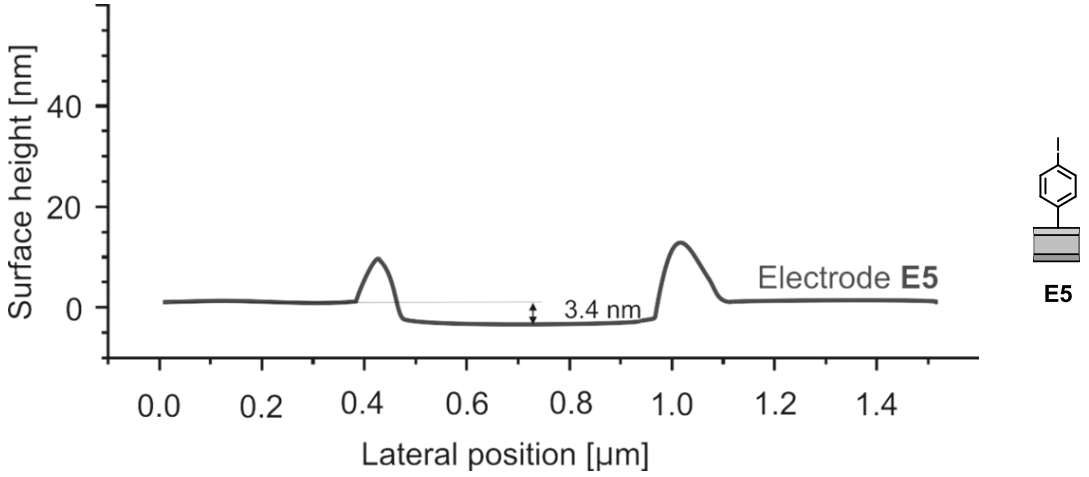

Figure 42 Lateral cut of the scratched squares of the AFM pictures for electrode **E5**. The difference in height represents the layer thickness of the organic film on the platinum electrode.

In **Figure 43** the static water contact angle pictures are shown. The contact angle is the angle at which the water droplet meets the functionalized electrode surface. The measured angle is specific for any given system and is determined by the interactions across the two interfaces. The shape of the droplet was determined by the Young – Laplace equation[240] and gives information about the hydrophobicity of the surface. Hence the contact angle is a suitable tool to obtain information about the functionalities point out of the functionalized surface.

For each sample, contact angle measurements were repeated three times at different positions of the electrodes and the average value was taken as the contact angle of the corresponding sample. Considerable differences in the contact angle of a static water droplet were measured upon electroreduction of 4-iodobenzene diazonium ions. While for the bare platinum electrode **E0** a contact angle of 71 ± 2° was obtained, an angle of 48 ± 1° was measured on the iodobenzene covered electrode **E5**. This significant decrease of 23° indicates a

decreased hydrophobicity and further corroborates the surface coating with iodophenyl moieties exposing a polarized I-C bond.

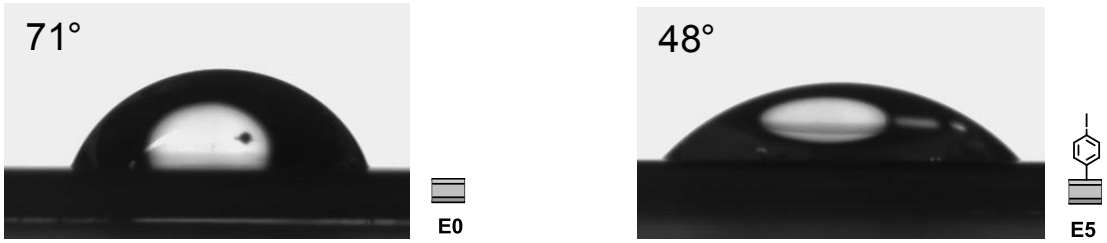

Figure 43 Static water contact angle picture of electrode **E0** and electrode **E5** after the electroreduction step. The contact angles were measured at RT and calculated using the Young-Laplace equation.

The elemental composition of the films was analyzed by X-ray photoelectron spectroscopy (XPS). In particular the ratio between the carbon and the iodine signal, the two elements (in addition to hydrogen) present in the grafted molecule, were investigated. For the analysis the peak counts were determined by integration over the counts after subtraction of a suitable background. To determine the relative amounts of elements on the surface the tabulated elemental sensitivity factors of both Wagner[241] and Scofield[242] were used. The discrepancy between such measurements of different XPS peaks and between the two sets of sensitivity factors were added to the uncertainty of the measurement. While an I/C ratio of 0.17 was expected for immobilized C_6H_4I units, an I/C ratio of 0.08 ± 0.04 was measured for the coated platinum electrodes **E5**. The deviation from the expected ratio suggests that 52% of the incorporated material either lacks or loses the iodine atom. Some of the iodines can be replaced by hydrogen atoms and some are maybe substituted by a diazonium salt during the radical immobilization step.

In a control experiment on a platinum electrode **E0**, which was exposed to the same solvents but not to 4-iodobenzene diazoniumsalt **48** some small amounts of oxygen and traces of carbon were found. The oxygen was attributed to inevitable oxide on the surface and the carbon to traces of contamination or residues. Apart from the elements comprised in the immobilized molecules, nitrogen was also

found and can be explained through “dendritically growth” as sketched in **Figure 44B**.

In summary, the analytical data of the platinum electrode **E5** coated with the iodo precursor **48** suggest the grafting of a compact and closed organic layer onto the platinum electrode. The rather uniform film with a thickness of 3.4 ± 0.1 nm points at a “dendritic” morphology with at least five molecular layers (**Figure 44B**), since for a monolayer a layer thickness of only 0.7 nm was calculated (**Figure 44A**). Films made by electroreduction of diazonium salts have been reported to grow upon attachment of formed radicals on the electrode surface as well as on already immobilized organic molecules. Furthermore, reactions of diazonium species with immobilized radicals results in moieties immobilized by azo groups.[237] Covalent grafting of a compact organic layer bearing aryl iodide moieties is important, especially for the subsequent modification by wet chemistry substituting iodine atoms attached to the phenyl rings.

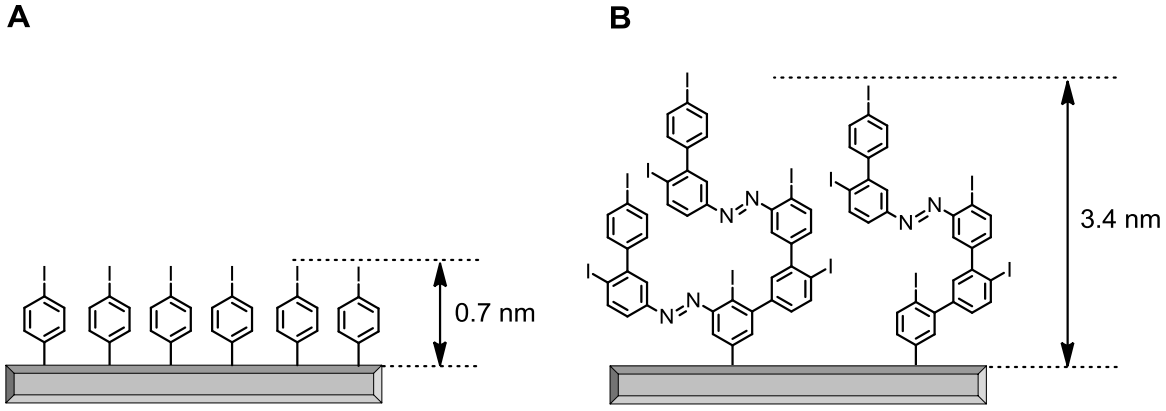

Figure 44 Sketch of the surface morphology: (A) Ideal molecular monolayer with a calculated thickness of 0.7 nm and (B) hypothesized “dendritically” grown and densely packed multilayer surface coating, resulting in a thickness of 3.4 nm.

3.3 Modification of Iodophenyl Functionalized Platinum Surfaces

In order to introduce various surface functions the exposed iodophenyl groups at the surface of electrode **E5** were subjected to subsequent chemical modification. Iodo substituents on phenyl rings are known to be excellent leaving groups in metal catalyzed cross coupling reactions.[149] In particular the substitution of iodines by acetylenes assisted by palladium catalysts has been found to be a powerful and modular approach in materials chemistry. In the present case this strategy is highly promising as various functional subunits comprising acetylenes are either commercially and/or synthetically available.

3.3.1 Synthesis of Functionalized Acetylenes

In the following, the synthesis of non-commercial acetylene precursors **54** and **58** are described. In **Scheme 27** the synthesis to the 2,2'-bis(3,4-ethylene-dioxythiophene) (BiEDOT) functionalized acetylene precursor **54** is shown.

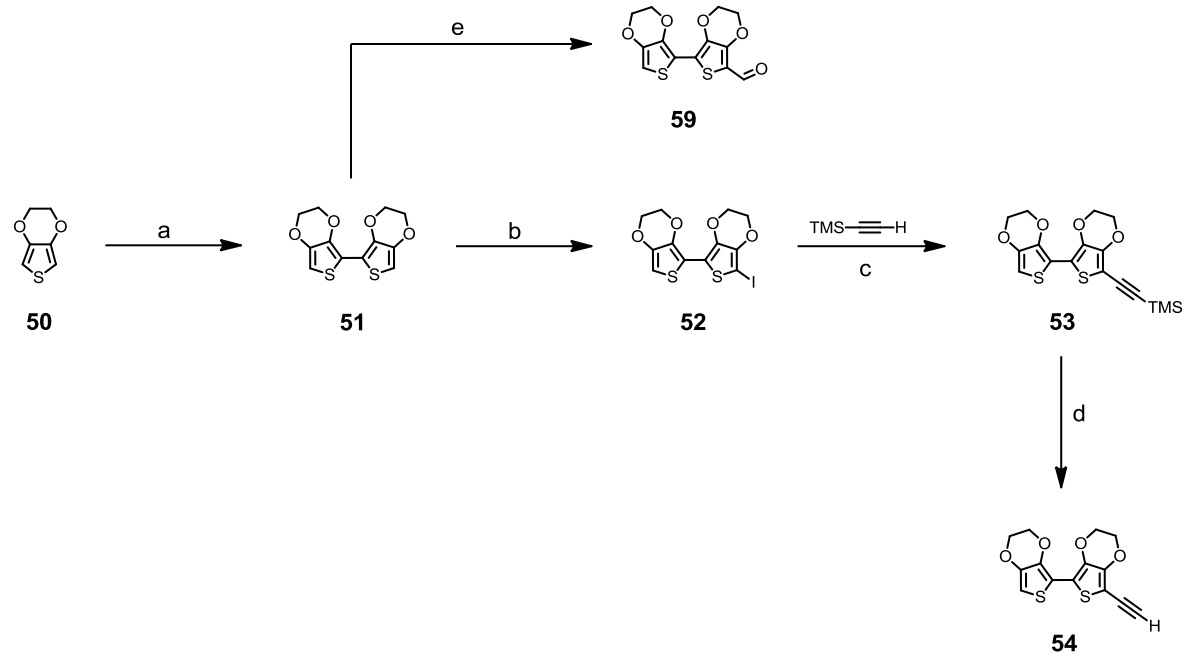

Scheme 27 Synthesis to the BiEDOT functionalized acetylene precursor **54**. Reagents and conditions. (a) *n*-BuLi, $CuCl_2$, THF, -78°C → 40°C, 2.5 h, 75%. (b) *n*-BuLi, I_2, THF, -78°C, 1 h, 74%. (c) [$Pd(PPh_3)_4$], CuI, DIEA, THF, RT, 15 h, 88%. (d) K_2CO_3, THF, CH_3OH, RT, 20 min, 53%. (e) DMF, $POCl_3$, AcONa, $C_2H_4Cl_2$, 90°C, 2 h, 2%.

In a first step two commercially available ethyldioxythiophnes (EDOT, **50**) were coupled following a literature procedure.[243] EDOT was lithiated with *n*-butyllithium in tetrahydrofuran and insitu coupled in an Ullmann coupling with copper(II) chloride. The crude was purified by column chromatography with silica gel to afford the desired BiEDOT **51** as white crystals in 75% yield.

In order to introduce the acetylene function via a Corey – Fuchs reaction an aldehyde precursor **59** is needed. Compound **51** was treated with DMF, phosphoryl chloride and acetic acid in dichloroethane, after purification by column chromatography with silica gel, the desired aldehyde **59** was isolated in a rather poor yield. Due to this low yield of just 2% in the aldehyde functionalization step of BiEDOT **51**, a detour over the iodinated BiEDOT **52** was performed. Hence, compound **51** was lithiated just on one side by using exactly one equivalent of *n*-butyllithium in tetrahydrofuran.[244] In a subsequent lithium ─ iodine exchange the mono-iodinated BiEDOT **52** was isolated as a yellowish solid. The iodinated compound **52** was used without further purification in the subsequent Sonogashira cross coupling reaction under standard palladium catalyzed conditions.[149] The TMS protected acetylene **53** was isolated after column chromatography with silica gel as a light brown powder in 65% yield over both steps. For the deprotection of the TMS protecting group with potassium carbonate in methanol, oxygen free conditions were used in order to reduce the acetylene homo coupling. Therefore the solvent was degassed for 15 minutes with argon. The free acetylene **54** was isolated analytically pure after purification by column chromatography with silica gel. Despite the known instability of free acetylenes, compound **54** was stable for about two weeks when stored at -20°C under argon.

The dibromo precursor **58** was synthesized straight forward in three steps starting from commercially available 1,3,5-tribromobenzene (**55**). The synthesis is shown in **Scheme 28**. In a first step compound **55** was lithiated by using one equivalent of *n*-butyllithium in tetrahydrofuran. In order to exchange only one bromine by a lithium atom the temperature was decreased to -90°C. The reaction mixture was

then treated with iodine at room temperature affording the mono iodinated compound **56** as brown needles after column chromatography with silica gel. In a palladium and copper catalyzed Sonogashira cross coupling reaction the iodide of **54** was substituted by a TMS protected acetylene and compound **57** was isolated as a colorless liquid. For the subsequent TMS deprotection the same conditions as described above were applied. The free acetylene was synthesized over three steps with an overall yield of 68%.

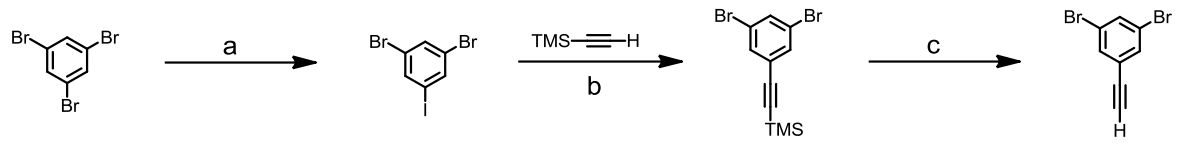

55 **56** **57** **58**

Scheme 28 Synthesis of the dibromo functionalized acetylene precursor **58**. Reagents and conditions. (a) *n*-BuLi, I_2, Et_2O, -90°C, 2.5 h, 77%. (b) [$Pd(PPh_3)_4$], CuI, DIEA, THF, 0°C → RT, 2.5 h, 89%. (c) K_2CO_3, THF, CH_3OH, RT, 30 min, 99%.

The alkyl functionalized acetylene **60** and the ferrocene functionalized acetylene **61** which were used for the functionalization of the platinum electrode **E5** are commercially available.

3.3.2 General Protocol for the Sonogashira Cross Coupling Reaction on Iodophenyl Functionalized Platinum Surfaces

In order to demonstrate the modularity and broad applicability of the modification method, four different functionalized platinum electrodes **E1**-**E4** were assembled (**Scheme 29**).

First a simple alkyl chain was immobilized to yield in the surface functionalized electrode **E1** which is expected to have a very hydrophobic surface. As second electrode **E2** is modified using 3,5-dibromoethynylbenzene **58**. With the two bromines as potential, but less reactive than iodine, leaving groups in cross

coupling reactions, this surface is geared towards a dendritic branching unit after further functionalization. At the surface of electrode **E3** a redox active ferrocene unit is immobilized. And finally, BiEDOT is immobilized at the surface of electrode **E4**. In this case BiEDOT is not only interesting as a redox active subunit, it might also be considered as potential anchor group of an electrochemically grown EDOT polymer.[237]

First attempts using a classical Sonogashira cross coupling protocol mainly provided diacetylenes as product, probably due to a copper ion catalyzed oxidative acetylene homo-coupling reaction.[245][246] To avoid this competing homo-coupling and to increase the reproducibility of the procedure, a “copper free” Sonogashira protocol was chosen.[147] It has to be mentioned that “copper free” means that no copper ions were added. However, the presence of traces of copper ions for example from the cleaning detergents or as impurity of the palladium source cannot be completely excluded in these experiments.

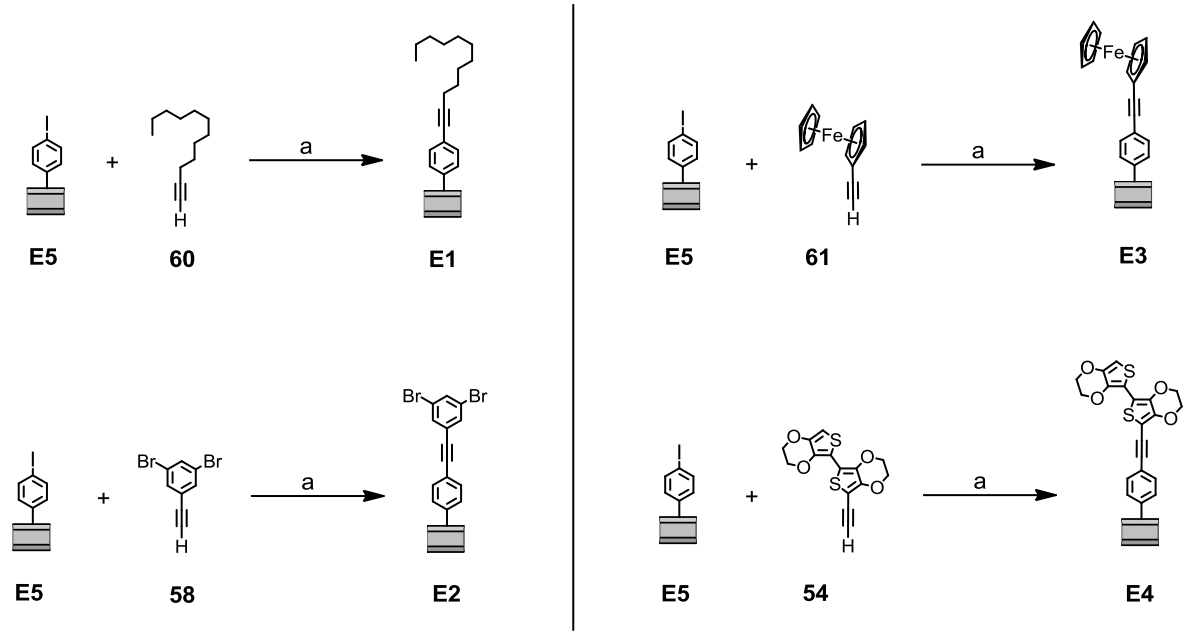

Scheme 29 Overview of the general procedure for the Sonogashira cross coupling reaction with various acetylenes **54**, **58**, **60** or **61** on platinum surface. Reagents and conditions. (a) $PaCl_2$, pyrrolidine, H_2O, 50°C, 24 h.

The general procedure for the electrode functionalization with the “copper free” coupling protocol is shown in **Scheme 29**. The pre-functionalized electrodes **E5** was heated to 50°C under aerobic conditions in the presence of palladium(II) dichloride as catalyst, pyrrolidine as base and water as solvent. The corresponding acetylene was added and the reaction mixture was kept at 50°C for 24 hours. The electrodes were removed from the reaction mixture, rinsed extensively with acetone and dichloromethane. After sonication for 5 minutes in dichloromethane the electrodes were dried under an argon stream. All functionalized platinum electrodes **E1**-**E5** were stored at ambient conditions and no degeneration was observed for more than one year.

3.4 Characterization of the Modified Electrodes

The surface functionalized electrodes **E1**-**E4** were analyzed by up to four different methods. Wetting was determined by static water contact angle (CA) measurements and elemental compositions were investigated by X-ray photoelectron spectroscopy (XPS). Atomic force microscopy (AFM) was used to determine the roughness and a scratching protocol was applied to determine the thickness of the films. Cyclic voltammetry (CV) was used to investigate immobilized redox chromophores.

The analytical data for the electrodes **E1**-**E6** obtained by the first three methods are summarized in **Table 5**.

Table 5 Static water contact angle measurement for all electrodes **E0**-**E6** and layer thickness determined by AFM scratching experiments together with I/C ratio and the conversion of the wet Sonogashira cross coupling reaction on electrode **E5** measured by XPS for the electrodes **E1**-**E4**.

	 E0	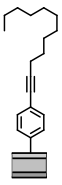 E1	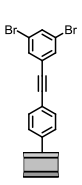 E2	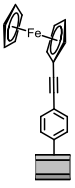 E3	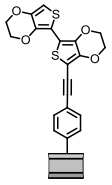 E4	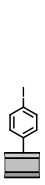 E5	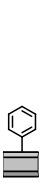 E6
Contact angle	71±2°	79±1°	59±3°	58±1°	52±2°	48±1°	65±2°
Layer thickness[a]	-	4.4±0.05nm	4.1±0.1nm	3.6±0.05nm	4.6-5.9 nm[b]	3.4±0.1nm	1.9±0.1nm
I/C ratio (XPS)	-	0.005±0.0005	0.032±0.01	0.059±0.03	0.06±0.02	0.08±0.04	0
Approx. conversion	-	88%	48%	18%	14%	-	-

[a] determined by AFM scratching experiment.
[b] slightly inhomogeneous surface, some little debris on surface.

3.4.1 Dodec-1-yne Functionalized Electrode (E1)

Dodec-1-yne **60** was considered as interesting model acetylene as its immobilization on a surface is expected to increase the hydrophobicity considerably. Furthermore, its slim shape having minimal spatial requirements is expected to allow access to iodine groups in a crowded surrounding on the rough electrode surface.

As displayed in **Figure 45**, the contact angle increases considerably from 48 ± 1° for **E5** to 79 ± 1° **E1** upon functionalization with the long alkyl chain. The expected increase of the surface hydrophobicity corroborates the successful surface functionalization with long alkyl chains.

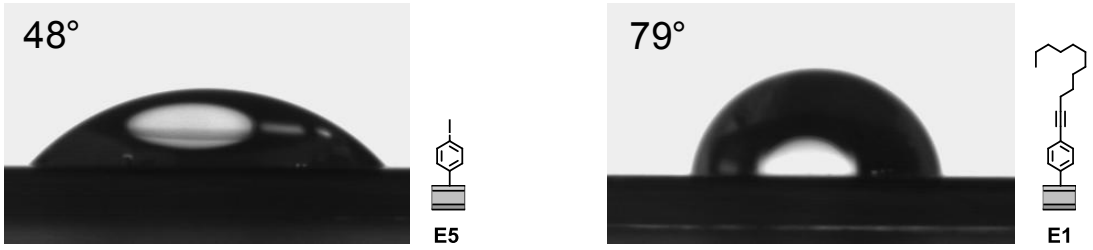

Figure 45 Static water contact angle picture of electrode **E5** (before the functionalization with dodec-1-yne) and electrode **E1** (after the Sonogashira reaction). The contact angles were measured at RT and calculated using the Young-Laplace equation.

To determine the film thickness of the organic coating the same AFM scratching protocol as described above (see **Figure 41**) was applied. In **Figure 46** the lateral cut of the scratched squares of the AFM pictures for all functionalized electrodes are shown. In this section electrode **E1** functionalized with a long alkyl chain will be discussed. The other electrodes are discussed subsequently in their corresponding sections.

The increase of the thickness of the organic coating by about 1 nm after the Sonogashira cross coupling reaction fits perfectly with the estimations for the replacement of iodine by a dodec-1-ynyl substituent and indicating the functionalization of the outer sphere. According to simple MM2 estimations, the difference between the van der Waals (vdW) radius of an iodine substituent,

compared to a dodec-1-ynyl substituent is up to 1.2 nm for a fully stretched alkyl chain.

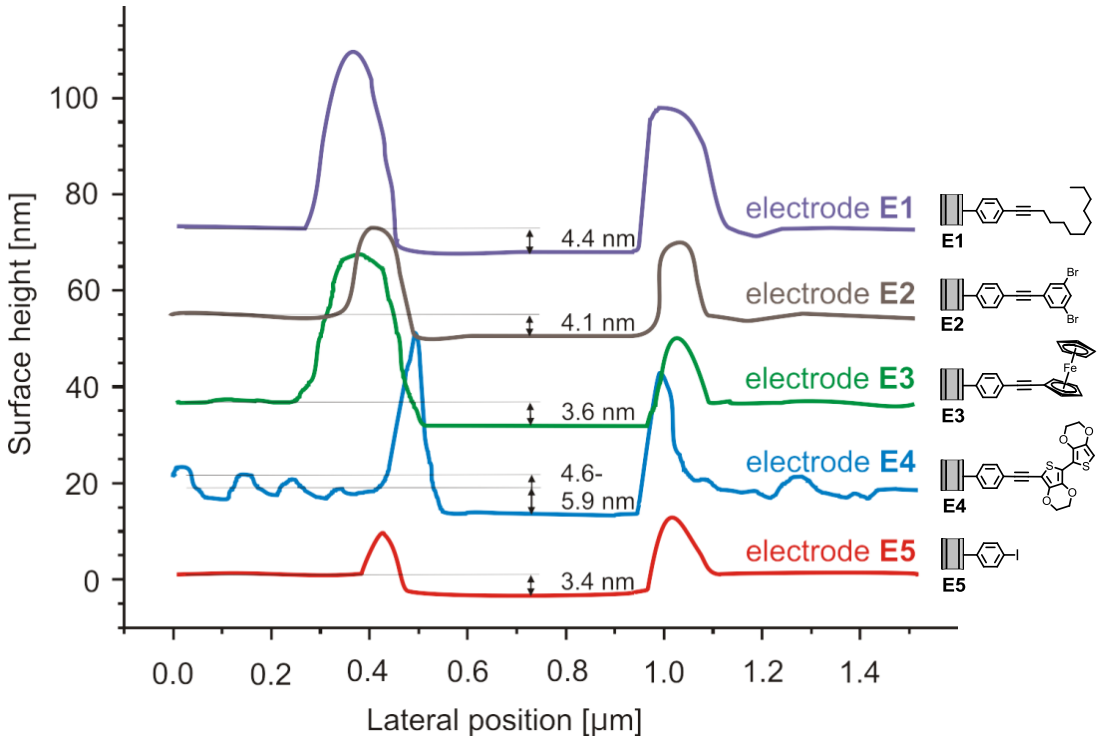

Figure 46 Lateral cut of the scratched squares of the AFM pictures for each electrode **E1**-**E5**. The difference in high represents the layer thickness of the organic film on the platinum electrode.

As a last analysis for electrode **E1** the I/C ratio of 0.005 ± 00005 determined by XPS allows estimations about the completeness of the substitution reaction. Together with the I/C ration of 0.08, before the Sonogashira functionalization step, the effective conversion was calculated as following:

$$\frac{I_{end}}{C_{end}} = 0.005 \qquad \text{(1) ratio of XPS measurement after Sonogashira reaction}$$

$$\frac{I_{start}}{C_{start}} = 0.08 \qquad \text{(2) ratio of XPS measurement before Sonogashira reaction}$$

$$I_{start} = 0.08 \cdot C_{start} \qquad \text{(2a)}$$

$C_{acetylene(alkyl)} = 12$ (3) number of carbon atoms added per substituted iodine atom during the Sonogashira reaction

With *n* being the number of iodine atoms which were substituted by a dodec-1-yne **60** during the coupling reaction the I/C ratio after the reaction is given as:

$$\frac{I_{end}}{C_{end}} = \frac{I_{start} - n}{C_{start} + n \cdot C_{acetylene}} \quad (4)$$

(1), (2a) and (3) in (4):

$$0.005 = \frac{0.08 \cdot C_{start} - n}{C_{start} + n \cdot 12}$$

$$0.005 \cdot C_{start} + 0.06 \cdot n = 0.08 \cdot C_{start} - n$$

$$1.06 \cdot n = 0.075 \cdot C_{start}$$

$$n = \frac{0.075 \cdot C_{start}}{1.06} \cong 0.0708 \cdot C_{start}$$

All iodine atoms present before the Sonogashira reaction correspond to 100% and can be expressed in terms of C_{start} according to (2a):

$$0.08 \cdot C_{start} = 100\%$$

Since *n* is defined as all iodines replaced during the Sonogashira reaction and can therefore be expressed as a percentage of iodine atoms initial presented.

$$n = 0.0708 \cdot C_{start} = x\ \%$$

$$x = \frac{0.0708 \cdot C_{start} \cdot 100}{0.08 \cdot C_{start}}\ \% = 88\%$$

Thus, 88% of the iodines were substituted in the Sonogashira reaction, assuming that the substitution reaction is the only mechanism to remove iodine atoms. With the dodec-1-yne **60** as a very compact acetylene the intensity of the XPS iodine signal of the functionalized surface dropped almost below the detection limit. While the disappearance of the signal of the iodine atoms perfectly fits with the

expectations for a completed substitution reaction the analytical data should be treated with a degree of skepticism. Dehalogenation is a well known side reaction during palladium catalyzed coupling reactions[149][247] and thus, the disappearance of the iodine signals is not necessarily proof that all iodine atoms have been replaced by a dodec-1-ynyl chain. The halide can be substituted by a hydrogen atom in a palladium catalyzed cross coupling reaction, but the reaction between acetylenes and the aryl iodides are highly favored over the dehalogenation.[247][248] Hence due to the relatively long reaction time of 24 hours it is possible that a minor not quantifiable amount of iodines are replaced by a hydrogen atom. However it is most likely that the dehalogenation is not in a competition to the Sonogashira reaction with the acetylene, but it can be dominant when all accessible iodines are substituted by acetylenes.

All together, the analytical data of the dodec-1-ynyl functionalized platinum electrode **E1** match perfectly with a successful and complete substitution of the iodine atoms of the pre-coated electrode **E5** by acetylenes bearing long alkyl chains.

3.4.2 3,5-Dibromo-ethynylbenzene Functionalized Electrode (E2)

2,5-Dibromo-ethynylbenzene **58** was of interest as a more bulky model acetylene comprising two bromine atoms as labels for the XPS investigations. Furthermore, the two bromines may also act as leaving groups under metal catalyzed cross coupling conditions providing a potential access to dendritic surface functionalization.

Applying the general procedure for the Sonogashira cross coupling reaction on platinum surface described in section 3.3.2, the 2,3-dibromophenylethynyl functionalized electrode **E2** was obtained. The contact angle of a water droplet increased from 48 ± 1° for **E5** to 59 ± 3° for the functionalized electrode **E2** and is shown in **Figure 47**.

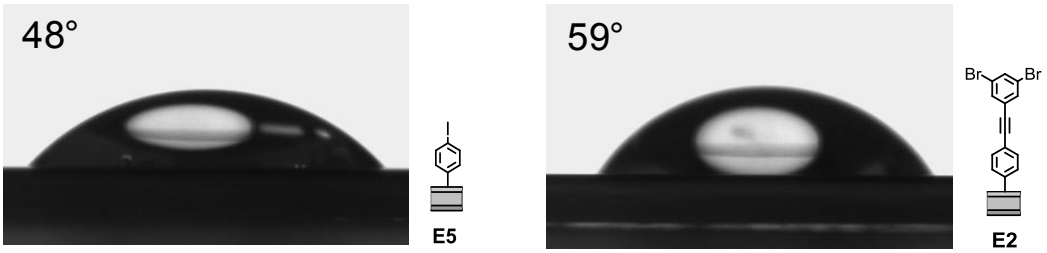

Figure 47 Static water contact angle picture of electrode **E5** (before the Sonogashira reaction) and electrode **E2** (after the Sonogashira reaction). The contact angles were measured at RT and calculated using the Young-Laplace equation.

The AFM scratching experiment (**Figure 41**) showed an increase of the layer thickness by 0.7 nm. The organic coating was increased from 3.4 nm (electrode **E5**) to 4.1 ± 0.1 nm (electrode **E2**), the lateral cut of both line scans are shown in **Figure 48**. This value exceeds the increase expected for the substitution of surface iodine atoms by the acetylene **58**. Rough MM2 estimations considering the van der Waals radii of the involved atoms suggest an increase of about 0.5 nm. Whether this increase is due to dendritic growth at the surface, due to substitution of the bromine atoms under the applied coupling conditions, or simply due to swelling of the film emerging from the steric requirements of the acetylene, remains unclear.

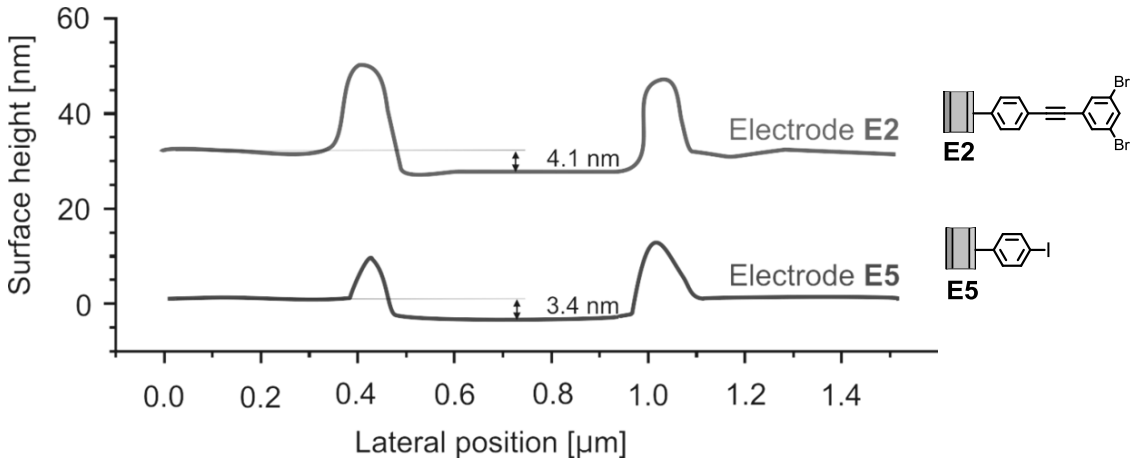

Figure 48 Lateral cut of the scratched squares of the AFM pictures for electrode **E5** (before Sonogashira reaction) and electrode **E2** (after Sonogashira reaction). The difference in high represents the layer thickness of the organic film on the platinum electrode.

Of particular interest were the XPS investigations providing insight concerning the composition of the coated film. The conversion efficiency was calculated in the same way as showed in section 3.4.1 for electrode **E1**.

$$x = \frac{0.0382 \cdot C_{start} \cdot 100}{0.08 \cdot C_{start}} \% = 48\%$$

The observed I/C ratio of 0.032 ± 0.01 therefore suggested a substitution of about 48% of the iodine atoms initially present. However, the presence of two bromine atoms in the coupled acetylene allowed a more detailed inspection of the coupling success. A value of only 0.5 ± 0.2 was measured for the Br/I ratio of the electrode **E2**. If these ratios obtained by XPS are reliable, the low bromine content compared to iodine can only be explained by considerable dehalogenation during the applied reaction conditions. Either most of the iodines are substituted by the dibromophenyl acetylene **58** and subsequently, the bromine content is reduced by dehalogenation, or considerably less iodines are substituted by the acetylene **58** but instead by a proton during dehalogenation.

Considering the considerable increase in the thickness of the organic coating (0.7 nm) and the contact angle close to the value measured for the phenyl functionalized control electrode **E6** (65 ± 2°), our favored hypothesis is the first one, namely the loss of the majority of the exposed bromines by a dehalogenation reaction. As already pointed out above, dehalogenations are frequently observed side reactions during palladium catalyzed coupling protocols.[149][247]

The reduced coupling efficiency observed for electrode **E2** compared with electrode **E1** probably arises from the increased bulkiness of the dibromophenyl acetylene **58** compared with decylacetylene **60**.

3.4.3 Ethynyl-ferrocene Functionalized Electrode (E3)

Ethynyl ferrocene **61** as a bulky acetylene was of particular interest due to its redox activity allowing the electrochemical investigation of the functionalized electrode **E3**. Applying the general Sonogashira surface immobilization protocol described above (see section 3.3.2), the ethynyl ferrocene **61** was immobilized to obtain **E3**.

The electrochemical activity of the coating of the iodophenyl functionalized electrode **E5** and of the ethynyl ferrocene **61** functionalized electrode **E3** were investigated in a CV experiment. Cyclic voltammograms were recorded using a three electrode set-up with the electrode under investigation as working electrode, an Ag/AgCl reference electrode and a platinum wire as counter electrode. An acetonitrile solution comprising 100 mM $TBABF_4$ as electrolyte and a scan rate of 100 mVs^{-1} was used for the experiment. **Figure 49** displays the CV curves recorded with both electrodes **E5** (before the Sonogashira cross coupling reaction step, dashed line) and **E3** (after the Sonogashira modification step, solid line).

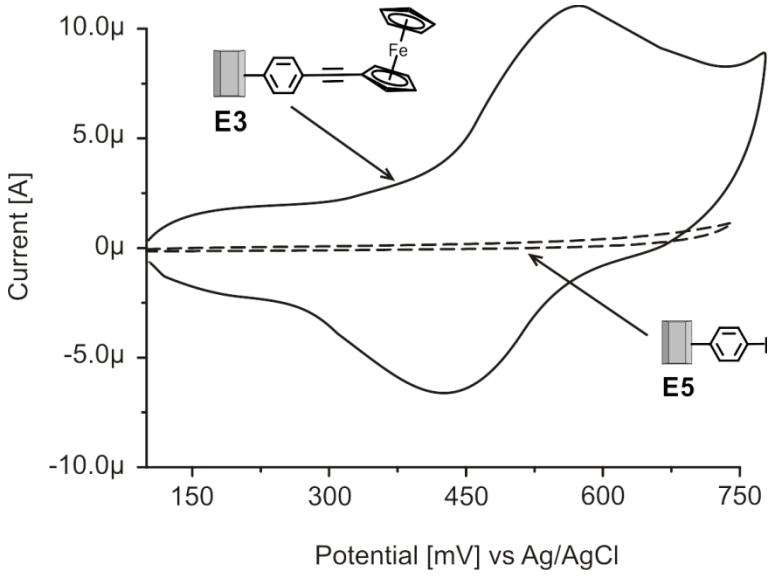

Figure 49 CV before and after the Sonogashira cross coupling reaction with ethynyl ferrocene **61**. The surface **E5** is redox inactive (dashed line) before the modification step but the surface **E3** is redox active (solid line) after the modification. The CV measurements were performed in acetonitrile, 100 mM $TBABF_4$, and with a scan rate of 100 mVs^{-1}. Reference electrode Ag/AgCl.

A pronounced and broad oxidation peak with a maximum at 572 mV and the corresponding reduction peak with a maximum at 429 mV was recorded for the ethynylferrocene functionalized electrode **E3** (solid line **Figure 49**), while the iodophenyl functionalized electrode **E5** did not display redox activity in this potential range (dashed line **Figure 49**). The two redox peaks clearly demonstrated the presence of ferrocene units at the surface of **E3**. However, the redox peaks of **E3** did not show a linear variation in peak current with the scan rate as expected for a redox species immobilized within the *Helmholtz* layer of the electrode (adsorption-type signals). On the other hand, a linear variation of the redox peak current varying with the square root of the scan rate was not observed as it would be expected for a freely diffusing species (diffusion-type signals).[249] A behavior of the redox peak current in between these two extreme cases was observed which can be attributed to the ferrocene subunit being located in a range of different environments at various distances to the platinum surface resulting in a range of formal electrode potentials (E_0).[250][251] In fact, the observed behavior of the ferrocene redox signal is expected for the functionalization of a dendritically grown multilayer as displayed in **Figure 44**.

To exclude non-specifically bound ferrocene molecule **61** as the origin of the redox peaks of **E3**, a control experiment with electrode **E6** (**Scheme 26**) lacking the iodophenyl groups, which are required for the Sonogashira coupling reaction, was performed. The electrode **E6** was exposed to the same general coupling protocol with ethynyl ferrocene **61** as experienced **E5** in order to provide **E3**. Due to the absence of iodines, a covalent coupling of the ethynyl ferrocene **61** was excluded in the case of **E6**. After this exposure, the electrode **E6** still did not display any redox activity in the voltage range in which **E3** displayed the ferrocene redox chemistry. This corroborates the hypothesis that the electrochemical signals of **E3** are due to covalently immobilized ferrocene units at the electrode surface.

The number of redox active ferrocene molecules attached to the surface was determined from the total charge passed derived from the area of the Faradic peak in the ferrocene modified platinum electrode **E3**, and is approximately $(4 \pm 1.3) \times 10^{-10}$ mol cm^{-2}. Chidsey et al. first studied the electrochemistry of ferrocene alkanethiol SAMs in 1 M $HClO_4$.[252] Based on a close-packed layer of

electro active ferrocene groups modeled as spheres with a diameter of 6.6 Å (for the $\sqrt{3} \times \sqrt{3}$ R30° lattice on Au (111)), they estimated the maximum theoretical coverage on the plane gold substrate to be 4.64×10^{-10} mol cm^{-2}. The obtained surface coverage for **E3** is with $(4 \pm 1.3) \times 10^{-10}$ mol cm^{-2} close to the one expected for a compact monolayer on a plane substrate. Even though the topology of the electrodes coated with a dendritically grown organic film increases the surface area, the density of redox active subunits close to the theoretical value of a compact monolayer is impressive, demonstrating the potential of this technique.

According to the analysis of the electrode **E5** described in section 3.2.2 above, about 2×10^{-8} mol cm^{-2} were deposited from which 52% have lost their iodines during the electrochemical reduction procedure. Thus the number of iodophenyl subunits on **E5** is about 1×10^{-8} mol cm^{-2} and the electrochemically determined surface converge of 4×10^{-10} mol cm^{-2} suggests that about 4% of the iodines were transferred to a redox active ferrocene subunit. The bulky ethynyl ferrocene **61** can only react with accessible aryl iodides on the outside of the surface to form carbon ─ carbon bonds in the Sonogashira cross coupling reaction. Hence, the packing of ferrocenes in this case is not only determined by interaction between ferrocene redox centers, but also by the underlying layer of iodobenzene subunits exposed by the organic film.

The modification of the electrode surface **E3** was further studied by contact angle measurements. An increase of 10° was observed form the parent electrode **E5** (48 ± 1°) exposing iodophenyl groups to the ferrocene modified electrode **E3** (58 ± 1°), as shown in **Figure 50**.

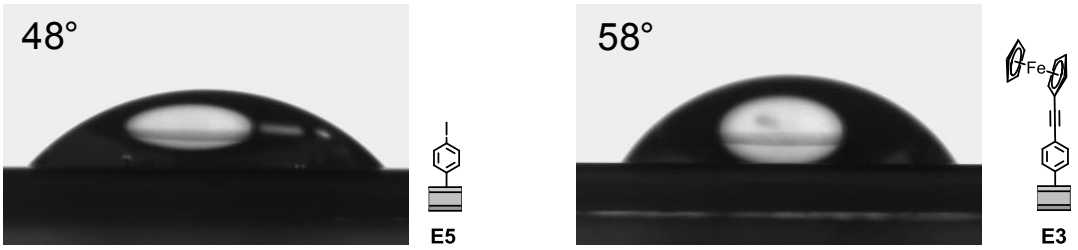

Figure 50 Static water contact angle picture of electrode **E5** (before the Sonogashira reaction) and electrode **E3** (after the Sonogashira reaction). The contact angles were measured at RT and calculated using the Young-Laplace equation.

AFM scratching experiments displayed an increase in film thickness of 0.2 nm from 3.4 ± 0.1 nm for the unmodified electrode **E5** to 3.6 ± 0.05 nm for the ethynyl ferrocene functionalized electrode **E3** (**Figure 51**). Estimations based on MM2 calculations predicted an increase of the van der Waals surface of only about 0.3 nm for the substitution of an iodine pointing perpendicular from the surface by ethynyl ferrocene. Hence, the observed value corresponds within the accuracy of the method to this expectation.

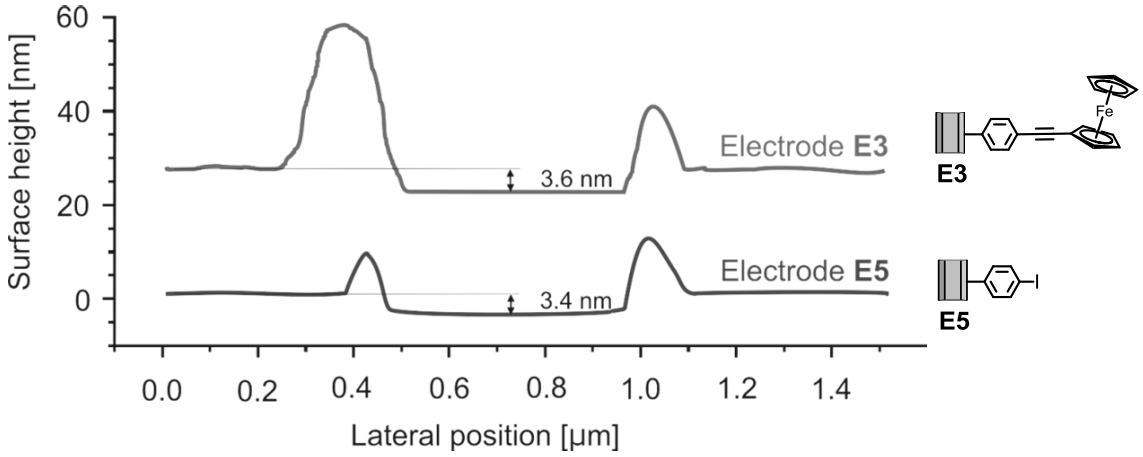

Figure 51 Lateral cut of the scratched squares of the AFM pictures for electrode **E5** (before Sonogashira reaction) and electrode **E3** (after Sonogashira reaction). The difference in high represents the layer thickness of the organic film on the platinum electrode.

The atomic composition of the coating of electrode **E3** was investigated by XPS experiments. The poor sensitivity of the method towards iron did not allow determining the amount of incorporated ferrocene subunits directly. Instead, the I/C ratio as a measure of the completeness of the substitution reaction was determined. For **E3** the I/C ratio was with 0.056 ± 0.02 significantly smaller than for the unmodified electrode **E5** (0.08 ± 0.04). The conversion efficiency was calculated in the same way as described in section 3.4.1 for electrode **E1**.

$$x = \frac{0.0144 \cdot C_{start} \cdot 100}{0.08 \cdot C_{start}} \% = 18\%$$

Thus, about 82% of the iodines remained and a “completeness” of the substitution reaction of about 18% was estimated based on the XPS data. This value is about

five times larger than the one determined by the electrochemical signal of the immobilized ferrocenes. Whether this difference is due to dehalogenation during the coupling reaction or due to electrochemically “silent” ferrocene subunits (e.g. located too far away from the platinum electrode) cannot be determined experimentally. Considering the experiences made with all acetylenes, our favored hypothesis is a decrease of the iodine content by dehalogenation during the coupling reaction as mentioned before in section 3.4.2.

3.4.4 BiEDOT-ethhynyl Functionalized Electrode (E4)

2,2’-bis(3,4-ethylenedioxythiophene) (BiEDOT) was not only of particular interest as another redox active subunit, but also as potential electrode functionalization enabling the growth of a conjugated EDOT polymer by electro polymerization on the pre functionalized electrode surface. After exposure of the iodophenyl electrode **E5** to the general coupling protocol with the BiEDOT-acetylene **54** (see section 3.3.2), the BiEDOT functionalized electrode **E4** was obtained.

To demonstrate the covalent immobilization of the BiEDOT-acetylene **54** the functionalized electrode **E4** was investigated by electrochemistry. Cyclic voltammetry using electrode **E4** as the working electrode, an Ag/AgCl reference electrode and a platinum wire as counter electrode showed a typical redox signature. [134][237] The CV displayed in **Figure 52** (solid line) showed an oxidation peak with a maximum at 729 mV and a broadened reduction peak at about 100 mV for the BiEDOT functionalized electrode **E4**. The iodophenyl functionalized electrode **E5** did not display redox activity in this potential range (dashed line in **Figure 52**). The two redox peaks clearly demonstrated the presence of BiEDOT units at the surface **E4**. To exclude non specific bound BiEDOT acetylenes **54** as the origin of the redox peak of electrode **E4**, the same control experiment as described above (see section 3.4.3) with electrode **E6** lacking the iodophenyl groups required for the Sonogashira coupling reaction was performed. After the exposure of **E6** to the same general Sonogashira coupling conditions the electrode still did not display any redox activity in the voltage range in which **E4** displayed the

BiEDOT redox chemistry. This corroborates that the origin of the electrochemical signals of **E4** are due to covalently immobilized BiEDOT functionalities at the electrode surface.

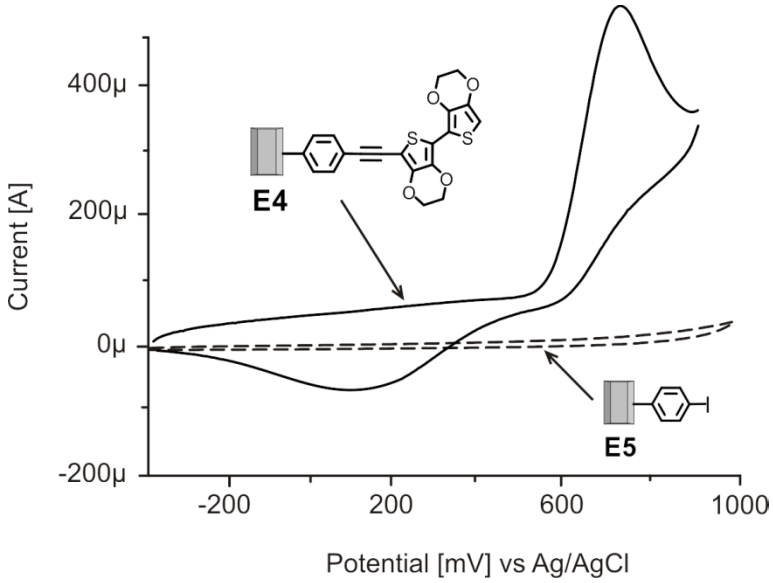

Figure 52 CV before and after the Sonogashira cross coupling reaction with BiEDOT acetylene **54**. The surface **E5** is redox inactive (dashed line) before the modification step but the surface **E4** is redox active (solid line) after the modification. The CV measurements were performed in acetonitrile, 100 mM $TBABF_4$, and with a scan rate of 100 mVs^{-1}. Reference electrode Ag/AgCl.

The contact angle of a static water droplet of electrode **E5** and **E4** is displayed in **Figure 53**. Upon immobilization of the BiEDOT-acetylene **54** on electrode **E4** the contact angle was shifted to a slightly higher value (52 ± 2°) compared with the iodophenyl electrode **E5** (48 ± 1°). As the hydrophobicity of the surface did not significantly change upon functionalization with BiEDOT-acetylene **54** the change of the contact angle was expected to by small.

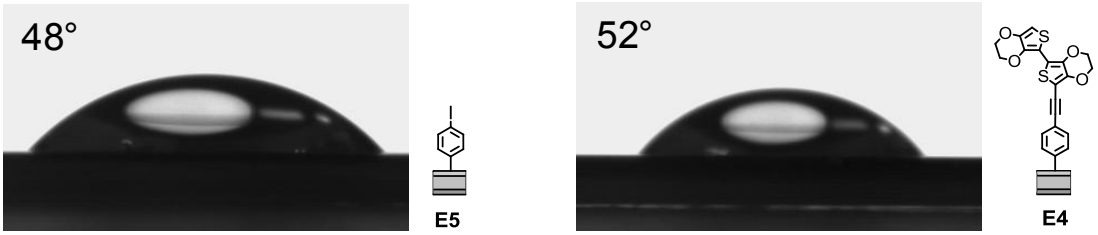

Figure 53 Static water contact angle picture of electrode **E5** (before the Sonogashira reaction) and electrode **E4** (after the Sonogashira reaction). The contact angles were measured at RT and calculated using the Young-Laplace equation.

The film thickness was also determined by AFM scratching experiment (**Figure 41**). In **Figure 54** the obtained lateral cuts of the scratched squares are displayed and an increase of about 1.75 nm was measured. Based on MM2 estimations an increase of about 0.7 nm was expected. This rather large value may point to a swelling of the film due to sterical requirements of the BiEDOT molecule. Not only the thickness was increased but also the roughness of the electrodes surface **E4** was slightly inhomogeneous and showed some little debris on the surface, which can also be attributed to a certain local surface polymerization of the organic film.

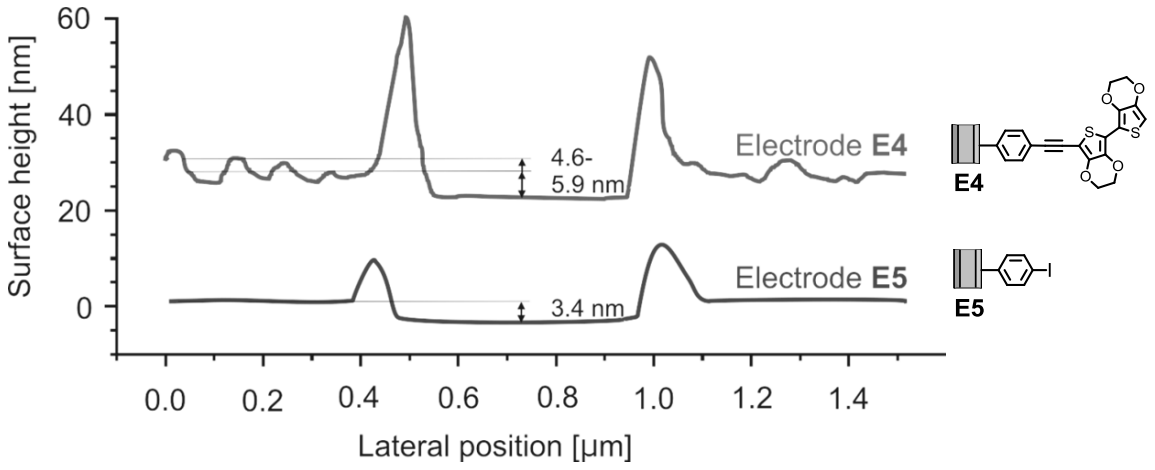

Figure 54 Lateral cut of the scratched squares of the AFM pictures for electrode **E5** (before Sonogashira reaction) and electrode **E4** (after Sonogashira reaction). The difference in height represents the layer thickness of the organic film on the platinum electrode.

The atomic composition of electrode **E4** was analyzed by XPS in order to study the extent of iodine substitution during the coupling reaction. With an I/C ratio of 0.06 ± 0.02, the conversion efficiency was calculated in the same way as described in section 3.4.1 for electrode **E1**.

$$x = \frac{0.0109 \cdot C_{start} \cdot 100}{0.08 \cdot C_{start}} \% = 14\%$$

Hence, about 14% of the initially present iodines were substituted by a BiEDOT acetylene **54**. Initial ideas to benefit from the oxygen atoms present in the acetylene as additional XPS label turned out to be troublesome. The oxygen content of these films tends to vary considerably (from electrode to electrode as well as from measurement to measurement) probably due to various oxide species on the platinum surface such as platinum oxides.

In conclusion, we successfully decorated the electrode surface with BiEDOT which is even more sterically demanding than ferrocene.

3.5 Conclusion of Platinum Electrode Modification

In this section a new modular technique for the functionalization of platinum electrodes was discussed. Combining the technique of electro reduction of aryl diazonium salts with Sonogashira cross coupling reactions, it is possible to modify platinum surfaces with a high surface coverage. This new technique allows introducing of a wide range of functional groups onto an electrode surface. To demonstrate the scope of this method, platinum electrodes were functionalized with four different acetylenes **54**, **58**, **60**, **61** resulting in four different surface functions. Namely a simple alkyl chain as an insulating layer (electrode **E1**), a more bulky substituent with further functionalization options (electrode **E2**), a redox active ferrocene species (electrode **E3**) and a redox active BiEDOT functionality (electrode **E4**) paving the way towards the growth of a conjugated EDOT polymer by electro polymerization directly on the electrode's surface.

The electro reduction of the diazonium salt yielded in a dendritic growth of multilayers (about 5 layers). According to the surface analysis, the Sonogashira cross coupling reaction of sterically demanding acetylenes mainly occurred at exposed iodophenyls at the surface. Considering the experiences made with all acetylenes, a decrease of the iodine contents by dehalogenation during the coupling reaction was found.

Furthermore, the molecular carpet made of iodophenyl moieties after electroreduction of *para*-iodophenyl diazonium salt **48** allows further functionalization by Sonogashira cross coupling reactions. The reaction completeness estimated using XPS, the moderate increase in film size and the quantification of the CV scans consistently indicate a significant conversion at the electrodes surface

The investigations discussed here pave the way towards further possible functionalization of electrodes. The subsequently described conducting biphenyl with an azobenzene bridge could act as a potential switching unit on an electrode. Thanks to the integration via Sonogashira cross coupling reaction a broad variety of functional molecules are accessible.

4 Switchable Conducting Azo Biphenyls

The exact understanding of charge transport properties of molecules in single metal–molecule–metal junctions is of great interest and represents a key step towards the realization of molecular based electronics.[154][156][179] The concept of molecules as tailor made functional building blocks with atomic precision for electronic applications ranging from single molecules,[153][253] through molecular devices,[254]-[258] to bulk materials leads to new challenges in organic chemistry. Of particular interest are conjugated π systems as their delocalized electrons are expected to considerably favor electronic transport through their planer structures. Thus π conjugated molecules, either as single molecule wires,[136][154][156] or as polymers,[259]-[262] have received considerable attentions as potential functional subunits or materials in emerging areas such as molecular electronics,[263] photovoltaics,[264][265] or light emitting systems.[266] A detailed understanding of the structural factors controlling electron transport processes is not only of fundamental interest, but also a crucial requirement for the development of design criteria.[178]

Theoretical studies towards biphenyl systems[164][165][175][176] and molecular junctions comprising biphenyls have gained considerable attention over the last decade. [163] The physical properties of biphenyls can be altered by different parameters. In particular the electron density in the phenyl rings[267] and the torsion angle between both phenyl rings play an important role in the transport properties through a biphenylic system.[157][177][179] The systematic variation of the torsion angle (θ in biphenyl subunits with almost negligible alterations in electronic properties of the phenyl rings was found to show a linear correlation of the single molecule conductance with the $\cos^2 \theta$ of the torsion angle.[179]

A new approach towards novel molecular switches and memory devices based on “mechanical” motion in molecular biphenylic structures is introduced here. In particular biphenyl systems possessing electronic transport properties depending on an intramolecular torsion angle of the two neighboring π-systems are interesting.[176][179] In a bridged biphenyl system (**Figure 55A**), the torsion angle (θ) and thus the electronic conductance of the molecule, depends on the length of the linking chain.[179] The torsion angle between the two phenyl rings is dictated by the

number of CH_2 units and thus the π-electron delocalization. The overall electronic structure and the length of the molecule are maintained. Furthermore the rather rigid cyclic structure and the thermal fluctuation around the equilibrium values of the torsion angle are expected to be reduced.

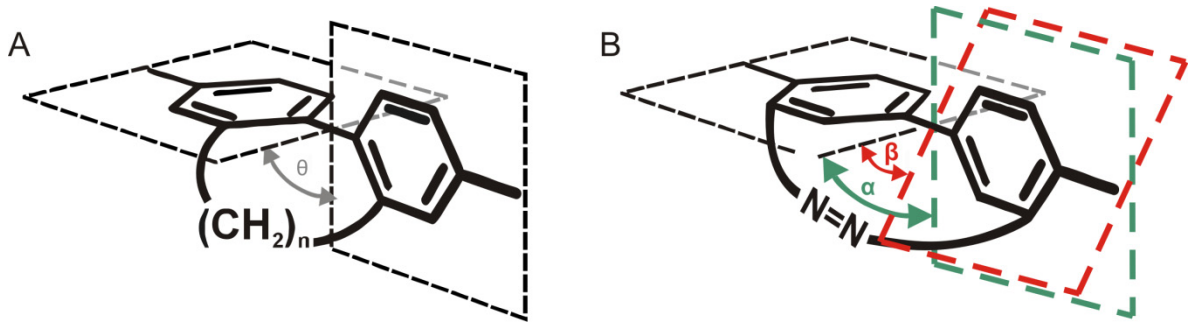

Figure 55 (A) The fixed interplanar torsion angle θ of the biphenyl system is adjusted by the length of the interlinking alkyl chain.[157] (B) The interplanar torsion angle can by varied between α and β by altering the conformation of the azo functionality.

In order to alter the transport properties by an external stimulus, such as light, we planned to integrate bistable molecular sub units with state dependent length as bridging systems. Potential candidates as bridging sub units are azo compounds due to their optically addressable *cis*/*trans* isomerization (**Figure 55B**).

The mechanically controllable break-junction (MCBJ) technique has become a valuable tool to investigate the correlation between molecular structures and electronic properties on a single molecule level.[268]-[270] The systematic variation of the molecular structure enabled fundamental MCBJ experiments that revealed the molecules symmetry,[271] the reduced electronic conductance of separated π-systems[272] and the investigation of *meta*-position immobilized rods.[159] Furthermore, even single molecule diode,[273] and recently the transport properties in correlation to the torsion angle of a biphenyl system have been realized.[177][179]

The envisaged molecular switch, based on light induced “mechanical” motion in a molecular biphenylic structures assembled between two gold electrodes in a MCBJ is shown in **Figure 56**. By irradiating light at a specific wave length the biphenylic system can be switched between an “on – state” (**Figure 56A**) and an “off – state”

(**Figure 56B**). MM2 calculations[274] have shown a highly conducting conformation (**Figure 56A**) with both phenyl rings almost planar to each other for an azo *cis* isomer as bridging unit. In contrast to that, a low conducting state (**Figure 56B**) with both phenyl rings almost perpendicular to each other is expected for an azo *trans* isomer as bridging unit.

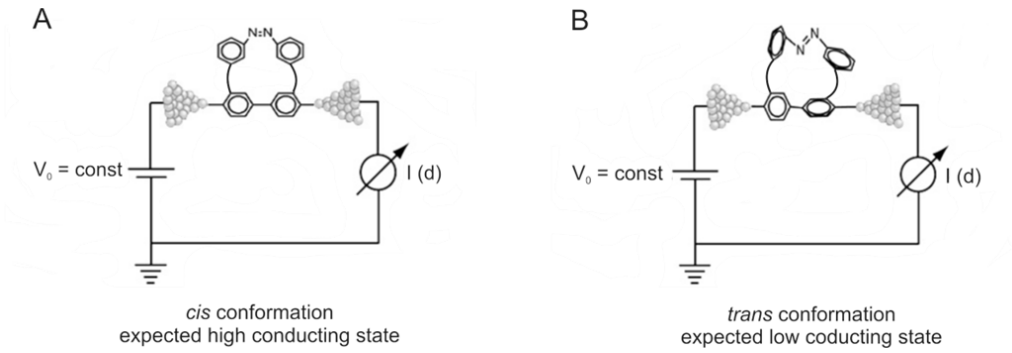

Figure 56 Light driven molecular switch assembled between two gold electrodes in a mechanically controllable break-junction (MCBJ). (A) “On – state” with phenyl rings almost planar to each other when having a *cis* conformation of the azo unit. (B) “Off – state” with phenyl rings almost perpendicular to each other when having a *trans* conformation of the azo unit.

With a modular design, the investigation of the switching behavior of these derivatives will not be limited to single molecule investigations in the MCBJ. The modular synthesis allows the functionalization with different terminal groups. For the industry the integration of potential light driven switches into CMOS devices is of great importance.[121]

4.1 Molecular Design of Azo Biphenyls

For the integration of the required properties and for a successful synthesis a clever molecular design is of prime importance. In **Figure 57** the principle construction plan of a biphenyl system including a sub unit which allows altering the torsion angle between the two phenyl rings is shown.

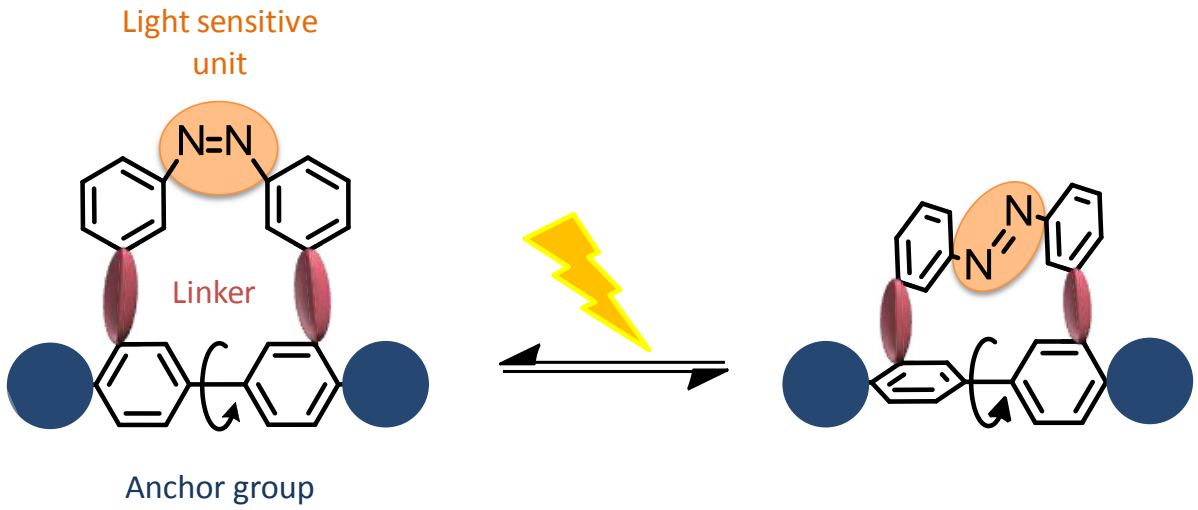

Figure 57 Schematical construction plan of a light sensitive biphenyl system. With anchor groups to attach to different possible surfaces and setups; with a light sensitive unit (preferable an azo function) and with a linker between the photo sensitive unit and the biphenyl.

The light sensitive unit is given by an azo functionality, building on the previous work (section 2 Azo Macrocycles) where a broad experience of azo groups was collected. But an azo functionality also has important advantages over other light sensitive units. The switching behavior of azo compounds is well understood[48] and causes a significant difference of the exterior form depending on the present state of the isomerization. The spatial difference of the *cis* and *trans* isomer of an azobenzene is significant, but to pass this spatial alteration to the biphenyl systems the linking part is as important as the altering unit itself. While too short and stiff linkers would hinder the *cis*/*trans* isomerization of the azo unit an overly flexible linker would weaken the altering information to the biphenyl system. Another important point is the electron density in the phenyl ring of the biphenylic system, since it also affects the transport properties of the biphenyl.[267] For all this reasons

the best linker would be a short alkyl chain. But also a linking via a hetero atom such as oxygen or sulfur would be possible; in this case a more general strategy could be envisaged (see section 4.3 Second Generation of an Azo Bridged Biphenyl).

In comparison to previously reported azo functionalized small ring systems[47][77][182] and based on preliminary calculations, a macrocycle with a small CH_2 linker is flexible enough to allow the optically triggered *cis*/*trans* isomerization reaction. Owing to the short and stiff linker, the spatial difference of the linking subunits is expected to considerably alter the rotation angle between both neighboring phenyl rings in the biphenyl backbone.

In order to design a modular switchable biphenylic system which is easy adaptable to different applications and physical setups a careful choice of the anchor group is crucial. A schematical overview of possible modification reaction for different anchor groups is shown in **Figure 58**.

To achieve generally interesting model structures the terminal functional group modification should be performed in the very last step. To enable functionalization and/or integration into molecular devices and materials, the anchor groups of the biphenylic systems were functionalized in *para*-positions in order to guaranty the best possible transport properties.[136][273] Typical leaving groups for further modifications such as halogen atoms or triflate groups were envisaged. Such bromine-, iodine- and triflate functionalized building blocks are suitable candidates for a series of different modification reactions. Besides the palladium catalyzed cross coupling reactions such as Sonogashira – Hagihara-,[146][148] Suzuki-,[192]-[194] Hartwig – Buchwald-,[36][275][276] Heck-[277][278] or Stille reactions;[279] these halogen building blocks would also be suitable for Sandmeyer-,[280]-[282] Appel-[283] and even S_NAr-type[178][204] reactions. Furthermore, metal mediated reaction such as Ullmann-[284] and Grignard reaction[285] can be envisaged as well.

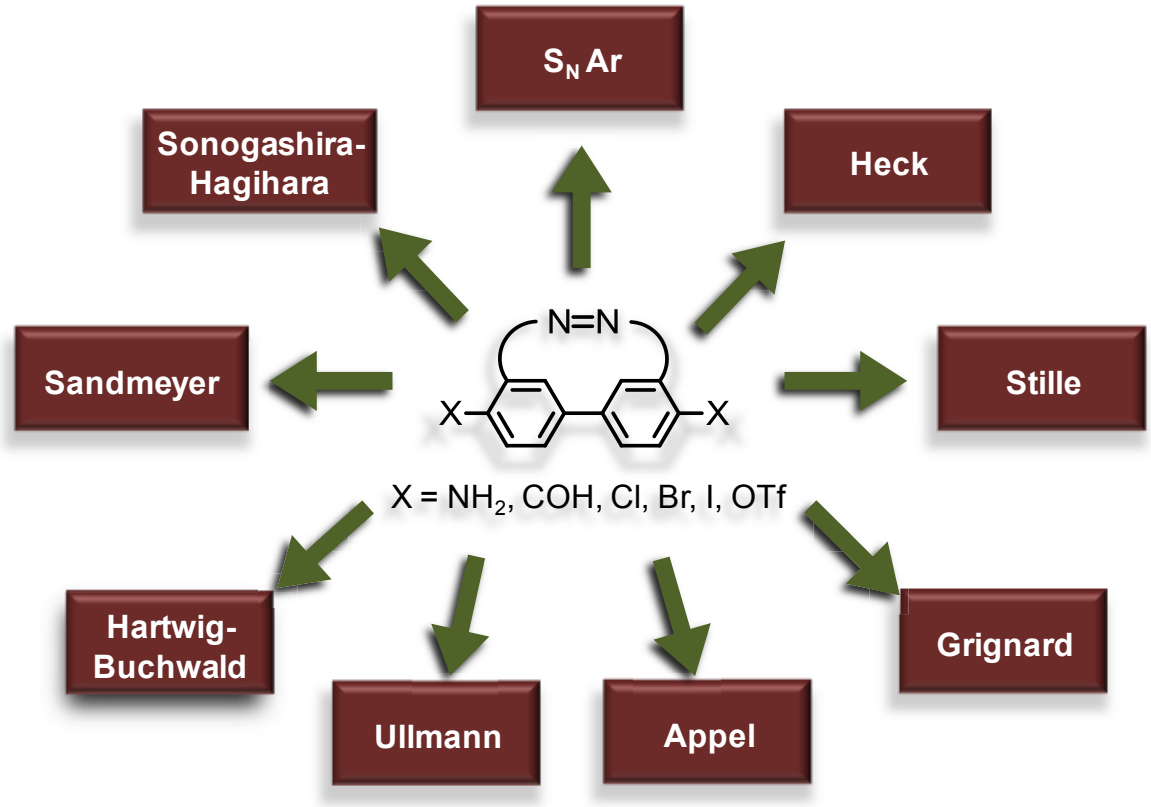

Figure 58 The biphenyl is bridged by a linker and light sensitive azo unit. The biphenylic building block is terminally *para* functionalized with leaving groups X. The various leaving groups of the modular building block provides substrates for many reactions, such as Sandmeyer-, Sonogashira – Hagihara-, Heck-, Stille-, Appel-, Ullmann-, Hartwig – Buchwald-, Grignard or S_NAr type reactions.

4.2 First Generation of an Azo Bridged Biphenyl

In this section the first generation of an azo bridged biphenyl **76** is described (**Figure 59**). The first envisaged biphenyl **76** is based on the smallest possible linker, namely a CH_2 unit and halogenides as precursors for the introduction of different possible anchor groups. The ring strain of such a small cyclic molecule is not insignificant but based on MM2[274] calculations the macrocycle **76** should be flexible enough to allow the optically triggered *cis*/*trans* isomerization and should lead to a significant difference of the torsion angle between the two phenyl units of the biphenylic system.

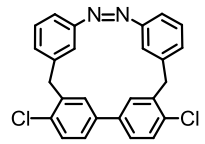

Macrocycle **76**

Figure 59 Azo bridged biphenyl with a CH_2 linker and halogenides as functional groups, allowing the introduction of different possible anchor groups.

4.2.1 Retro Synthesis

The cyclic target structure **76** consists of a biphenyl and an azobenzene interlinked by a short CH_2 alkyl chain. An overview of the retro synthesis is shown in **Scheme 30**.

The key step in this pathway will be the cyclization together with the formation of the azo joint. The previously investigated reductive cyclization procedure with lithium aluminium hydride (section 2 Azo Macrocycles) allows the closing of the ring with the formation of the azo joint. The azo functionality could also be built via an oxidative procedure,[16][30][216] but owing to the synthetic availability of the precursors, a reductive procedure was favored.[180] A Suzuki cross coupling reaction should provide the dinitro functionalized precursor **70** for the subsequent reductive cyclization reaction. The dibromo precursor **69** for the Suzuki reaction can be provided by a bromination of 4,4'-dichloro-3,3'-dimethyl-1,1'-biphenyl (**68**). Through a benzidine rearrangement from commercially available 2-nitro-

toluene (**66**) the 3,3'-dimethyl-[1,1'-biphenyl]-4,4'-diamine (**67a**) will be obtained. A subsequent Sandmeyer reaction will provide chlorines as potential leaving groups in *para* positions of the biphenyl for further functionalization with different anchor groups at a later stage of the synthesis.

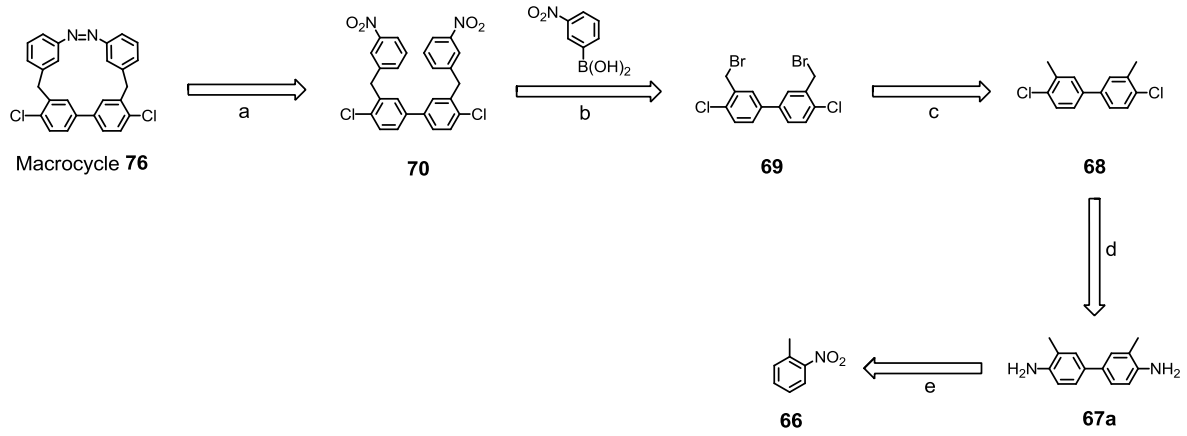

Scheme 30 Retrosynthetic scheme for the synthesis of an azo bridged biphenyl **76** with a CH_2 linker. (a) Reductive azo formation. (b) Suzuki cross coupling reaction. (c) Bromination. (d) Sandmeyer reaction. (e) Benzidine rearrangement.

4.2.2 Synthesis and Characterization of the first Biphenyl Generation

Initially the dinitro precursor **70** for the final cyclization reaction was synthesized. Later the focus will then be changed to the different possible anchor groups in *para* positions of the biphenyl and to the final cyclization step. The synthesis to the dinitro intermediate **70** is shown in **Scheme 31**.

The dichloro biphenyl intermediate **68** was obtained in two steps from commercially available 2-nitrotoluene (**66**). The terminally amino functionalized biphenyl structure comprising two methyl groups in the 3,3' positions **67** was assembled in a benzidine rearrangement from commercial 2-nitrotoluene (**66**). Contrasted from the literature[286][287] the reaction mixture was heated to 80°C-90°C and the reaction time was elongated to 2 hours, in order to increase the yield to 88%. After acidification the product **67** was isolated as the dichloride salt. In a Sandmeyer type reaction both ammonium groups of **67** were substituted by chlorides. To

obtain acceptable yields the literature procedure[286][288] had to be adapted, as follows. The biphenyl **67** was first treated with sodium nitrite and an aqueous hydrochloride solution at -5°C. The -5°C cold freshly prepared diazonium solution was then added over a period of 30 min to a 100°C warm aqueous acidic copper(I)chloride solution. After purification by column chromatography with silica gel the chlorinated biphenyl **68** was isolated as a white solid in 30% yield. As byproduct the monochlorinated compound was also isolated. While elongation of the reaction time to 1.5 hours reduced the byproduct to 15%, further elongation reduced the overall yield below 30%, hence 2 hours turned out to be the best reaction time. Following a known one pot procedure[289] for delicate Sandmeyer type reaction with copper(II)chlorides the yield could not be further improved. The Sandmeyer reaction with the methyl group in *ortho* position turned out to be much more challenging compared to the reaction when the methyl group is in *meta* position,[178][286] possibly due to a change in the relative solubility of the salt.

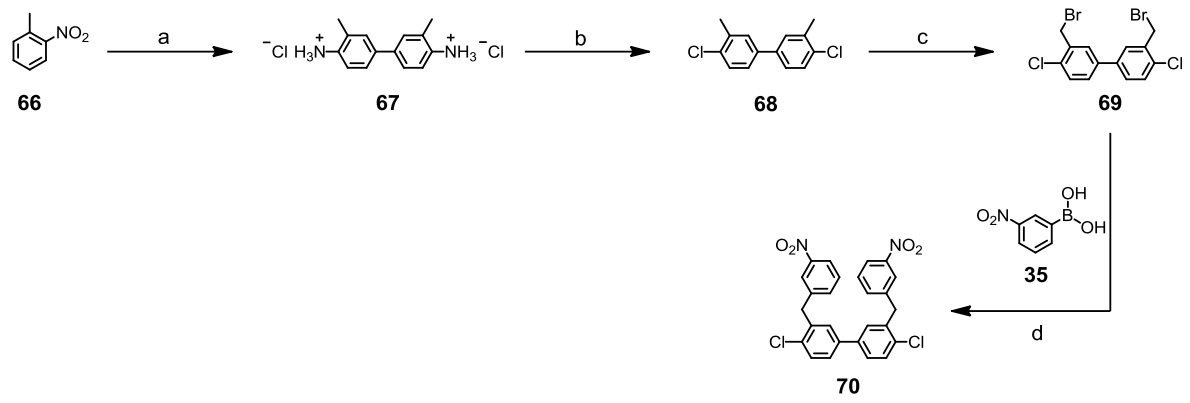

Scheme 31 Synthetic route to the dinitro intermediate **70**. Reagents and conditions. (a) Zn, NaOH, EtOH, H_2O, 90°C, 2 h, 88%. (b) 1) conc. HCl, $NaNO_2$, H_2O, -10°C, 30 min. 2) CuCl, H_2O, 100°C, 30 min, 30%. (c) NBS, CCl_4, hv, reflux, $(PhCO_2)_2$, 2 h, 58%. (d) $[Pd(PPh_3)_4]$, K_2CO_3, $CH_3C_6H_4CH_3$, 130°C, 10 h, 30% or $[Pd(PPh_3)_4]$, K_2CO_3, $C_6H_5CH_3$, EtOH, 85°C, 30 min in MW, 95%.

The biphenyl **68** was subsequently brominated in carbon tetrachloride with *N*-bromosuccinimide (NBS) and benzoyl peroxide as a radical starter. The reaction mixture was irradiated with visible light (200 W) at such a distance from the reaction flask that reflux was maintained. After 2 hours of irradiation the reaction

mixture was cooled to 0°C and the white precipitate was filtered off. After recrystallization the brominated biphenyl **69** was isolated as a white powder in a yield of 58%. By decreasing the reaction time from 18 hours to 2 hours the over bromination, which is known to be a major problem of radical bromination,[290] could be minimized and the overall yield was increased from 30% to 58%.

The subsequent Suzuki cross coupling reaction of a benzylic bromide **69** and an aryl boronic acid **35** behaved similar to the one discussed in section 2.2.3.2. While conventional conditions in *m*-xylene at 130°C afforded the product **70** only in 30% yield, the yield was increased by using microwave conditions to an excellent 95%. In an inert argon atmosphere 2.6 equivalents of the commercially available 3-nitrophenyl-boronic acid (**35**) and the dibromo biphenyl **69** with 10 mol-% [$Pd(PPh_3)_4$] and potassium carbonate as base were dissolved in a solvent mixture of toluene:ethanol (3:1). The reaction mixture was heated using microwave conditions to 85°C for 3 hours and provided after column chromatography with silica gel the desired dinitro compound **70** as a white powder.

4.2.2.1 Reductive Azo Formation

With the dinitro intermediate **70** in hand, the two key steps, namely the cyclization reaction and the introduction of the desired anchor groups were investigated. The two synthetic steps are shown in **Scheme 32**.

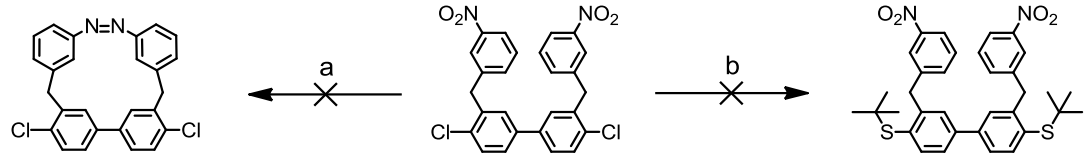

76 **70** **75**

Scheme 32 Synthetic strategy towards macrocycle **76** and sulfur functionalized biphenyl intermediate **75**. Reagents: (a) $LiAlH_4$, THF. (b) NaS-*tert*-butyl, DMI.

First we focused on the cyclization to the target macrocycle **76**. Since a reductive azo cyclization procedure with dinitro precursor was investigated (see section 2 Azo Macrocycles) similar conditions were applied here. To avoid excessive polymerization high dilution conditions were chosen. In order to guaranty the best possible conditions the tetrahydrofuran was dried over potassium and sodium and the lithium aluminium hydride was used freshly. All reactions were carefully performed using Schlenk technique under an argon atmosphere. In **Table 6** the different reaction conditions are listed.

Table 6 Different reaction conditions for the key cyclization together with the azo formation. All reactions were performed under inert atmosphere, in dry THF (dried over K and Na) and a freshly distilled 1 M $LiAlH_4$ solution in *n*-hexane was used. $NaBH_4$ powder from *Aldrich* was used as received.

entry	reducing agent	concentration of **70** [mol/L]	temperature [°C]	reaction time [h]	yield
1	$LiAlH_4$	5.0×10^{-3}	RT	2	no
2	$LiAlH_4$	5.8×10^{-4}	0-5°C	2	traces
3	$LiAlH_4$	5.8×10^{-4}	0°C	10	traces[a]
4	$LiAlH_4$	5.8×10^{-4}	40°C	2	no[b]
5	$LiAlH_4$	5.8×10^{-4}	reflux	2	no[b]
6	$LiAlH_4$	5.8×10^{-4}	-10°C	4	traces[c]
7	$LiAlH_4$	6.6×10^{-5}	0°C	6	traces[d]
8	$NaBH_4$	5.8×10^{-4}	0°C	6	no[e]
9	$NaBH_4$	5.8×10^{-4}	RT	6	no[e]

[a] after about 6 h, decomposition was observed.
[b] slowly decomposition of starting material, extensive formation of polymers.
[c] at least 50% starting material was isolated, almost no conversion.
[d] much slower conversion compare to entry 2.
[e] almost no conversion.

All reactions had the unwanted polymerization in common. As already investigated above a slow addition of the reducing agent is required, the best results were obtained with a continuous addition over a period of about 1 h. The temperature plays also a very important role, if the temperature is too low (<RT) the complete

reduction to the amine is favored over the selective reduction to the nitroso compound, which can further react and form the azo joint. But if the temperature is too high (>40°C) it seems that the formation of larger polymers is favored and significant decomposition of the starting material **70** and/or the product **76** occurred (entry 4 in **Table 6**). At temperatures <0°C the conversion was observed to be much slower, the same is true for high dilution conditions of 6.6×10^{-5} (40.0 mg of **70** in 1500 mL). In entry 5 the reaction temperature was increased in order to provide enough energy to overcome the expected ring strain in the cyclic system, but also here mostly decomposition was observed.

As another option the reducing agent was changed from lithium aluminum hydride to sodium borohydride, but with the slightly decreased reactivity of the reducing agent almost no conversion was observed, even with increased reaction times (entry 8 and 9 in **Table 6**).

The best results were obtained at 0-5°C at a reaction time of 2 hours (entry 2 in **Table 6**), but even here the product was only observed in a MALDI-TOF mass spectrum from the crude reaction mixture (see **Figure 61B**). Beside the expected peak for the product **76** at 429.09, a peak at 862.82 was observed as well, this peak corresponds to the open fully reduced dimer **D76** (**Figure 60**).

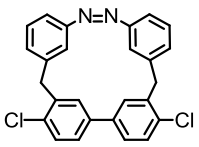

Macrocycle **76**
Chemical Formula: $C_{26}H_{18}Cl_2N_2$
Molecular Weight: 429.34

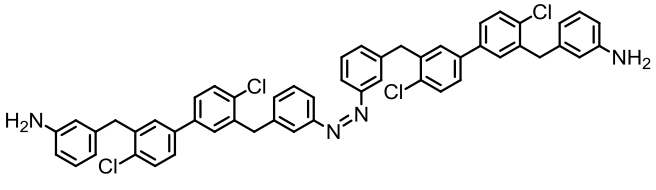

Reduced Dimer **D76**
Chemical Formula: $C_{52}H_{40}Cl_4N_4$
Molecular Weight: 862.71

Figure 60 Formed products in the reductive azo formation reaction.

In **Figure 61A** the GPC chart of the crude reaction mixture is shown, the chart displayed a main peak at a retention time of 7.51 minutes which clearly showed many impurities at almost the same retention time. At a shorter retention time of

3.68 minutes a small peak was detected which probably corresponds to the dimer **D76**, but due to the low yield of this peak (0.9%) it was not further analyzed. All attempts to purify the compound **76** failed, neither the purification by column chromatography with silica gel, nor a preparative TLC, nor preparative SEC (with a molecular weight of 429.34 g/mol is the product almost at the separation limit of SEC method), nor a crystallization was possible. Even so the product **76** was formed it turned out that the conversion towards the cyclized compound **76** is very weak and far away from an acceptable yield. Due to this fact and the lack of a purification method of the final cyclization, a different synthetic strategy has to be found (see below).

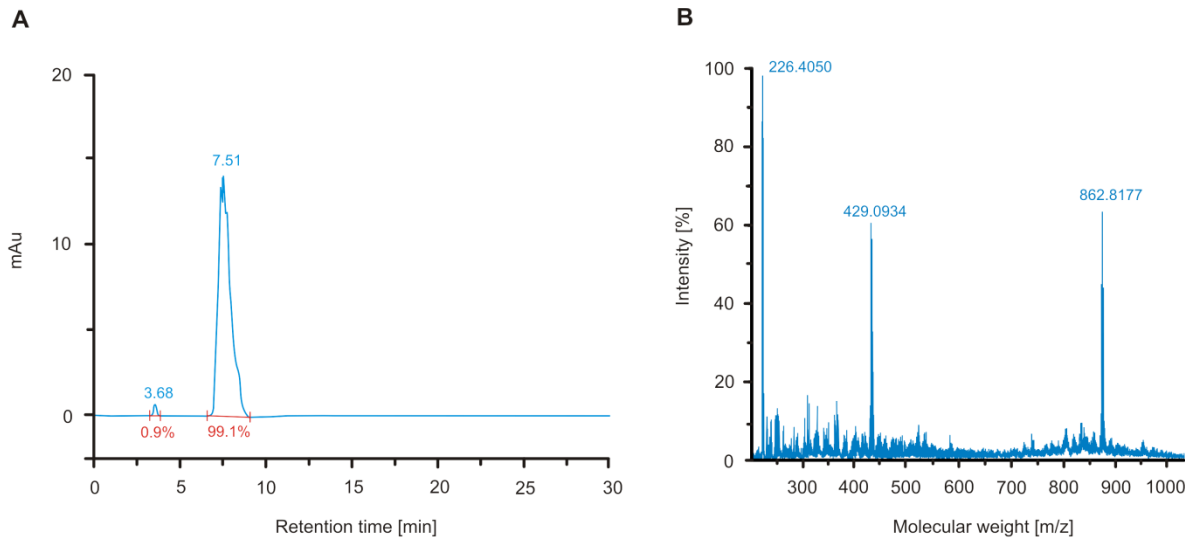

Figure 61 (A) GPC chart of the crude reaction mixture of the reductive cyclization reaction towards **76**. Analyzed in toluene with a flow rate of 0.5 mL/min at λ = 220 nm. The integrations are shown in red and the retention times in blue. (B) MALDi-TOF mass spectrum of the crude reaction mixture showing peaks at 429.0934 (product **76**) and 862.8177 (dimer **D76**).

The intermediate **70** with its two chlorides in *para* position of the biphenyl is also a potential precursor for the introduction of a sulfur anchor group (**Scheme 32**). Sulfur functionalities can be introduced to aryl chlorides by a nucleophilic aromatic substitution reaction.[30][221][222] Applying similar conditions to compound **70**, no conversion at all was observed even in refluxing 1,3-dimethyl-2-imidazolidinone

(DMI) (bp. 226°C). The anchor group can also be introduced as acetyl protected sulfur[178] and not necessarily as *tert*-butyl protected sulfur, but for the subsequent reaction steps the more stabile *tert*-butyl protecting group is essential. The introduction via an acetyl protected sulfur needs to be the final reaction step in the synthesis. Due to this fact, the focus of the synthetic strategy was first to find a suitable strategy for the cyclization and to form a biphenyl interlinked by an azobenzene bridge.

4.2.2.2 Palladium Catalyzed Azo Formation

A further option for a possible cyclization including the azo formation is the palladium catalyzed coupling reaction of aryl hydrazides with aryl halides followed by direct oxidation (**Scheme 34**).[35][186] For this approach a halogenide functionalized precursor is needed. In **Scheme 33** the synthesis to an iodide functionalized biphenyl precursor is shown.

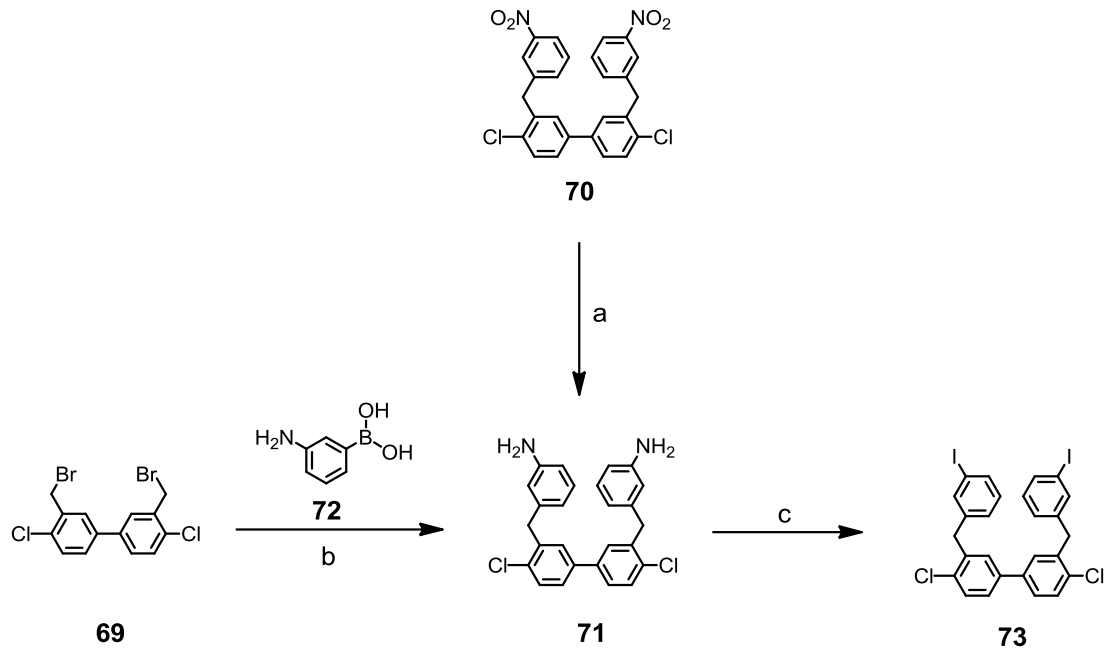

Scheme 33 Synthetic route to the diiodo intermediate **73**. Reagents and conditions. (a) Sn, conc. HCl, THF, RT, 2 h, 45%. (b) $[Pd(PPh_3)_4]$, K_2CO_3, $C_6H_5CH_3$, EtOH, 90°C, 20 min in MW, 51%. (c) 1) $NaNO_2$, conc. HCl, DMF, 0°C, 20 min. 2) CuI, aq. HCl, 50°C, 2 h, 9%.

The dinitro functionalized compound **70** was reduced with tin powder in concentrated hydrochloric acid,[25] after basic work up the reduced compound **71** was isolated as a white solid in a moderate yield of 45%. The diamino compound **71** was unstable and therefore no elemental analysis could be obtained.

In an alternative route (b in **Scheme 33**) the amine **71** was synthesized in a Suzuki cross coupling reaction. Applying literature known Suzuki reaction microwave conditions[180] the amine **71** was synthesized in a slightly higher yield of 51% compare to pathway a in **Scheme 33**. To further improve the yield, microwave assisted aqueous Suzuki cross coupling conditions were applied.[291] With these conditions the desired amine **71** was isolated as well, but only in 41% yield.

However, the amine **71** was synthesized and had to be directly exposed to Sandmeyer conditions, due to its instability.[280][281][292] The amine **71** was treated with sodium nitrite and concentrated hydrochloric acid, the obtained diazonium solution was cooled to 0°C and added over a period of 30 min to a solution of copper(I)iodide in an aqueous hydrochloride solution. The reaction mixture was stirred at 50°C for 2 hours and then purified by column chromatography with silica gel. The desired iodinated compound **73** was isolated as white solid in a yield of 9%. During the Sandmeyer reaction under the applied condition considerable chlorine-iodine exchange was observed, reducing the yield dramatically. However, the isolated amount of **73** was enough for further investigations (see below). To exclude a halogen exchange the molecule should bare a different anchor group to chloride and the reaction conditions need to be chlorine free. In section 4.4 the synthesis of a more stable methoxy functionalized precursor will be discussed on which some chlorine free acids as sulfuric acid and hydroiodic acid can be used for the Sandmeyer reaction.[281][293][294]

The palladium catalyzed coupling reaction of aryl hydrazides with aryl halides followed by direct oxidation is shown in **Scheme 34** and is envisaged as strategy for a cyclization together with an azo formation.[35][186] *Tert*-butyl carbazate (Boc-hydrazine, **A2**) is first cross coupled with an aryl halide **A1** and then further treated

with another aryl halide **A4** to form the diphenylhydrazine intermediate **A5** which is then oxidized to the azobenzene derivative **A6**. This synthetic procedure is applicable for symmetric and asymmetric reactions. The first coupling reaction to **A3** tolerates electron donating and electron withdrawing R-groups while the second coupling to **A5** is favored with electron withdrawing R'-groups.[39][295][296] In our case we therefore have a slight deactivation, but this method has been successfully applied to similar systems and was also used for a macrocyclization step for simple azobenzeneophanes.[38]

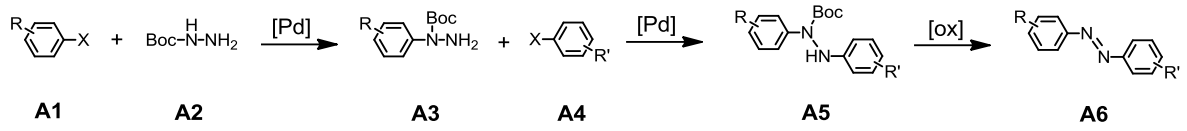

Scheme 34 Palladium catalyzed coupling reaction of aryl hydrazides with aryl halides followed by direct oxidation.[35]

In consideration of the fact, that the existing conditions are delicate some test reactions were performed, before using intermediate **73** which required 6 steps to prepare. The reaction scheme of the test reaction is shown in **Scheme 35**. While the electrochemical conditions can be simulated quite well with 3-iodotoluene **85** as starting material, the simulation of the expected ring strain in the macrocycle **76** is not possible with commercially available starting materials. By using the less expensive hydrazine compared to the expensive *tert*-butyl carbazate (Boc-hydrazine, **A2**) the reaction temperature needed to be increased, due to the slightly reduced activity of the hydrazine. In such palladium catalyzed Hartwig – Buchwald type reactions secondary amines are more reactive compare to primary amines,[35][275][296] but in order to investigate the conditions under the existing electrochemical conditions, this fact is irrelevant as on one point the primary amine has to react anyway in order to form the macrocycle.

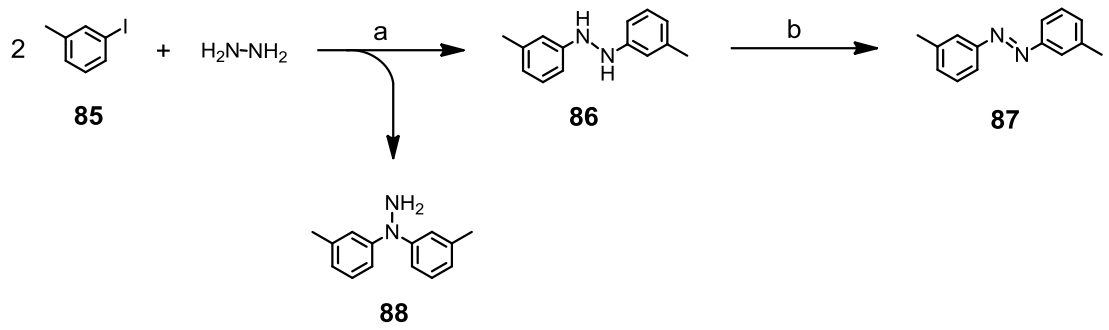

Scheme 35 Test reaction for a palladium catalyzed azo cyclization via a diphenylhydrazine intermediate **86**. Hydrazine was used as 1 M THF solution. (a) Reagents and conditions are listed in **Table 7**. (b) Different oxidation conditions.

However, 3-iodotoluene **85** was treated with a 1 M hydrazine solution in THF under an inert argon atmosphere, applying different possible reaction conditions (**Table 7**). First (entry 1, **Table 7**) general Hartwig – Buchwald conditions, with a stronger base (sodium *tert*-butoxide) were applied.[36][37] As expected, the secondary amine was found to be much more reactive and since just 2.0 eq. of 3-iodotoluene were used, the major product was compound **88** in a yield of 63%. Compound **86** could be found as traces in a crude MALDI-TOF mass spectrum. Similar results were found for palladium acetate as catalyst (entry 6, **Table 7**), while in all other attempts (entry 2-5, **Table 7**) hardly any conversion was observed.

The best conditions found (entry 1 and 6, **Table 7**) were also tested with the more expensive *tert*-butyl carbazate (Boc-hydrazine, **A2**) instead of simple hydrazine. With the applied conditions the tolylhydrazine **86** was formed and in situ oxidized, following the reported protocol,[35] to form the desired azo compound **87** (**Scheme 35**).

This successfully tested reaction conditions were now applied to the iodide functionalized biphenyl **73** (**Scheme 36**). For both conditions (entry 1 and 6, **Table 7**) no conversion towards a cyclized hydrazine derivative **74** was observed. The reaction was monitored by thin layer chromatography (TLC) and after a reaction time of 24 hours, instead of product formation, just a massive spot on the TLC base line was observed, pointing towards complete decomposition of the

starting material **73**. Neither a linear, nor a cyclic addition product could be found. Due to the fact, that the same reaction conditions were successful tested in an acyclic system (**Scheme 35**) it seemed that the problem of the ring strain is larger than expected. Since there was no conversion at all and more than that, the starting material was decomposed under the applied relatively harsh conditions there was no use to further follow this synthetic strategy. To overcome this problem a new and modular synthetic strategy is needed in order to reduce the ring strain in the closed system (see section 4.3 Second Generation of an Azo Bridged Biphenyl)

Table 7 Different reaction conditions tested for the palladium catalyzed diphenylhydrazine **86** formation ((a) in **Scheme 35**). All reactions were performed under an inert argon atmosphere using dry solvents.

entry	catalyst	ligand	base	solvent	temperature [°C]	reaction time [h]	yield
1	$Pd_2(dba)_3$	BINAP	NaO*t*bu	toluene	90	6	63%[a]
2	$Pd_2(dppf)_3$	-	$CsCO_3$	toluene	110	8	no
3	$Pd_2(dba)_3$	BINAP	$CsCO_3$	toluene	120	6	no[b]
4	$Pd_2(dba)_3$	BINAP	$CsCO_3$	toluene	RT→80	24	no[b]
5	$Pd_2(dba)_3$	BINAP	NaO*t*bu	toluene	RT→60	7	no
6	Pd(OAc)	xantphos	$CsCO_3$	DMF	RT→110	23	69%[a]

[a] traces of **86**, yield corresponds to the basically formed **88**.
[b] almost no conversion, starting material isolated.

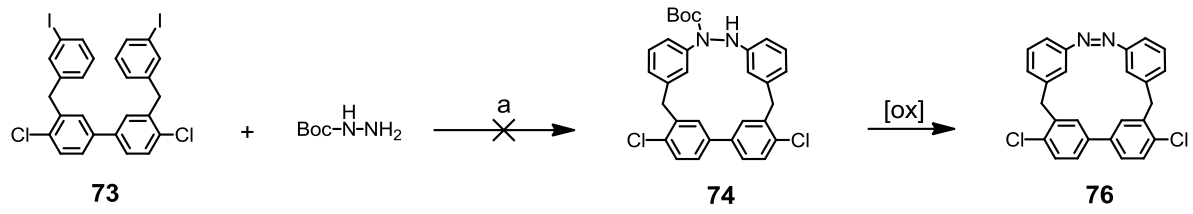

73 **74** **76**

Scheme 36 Synthetic route towards macrocycle **74**. Reagents and conditions: (a) $Pd_2(dba)_3$, BINAP, NaO-*tert*-butyl, toluene, RT → 90°C, 24 h or Pd(OAc), xantphos, $CsCO_3$, DMF, RT → 110°C, 24 h.

4.2.2.3 Oxidative Azo Formation

Similar to the extensively discussed reductive azo formation (**Scheme 37B**) an oxidative azo formation (**Scheme 37A**) starting from the amino precursor **71** is also possible.[29][30]

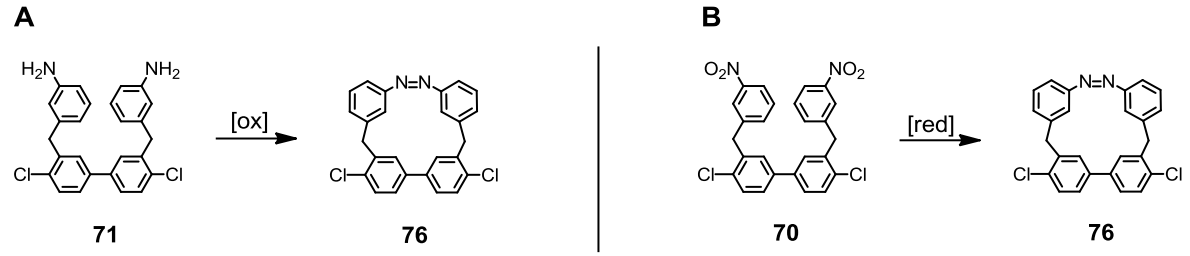

Scheme 37 Oxidative and reductive azo formation in the key cyclization step.

The amino precursor **71** was treated in three different reactions with different oxidizing agents, namely manganese(IV)oxide, sodium hypochlorite and silver(II)oxide. At low reaction temperatures (0°C-RT) hardly any conversion was observed. By increasing the reaction temperature up to 40°C, decomposition of the delicate amino precursor **71** began and some polymer formation was observed. Since for all oxidizing agent the same behavior was observed, no further reaction conditions were investigated. Closing the ring at one specific point turned out to be delicate, probably due to the increased ring strain of the closed system.

4.2.2.4 Cyclization via Suzuki Reaction

A final cyclization via Suzuki cross coupling reaction is the next investigated synthetic strategy, in the context of the first generation of an azo bridged biphenyl. In **Scheme 38** the synthesis of the boronic acid functionalized azobenzene **79** and the subsequent Suzuki cyclization step is shown.

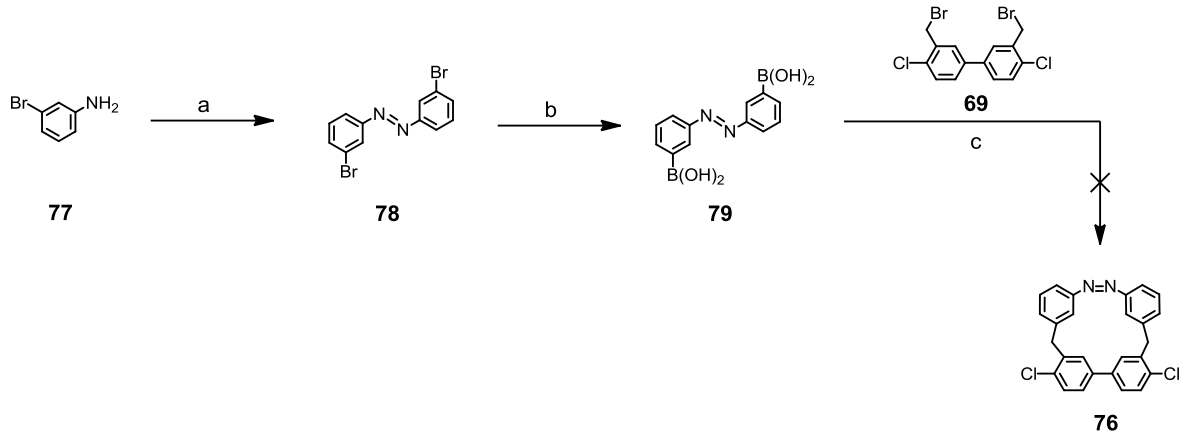

Scheme 38 Synthetic route to a boronic acid functionalized azobenzene **79**, as precursor for a cyclization via a Suzuki cross coupling reaction. Reagents and conditions: (a) MnO_2, $C_6H_5CH_3$, molecular sieves, RT → 110°C, 14 h, 85%. (b) *n*-BuLi, $B(OCH(CH_3)_2)_3$, THF, -78°C → -20°C, 2.5 h, 80%. (c) $[Pd(PPh_3)_4]$, K_2CO_3, $C_6H_5CH_3$, EtOH, 90°C, 20 min in MW.

3-Bromaniline (**77**) was oxidized with mangan(IV)oxide in toluene with molecular sieves (4 Å) instead of using a Dean-Stark apparatus.[297] The reaction mixture was heated to reflux for 14 hours and then filtered over a plug of *Celite*®. Column chromatography with silica gel afforded the azobenzene derivative **78** as an orange powder in a yield of 85%. The subsequent substitution of the bromines with the boronic acid functionalities turned out to be troublesome. The dibromo compound **78** was first treated with *n*-BuLi at -78°C for a bromine ─ lithium exchange. The lithiated compound was further reacted with triisopropylborate at -20°C and after quenching with aqueous hydrochloride the reaction mixture was filtered over a plug of silica gel to afford the product **79** as an orange resin in a crude yield of 80%.[222] Further purification was troublesome, since the boronic acid **79** already started to decompose in the timeframe of the ^{1}H-NMR measurement. Beside slight decomposition the formation of boroxine was also observed, but fortunately such boroxine are as reactive as boronic acids in Suzuki cross coupling reactions.[298] Normally, azo functions are not sufficiently stable to *t*-BuLi but it seemed that *n*-BuLi followed by subsequent quenching with aqueous hydrochloride solution did not destroy the azo functional group.[299] However, according to the analytical data from ^{1}H-NMR- and MALDI-TOF measurements the desired boronic acid **79** was formed and directly used for the subsequent Suzuki cyclization step without further purification.

The Suzuki cross coupling reaction for the cyclization (c in **Scheme 38**) was performed under similar conditions as already successfully investigated above for benzylic bromines (see section 4.2). To favor the cyclization reaction over the possible polymer formation, high dilution conditions (of at least 6.0×10^{-4} mol/L) were applied. The reaction was first performed using microwave conditions with $[Pd(PPh_3)_4]$ as catalyst and potassium carbonate as base in a solvent mixture of toluene and ethanol. Different reaction conditions ranging from temperatures (50°C to 120°C) and different reaction times (10 min to 60 min) were investigated. All applied conditions resulted in extensive polymer formation at which no product **76** could be detected, neither in MALDI-TOF mass spectrometry nor in LC-MS.

In order to reduce the reactivity of the Suzuki cross coupling conditions, standard conditions were also applied. The reaction was performed with $[Pd(PPh_3)_4]$ as catalyst and potassium carbonate as base in a solvent mixture of toluene and ethanol under an inert argon atmosphere. The reaction temperature was slowly increased form 0°C to 60°C while the conversion was monitored by thin layer chromatography (TLC). At a temperature of about 30°C first conversion was observed. By continuous increasing the temperature every 5°C a test sample was investigated in order to analyze the product formation by mass spectrometry. After reaching 60°C no starting material was left and no product could be detected neither. Since the conversion of the Suzuki reaction was closely monitored and despite that no cyclized product **76** could be observed pointed to a strategic problem of the synthesis.

All this investigations show clearly the need of a completely new synthetic strategy. Especially the internal ring strain was found to be a major problem therefore a modular strategy, where the length of the linker can be varied, was envisaged.

Even if the cyclization is possible, there is still a certain chance that the ring strain may be so large as it preclude the possibility of the formation of an *trans* conformation.

4.3 Second Generation of an Azo Bridged Biphenyl

In this section the second generation of an azo bridged biphenyl (**Figure 62**) is described. The main difference in this series of envisaged biphenyls, compared to target macrocycle **76** (described in section 4.2) is the modularity of the alkyl linker. With this approach different linker length between zero and two CH_2 units including a heteroatom can easily be introduced. This variation of the linker allows the stepwise reduction of the ring strain, the longer the linker, the lower the ring strain. But in contrast to a desired low ring strain for the synthesis a high stiffness is required for a significant change in the torsion angle between the two phenyl units while switching the azo unit between its *cis* and *trans* conformation. Based on MM2[274] calculations for each additional CH_2 unit the ring strain is reduced by about 5 kcal/mol.

The disadvantage of the reduced ring strain is, as already mentioned, the smaller change in the torsion angle after the isomerization reaction. While a simple CH_2 linker seemed to be too stiff a linker, longer then two CH_2 units may lead to a difference of the torsion angle of less than 10° and is therefore impracticable for switching experiments, as a higher difference in the torsion angle is required in order to sufficient effect the conductance for measurements in the mechanically controlled break junction (MCBJ).

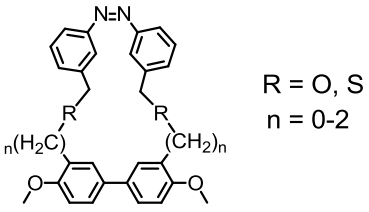

Macrocycle with modular linker

Figure 62 Azo bridged biphenyl with a modular linker length and more stabile methoxy groups as anchor group precursor.

Another difference concerns the anchor groups, in the previous described investigations the chlorines were found to be unstable under certain conditions,

especially in Sandmayer reaction halogen exchange was observed. To avoid such unwanted side reaction and dehalogenation, the chlorines as possible leaving groups were exchanged to more stable methoxy groups as anchor group precursors.

4.3.1 Design and Retro Synthesis

To build up such a macrocyclic structure two key intermediates are envisaged: A biphenylic system with two methoxy groups in *para* position and a "protected" azobenzene precursor. The key intermediate **K1** and **K2** with the macrocyclic structures are shown in **Scheme 39**. The "protecting group" is more a "fixing" unit to lock the azo unit in the thermodynamically less favored *cis* conformation allowing the cyclization reaction via a nucleophilic substitution reaction in the final step.

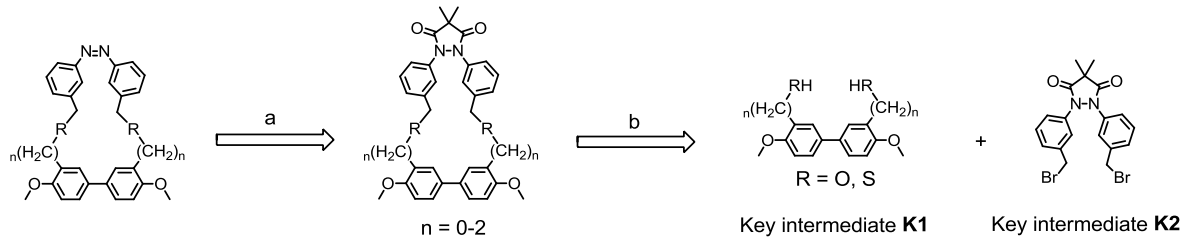

Scheme 39 Retrosynthetic scheme for the final cyclization step. (a) Oxidative deprotection. (b) Nucleophilic substitution reaction.

Methoxy groups are chosen as precursors for the anchor group in *para* position of the biphenyl. In contrast to the previously chosen chlorine precursors in macrocycle **76**, the methoxy groups are more stable and in particular for substitution- and Sandmeyer reactions the better choice as protecting groups. They can easily be deprotected with a Lewis acid and transferred to triflates, which are known to be suitable precursors for further modifications.[149][300]

For the final cyclization, a nucleophilic substitution was chosen, using oxygen and sulfur as nucleophiles. While oxygen as nucleophile is more easily accessible,

sulfur is due to its polarizability considerably more nucleophilic. Benzylic bromines were envisaged as electrophiles.

In **Scheme 40** the retrosynthetic strategy for the key intermediate **K1a** and **K1b** are shown. The key step for both strategies was the coupling reaction to form the biphenylic system, followed by standard protecting group transformations.[300]

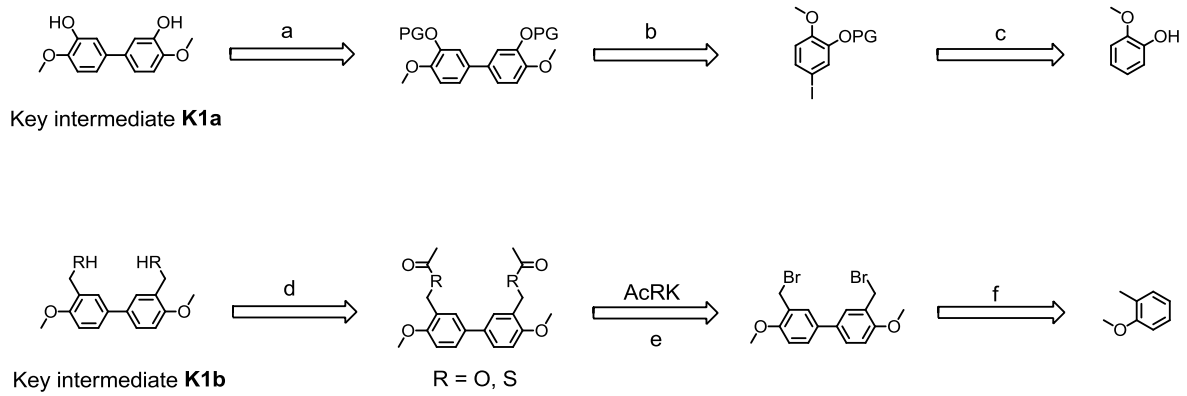

Scheme 40 Retrosynthetic scheme for the synthesis of key intermediate **K1a** and **K1b**. (a) Deprotection. (b) Ullmann type reaction. (c) Protection group chemistry and iodination. (d) Deprotection. (e) Heteroatom introduction, nucleophilic substitution reaction. (f) Oxidative coupling reaction and bromination.

The key intermediate **K1a** can be assembled by an Ullmann type reaction and subsequent deprotection to the free alcohols. The phenolic position of the commercially available 2-methoxyphenol can be transferred by standard organic reactions to an electron donating substituent. The two electron rich intermediates can be coupled, after iodination, in an Ullmann type reaction to the desired key intermediate **K1a**.

Key intermediate **K1b** can be assembled through an oxidative coupling of 1-methoxy-2-methylbenzene and subsequent bromination, which forms the brominated biphenylic system. In a nucleophilic substitution reaction at the benzylic position, the heteroatoms can be introduced, either as acetyl protected sulfur or as acetyl protected oxygen. To obtain the desired key intermediate **K1b** a deprotection of the acetyl protection group under basic conditions was envisaged.

In **Scheme 41** retrosynthetic strategy for the second key intermediate **K2** is shown. 1-Methyl-3-nitrobenzene can be coupled under reductive conditions to a hydrazine derivative. Remarkable in this strategy is the subsequent “fixation” of the hydrazine derivative in a *cis* conformation with a 4,4-dimethylpyrazolidine derivative. The pyrazolidine holds the hydrazine derivative in a *cis* conformation which is needed for the cyclization step, in order to favor the cyclization over the polymer formation. The addition of the hydrazine derivative and 2,2-dimethylmalonyl dichloride should provide the desired locked structure. In a last step, bromines can be introduced as leaving groups for the final nucleophilic substitution reaction.

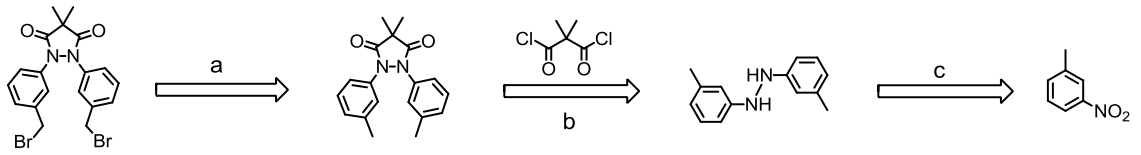

Key intermediate **K2**

Scheme 41 Retrosynthetic scheme for the synthesis of key intermediate **K2**. (a) Bromination. (b) *Cis* conformation “fixation”. (c) Reductive coupling reaction

4.3.2 Synthesis and Characterization of the second Biphenyl Generation

In a first step the key intermediate **K2** (**Scheme 41**) and in a second step the different biphenyl intermediates **K1a** and **K1b** (**Scheme 40**) were synthesized. In a final section the cyclization step as nucleophilic substitution reaction will be discussed.

4.3.2.1 The “Locked” Dibromo Hydrazine Intermediate

In **Scheme 42** the tree step synthesis to the locked dibromo hydrazine intermediate **94** is shown.

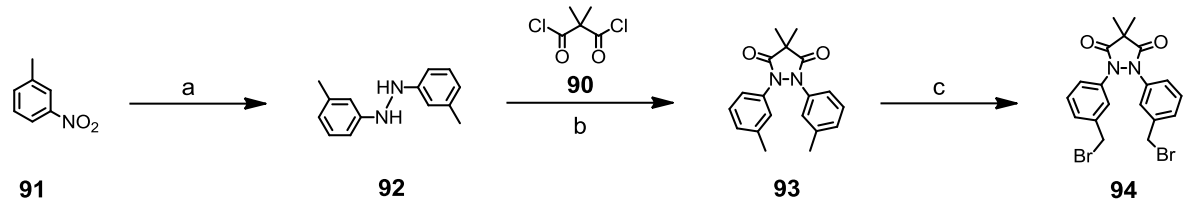

Scheme 42 Synthetic route to the locked dibromo hydrazine intermediate **94**. Reagents and conditions. (a) Al, KOH, CH_3OH, RT → 65°C, 1.5 h, 90%. (b) DMAP, py, CH_2Cl_2, -20°C → RT, 7 h. (c) NBS, AIBN, CCl_4, hv, 35°C, 1.5 h, 35%.

1,2-Di-*m*-tolylhydrazine (**92**) was obtained by a reductive coupling of commercially available 1-methyl-3-nitrobenzene (**91**) with aluminium metal and potassium hydroxide in methanol.[301] The nitro compound **91** was treated with 8 equivalents of aluminium powder and potassium hydroxide in methanol. Due to the high reduction potential of aluminium ($Al \rightarrow Al^{+III}$) in alkaline solution a complete reduction via azobenzene derivative to the hydrazine derivative was possible. During the reaction a bright orange color was observed which was attributed to the formation of the azobenzene derivative. After 1.5 hours the orange color disappeared again indicating the completeness of the reduction to the desired hydrazine derivative **92**. After purification by column chromatography with silica gel the product **92** was isolated as a yellow oil in a yield of 90%.

In the next step the hydrazine derivative **92** was treated with 2,2-dimethylmalonyl dichloride (**90**) to form the pyrazolidine derivative **93** and to fix the conformation of the N─N bond in its *cis* conformation.[302] In order to increase the yield, the dichloride **90** was slowly added at -20°C under an inert argon atmosphere and the reaction mixture was further treated with pyridine and 1,3-dimethyl-2-imidazolidinone (DMAP). The pure "fixed" product **93** was isolated after purification by column chromatography with silica gel as a beige solid in 95% yield.

The subsequent bromination turned out to be troublesome in order to separate the product from the over brominated side products. The bromination was done following a literature protocol.[302] The pyrazolidine derivative **93** was treated with *N*-bromosuccinimide (NBS) under an inert argon atmosphere and as radical starter 2,2-azobis(2-methylpropionitrile) (AIBN) was used. The reaction mixture was irradiated with visible light (200 W) and the lamp was fixed at such a distance from

the reaction flask that the desired inner temperature was reached (temperatures in **Table 8**). Applying exactly the published conditions form *Grützmahcher* et al.[302] mainly over bromination was observed. Therefore different reaction conditions for this bromination were tested and are listed in **Table 8**. First, different solvents which are known to be suitable for delicate bromination reactions were tested.[303][304] The use of the toxic carbon tetrachloride could not be avoided, in fact this solvent afforded the best results. Methyl formate (entry 1 in **Table 8**) showed almost no conversion. While the conversion in benzene (entry 6 in **Table 8**) was reduced, the purity was better than in other solvents. The best results were obtained in carbon tetrachloride at a temperature of 35°C (entry 2 in **Table 8**). At increased temperatures the over bromination was even more dominant and at lower temperature the mono brominated compound was favored but even there some over brominated compound was already observed.

Table 8 Reaction conditions for the bromination to compound **94** with 2.07 eq. NBS and light (200 W). For all reaction dry solvents were used, the reactions were performed under an inert argon atmosphere and AIBN was used as radical starter.

entry	solvent	temperature [°C]	reaction time [h]	yield	purity[a]
1	methyl formate	reflux	12 h	no[b]	-
2	CCl_4	35°C	1.5 h[c]	35%	95%
3	CCl_4	reflux	1 h	20%	90%[d]
4	CCl_4	10°C	2 h	15%	95%
5	*c*-hexane	50°C	7 h	20%	80%
6	benzene	40°C	6 h	13%	95%

[a] purity calculated from ^{1}H-NMR measurements.
[b] just mono brominated product isolated.
[c] for longer reaction times, significantly more over bromination was observed.
[d] more over bromination.

In the purification method of *Grützmahcher* et al.[302] the brominated compound **94** was nicely purified by flash column chromatography (silica gel, petrolether:ethyl

acetate, 4:1). With the same purification method compound **94** was separated from the mono brominated compound but it was not possible to separate the over brominated side products. To further purify the product **94**, four sequenced column chromatographies (silica gel, dichloromethane) were performed and product **94** was finally isolated as white powder in a yield of 35%. Despite three subsequent recrystallization of the already chromatographed product, there was still some over brominated product left. The impurity was calculated from ^{1}H-NMR measurements to be smaller than 5%. In order to obtain the brominated compound **94** in a higher purity the reaction conditions were optimized, so that less over brominated product was formed, as well as different purification procedure were investigated. All purification methods had in common that smaller amounts of the over brominated product could not be separated and this could maybe hinder the final cyclization step.

4.3.2.2 The Variable Biphenyl Intermediates

Now we turn to the synthesis of the different biphenyl key intermediates **K1a** and **K1b** (**Scheme 40**) in order to vary the length of the linker. In **Scheme 43** the synthesis to the biphenyl **99** with a ─CH_2O─ linker is shown.

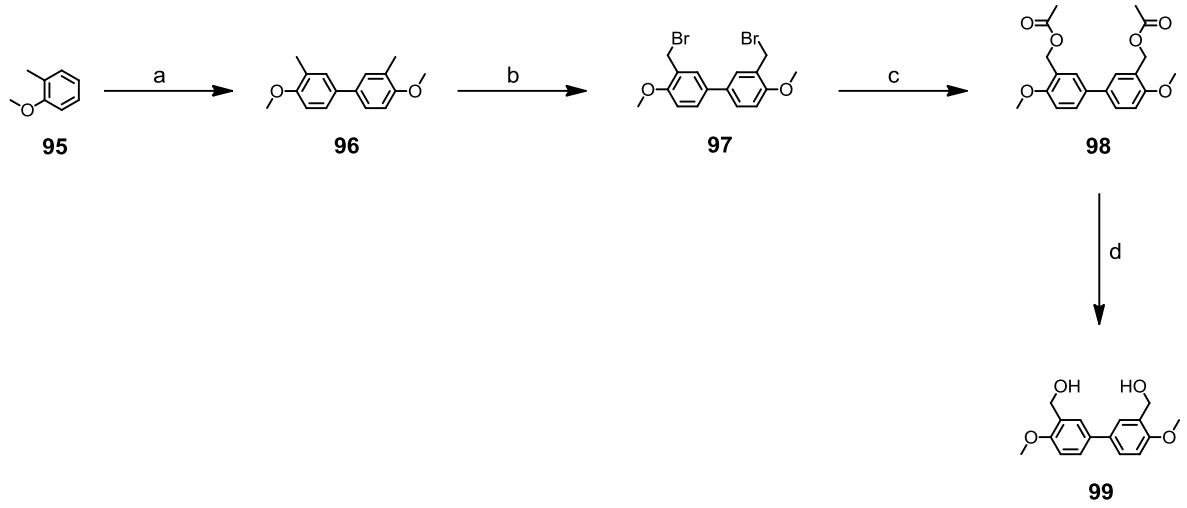

Scheme 43 Synthetic route to the biphenyl intermediate **99**. Reagents and conditions. (a) $MoCl_5$, CH_2Cl_2, 0°C, 1 h, 69%. (b) NBS, CCl_4, hv, reflux, 1.5 h, 63%. (c) AcOK, $CH_3CH_2CO_2H$, 105°C, 2.5 h, 96%. (d) NaOH, H_2O, EtOH, 80°C, 4 h, 91%.

Anisole derivatives can be coupled in a selective oxidation to their corresponding biphenyl derivatives.[305] Thanks to the methyl group in 1-position and the spatial demand close to the donor function of the anisole the 4,4'-coupled product was formed exclusively. The commercially available 2-methylanisole (**95**) was treated with molubdenum(V)chloride under an inert argon atmosphere at 0°C for 1 hour. The reaction mixture was quenched with sodium hydrocarbonate and purified by column chromatography with silica gel affording the pure product **96** as a white powder in 69% yield. The molubdenum(V)chloride was dried under high vacuum conditions prior to use, this resulted in a increased yield of about 10%.

For the subsequent delicate bromination the reaction conditions were carefully chosen. The bromination of compound **96** under standard bromination conditions[25][290][306] afforded the product **97** in 38% yield, while 45% of the over brominated product was also isolated. The biphenyl **96** was therefore only treated with NBS (without radical starter) in carbon tetrachloride under an inert argon atmosphere. The reaction flask was illuminated with visible light (200 W) for 90 minutes at such a distance from the reaction flask that the reflux was maintained. The yellow crude was recrystallized from hot TBME to give the desired brominated biphenyl **97** as a white powder in a yield of 63%. By leaving the radical starter out, the yield was increased by 25% and the formation of the over brominated side products was drastically reduced.

The bromines were substituted by oxygen following a literature procedure.[307][308] The dibromo biphenyl **97** was treated with potassium acetate under strong acidic condition in glacial acetic acid. Recrystallization form hot TBME afforded the pure acetylated product **98** as a white powder in an excellent yield of 96%. The subsequent deprotection was performed under basic conditions in ethanol. Purification by column chromatography afforded the analytical pure deprotected compound **99** as a white powder in a yield of 91%.

The nucleophilic precursor **99** was synthesized straight forward with standard organic reactions in four steps in a good overall yield of 39%. All intermediates

96-**98** and the final product **99** were fully characterized by ^{1}H- and ^{13}C-NMR spectroscopy, mass spectrometry and elemental analysis.

In order to be able to vary the length of the linker a second biphenyl intermediate **106** was synthesized. The synthetic route to the phenolic biphenyl **106** with a short ─O─ linker is shown in **Scheme 44**. As starting material for the synthesis of biphenyl **106**, commercially available 2-methoxyphenol (**100**) was chosen. The characteristic in this synthetic strategy were the requirement for different electronic properties of the phenyl precursors. For the iodination in *para* position to the methoxy group an electron withdrawing protection group of the alcohol is required in order to obtain the desired iodide for the subsequent Ullmann coupling. On the other hand an electron donating protecting group of the alcohol is required for the Ullmann coupling itself, since an electron withdrawing group would deactivate the coupling reaction. Therefore first some protection group chemistry had to be performed.

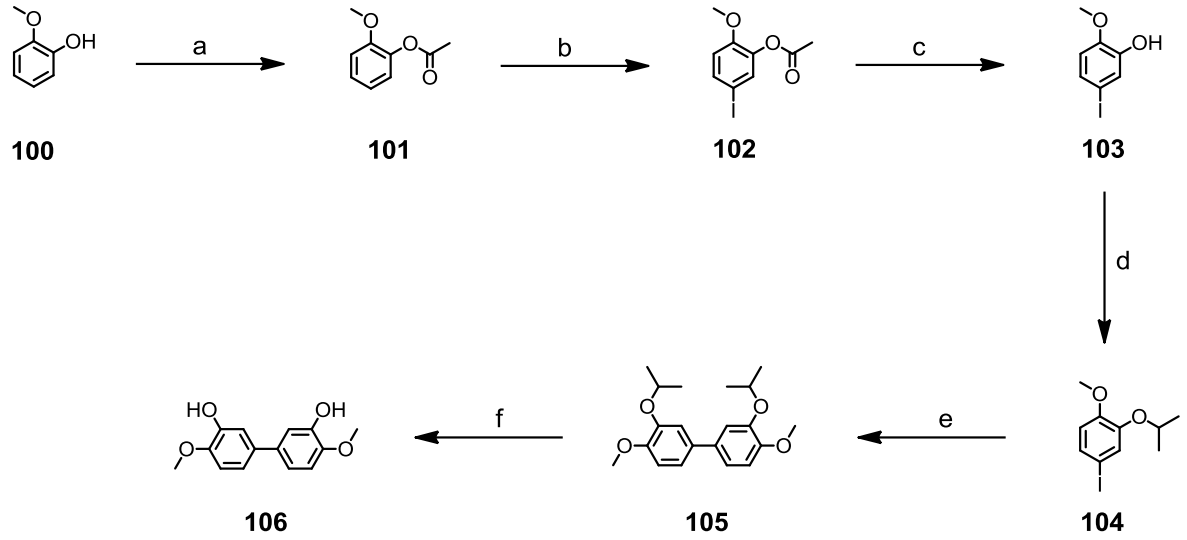

Scheme 44 Synthetic route to the biphenyl intermediate **106**. Reagents and conditions. (a) AcCl, py, CH_2Cl_2, 0°C → RT, 1 h, 99%. (b) ICl, CH_2Cl_2, 0°C → RT, 18 h, 93%. (c) 1) LiOH, CH_3OH, H_2O, RT, 20 h. 2) 1 M aq. HCl, RT, 10 min, 87%. (d) $CH_3CHBrCH_3$, K_2CO_3, EtOH, 70°C, 18 h, 94%. (e) Cu, neat, 250-260°C, 1.5 h, 78%. (f) $FeCl_3$, CH_2Cl_2, RT, 18 h, 54%.

The commercially available 2-methoxyphenol (**100**) was first protected with an electron withdrawing protecting group.[309] The phenol **100** was dissolved in degassed dichloromethane and treated with 1.2 equivalents of acetyl chloride, after extraction the acetylated product **101** was obtained analytically pure as a yellow oil in a quantitative yield. After the introduction of the electron withdrawing group an electrophilic aromatic substitution reaction with iodine monochloride was performed. In this type of iodination the iodine from the iodine monochloride is partial positively charged and acts as electrophile.[293] Compound **101** was dissolved under an inert argon atmosphere in dichloromethane and cooled down to 0°C. The pure iodine monochloride was dissolved in dry dichloromethane and added drop wise over a period of 70 min to the reaction mixture. A slow addition of the electrophile was essential in order to obtain a good yield with as little as possible over iodination. The iodinated compound **102** was purified by column chromatography with silica gel and isolated after drying under high vacuum conditions as a white powder in an excellent yield of 93%.

In order to trans protect compound **102** with an electron donating protecting group, the acetate **102** was first deprotected to the free alcohol under basic conditions.[310] The deprotection was performed in tetrahydrofuran and methanol with lithium hydroxide at room temperature. The crude was recrystallized form hot *n*-hexane with a few drops of TBME affording the free alcohol **103** analytically pure as white crystals in a yield of 87%. In a subsequent nucleophilic substitution reaction the free alcohol **103** was treated with 2-brompropane and potassium carbonate in ethanol to obtain the trans-protected phenyl derivative **104** as a white powder in 94% yield.

With the introduced electron donating group in compound **104**, the Ullmann type coupling[284][296][311] was performed. The iodinated compound **104** and 8.5 equivalents copper powder were mixed without solvent and slowly heated to 250°C. At this temperature an exothermic reaction began and the temperature rose to 260°C, after 15 minutes the exothermic reaction subsided and the liquid reaction mixture was stirred for a further 90 minutes. The crude was recrystallized from hot methanol to afford the coupling product **105** as a white powder in a good 78% yield.

The isopropyl protecting group of **105** had to be removed with a weaker Lewis acid than boron tribromide, in order to leave the methoxy groups untouched. Iron(III) chloride in dry dichloromethane was found to be a suitable Lewis acid for such selective deprotection reaction and the selectively deprotected compound **106** was isolated as a white solid in 79% yield. The phenolic biphenyl **106** turned out to be slightly unstable and had to be used directly for the cyclization reaction (see section 4.3.2.3 The Cyclization Reaction). However, the protected biphenyl **105** was synthesized over five steps in an excellent overall yield of 59% and could be stored under ambient conditions and was stable for more than one month.

In order to obtain a stable and synthetically easier available phenolic biphenyl intermediate, compound **110** was also synthesized in a two step procedure according to a literature known protocol[312] and is shown in **Scheme 45**.

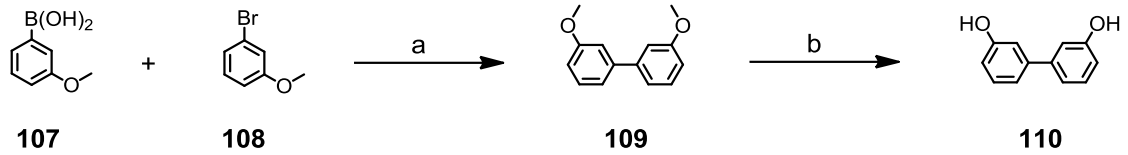

Scheme 45 Synthetic route to the phenolic biphenyl **110**. Reagents and conditions. (a) $[Pd(PPh_3)_4]$, K_2CO_3, $C_6H_5CH_3$, EtOH, 85°C, 4 h, 94%. (b) BBr_3, CH_2Cl_2, 0°C, 3 h, 90%.

The Suzuki reaction was performed under the same conditions as already investigated (see section 2 Azo Macrocycles) using the commercially available 3-methoxyphenylboronic acid (**107**) and 3-bromanisole (**108**). The coupling product **109** was isolated as a colorless liquid in 94% yield. The subsequent deprotection of the methoxy groups was performed in dry dichloromethane at 0°C with 3.5 equivalents of boron tribromide. The crude was recrystallized from hot dichloromethane to afford the deprotected product **110** as a white solid in 90% yield.

All intermediates **101**-**105**, **109** and the final products **106** and **110** were fully characterized by ^{1}H- and ^{13}C-NMR spectroscopy, mass spectrometry and elemental analysis.

To obtain a slightly more nucleophilic biphenyl precursor, compared to the oxygen functionalized ones **99**, **106** and **110**, the sulfur functionalized biphenyl **112** was synthesized as well. The synthetic route profited from the already synthesized dibromo precursor **97** and is shown in **Scheme 46**.

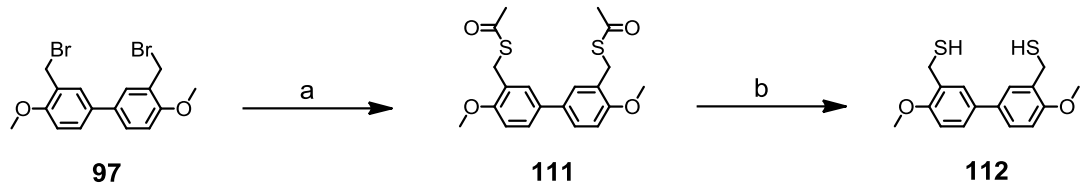

97 **111** **112**

Scheme 46 Synthetic route to the sulfur functionalized biphenyl **112**. Reagents and conditions. (a) AcSK, DMF, RT, 2 h, 81%. (b) AcCl, CH_3OH, CH_2Cl_2, 0°C → 35°C, 5 h, 94%.

The introduction of the sulfur via a nucleophilic substitution reaction was performed in a similar way as already described for the introduction of the oxygen.[313] Potassium thioacetate and the dibromo compound **97** were reacted in DMF at room temperature. The substituted product **111** was isolated after column chromatography with silica gel as a white powder. In a subsequent deprotection of the acetyl protecting group with acetyl chloride and methanol in dichloromethane the free thiol was isolated as a white powder. Due to the strong disulfide formation tendency the reaction mixture was directly evaporated to dryness and used for the cyclization reaction (see section 4.3.2.3 The Cyclization Reaction) without further purification. However, the sulfur functionalized biphenyl **111** was synthesized over four steps in a good overall yield of 34%. The protected sulfur compound **111** could be stored under ambient conditions and was stable for more than one month.

4.3.2.3 The Cyclization Reaction

In this section the nucleophilic substitution reaction to form the desired macrocyclic structure will be discussed. With the different key intermediates (**Figure 63**) in

hand, a modular synthesis to different biphenylic macrocycles with different linker lengths was envisaged.

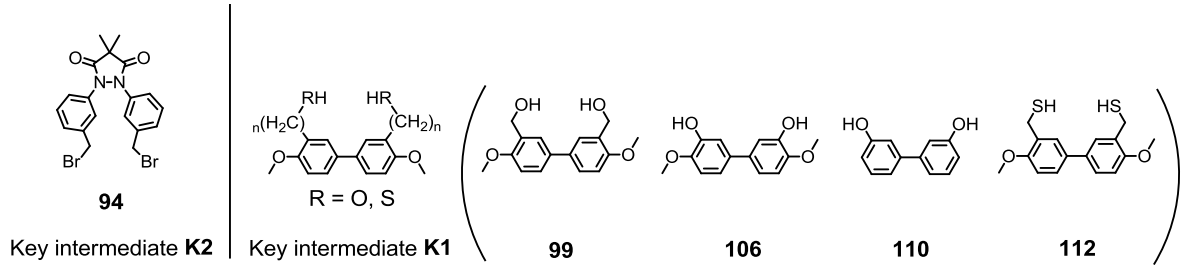

Figure 63 The synthesized key intermediates **K2** and **K1**. For the modular key intermediate **K1** four different biphenyls **99**, **106**, **110** and **112** were synthesized with different linker length or different nucleophiles (oxygen for **99**, **106** and **110** as well as sulfur for **112**).

In a first attempt the dibromo compound **94** was coupled with biphenyl **99** (**Scheme 47**). The cyclization of dibromo compound **94** with 1,3-phenylene-dimethanethiol derivatives and 1,4-phenylenedimethanethiol derivatives is literature known.[314] The cyclized product was obtained by a nucleophilic substitution reaction with potassium carbonate and 18-crown-6 in refluxing benzene. Even so the nucleophile was much more flexible this protocol seemed promising, since also two substitutions had to take place at the same time in order to form the desired macrocyclic structure.

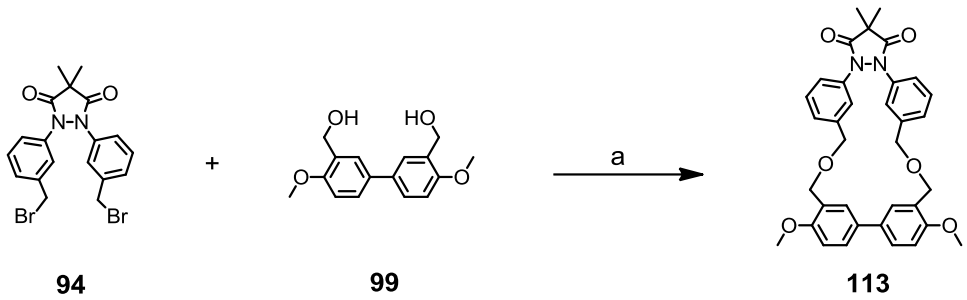

Scheme 47 Synthetic route of the cyclization reaction towards biphenyl macrocycle **113**. With a $-CH_2OCH_2-$ linker between the azobenzene derivative and the biphenylic system. (a) The different tested reaction conditions are listed in

Table 9.

For a first attempt the literature known protocol[314] was applied to form macrocycle **113**, but since it ended in extensive polymer formation instead of macrocyclization, different reaction conditions had to be tested, which are listed in

Table 9. The different tested conditions clearly indicated the dependency on the solvent and the reaction temperature. The base was an important parameter as well, but because of the lability of the pyrazolidine derivative **94** to base, only weak bases such as potassium carbonate could be used. Sodium hydride (entry 8 in

Table 9) resulted in "deprotection" of the azo group, and the pyrazolidine was cleaved, even at a temperature of -20°C.

Performing the reaction in benzene at 60°C (entry 1 in

Table 9) resulted in extensive polymer formation, despite the applied high dilution conditions of 6×10^{-5} mol/L and when the reaction temperature was reduced (entry 2 in

Table 9) no conversion was observed at all. By changing the solvent to toluene almost the same behavior was observed, at temperatures below 55°C hardly any conversion occurred and as soon as the temperature was raised, the dibromides started to decompose or some polymers were formed (entry 3 and 4 in

Table 9). Further investigations in more polar solvents such as DMF did not yield in the expected macrocycle **113**, but in decomposition of the dibromo compound **94**. In all cases were decomposition of the starting material **94** was observed it was possible to re-isolate the corresponding alcohol starting material **99** in various quantities.

In conclusion we can say that the dibromo compound **94** is just stable at temperatures below 60°C and it seems that compound **94** is additionally destabilized in polar solvents. Even so the substitution reaction occurred under specific reaction conditions the formation of the macrocycle **113** could not be observed, pointing at a cyclization problem with a rigid biphenyl like **99** as counterpart.

Table 9 Different tested reaction conditions for the cyclization reaction of compound **94** with **99**. All reactions were performed under an inert argon atmosphere using dry solvents under high dilution conditions of at least 10^{-4} mol/L.

entry	additives	solvent	temperature [°C]	reaction time [h]	yield
1	K_2CO_3 18-crown-6	C_6H_6	60°C	3 h	polymer
2	K_2CO_3 18-crown-6	C_6H_6	RT	12 h	no conversion
3	K_2CO_3 18-crown-6	$C_6H_5CH_3$	<55°C	8 h	no conversion
4	K_2CO_3 18-crown-6	$C_6H_5CH_3$	60-75°C	3 h	no[a][b]
5	K_2CO_3 18-crown-6	DMF	80°C	26 h	no[b]
6	K_2CO_3	DMF	<RT	8 h	no[b]
7	K_2CO_3	THF	50°C[c]	4 h	no[a][b]
8	NaH	THF	40°C	2 h	no[b]

[a] some polymer formation observed.
[b] decomposition of the dibromo starting material **94**.
[c] at lower temperatures no conversion was observed.

Thanks to the modular strategy, some other nucleophiles can be investigated for the cyclization reaction. Subsequently the two different phenol derivatives **106** and **110** were investigated in order to obtain the desired macrocycle **114a** or **114b**, respectively. The synthetic strategy is shown in **Scheme 48** and the different tested reaction conditions are shown in **Table 10**.

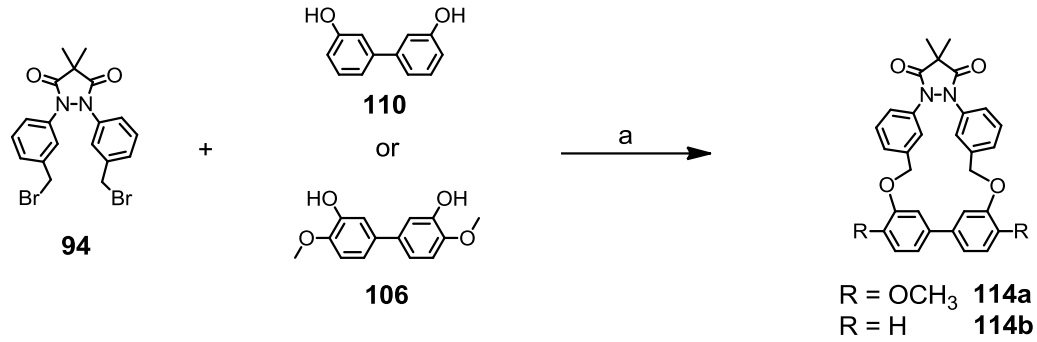

Scheme 48 Synthetic route of the cyclization reaction towards biphenyl macrocycle **114a** or **114b**. With a –OCH_2– linker between the azobenzene derivative and the biphenylic system. (a) The different tested reaction conditions are listed in **Table 10**.

Table 10 Different tested reaction conditions for the cyclization reaction of compound **94** with **110**. All reactions were performed under an inert argon atmosphere using dry solvents under high dilution conditions of at least 10^{-4} mol/L.

entry	additives	solvent	temperature [°C]	reaction time [h]	yield
1	K_2CO_3 18-crown-6	C_6H_6	60°C	3 h	polymer
2	K_2CO_3	C_6H_6	60°C	4 h	polymer
3	K_2CO_3 18-crown-6	THF	60°C[b]	6 h	no[a][c]
4	K_2CO_3	THF	60°C[b]	6 h	no[a][c]
5	K_2CO_3	DMF	RT[b]	6 h	no[a][c]

[a] decomposition of the dibromo starting material **94**.
[b] no conversion at lower temperatures.
[c] starting material **110** was re-isolated.

The main biphenyl **106** with its two methoxy groups in *para* position was replaced for the subsequent test reaction by a synthetically easy accessible synthon **110**. According to the previous investigations above, just reaction conditions below 60°C were chosen, since this temperature seemed to be the critical temperature for the decomposition of the dibromo compound **94**. Despite the increased nucleophilicity of compound **110** the obtained results are comparable to those found for

compound **99**. In benzene a relatively good conversion was observed no matter if 18-crown-6 was added as additive or not (entry 1 and 2 in **Table 10**), but equal to above, just polymers were formed. The molecular mass of macrocycle **114b** was not detectable by mass spectrometry, neither in ESI-, nor in MALDI-TOF mass spectrometry. Similar results were obtained in THF and DMF as solvent (entry 3-5 in **Table 10**). While decomposition of the dibromo compound **94** already at room temperature was observed in DMF, but the temperature could be raised to 60°C for THF until decomposition started. In both cases the biphenylic starting material **110** could be re-isolated, pointing at a too low nucleophilicity of compound **110** or at a too weak base. Since the base cannot be changed in order to not deprotect the azo function of **94**, only the nucleophilicity can be changed.

In order to increase the nucleophilicity the alcohol function was replaced by a sulfur unit.[204][207] The synthetic route of the cyclization reaction with the sulfur functionalized biphenyl **112** is shown in **Scheme 49**.

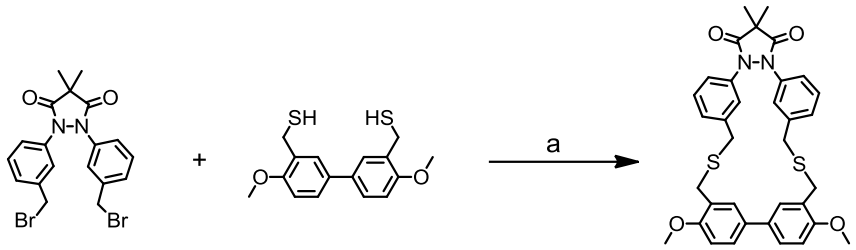

Scheme 49 Synthetic route of the cyclization reaction towards biphenyl macrocycle **115**. With a $-CH_2SCH_2-$ linker between the azobenzene derivative and the biphenylic system. (a) The different tested reaction conditions are listed in **Table 11**.

In a first attempt the literature known protocol[314] was applied and the sulfur compound was almost instantly consumed, due to disulfide formation of the starting material **112**. Therefore all subsequent reaction mixtures were degassed for at least 15 minutes with argon prior the addition of the sulfur functionalized biphenyl **112**. The results of the investigated reaction conditions are summarized in

Table 11. The results for benzene as solvent (entry 1 in **Table 11**) are the same as already observed above, both starting materials were consumed and formed polymers despite the use of high dilution conditions. For the attempts with toluene and tetrahydrofuran the reaction temperature was decreased to 50°C in order to obtain milder conditions with the hope of a higher stability of the dibromo precursor **94**. And in fact, the compound **94** was more stable under the applied condition. But even though the sulfur counterpart **112** was more nucleophilic than the alcohol **110**, neither product nor polymer formation was observed. After a reaction time of about 3 hours, compound **94** started to decompose anyway and for the sulfur compound **112** some disulfide formation was observed.

Table 11 Different tested reaction conditions for the cyclization reaction of compound **94** with the sulfur functionalized biphenyl **112**. All reactions were performed under an inert argon atmosphere using dry solvents under high dilution conditions of at least 10^{-4} mol/L. The reaction mixture was degassed for 15 min with argon prior adding the sulfur compound **112**.

entry	additives	solvent	temperature [°C]	reaction time [h]	yield
1	K_2CO_3 18-crown-6	C_6H_6	60°C	3 h	polymer[a]
2	K_2CO_3 18-crown-6	$C_6H_5CH_3$	50°C	8 h	no[a][b]
3	K_2CO_3 18-crown-6	THF	50°C[c]	8 h	no[a][b]

[a] disulfide was formed.
[b] decomposition of the dibromo starting material **94**.
[c] no conversion at lower temperatures.

Despite using all the different investigated biphenyls **99**, **106**, **110** and **112** and different conditions it was not possible to obtain the desired macrocycles **113**-**115**. Since the nucleophilic substitution reaction proceeded and only polymer was formed, the favored hypothesis is that the biphenylic precursors are too rigid for a successful cyclization reaction. For a cyclization two substitution reactions had to take place at the same moment and if the conformation of the two molecules is not

perfectly fitting a polymerization reaction is favored. And due to the instability of the dibromo compound **94** only smooth reaction conditions and weak bases could be used. Higher reaction temperatures would also increase the energy of the molecules, so that they could more easily cyclize.

Even so there are still some further options for a possible cyclization like e.g Mitsunobu type reactions[315] this synthetic strategy was not further investigated. Not only because the synthetic success is unlikely due to the investigations done above, but also the relatively long linker in this strategy, is a disadvantage. The reason for this strategy with the longer linker was originally to overcome the in section 4.2 observed ring strain, but from the results presented above one can conclude that this is not necessarily the case, since the cyclization with longer and more flexible linkers was still not possible either.

4.4 Third Generation of an Azo Bridged Biphenyl

As the first and second attempt to synthesize an azo bridged biphenyl failed, a third strategy is described here. The target structures **120** and **125** are nearly the same as the one already described in section 4.2 and are shown in **Figure 64**. The only difference of the structure affects the *para* position of the biphenyl; the halogenides were substituted by either a methoxy group or a triflate. With this change to more stable methoxy groups we expect an easier access to iodinated Sandmeyer reaction precursors and/or the possibility of using harsher conditions for a cyclization reaction. The introduction of a triflate as good leaving group in cross coupling reaction[149] opens the possibility of the introduction of anchor groups via palladium catalyzed reactions.

As already mentioned in section 4.2 there will be a certain ring strain in such small cyclic molecules, but based on MM2[274] calculations the macrocycles **120** and **125** should be flexible enough to allow the optically triggered *cis*/*trans* isomerization and should lead to a significant difference of the torsion angle between the two phenyl units of the biphenylic system.

Since the MALDI-TOF measurements described in section 4.2 showed the desired macrocycle **76**, it is worth trying to synthesize slightly modified macrocycles **120** and **125** (**Figure 64**). On one hand we lose the modularity of the approach described in section 4.3 but on the other hand it is easier to close a cycle on one side instead of two simultaneously closing points.

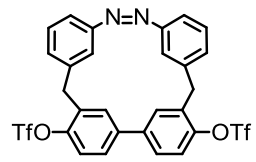

Macrocycle **120**

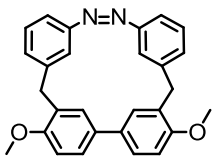

Macrocycle **125**

Figure 64 Azo bridged biphenyls with a CH_2 linker and methoxy or triflate groups in *para* position of the biphenyl.

4.4.1 Retro Synthesis

The cyclic target structures **120** and **125** consist of a biphenyl and an azobenzene interlinked by a short CH_2 alkyl linker. The two target structures **120** and **125** differ only in their functionalities of the biphenylic system. Macrocycle **120** has triflate functionalities in 1,6-positions and macrocycle **125** has methoxy groups in 1,6-position. An overview of the retro synthetic analysis is shown in **Scheme 50**.

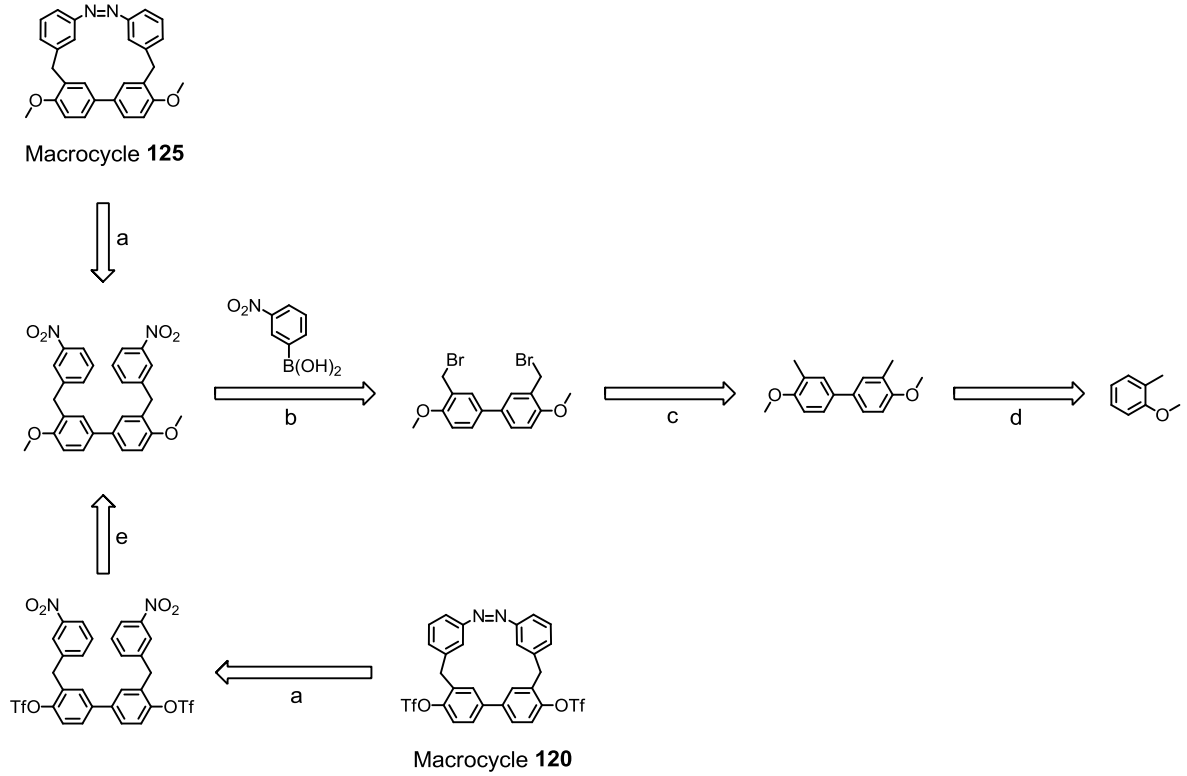

Scheme 50 Retrosynthetic scheme for the synthesis of an azobenzene bridged biphenyl **120** and **125** with a CH_2 linker. (a) Reductive azo formation. (b) Suzuki cross coupling reaction. (c) Bromination. (d) Oxidative coupling. (e) Deprotection and triflate introduction.

The key step in this synthetic pathway will be the cyclization during the formation of the azo joint. The previously investigated reductive cyclization procedure with lithium aluminium hydride (section 2 Azo Macrocycles) allows the closing of the ring with the formation of the azo joint. The investigation performed for the first generation of an azo bridged biphenyl (see section 4.2) gives further evidence for a cyclization. Before the final cyclization step, the methoxy groups of the dinitro

precursor can be modified to e.g. triflate functionality, which are known to be suitable leaving groups for further modification and anchor group introduction.[149] A Suzuki cross coupling reaction should provide the dinitro functionalized precursor for the subsequent reductive cyclization reaction. The dibromo precursor for the Suzuki reaction can be assembled through an oxidative coupling of 1-methoxy-2-methylbenzene and subsequent bromination.

4.4.2 Synthesis and Characterization of the third Generation Biphenyls

4.4.2.1 Synthesis of the Triflate Functionalized Biphenyl

In a first step the nitro functionalized biphenyl **116** comprising two methoxy groups was synthesized. The key intermediate **116** was further modified with two triflate groups to form precursor **118** on which the introduction of different functionalities and anchor groups is possible as well as acting as potential precursor for the final cyclization step to macrocycle **120**. The synthesis to the macrocycle **120** via the dinitro key intermediates **116** and **118** is shown in **Scheme 51**.

As already investigated in section 4.3.2.2 the dibromo compound **97** was synthesized in a two step procedure. The commercially available anisole derivative **95** was coupled in a selective oxidation with molubdenum(V) chloride to the corresponding biphenyl **96** and subsequently brominated with *N*-bromosuccinimide (NBS) in carbon tetrachloride affording the brominated biphenyl **97** in 43% yield over the two steps. Since the deprotection of the methoxy group with boron tribromide of intermediate **97** was not possible and yielded in decomposition of the starting material, the synthesis was continued and the trans protection will take place at a later stage of the synthesis.

The following Suzuki cross coupling reaction between the benzylic bromide **97** and an aryl boronic acid **35** behaved similar to the one discussed in section 2.2.3.2 for the similar chlorine substituted precursor **70** (**Scheme 31**). Under an inert argon atmosphere 3.5 equivalents of the commercially available 3-nitrophenyl-boronic acid (**35**) and the dibromo biphenyl **97** with 10 mol-% [$Pd(PPh_3)_4$] as catalyst and

potassium carbonate as base were dissolved in a solvent mixture of toluene and ethanol. The reaction mixture was heated using microwave conditions to 85°C for 50 minutes and provided after column chromatography with silica gel the desired dinitro compound **116** as a white powder in 91% yield.

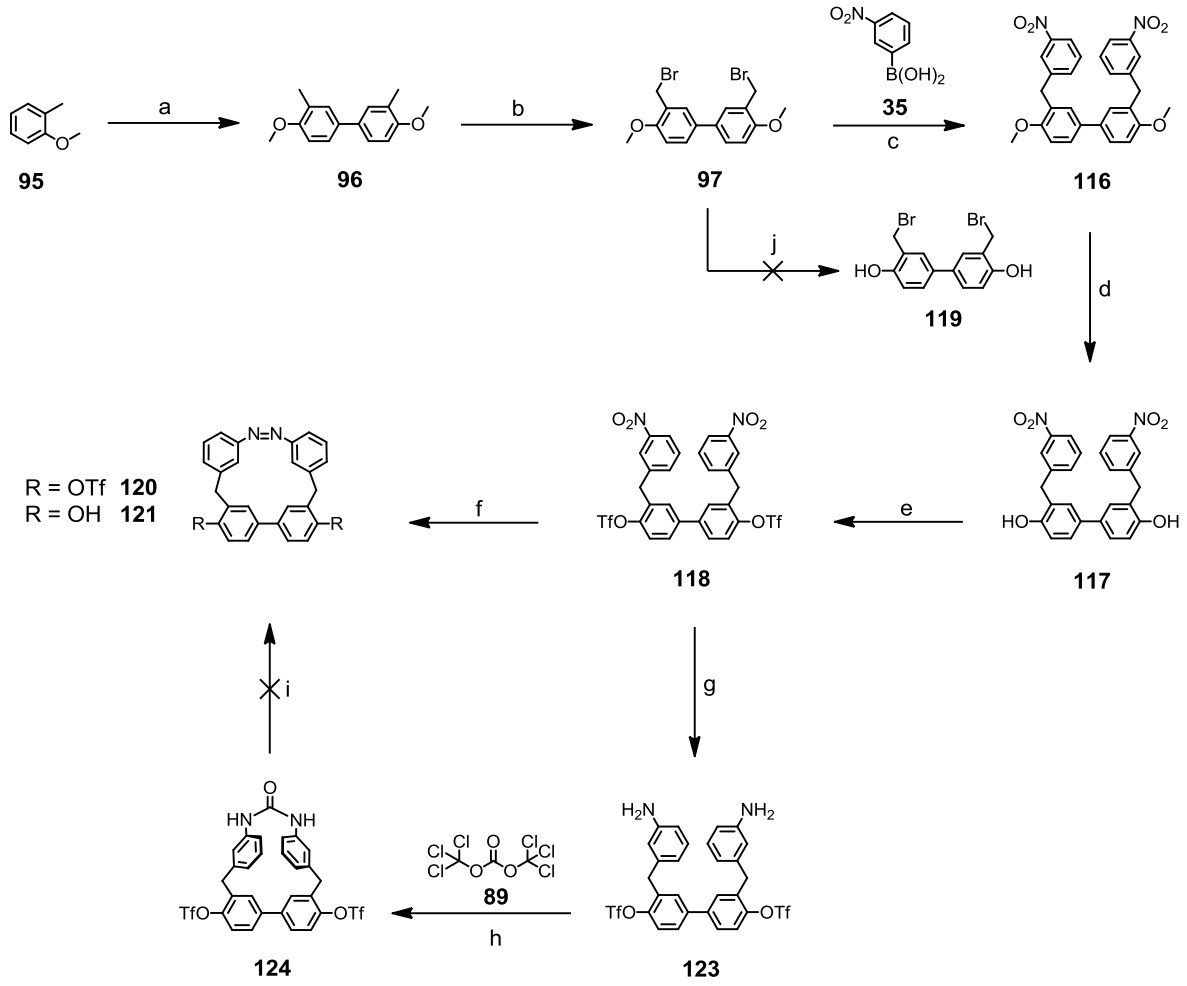

Scheme 51 Synthetic route to the macrocycle **120**. Reagents and conditions. (a) $MoCl_5$, CH_2Cl_2, 0°C, 1 h, 69%. (b) NBS, CCl_4, hv, reflux, 1.5 h, 63%. (c) $[Pd(PPh_3)_4]$, K_2CO_3, $C_6H_5CH_3$, EtOH, 85°C, 50 min in MW, 91%. (d) BBr_3, CH_2Cl_2, -78°C → RT, 4 h, 91%. (e) Tf_2O, py, 0°C → RT, 2 h, 75%. (f) $LiAlH_4$, THF, RT → 40°C, 16 h, <1% of **121**. (g) H_2, Pd/C, CH_2Cl_2, EtOH, RT, 17 h, 98%. (h) DMAP, CH_2Cl_2, RT, 18 h, 10%. (i) Ag_2O or silver foil, Ph_2O/DMI, 350°C, 27 h. (j) BBr_3, CH_2Cl_2, -78°C → RT, 3 h.

In order to exchange the stable methoxy protecting group with triflate functionalities as halogenide syntons for further modification, compound **116** was deprotected to

the free alcohol. The methoxy groups of **116** were deprotected using a 1 M boron tribromide solution in dichloromethane, after slow addition of the deprotecting agent at room temperature and acidic work up, the free alcohol **117** was isolated after flash column chromatography with silica gel as a brown solid in 91% yield. Since the free alcohol **117** was unstable at ambient conditions, it was directly treated with triflic anhydride in order to insert the triflate functionality. The diol **117** was first dried under high vacuum conditions and then dissolved under an inert argon atmosphere in dry pyridine. A slow addition of triflic anhydride seemed to be crucial since the yield was improved from 40% to 75% by an addition over a period of 1 hour. After basic work up and purification by column chromatography the desired product **118** was isolated as a white solid.

With the precursor **118** in hand, two possible strategies for the cyclization steps are possible (see **Scheme 51**). Either a direct cyclization by reduction of the nitro groups, or a step wise procedure including a complete reduction to the amine **123** followed by a cyclization step via an urea derivative **124** with subsequent azo formation to the desired macrocycle **120**. First the direct azo formation (f in **Scheme 51**) was investigated.

The same conditions as already successfully applied in the reductive dimerization in the formation of azo macrocycles **1**-**7**, were applied to **118** (see section 2 Azo Macrocycles). The dinitro precursor **118** was dissolved under high dilution conditions in dry THF (1.7×10^{-4} mol/L). After slow addition (over a period of 1 hour) of lithium aluminium hydride as reducing agent at room temperature the reaction mixture was analyzed after 16 hours by preparative thin layer chromatography. Aside from the significant start band, which was attributed to polymer formation, an orange band was isolated. Since the isolated amount of 0.2 mg was not enough for ^{1}H-NMR investigations, the product was analyzed by MALDI-TOF mass spectrometry (**Figure 65**). A single peak at 393.26 was observed which nicely fits with the molecular weight of the deprotected free alcohol **121**. This result gives further evidence that in principle the formation of such a macrocycle is possible although the yield needs to be improved significantly. Since the yield was below 1%, the detour via a urea derivative **124** was envisaged.

The dinitro compound **118** was reduced by hydrogenation with palladium on activated carbon as catalyst. While hydrogenation in an autoclave with 50 bars at room temperature for 16 hours gave a yield of just 33%, a smooth hydrogenation with three hydrogen balloons at room temperature for 17 hours afforded the diamino compound **123** as yellow oil in an excellent yield of 98%. Due to the instability of compound **123** it was directly treated with triphosgene **89** as a very reactive electrophile in order to form the cyclized urea derivative **124**.[316] After basic work up and purification by column chromatography the cyclized product **124** was isolated as a beige solid in 10% yield.

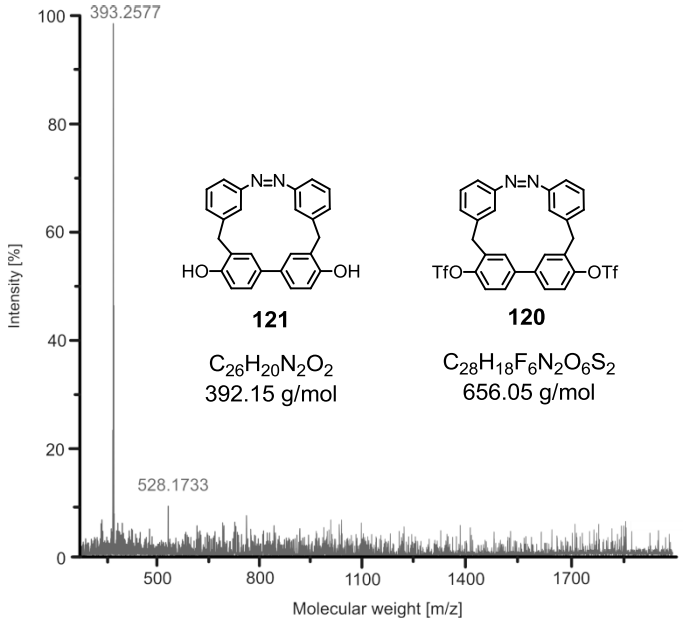

Figure 65 MALDI-TOF mass spectrum of the isolated band of the preparative TLC. Under the applied reductive conditions with $LiAlH_4$ the single protonated free alcohol **121** was observed instead of the expected macrocycle **120**.

The addition of an extra carbon in the urea derivative **124** during the cyclization reduced the ring strain and favored the ring closing. But in order to obtain a light sensitive switching unit in the form of an azo joint, the urea function needed to be transformed. It has already been shown, that a transformation of a urea derivative to an azo compound on silver surface under high vacuum conditions and at high temperatures is possible.[317] This reaction which occurred on single molecules

adsorbed on a silver surface under reduced pressure was mimicked as a wet chemistry reaction. Since macrocycle **120** needed to be synthesized in a larger scale, surface chemistry is not practicable. The urea derivative **124** was dissolved in polar high boiling solvents such as a solvent mixture of DMI and phenyl ether, as reactant silver foil or silver(I) oxide were added. Even so the reaction mixture was heated in a pressure tube up to 350°C, no conversion to the desired azo macrocycle **120** could be observed. It seemed that the absorption on silver surface together with the reduced pressure is crucial for a successful transformation of an urea derivative to an azo compound.

Since urea derivatives are rather stable in solution comparable reactions have not yet been reported, thus this reaction sequence was not further investigated. But for the direct reduction of the dinitro compound **118** a cyclization product was observed, even so the triflate functionality was lost. It was worth trying this reaction sequence with a suitable, more stable protecting group, such as a methoxy group.

4.4.2.2 The Methoxy Functionalized Biphenyl

As an alternative for the delicate reductive cyclization with the triflate functionalized precursor **118** or the chlorine functionalized precursor **70**, the more stable methoxy functionalized precursor **116** was envisaged. The reductive cyclization with the already synthesized dinitro precursor **116** to macrocycle **125** is shown in **Scheme 52**.

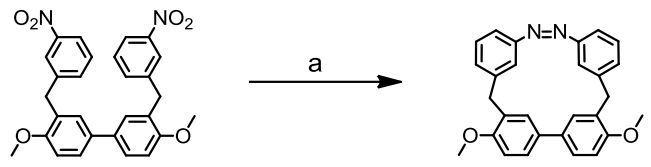

116 **125**

Scheme 52 Reductive cyclization to target macrocycle **125**. Reagent and condition. (a) $LiAlH_4$, THF, RT → 40°C, 16 h, 2%.

For the dinitro key intermediate **116** a crystal structure was obtained. The observed conformation in the solid state (**Figure 66**) showed the structure in its favored form. The nitrophenyl substituents of the biphenylic systems are on opposite sides. For a successful cyclization a rotation of the biphenyl with a simultaneous rotation around the benzylic position is crucial in order to form the desired macrocycle **125**.

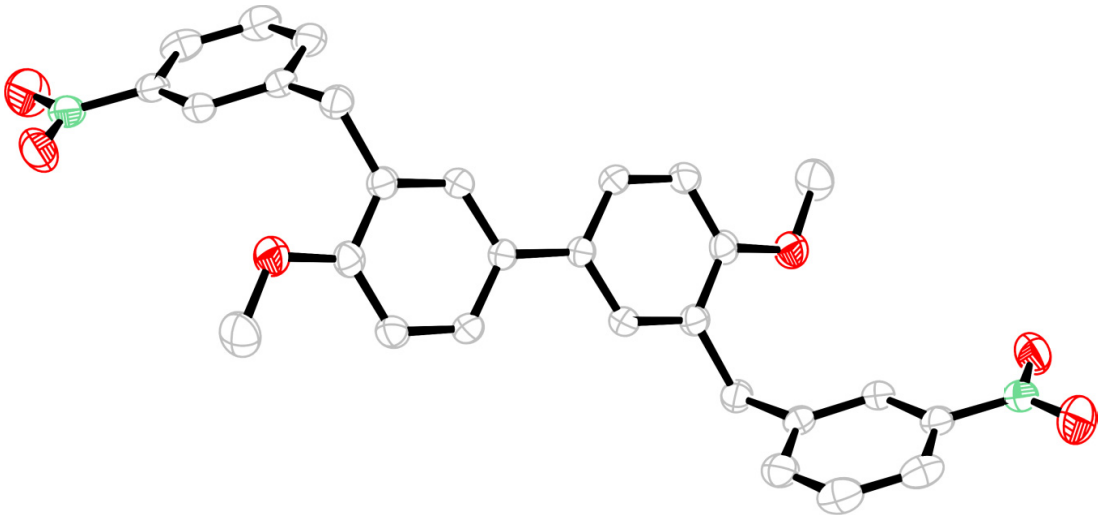

Figure 66 Solid state structure of the dinitro key intermediate **116**. The structure is slightly twisted in its sterically favored conformation.

The dinitro compound **116** was dissolved under an inert argon atmosphere under high dilution conditions (2.3×10^{-4} mol/L) in dry tetrahydrofuran. As a reducing agent 6.0 equivalents of lithium aluminium hydride were slowly added at room temperature. The reaction mixture was then stirred at 40°C for 16 hours. For the delicate purification a sequence of preparative thin layer chromatographies were made (see experimental section 6.4). The desired cyclized azo compound **125** was isolated analytically pure as an orange solid in 2% yield. The purity of the compound was shown by a single peak in the GPC chart at a retention time of 34.6 minutes (area: 99.2%) at a flow rate of 0.5 mL/min in toluene. While the majority of the products formed were attributed to the formation of polymers, the formation of larger oligomers was also observed. MALDI-TOF measurements have shown the formation of dimers up to pentamers and the overall yield of these larger oligomers was calculated to be 8%. Macrocycle **125** was fully characterized by

^{1}H and ^{13}C-NMR spectroscopy, mass spectrometry and gel permeation chromatography in order to demonstrate its purity.

The MALDI-TOF mass spectrum of the isolated macrocycle **125** is shown in **Figure 67**. Just one single peak at 420.20 was observed and gave further evidence of a successful cyclization to macrocycle **125**.

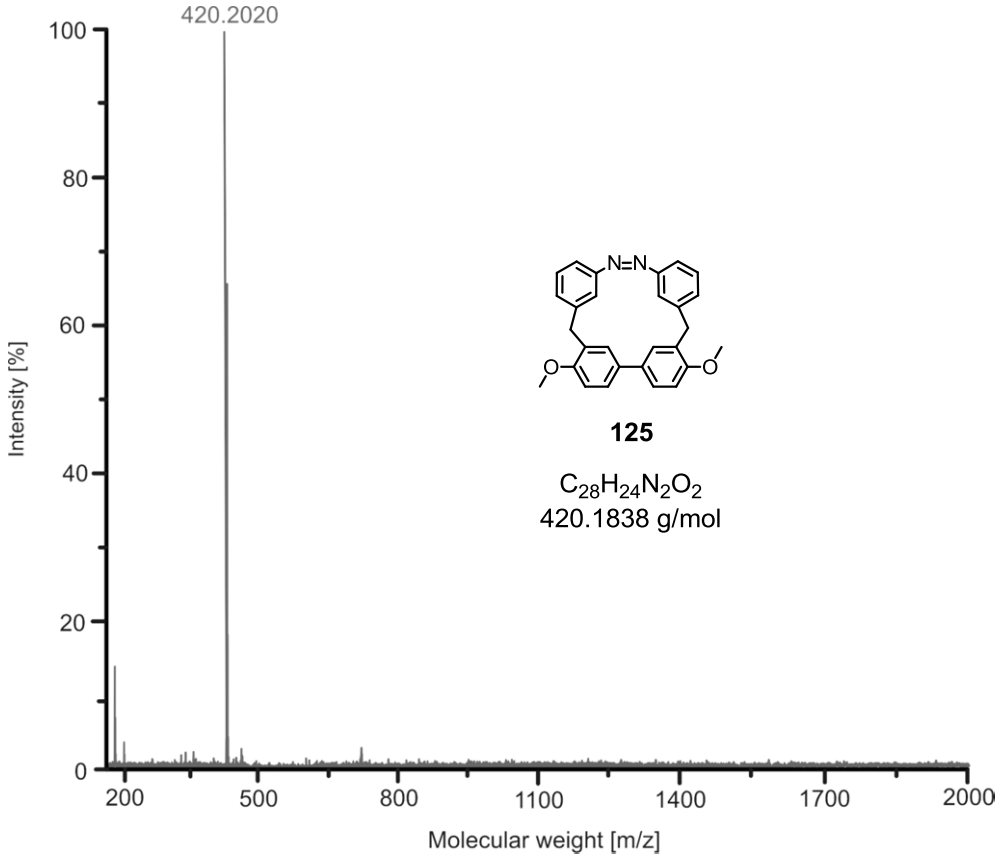

Figure 67 MALDI-TOF mass spectrum of the pure macrocycle **125** (Isomer A is equal Isomer B in terms of the observed molecular weight).

To further analyze the obtained product **125** in terms of a possible *cis*/*trans* mixture the ^{1}H-NMR spectrum is shown in **Figure 68**. All peaks were assigned by HMBC, HMQC and COSY methods. The displayed ^{1}H-NMR spectrum of macrocycle **125** was recorded in deuterated chloroform at room temperature in a 500 MHz spectrometer with 256 scans.

The color code shows the assignment of the protons in structure **125** to the observed ^{1}H-NMR peaks of both observed isomers. While isomer A was the major one, isomer B (dots are surrounded by a solid black line) was the minor one with observed ration of 2:1. The difference in the chemical shift of the corresponding peaks of the two isomers was surprisingly high. This could point at a significant difference of the two conformations. The exact same ^{1}H-NMR spectrum with the same ratio was also observed after further purification steps by additional preparative TLC and preparative SEC.

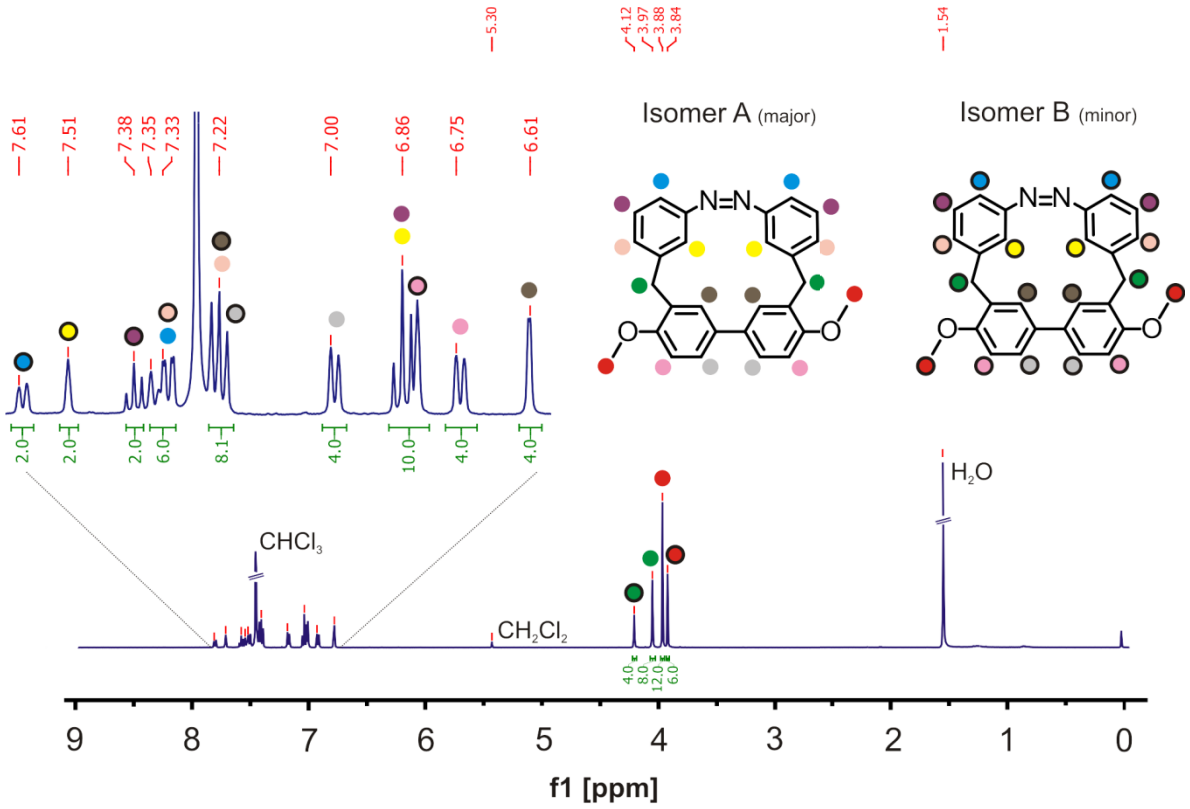

Figure 68 ^{1}H-NMR spectrum of the isolated macrocycle **125** in $CDCl_3$ at room temperature, recorded with 256 scans on a 500 MHz spectrometer. The signals were assigned by supporting HMBC, HMQC and COSY investigations to the different protons depicted by the color code. The dots of the minor isomer B are surrounded by a solid black line.

In some additional ^{1}H-NMR measurements the observed *cis*/*trans* mixture of **125** was measured at different temperatures and after irradiation of different

wavelength in order to change the ratio of the isomers. In **Figure 69** the measurements at the different conditions are shown.

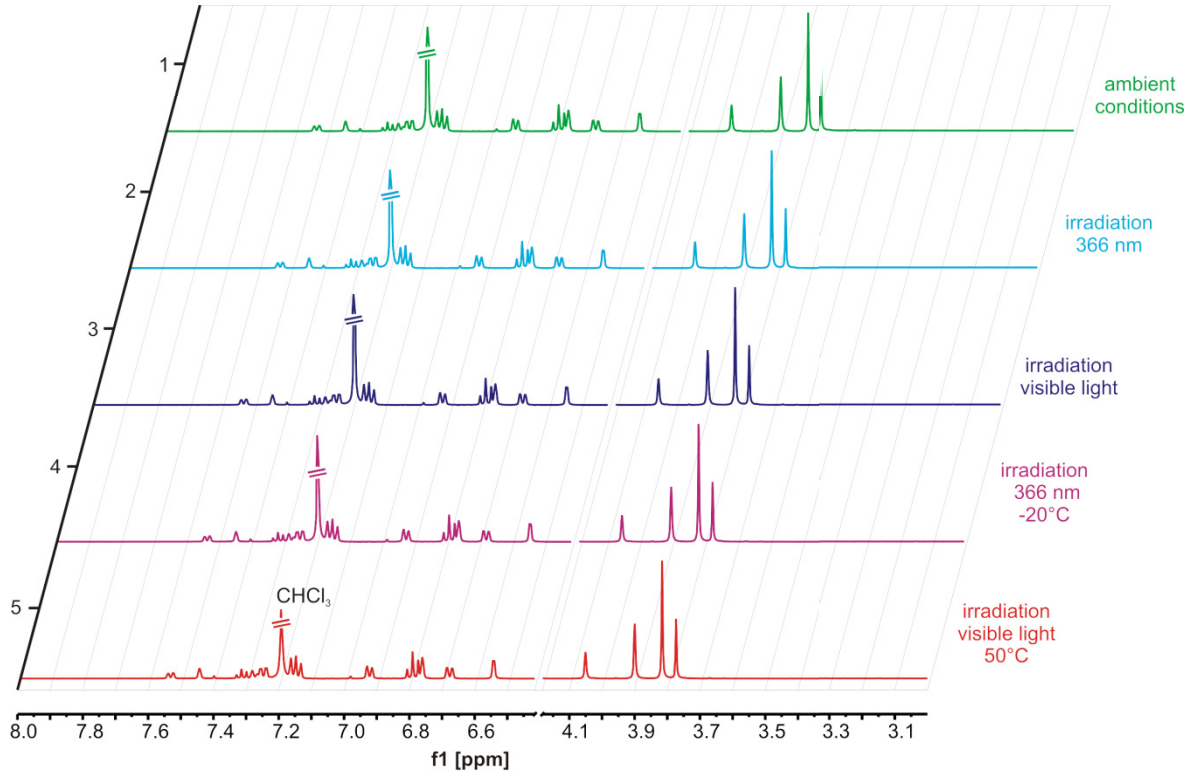

Figure 69 ^{1}H-NMR measurements of macrocycle **125** in $CDCl_3$, recorded with 128 scans on a 500 MHz spectrometer. Just the relevant parts of the spectra are shown in order to simplify the visualization. The green top spectrum is recorded after purification at room temperature. The samples which were irradiated at 366 nm were kept in the dark for 2 min until the ^{1}H-NMR spectrum was recorded. The samples which were cooled and warmed respectively were kept at the mentioned temperature until the ^{1}H-NMR spectrum was recorded. The ^{1}H-NMR spectrum itself were recorded in the dark at RT.

The first green spectrum shown in **Figure 69** was recorded after purification at room temperature without any irradiation and was the comparison spectrum. The same sample was then irradiated at 366 nm for 15 minutes at room temperature, in order to increase the amount of *cis* isomer in solution, but surprisingly the second spectrum was identical to the first one, neither the chemical shift nor the integration changed. And the same behavior was observed for all subsequent measurements. The third spectrum was irradiated with visible light to increase the *trans* isomer and even heating to 50°C did not favor the *trans* conformation (spectrum 5). The sample was then irradiated over night at 366 nm and cooled down to -20°C to favor

the *cis* isomer, but the recorded spectrum 4 did not show any increase of a specific isomer. The fact that in all these measurements no change at all could be observed in the *cis*/*trans* ratio of macrocycle **125**, neither in the chemical shift nor in the integration, indicating either a high stability of each isomer or that the cycle is not flexible enough to switch between both states. Since for the *cis* isomerization the TLC visualizer (12 W, 366 nm) was used, one could argue that the intensity of the lamp was too low for the isomerization reaction, but for the *trans* isomerization a 500 W lamp and temperatures of up to 60°C were used and even here no change was observed.

In order to further investigate the isomerization mechanism, macrocycle **125** was irradiated at 313 nm (wavelength of azo groups) in a 10^{-5} molar THF solution (**Figure 70A**). For the irradiation a 200 W mercury lamp with a dichromic filter (280-400 nm) and a 320 nm band-pass filter to select only the peak at 313 nm were used. After 30 minutes no further change in the conformation was observed. The thermal back reaction (**Figure 70B**) where the equilibrium was reached after 5 hours was also measured, in order to investigate the reversibility of the switching mechanism.

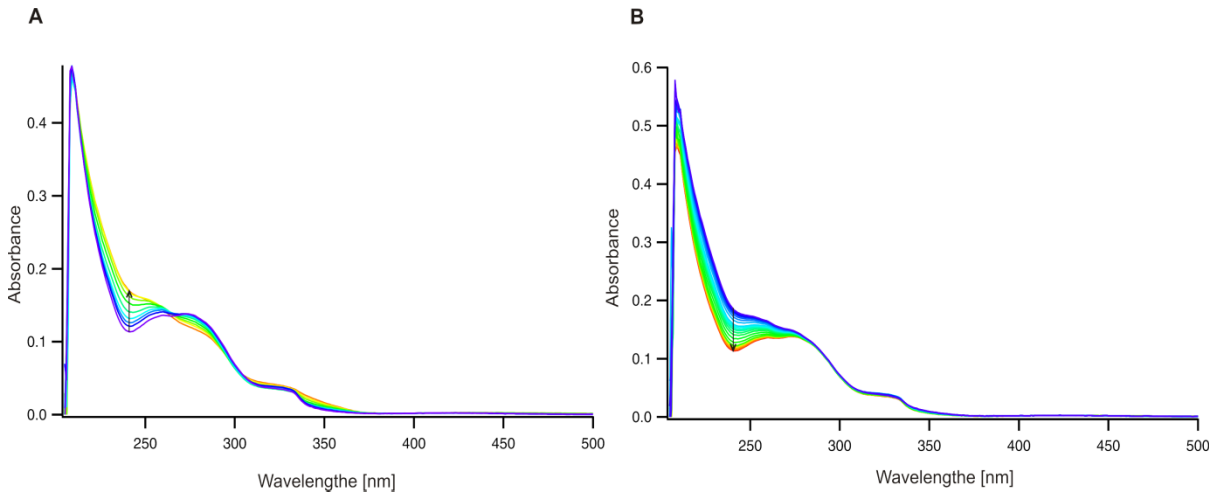

Figure 70 (A) Change of the absorbance spectra of macrocycle **125** in 10^{-5} molar THF solution upon irradiation at 313 nm. The overall irradiation was 30 min and every 3 min a measurement was done. (B) Change of the absorbance spectra of the thermal back reaction. Reaction was followed for 5 h, at least every 15 min a measurement was done.

The observed UV/Vis spectrum for macrocycle **125** is quite unexpected. Azo compounds are known to have an absorbance at about 320 nm, which is attributed to the thermodynamically favored *trans* conformation of the azo function.[26] Usually a decrease in the absorbance of the π → π* band and the increase in the n → π* absorbance upon irradiation over time is found attributed to the formation of the *cis* isomer.

In the investigated UV/Vis spectrum (**Figure 70**) a weak absorbance at 325 nm was observed, which can be attributed to a certain amount of *trans* isomer, but since this absorbance is rather weak, possibly the major isomer observed in the ^{1}H-NMR spectrum is the *cis* isomer (see **Figure 68**). Furthermore no change of the absorbance at 320 nm upon irradiation was observed. Together with the absence of an absorbance at about 450 nm upon irradiation, this indicates that there is no *cis* → *trans* isomerization of the azo functionality. These facts further corroborate a high ring strain and a rather stiff, nonelastic macrocycle **125**.

However, upon irradiation with UV light an absorbance change at 240 nm and at 275 nm was observed, but for the thermal back reaction only an absorbance change at 240 nm could be observed. This rather strange behavior for an azo compound points at an irreversible mechanism, or an alteration of the molecular structure. A change of the molecular structure of **125**, such as ring opening or deprotection could be excluded, as the ^{1}H-NMR spectrum before and after irradiation are the same. This absorbance change is more due to a slight deformation of macrocycle **125** instead of a proper *cis* → *trans* isomerization. The increased internal ring strain in the system may hinder the isomerization and just a deformation of the cyclic system may be observed.

In consideration of the performed investigation the macrocycle **125** was successfully synthesized in a low 2% yield. All attempts to increase the yield failed, even when applying high dilutions of up to 1.1×10^{-4} mol/L, only a small amount of the desired macrocycle **125** was isolated. Due to the ^{1}H-NMR- and UV/Vis investigations a *cis*/*trans* mixture was isolated and the internal ring strain, in order to switch between these two conformations, could not be overcome.

4.5 Summary and Conclusion of the Azobenzene Bridged Biphenyls

In this section the synthesis of a novel molecular switch and memory device based on “mechanical” motion in molecular biphenylic structures was described. A light sensitive azobenzene bridge was introduced in the biphenylic system as switching unit. A conformation change should cause a significant difference of the exterior form depending on the degree of isomerization.

In the first generation a dinitro key intermediate **70** with chlorines as further functionalities was synthesized and cyclized via a reductive azo formation. The formation of the product **76** was observed, but further improvement of the yield was necessary. The strategy was slightly adapted and a cyclization via Suzuki cross coupling reaction or a palladium catalyzed azo formation was envisaged. Both strategies ended in extensive polymer formation and no cyclized product was observed.

A modular strategy with different linker lengths was envisaged for the second generation. A series of different biphenyl precursors **99**, **106**, **110** and **112** was successfully synthesized and fully characterized. The cyclization with the “fixed” dibromo azo derivative **94** turned out to be troublesome. Either polymerization or decomposition of the starting material **94** before any conversion occurred was observed.

For the third generation a dinitro compound **116** with two methoxy groups as anchor group precursors was synthesized. While a cyclization via the urea derivative **124** remained unsuccessful, a reductive azo formation afforded the desired macrocycle **125** in rather low 2% yield. Further ^{1}H-NMR- and UV/Vis investigation have shown, that the product **125** was isolated as a *cis*/*trans* mixture and a normal isomerization of the azo function was not possible, probably due to the increased internal ring strain and the reduced flexibility of the cycle.

Since the switching behavior of macrocycle **125** was not reversible and did not lead to the two expected stable *cis* and *trans* isomers respectively, the conducting properties were not further analyzed. Also the introductions of different possible anchor groups were not further investigated. Several possible precursors such as

fluorides- and iodide derivatives were synthesized and characterized (see experimental section 6.4)

5 Summary and Conclusion

5.1 Azo Macrocycles

The goal of this thesis is the design and synthesis of new functional molecules, in particular azo macrocycles for surface modifications and as conductance switch.

A series of shape switchable azo macrocycles **1**-**7** consisting of *m*-terphenyl semicircles interlinked by two azo joints were designed and synthesized (**Figure 71**).

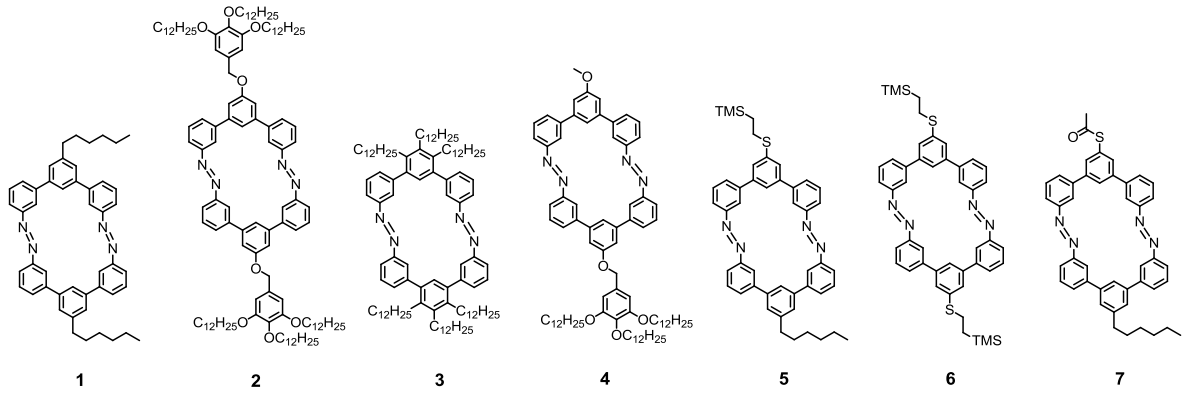

Figure 71 A series of shape switchable azo macrocycles **1**-**7**. Macrocycles **1**-**4** functionalized with long alkyl chains and macrocycles **5**-**7** functionalized with sulfur anchor groups.

All seven azo macrocycles **1**-**7** were obtained by reductive dimerization of the corresponding dinitro semicircles. A synthetic strategy for asymmetric azo coupling via a nitroso intermediate (see section 2.1.3) was investigated, however the isolation of the corresponding dinitroso semicircle, which is essential for the asymmetric coupling reaction, turned out to be troublesome. Hence, the asymmetric macrocycles **4** and **5** had to be synthesized through a statistical dimerization.

In a first series the alkyl functionalized azo macrocycles **1**-**4** were investigated (see section 2.1). Considering the polymerization potential of the synthetic strategy, the four azo macrocycles **1**-**4**, which could be purified by size exclusion

chromatography (SEC), were isolated in surprisingly good yields, ranging from 34% for **2**, to 44% and 49% for **4** and **3**, respectively, up to 50% for macrocycle **1**. These macrocycles were characterized by ^{1}H and ^{13}C-NMR spectra, profiting from the more sensitive ^{1}H-decoupled HMBC and HMQC techniques in the case of macrocycle **2** and **3**. Although the purity of **1**-**4** was shown by analytical GPC, the determination of their molecular weights turned out to be more troublesome in the case of **2** and **4**, but finally the molecular weights were determined by VPO.

All four macrocycles **1**-**4** displayed comparable absorbance spectra, and showed similar *trans* → *cis* photoisomerization upon irradiation at 313 nm. A *trans*/*cis* ratio of 15:85 of the isomers was determined in their photostationary states. The full thermal back reaction required several weeks. Hence, the thermodynamically less favored *cis* isomer showed substantial stabilization by the rigid macrocyclic structure. Despite having two azo groups in the macrocyclic periphery, an intermediate mixed *trans*/*cis* isomer was not observed, the stiff *m*-terphenyl semicircles probably disfavor a strained mixed state.

These shape switchable macrocycles **1**-**4** were designed to investigate their spatial transformations by scanning probe methods. At the moment scanning probe investigations are ongoing.

In a second series the sulfur functionalized azo macrocycles **5**-**7** were investigated (see section 2.2). In contrast to the alkyl functionalized azo macrocycles **1**-**4**, these macrocycles can be covalently attached to a gold surface to investigate their spatial transformations by scanning probe methods.

Considering the minor difference in molecular weight of the two different semicircles **11** and **43**, a separation with size exclusion chromatography was not possible. Despite the potential for polymerization in the synthetic strategy and the separation difficulties, the asymmetric macrocycle **5** was isolated analytically pure in a rather low yield of 6%. The symmetric macrocycle **6** was also isolated by preparative TLC, in yield of 5%. These macrocycles were fully characterized by standard analytical methods. Although the purity of **5**-**7** was shown by analytical GPC, the determination of their molecular weights was, due to the presence of

more functional groups and hetero atoms, less challenging compared to macrocycles **1**-**4**. All molecular weights were determined by MALDI-TOF mass spectroscopy with a very good correlation to the calculated and measured isotopic distribution.

The sulfur functionalized azo macrocycles **5**-**7** displayed comparable absorbance spectra to the alkyl functionalized ones. The time to reach the photostationary state at 313 nm increased from macrocycle **1** (8 min) to macrocycle **7** (30 min). The full thermal back reaction required several weeks, and was found to be at least as long as for macrocycle **1**. The thermodynamically less favored *cis* isomer also showed substantial stabilization. A mixed *trans*/*cis* isomer was not observed, neither for macrocycle **1** nor for macrocycle **7**.

These shape switchable macrocycles **5**-**7** were designed to investigate their spatial transformations by scanning probe methods. So far, all attempts to immobilize a self assembled monolayer (SAM) of these macrocycles on a gold surface have not yet come to fruition in spite of the sulfur anchor group, which is known to have a high affinity to a gold surface.

5.2 Platinum Electrode Modification

In section 3 a new modular technique for the functionalization of platinum electrodes was discussed. Combining the technique of electro reduction of aryl diazonium salts with Sonogashira cross coupling reactions, it is possible to modify platinum surfaces with a high surface coverage (**Figure 72A**). This new technique allows introducing of a wide range of functional groups onto an electrode surface (**Figure 72B**). To demonstrate the scope of this method, platinum electrodes were functionalized with four different acetylenes **54**, **58**, **60**, **61** resulting in four different surface functions. Namely a simple alkyl chain as an insulating layer (electrode **E1**), a more bulky substituent with further functionalization options (electrode **E2**), a redox active ferrocene species (electrode **E3**) and a redox active BiEDOT functionality (electrode **E4**) allowing for the growth of a conjugated EDOT polymer by electro polymerization directly on the electrode's surface.

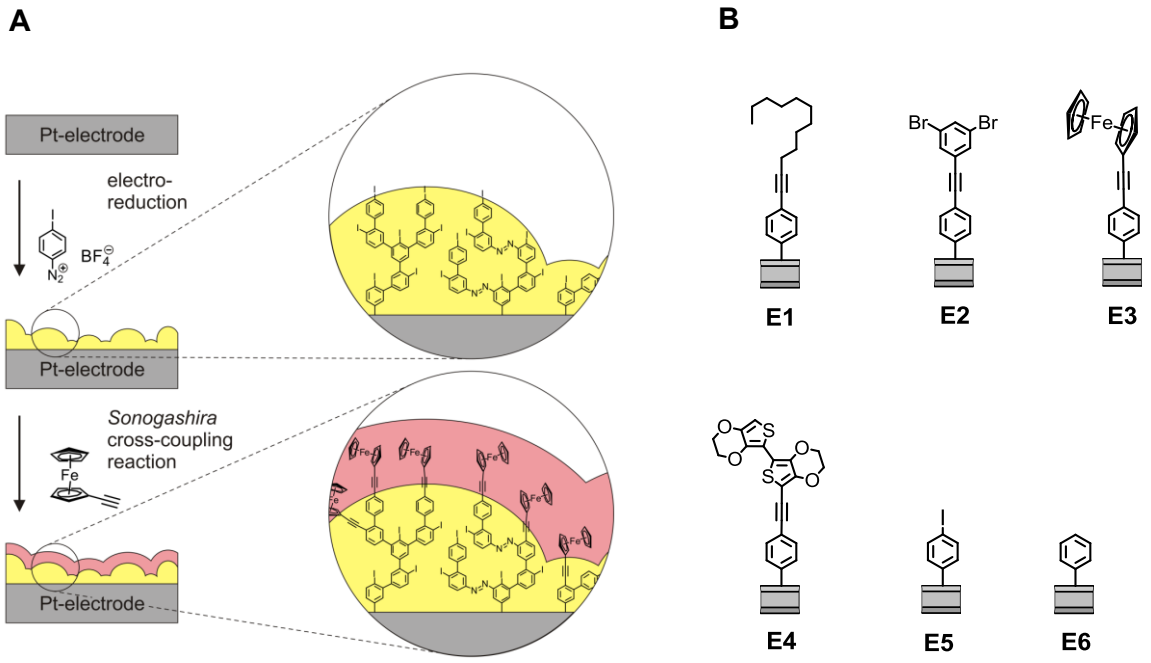

Figure 72 (A) Sketch for the stepwise functionalization of platinum electrodes. Electrochemical reduction of an iodoaryl diazonium salt in a first step and Sonogashira cross coupling reaction in the solid state as a second step to introduce a wide range of functional groups onto surfaces, with high surface coverage of the functional subunit. (B) Functionalized and investigated platinum electrodes **E1**-**E6**.

The electro reduction of the diazonium salt yielded a dendritic growth of multilayers (about 5 layers). According to the surface analysis, the Sonogashira cross coupling reaction of sterically demanding acetylenes mainly occurred at exposed iodophenyls at the surface. Considering the experiences made with all the acetylenes studied, a decrease of the iodine content by dehalogenation during the coupling reaction was found.

Furthermore, the molecular carpet made of iodophenyl moieties after electroreduction of *para*-iodophenyl diazonium salt **48** allows further functionalization by Sonogashira cross coupling reactions. The reaction completeness was estimated using XPS. The moderate increase in film size and the quantification of the CV scans consistently indicated a significant conversion at the electrodes surface.

The investigations discussed here pave the way towards further possible functionalization of electrodes. The conducting biphenyl described with an azobenzene bridge could act as a potential switching unit on an electrode. Thanks to integration via a Sonogashira cross coupling reaction a broad variety of functional molecules are accessible. These studies were geared mainly towards a proof of the concept for the two step functionalization of electrodes via electro reduction and subsequent Sonogashira cross coupling reactions. This general method can be applied for more exciting functions such as sensing or in storage devices.

5.3 Switching Conducting Azo Biphenyls

In section 4 the synthesis of a novel molecular switch and memory device based on “mechanical” motion in molecular biphenylic structures was described. A light sensitive azobenzene bridge was introduced in the biphenylic system as the switching unit. A conformation change should cause a significant change in the exterior form depending on the degree of isomerization.

In the first generation (**Figure 73**) a dinitro key intermediate **70** with chlorines as further functionalities was synthesized and cyclized via a reductive azo formation. The formation of the product **76** was observed, but further improvement of the yield was necessary. The strategy was slightly adapted and a cyclization via Suzuki cross coupling reaction or a palladium catalyzed azo formation was envisaged. Both strategies ended in extensive polymer formation and no cyclized product **76** was observed.

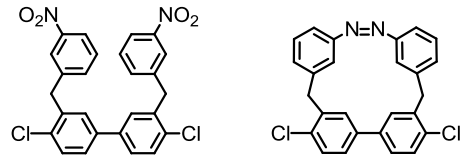

70 **76**

Figure 73 Synthesized key intermediate **70** and target macrocycle **76** of the first generation.

A modular strategy with different linker lengths was envisaged for the second generation (**Figure 74**). A series of different biphenyl precursors **99**, **106**, **110** and **112** was successfully synthesized and fully characterized. The cyclization with the “fixed” dibromo azo derivative **94** turned out to be troublesome. Either polymerization or decomposition of the starting material **94**, before any conversion occurred, was observed.

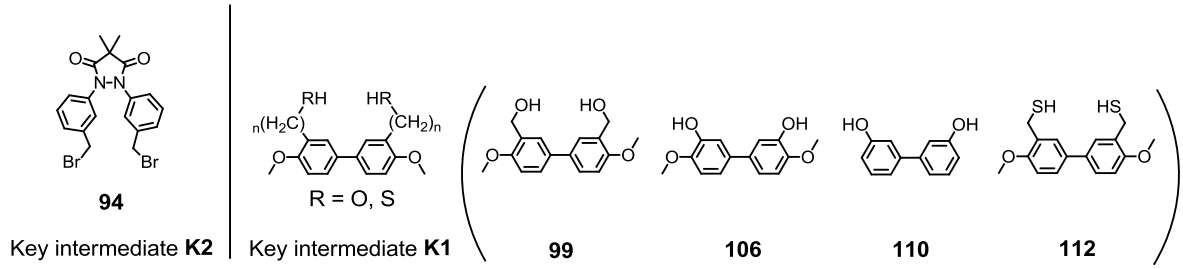

Figure 74 Modular strategy of the second generation with different linker length.

For the third generation a dinitro compound **116** with two methoxy groups as anchor group precursors was synthesized. While a cyclization via the urea derivative **124** remained unsuccessful, a reductive azo formation afforded the desired macrocycle **125** in rather low 2% yield. Further ^{1}H-NMR- and UV/Vis investigation have shown, that the product **125** was isolated as a *cis*/*trans* mixture and a normal isomerization of the azo function was not possible, probably due to the increased internal ring strain and the reduced flexibility of the cycle.

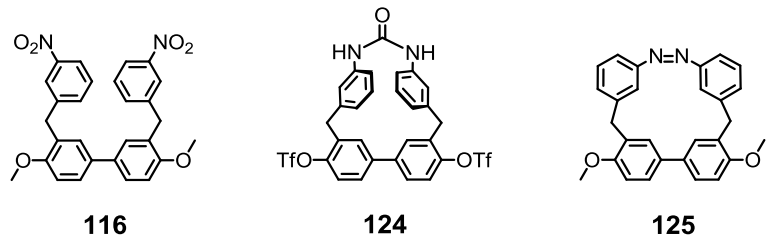

Figure 75 Synthesized key compounds **116, 124** and **125** of the third generation.

Since the switching behavior of macrocycle **125** was not reversible and did not lead to the two expected stable *cis* and *trans* isomers respectively, the conducting properties were not further analyzed. The introduction of different possible anchor group precursors such as fluorides- and iodide derivatives were synthesized and characterized (see experimental section 6.4). The macrocyclic structure of such a compound is probably too small and too rigid in order to obtain a stable switching unit and need to be investigated further.

6 Experimental Section

6.1 Materials and Analytical Methods

Reagents and solvents

All chemicals were directly used for the synthesis without further purification as received from *Fluka AG* (Buchs, Switzerland), *Acros AG* (Basel, Switzerland), *Merck* (Darmstadt, Germany), *Alfa Aesar* (Karlsruhe, Germany), *ABCR* (Karlsruhe, Germany) and *Aldrich* (Buchs, Switzerland) unless otherwise stated. The solvents for chromatography and crystallization were distilled once before use, the solvents for extraction were used in technical grade. Dry tetrahydrofuran (THF) was dispensed from a Pure Solv MD Solvent Purification System or distilled over sodium and potassium with benzophenone. Dry dichloromethane (DCM) was dispensed from a Pure Solv MD Solvent Purification System or distilled over calcium hydride. All other dry solvents were purchased over molecular sieves from *Fluka*. For an inert atmosphere *Argon 4.8* from *PanGas AG* (Dagmersellen, Switzerland) was used.

Synthesis

All reactions with reagents which are sensitive to air or moisture were performed under an argon atmosphere using Schlenk technique, only dry solvents were used and the glassware was heated out before use.

^{1}H-Nuclear Magnetic Resonance (^{1}H-NMR)

Bruker DRX-NMR (500 MHZ), *Bruker DPX-NMR* (400 MHz) and *Bruker BZH-NMR* (250 MHz) instruments were used to record the spectra. Chemical shifts (δ) are reported in parts per million (ppm) relative to residual solvent peaks ($CDCl_3$: 7.26 ppm) or trimethylsilane (TMS: 0.00 ppm), and coupling constants (*J*) are reported in Hertz (Hz). The bond distance of the coupling constant is stated with a superscript number (^{n}J). NMR solvents were obtained from *Cambridge Isotope Laboratories, Inc.* (Andover, MA, USA). The measurements were done at room temperature. The multiplicities are written as: s = singlet, d = doublet, t = triplet, q = quartet, quin = quintet, sext = sextet, hept = heptet, m = multiplet and br = broad.

^{13}C-Nuclear Magnetic Resonance (^{13}C-NMR)

Bruker DRX-NMR (126 MHz), *Bruker DPX-NMR* (101 MHz) and *Bruker* DRX-600 NMR (151 MHz) instruments were used to record the spectra. Chemical shifts (δ) are reported in parts per million (ppm) relative to residual solvent peaks ($CDCl_3$: 77.0 ppm or TMS: 0.0 ppm). The measurements were done at room temperature. Carbon valency is given as: Cp (primary carbon), Cs (secondary carbon), Ct (tertiary carbon) and Cq (quaternary carbon). The multiplicities are written as: s = singlet, d = doublet, t = triplet, q = quartet, quin = quintet, m = multiplet. The amount of carbon is stated due to intensity and calculation and could be wrong in rare cases. The coupling constants (*J*) are reported in Hertz (Hz) and are just stated in fluorine containing molecules. The bond distance of the coupling constant is stated with a superscript number (^{n}J). If the valency is stated the assignment is clear and confirmed with HMBC (heteronuclear multiple bond coherence) and HMQC (heteronuclear multiple quantum coherence).

^{19}F-Nuclear Magnetic Resonance (^{19}F-NMR)

A *Bruker DPX-NMR* (377 MHz) instrument was used to record the spectra. Chemical shifts (δ) are reported in parts per million (ppm), uncorrected. The measurements were done at room temperature. Coupling constants (J) are reported in Hertz (Hz). The multiplicities are written as: s = singlet, d = doublet, t = triplet, q = quartet, quin = quintet, m = multiplet.

Mass spectrometry (MS)

Mass spectra were recorded on a *Bruker esquire 3000 plus* for Electron Spray Ionization (ESI), a *finnigan MAT 95Q* for Electron Impact (EI), a *finnigan MAT 8400* for Fast Atom Bombardment (FAB), or a *Voyager-De™ Pro* for MALDI-TOF (using 1,8,9-anthracentriol or 2,5-dihydrosybenzoic acid as matrix). Significant signals are given in mass units per charge (*m/z*) and the relative intensities are given in brackets. EI-MS and FAB-MS measurements were performed by Dr. H. Nadig

Elementary Analysis (EA)

Elementary analyses were measured by W. Kirsch on a *Perkin-Elmer Analysator 240*. The values are given in mass percent.

Melting points (MP)

Melting points were determined in °C using a *Stuart SMP3* apparatus and are uncorrected.

Ultraviolet Spectroscopy (UV)

UV/Vis-spectra were recorded on an *Agilent* 8453 diode array detector spectrophotometer using optical 114-*QS Hellma* cuvettes (10 mm light path) at room temperature and ambient conditions unless otherwise stated. All macrocyclic azo compounds were analyzed by Dr. Klaus Schuermann in the group of Prof. Dr. Luisa De Cola. Spectra were recorded with a *Varian Cary* 5000 two beam spectrophotometer with baseline correction and pure solvent as reference. For irradiation a *Lot-Oriel* 200 W high pressure mercury lamp with a 280-400 nm dichroic mirror (to remove IR and visible light) and a *Perkin-Elmer* 320 nm band pass filter to allow only light from the 313 nm Hg line were used.

Infrared Spectroscopy (IR)

IR spectra were recorded neat with a *Shimadzu FTIR* 8400S fourier transform infrared spectrometer. Intensity of the peaks is written as: w = weak, m = middle, s = strong.

Cyclic Voltammetry (CV)

All electrochemical measurement were performed with a *Metrohm Autolab PGSTAT 1* and a conventional three-electrode system, comprising the modified substrate as working electrode, a platinum wire as counter electrode, and a Ag/AgCl 3.0 M KCl electrode from *Metrohm* as reference. All potentials were reported versus Ag/AgCl reference electrode at room temperature.

The surface concentration (Γ) was determined electrochemically using platinum electrode surfaces and applying the following equation:

$$\Gamma = \frac{Q}{nFA}$$

Where Q is the charge determined by integration of the voltammetric anodic peak corrected for the charging current, n is the number of electrons involved in electron-

transfer process (n = 1 for ferrocene/ferrocenium and reduction of aryl diazonium salt), F is the Faraday constant, and A is the electro-active surface area of the electrode surfaces use in the study.

Atomic Force Microscopy (AFM)

We used a commercial atomic force microscope from *Veeco Dimension V* with commercial tips from *Nanosensors* to study the layer thickness and morphology of the functionalized electrodes. For this a clean and homogenous area of the sample was imaged using the dynamic operation mode (tapping mode) first. Within that area a square of 500 nm × 500 nm was scratched off with the AFM tip at 2 Hz line frequency operating the same tip in the static operation mode (contact mode). During this scratching step a load force was chosen high enough to induce complete removal of the organic film, but yet low enough to leave the underlying platinum substrate intact. In a subsequent imaging step using the dynamic mode, a larger area was scanned, allowing determining the thickness of the removed layer.

X-ray Photoelectron Spectroscopy (XPS)

For XPS we used a commercial system from *Sigmaprobe by Thermo Scientific* applying a monochromatized aluminum X-ray source. No further sample preparation was undertaken prior to analysis of the samples.

Contact Angle Measurement (CA)

Water static contact-angle measurements were carried out at room temperature by the sessile drop method, using a *Standard Easy Drop* system from *Krüss*. The samples were placed on a flat, horizontal support. For each sample, contact angle measurement was repeated for three times at different sites, and the average value was taken as the contact angle of the sample. To extract the precise contact angle values, the drop images were fitted with commercial software (*Drop Shape Analysis, DSA v. 1.9, Krüss, Germany*) that uses the Young-Laplace equation.

Gel Permeation Chromatography (GPC)

Shimadzu LC-8A was used to record the chromatogram. The measurements were done at room temperature with an *OligoPore* 300 x 7.5 mm column (particle size 6 µm) from *Polymer Laboratories*, eluting with toluene, with a flow rate of 1.0 mL/min or 0.5 mL/min at λ = 220 nm and 330 nm.

Vapor Pressure Osmometry (VPO)

The VPO measurements were performed on a *Knauer* K-7000 vapor pressure osmometer. For the calculation the software *EuroOsmo* 7000 was used.

Column Chromatography (CC)

For CC *silica gel 60* (40-63 µm) from *Merck* or *silica gel 60* (40-63 µm) from *Fluka* was used. For preparative size exclusion chromatography (SEC) *Bio-Beads* S-X from *Bio Rad* with distilled toluene as eluent was used.

Thin Layer Chromatography (TLC)

Silica gel 60 F_{254} glass plates with a thickness of 0.25 mm from *Merck* were used. The detection was observed with a UV lamp at 254 nm by fluorescence quenching or at 366 nm by self fluorescence.

Preparative Thin Layer Chromatography (Prep TLC)

PLC Silica gel 60 F_{254} glass plates with a thickness of 0.5 mm from *Merck* were used. The detection was observed with a UV-lamp at 254 nm by fluorescence quenching or at 366 nm by self fluorescence.

6.2 Azo Macrocycles

6.2.1 Alkyl Functionalized Azo Macrocycles

2,6-Dibromo-4-hexylbenzenamine (9)

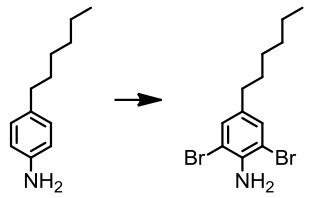

8 **9**

$C_{12}H_{17}Br_2N$
335.08 g/mol

4-Hexylaniline (**8**) (4.52 g, 25.5 mmol, 1.0 eq.) was dissolved in DMF (30 mL) and cooled to 0°C, *N*-bromosuccinimide (11.3 g, 63.7 mmol, 2.5 eq.) dissolved in DMF (30 mL) was added drop wise while stirring over a period of 30 min. The reaction mixture was stirred at 0°C for 30 min and for further 3 hours at room temperature. The reaction mixture was evaporated to dryness and the crude was purified by column chromatography with silica gel an toluene:dichloromethane (2:1) affording the brominated product **9** in 86% yield as dark red crystals after standing over night.

TLC: R_f = 0.73 (toluene:dichloromethane 2:1).

MP: 65-67°C.

^{1}H-NMR (250 MHz, $CDCl_3$): δ = 7.19 (s, 2H), 4.39 (br s, 2H), 2.45 (t, ^3J = 7.4 Hz, 2H), 1.53 (m, 2H), 1.28 (m, 6H), 0.88 (m, ^3J = 6.0 Hz, 3H) ppm.

MS (EI, m/z): 335.0 (100%) [M^+], 333.0 (51%), 337.0 (49%), 336.0 (13%).

1,3-Dibromo-5-hexylbenzene (10)

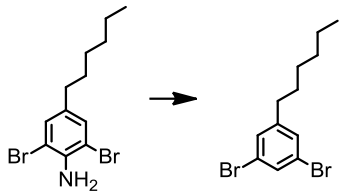

9 **10**

$C_{12}H_{16}Br_2$
320.06 g/mol

2,6-Dibromo-4-hexylbenzenamine (**9**) (7.26 g, 21.8 mmol, 1.0 eq.) was dissolved in ethanol (130 mL) and sulphuric acid 98% (10 mL). Sodium nitrite (4.50 g, 65.4 mmol, 3.0 eq.) was slowly added in small portions while stirring. Afterwards the reaction mixture was stirred at 75°C for 2 h. After the reaction mixture was cooled to 5 °C, water (50 mL) was added and the suspension was extracted with dichloromethane (2 × 30 mL), the combined organic layers were dried over $MgSO_4$ and evaporated. The black oily residue was purified by column chromatography with silica gel and *n*-hexane affording the product **10** as a light yellow liquid in a yield of 60%.

TLC: R_f = 0.56 (*n*-hexane).

^{1}H-NMR (400 MHz, $CDCl_3$): δ = 7.47 (t, ^4J = 2.0 Hz, 1H), 7.24 (d, ^4J = 2.0 Hz, 2H), 2.53 (t, ^3J = 7.6 Hz, 2H), 1.57 (m, 2H), 1.29 (m, 6H), 0.88 (t, ^3J = 7.1 Hz, 3H) ppm.

^{13}C-NMR (101 MHz, $CDCl_3$): δ = 147.3 (s, 1C), 131.7 (s, 1C), 130.7 (s, 2C), 123.1 (s, 2C), 35.8 (s, 1C), 32.0 (s, 1C), 31.4 (s, 1C), 29.2 (s, 1C), 23.0 (s, 1C), 14.5 (s, 1C) ppm.

MS (EI, m/z): 318.0 (17%), 320.0 (36%) [M^+], 322.0 (17%), 250.3 (100%), 169.3 (51%), 89.2 (22%).

EA: calculated C 45.03, H 5.04, N 0.00; found C 44.89, H 5.17, N 0.00.

5'-Hexyl-3,3''-dinitro-1,1':3',1''-terphenyl (11)

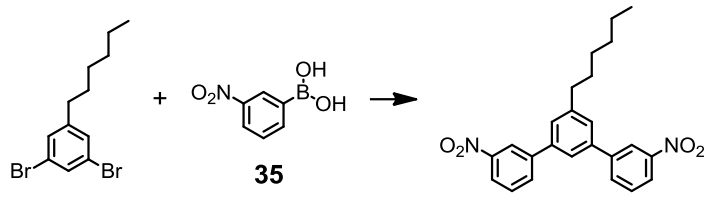

10 **35** **11**

$C_{24}H_{24}N_2O_4$
404.46 g/mol

Conventional conditions: To a solution of dry toluene (100 mL) and dry ethanol (30 mL), 1,3-dibromo-5-hexylbenzene (**10**) (1.00 g, 3.15 mmol 1.0 eq.), 3-nitrophenylboronic acid (**35**) (1.41 g, 8.18 mmol, 2.6 eq.), $[Pd(PPh_3)_4]$ (290 mg, 0.252 mmol, 8.0 mol-%) and K_2CO_3 (3.48 g, 25.2 mmol, 8.0 eq.) were added under argon. The reaction mixture was stirred vigorously at 85°C for 3 h. After cooling to room temperature the reaction mixture was filtered over 1 cm plug of silica gel, eluted with toluene and then washed with ethanol. The residue was adsorbed on silica gel and purified by column chromatography with silica gel and ethyl acetate:*n*-hexane (1:5) to give the product **11** as a light green solid in a yield of 95%.

Microwave conditions: To a solution of dry toluene (7 mL) and dry ethanol (3 mL), 1,3-dibromo-5-hexylbenzene (**10**) (100 mg, 0.315 mmol 1.0 eq.), 3-nitrophenylboronic acid (**35**) (141 mg, 0.818 mmol, 2.6 eq.), $[Pd(PPh_3)_4]$ (29.0 mg, 25.2 µmol, 8.0 mol-%) and K_2CO_3 (348 mg, 2.52 mmol, 8.0 eq.) were added under argon. The reaction mixture was heated to 120°C for 10 min in a microwave. After cooling to room temperature the reaction mixture was filtered over 1 cm plug of silica gel, eluted with toluene and then washed with ethanol. The residue was adsorbed on silica gel and purified by column chromatography with silica gel and ethyl acetate:*n*-hexane (1:5) to give the product **11** as a light green solid in a yield of 98%. With microwave conditions the yield could be improved compared to the yield obtained under conventional conditions.

TLC: R_f = 0.32 (ethyl acetate:*n*-hexane 1:5).

MP: 86-89°C.

^{1}H-NMR (400 MHz, $CDCl_3$): δ = 8.50 (t, ^4J = 2.0 Hz, 2H), 8.24 (m, 2H), 7.98 (m, 2H), 7.66 (t, ^3J = 8.1 Hz, 2H), 7.65 (t, ^4J = 1.5 Hz, 1H), 7.50 (d, ^4J = 1.5 Hz, 2H), 2.79 (t, ^3J = 7.6 Hz, 2H), 1.73 (quin, ^3J = 7.6 Hz, 2H), 1.42 (quin, ^3J = 7.6 Hz, 2H), 1.35 (m, 4H), 0.91 (t, ^3J = 7.1 Hz, 3H) ppm.

^{13}C-NMR (101 MHz, $CDCl_3$): δ = 149.2 (s, 2C), 145.6 (s, 1C), 143.0 (s, 2C), 140.2 (s, 2C), 133.6 (s, 2C), 130.2 (s, 2C), 127.9 (s, 2C), 123.9 (s, 1C), 122.8 (s, 2C), 122.5 (s, 2C), 36.5 (s, 1C), 32.1 (s, 1C), 32.0 (s, 1C), 29.5 (s, 1C), 23.0 (s, 1C), 14.5 (s, 1C) ppm.

IR (ATR, neat, $\tilde{\nu}$/cm^{-1}): 3072 (w), 2924 (m), 2854 (m), 1599 (m), 1519 (s), 1344 (s), 720 (s).

MS (EI, m/z): 404.2 (69%) [M^+], 405.2 (18%), 334.2 (100%), 287.2 (25%), 239.0 (43%), 226.0 (23%).

EA: calculated C 71.27, H 5.98, N 6.93; found C 71.10, H 5.96, N 6.87.

5'-Hexyl-[1,1':3',1''-terphenyl]-3,3''-diamine (12)

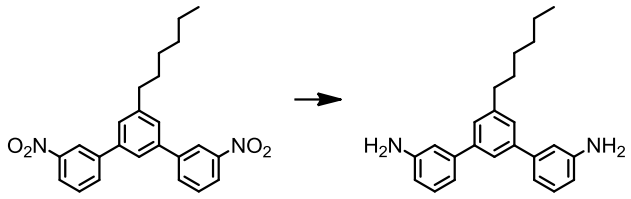

11 **12**

$C_{24}H_{28}N_2$
344.49 g/mol

5'-Hexyl-3,3''-dinitro-1,1':3',1''-terphenyl (**11**) (50.0 mg, 0.124 mmol, 1.0 eq) and palladium on activated carbon (8.00 mg, 0.0752 mmol, 0.6 eq) were suspended in dichloromethane (5 mL) and added into a sample glass, which was put in an autoclave with 20 bars of hydrogen. The reaction mixture was stirred at room temperature for 16 h. The reaction mixture was filtered over a 3 cm plug of *Celite*® and evaporated to dryness. After drying under high vacuum conditions the amine **12** was isolated as a light yellow solid in a yield of 87%.

TLC: R_f = 0.54 (ethyl acetate).

MP: 102-104°C.

^{1}H-NMR (400 MHz, $CDCl_3$): δ = 7.56 (t, ^4J = 1.5 Hz, 1H), 7.34 (d, ^4J = 1.5 Hz, 2H), 7.23 (t, ^3J = 7.8 Hz, 2H), 7.03 (m, 2H), 6.95 (t, ^4J = 1.5 Hz, 2H), 6.67 (m, 2H), 3.72 (br s, 4H), 2.70 (t, ^3J = 7.8 Hz, 2H), 1.69 (quin, ^3J = 7.8 Hz, 2H), 1.39 (quin, ^3J = 7.8 Hz, 2H), 1.32 (m, 4H), 0.89 (t, ^3J = 7.8 Hz, 3H) ppm.

^{13}C-NMR (101 MHz, $CDCl_3$): δ = 146.5 (s, 2C), 143.4 (s, 1C), 142.4 (s, 2C), 141.5 (s, 2C), 129.4 (s, 2C), 126.0 (s, 2C), 123.3 (s, 2C), 117.6 (s, 1C), 113.8 (s, 2C), 113.7 (s, 2C), 36.0 (s, 1C), 31.5 (s, 1C), 31.3 (s, 1C), 28.9 (s, 1C), 22.4 (s, 1C), 13.9 (s, 1C) ppm.

IR (ATR, neat, $\tilde{\nu}$/cm^{-1}): 3253 (br, m), 3072 (w), 2924 (m), 2854 (m), 1374 (s), 728 (s).

MS (EI, m/z): 344.2 (100%) [M^+], 345.0 (26%), 273.0 (32%).

EA calculated C 83.68, H 8.19, N 8.13; found C 82.86, H 8.18, N 8.01.

Symmetric hexyl functionalized azo macrocycle 1

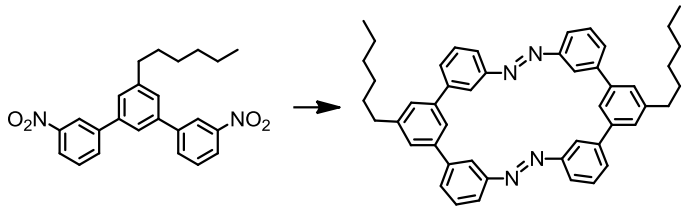

11 **1**

$C_{48}H_{48}N_4$
680.92 g/mol

5'-Hexyl-3,3''-dinitro-1,1':3',1''-terphenyl (**11**) (300 mg, 0.742 mmol, 2.0 eq.) was dissolved under argon in dry THF (1500 mL). 1 M $LiAlH_4$ solution in THF (3.00 mL, 2.97 mmol, 8.0 eq.) was carefully added over a period of 60 min. After complete addition, the reaction mixture was stirred at room temperature for 1 h and at 40°C for additional 4 h. After cooling down to room temperature, water (150 mL) was added carefully and after stirring for 5 min the reaction mixture was filtered. The filtrate was extracted with dichloromethane (2 × 500 mL) and the combined organic layers were dried over $MgSO_4$ and evaporated. The crude was purified by size exclusion column chromatography with *Bio-Beads*® S-X Beads and toluene, the almost pure crude was dissolved in 5 mL of a warm solvent mixture of ethanol:toluene (6:5). The solution was left for ten days in the freezer at -20°C and afterwards the solvent was decanted and the dark orange oily residue was washed with ethanol and dried under high vacuum conditions for 5 h to give a bright orange solid as macrocycle **1** in a yield of 50%.

TLC: R_f = 0.74 (dichloromethane).

MP: 155-157°C.

An alternative purification method resulted in a purer product but in a significant decrease of yield: The orange crude was chromatographed with silica gel and dichloromethane and the first few orange fractions were collected and evaporated. The resulting product was further purified by size exclusion column chromatography (SEC) with S-X Beads and toluene. The pre cleaned crude was purified on a preparative TLC plate (0.5 mm silica gel) with

dichloromethane:*n*-hexane (1:1). After extracting the top band, macrocycle **1** was isolated as orange crystals in a yield of 15%.

TLC: R_f = 0.75 (dichloromethane).

Prep TLC: R_f = 0.91 (dichloromethane:*n*-hexane (1:1).

MP: 159-160°C.

^{1}H-NMR (500 MHz, $CDCl_3$): δ = 8.63 (s, 4H), 8.21 (s, 2H), 8.02 (d, ^3J = 7.9 Hz, 4H), 7.89 (d, ^3J = 7.9 Hz, 1H), 7.64 (t, ^3J = 7.9 Hz, 4H), 7.58 (s, 4H), 2.80 (t, ^3J = 6.7, 4H), 1.75 (quin, ^3J = 6.7, 4H), 1.42 (m, 4H), 1.35 (m, 8H), 0.90 (t, ^3J = 6.7, 6H).

^{13}C-NMR (126 MHz, $CDCl_3$, clear determination by HMBC and HMQC): δ = 153.6 (s, Cq, 4C), 144.7 (s, Ct, 4C), 142.8 (s, Cq, 4C), 141.5 (s, Cq, 4C), 130.3 (s, Cq, 2C), 130.0 (s, Ct, 4C), 127.3 (s, Ct, 4C), 124.1 (s, Ct, 4C), 122.6 (s, Ct, 2C), 122.0 (s, Ct, 4C), 36.7 (s, Cs, 2C), 32.2 (s, Cs, 2C), 32.1 (s, Cs, 2C), 29.6 (s, Cs, 2C), 23.1 (s, Cs, 2C), 14.6 (2C, Cp, s) ppm.

IR (ATR, neat, $\tilde{\nu}$/cm^{-1}): 3051 (w), 3024 (w), 2924 (s), 2852 (m), 1593 (m), 1504 (w), 1445 (4), 1441 (m), 1155 (m).

UV (λ, nm): 248 (λ_{max}), 322, 443.

GPC (retention time, 0.5 mL/min): 11.85 min, area (100%).

VPO (determined molecular weight, gmol^{-1}): 709.

MS (EI, m/z): 680.3 (6%) [M$^+$], 681.3 (3%), 344.0 (100%), 85.0 (11%), 71.0 (17%), 57.0 (33%), 44.0 (35%).

MS (MALDI-TOF, m/z): 680.1 (100%) [M$^+$], 681.1 (65%), 682.1 (20%).

1,3-Dibromo-5-methoxybenzene (15)

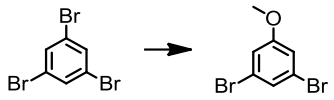

14 **15**

$C_7H_6Br_2O$
265.93 g/mol

Sodium methoxide (1.20 g, 22.2 mmol, 1.4 eq.) was added to a solution of 1,3,5-tribromobenzene (**14**) (5.10 g, 15.9 mmol, 1.0 eq.) in DMF (50 mL). The reaction mixture was stirred at 80 °C for 8 h, quenched with 10 % aq. HCl solution (20 mL) and extracted with TBME (3 × 30 mL). The combined organic layers were washed with brine (35 mL), dried over $MgSO_4$ and evaporated to dryness. The crude was purified by column chromatography with silica gel and *n*-hexane to give the desired product **15** as a white solid in a yield of 70%.

TLC: R_f = 0.30 (*n*-hexane).

MP: 42-43°C.

^{1}H-NMR (400 MHz, $CDCl_3$): δ = 7.25 (t, ^4J = 1.8 Hz, 1H), 6.99 (d, ^4J = 1.8 Hz, 2H), 3.78 (s, 3H) ppm.

^{13}C-NMR (101 MHz, $CDCl_3$): δ = 161.2 (s, 1C), 126.8 (s, 1C), 123.5 (s, 2C), 116.9 (s, 2C), 56.1 (s, 1C) ppm.

MS (EI, m/z): 265.8 (100%) [M^+], 263.8 (49%), 266.8 (7%), 267.8 (47%), 235.8 (19%).

EA: calculated C 31.62, H 2.27, N 0.00, found C 31.49, H 2.27, N 0.00.

5'-Methoxy-3,3''-dinitro-1,1':3',1''-terphenyl (16)

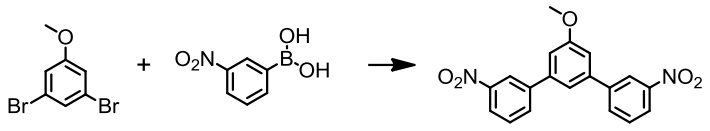

15 **35** **16**

$C_{19}H_{14}N_2O_5$
350.32 /mol

Conventional conditions: To a solution of 1,3-dibromo-5-methoxybenzene (**15**) (500 mg, 1.88 mmol, 1.0 eq.) in dry toluene (40 mL) and dry ethanol (15 mL) 3-nitrobenzeneboronic acid (**35**) (816 mg, 4.89 mmol, 2.6 eq.), $[Pd(PPh_3)_4]$ (174 mg, 0.152 mmol, 8.0 mol-%) and K_2CO_3 (2.07 g, 15.0 mmol, 8.0 eq.) were added under argon. The reaction mixture was stirred vigorously at 85 °C for 2 h. After cooling to room temperature the reaction mixture was filtered over a 1 cm plug of silica gel and washed with toluene (150 mL) and evaporated to dryness. The dark crude was recrystallized from hot toluene affording the title compound **15** as a white powder in a yield of 33%.

Microwave conditions: To a solution of 1,3-dibromo-5-methoxybenzene (**15**) (100 mg, 0.376 mmol, 1.0 eq.) in dry toluene (7 mL) and dry ethanol (3 mL) 3-nitrobenzeneboronic acid (**35**) (163 mg, 0.978 mmol, 2.6 eq.), $[Pd(PPh_3)_4]$ (43 mg, 0.0370 mmol, 10 mol-%) and K_2CO_3 (414 mg, 3.00 mmol, 8.0 eq.) were added under argon. The reaction mixture was heated at 120°C for 10 min in a microwave. After cooling to room temperature the reaction mixture was filtered over a 1 cm plug of silica gel and washed with toluene (150 mL) and evaporated to dryness. The dark crude was recrystallized from hot toluene, affording the title compound **15** as a white powder in a yield of 90%. With microwave conditions the yield could be improved significantly compared to the yield obtained under conventional conditions.

TLC: R_f = 0.35 (dichloromethane:*n*-hexane 1:1).

MP: 203-205°C.

^{1}H-NMR (400 MHz, d_6-DMSO): δ = 8.57 (t, ^4J = 2.0 Hz,), 8.28 (d, ^3J = 7.8 Hz,), 8.23 (dd, ^3J = 7.8 Hz, ^4J = 2.0 Hz,), 7.77 (t, ^3J = 7.8 Hz, 2H), 7.71 (t, ^4J = 1.4 Hz, 1H), 7.39 (d, ^4J = 1.4 Hz, 2H), 3.93 (s, 3H) ppm.

^{13}C-NMR (101 MHz, d_6-DMSO): δ = 161.4 (s, 1C), 149.3 (s, 2C), 142.3 (s, 2C), 141.1 (s, 2C), 134.7 (s, 2C), 131.3 (s, 2C), 123.4 (s, 2C), 122.6 (s, 2C), 119.3 (s, 1C), 113.7 (s, 2C), 56.5 (s, 1C) ppm.

IR (ATR, neat, $\tilde{\nu}$ /cm^{-1}): 3072 (w), 2939 (w), 1595 (m), 1518 (s), 1456 (m), 1344 (s), 1278 (m), 1209 (m), 1072 (m), 1041 (m), 854 (m).

MS (EI, m/z): 350.1 (100%) [M^+], 351.1 (21%), 352.1 (3%), 258.1 (13%), 215.1 (17%).

EA: calculated C 65.14, H 4.03, N 8.00; found. C 64.80, H 4.21, N 7.93.

3,3''-Dinitro-[1,1':3',1''-terphenyl]-5'-ol (17)

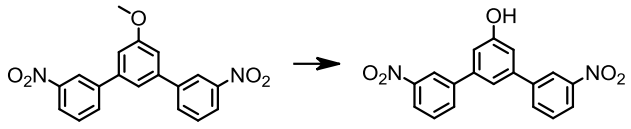

16 **17**

$C_{18}H_{12}N_2O_5$
336.30 g/mol

To a solution of the protected alcohol **16** (150 mg, 0.430 mmol, 1.0 eq.) in dry dichloromethane (15 mL), BBr_3 (170 µl, 1.82 mmol, 4.2 eq.) was slowly added at -78 °C. The orange reaction mixture was stirred at room temperature for 2.5 h and then poured onto ice water (20 mL). After extraction with dichloromethane (3 × 10 mL) the combined organic layers were washed with brine (20 mL), dried over $MgSO_4$ and evaporated to dryness, to afford the desired deprotected compound **17** as a pale yellow solid in a yield of 95%.

TLC: R_f = 0.45 (dichloromethane wtih 1% MeOH).

MP: 199-200°C.

^{1}H-NMR (400 MHz, $CDCl_3$): δ = 8.48 (m, 2H), 8.28 (m, 2H), 7.98 (m, 2H), 7.67 (t, ^3J = 8.1 Hz, 2H), 7.41(t, ^4J = 1.5 Hz, 1H), 7.17 (d, ^4J = 1.5 Hz, 2H) ppm.

MS (MALDI-TOF, m/z): 336.7 (30%) [M^+], 335.7 (100%).

Methyl-3,4,5-tris(dodecyloxy)benzoate (19)

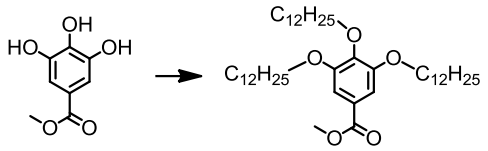

18 **19**

$C_{44}H_{80}O_5$
689.10 g/mol

To a solution of methyl-3,4,5-trihydroxybenzoate (**18**) (500 mg, 2.72 mmol, 1.0 eq.) in DMF (40 mL) 1-bromododecane (2.23 g, 8.96 mmol, 3.3 eq.), K_2CO_3 (1.31 g, 9.50 mmol, 3.5 eq.) and KI (676 mg, 4.07 mmol, 1.5 eq.) were added. After stirring at 70°C for 30 h the reaction mixture was cooled to room temperature, diluted with water (30 mL) and extracted with ethyl acetate (3 × 25 mL). The combined organic layers were dried over $MgSO_4$ and evaporated to dryness. The black crude was purified by column chromatography with silica gel and ethyl acetate:*n*-hexane (1:5). The alkylated product **19** was isolated as a pale yellow solid in a yield of 90%.

TLC: R_f = 0.57 (ethyl acetate:*n*-hexane 1:5).

MP: 46-49°C.

^{1}H-NMR (400 MHz, $CDCl_3$): δ = 7.25 (s, 2H), 4.01 (m, 6H), 3.89 (s, 3H), 1.84-1.70 (m, 6H), 1.47 (m, 6H), 1.26 (m, 48H), 0.88 (t, $^3J_{HH}$ = 6.9 Hz, 9H) ppm.

^{13}C-NMR (101 MHz, $CDCl_3$): δ = 167.4 (s, 1C), 153.2 (s, 2C), 142.7 (s, 1C), 125.0 (s, 1C), 108.4 (s, 2C), 73.9 (s, 1C), 69.6 (s, 2C), 52.5 (s, 1C), 32.3 (s, 3C), 30.0 (m, 21C), 26.5 (s, 3C), 23.1 (s, 3C), 14.5 (s, 3C) ppm.

MS (EI, m/z): 690.5 (12%), 689.5 (46%), 688.5 (100%) [M-H$^+$], 520.4 (27%), 184.0 (69%), 57.1 (32%).

EA: calculated C 76.69, H 11.70 N 0.00; found C 76.86, H 11.51, N 0.00.

3,4,5-Tris(dodecyloxy)phenyl)methanol (20)

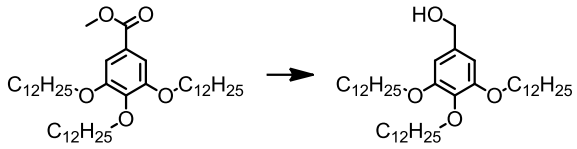

19 **20**

$C_{43}H_{80}O_4$
661.09 g/mol

To a solution of the benzoate **19** (1.50 g, 2.18 mmol, 1.0 eq.) in dry Et_2O (30 mL) $LiAlH_4$ powder (261 mg, 6.53 mmol, 4.5 eq.) was added under argon. After stirring at room temperature for 90 min the reaction mixture was diluted with water (10 mL) and 1 M aq. NaOH solution (10 mL). After stirring for additional 15 min at room temperature the grey viscous reaction mixture was diluted with THF (50 mL), filtered through *Celite*® and washed with TBME (100 mL). The water phase was extracted with TBME (3 × 20 mL). The combined organic layers were dried over $MgSO_4$, evaporated to dryness and dried under high vacuum conditions. The desired alcohol **20** was isolated as a white resin in a yield of 96%.

TLC: R_f = 0.14 (ethyl acetate:*n*-hexane 1:5).

^{1}H-NMR (400 MHz, $CDCl_3$): δ = 6.55 (s, 2H), 4.59 (s, 2H), 3.97 (m, 6H), 1.77 (m, 6H), 1.46 (m, 6H), 1.26 (m, 48H), 0.88 (t, $^3J_{HH}$ = 6.9 Hz, 9H) ppm.

^{13}C-NMR (101 MHz, $CDCl_3$): δ = 153.7 (s, 2C), 138.0 (s, 1C), 136.4 (s, 1C), 105.7 (s, 2C), 73.8 (s,1C), 69.5 (s, 2C), 66.1 (s, 1C), 32.4 (s, 3C), 30.0 (m, 21C), 26.5 (s, 3C), 23.1 (s, 3C), 14.5 (s, 3C) ppm.

MS (EI, m/z): 662.6 (11%), 661.6 (47%), 660.6 (100%) [M^+], 493.4 (15%), 492.4 (46%), 324.2 (13%), 156.1 (39%), 154.0 (10%), 127.0 (10%), 57.0 (15%).

EA: calculated C 78.12, H 12.20 N 0.00; found C 78.12, H 12.09, N 0.00.

5-(Chloromethyl)-1,2,3-tris(dodecyloxy)benzene (21)

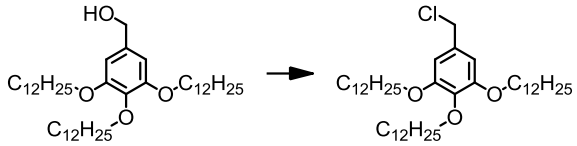

20 **21**

$C_{43}H_{79}ClO_3$
679.54 g/mol

To a solution of the alcohol **20** (1.33 g, 2.01 mmol, 1.0 eq.) in dichloromethane (30 mL) thionylchloride (204 µl, 2.82 mmol, 1.4 eq.) was added. After stirring at room temperature for 5 min, two drops of DMF were added. After further 45 min the reaction mixture was quenched with a 10 % aq. $NaHSO_3$ solution (5 mL) and water (5 mL). The reaction mixture was extracted with dichloromethane (2 × 15 mL).The combined organic layers were washed with brine (20 mL), dried over $MgSO_4$ and evaporated to dryness to afford the chlorinated compound **21** as pale yellow solid in a yield of 98%.

TLC: R_f = 0.64 (ethyl acetate:*n*-hexane 1:5).

MP: 49-52°C.

^{1}H-NMR (400 MHz, $CDCl_3$): δ = 6.57 (s, 2H), 4.51 (s, 2H), 3.97 (m, 6H), 1.78 (m, 6H), 1.46 (m, 6H), 1.26 (m, 48H), 0.88 (t, $^3J_{HH}$ = 6.9 Hz, 9H) ppm.

^{13}C-NMR (101 MHz, $CDCl_3$,): δ = 153.6 (s, 2C), 138.7 (s, 1C), 132.7 (s, 1C), 107.5 (s, 2C), 73.8 (s, 1C), 69.5 (s, 2C), 47.4 (s, 1C), 32.3 (s, 3C), 29.9 (m, 21C), 26.5 (s, 3C), 23.1 (s, 3C), 14.5 (s, 3C) ppm.

MS (EI, m/z): 678.4 (100%)[M^+], 679.4 (48%), 680.4 (44%), 681.4 (17%), 510.3 (54%), 174.0 (39%).

EA: calculated C 76.00, H 11.72, N 0.00; found C 76.10, H 11.42, N 0.00.

3,3''-dinitro-5'-((3,4,5-tris(dodecyloxy)benzyl)oxy)-1,1':3',1''-terphenyl (22)

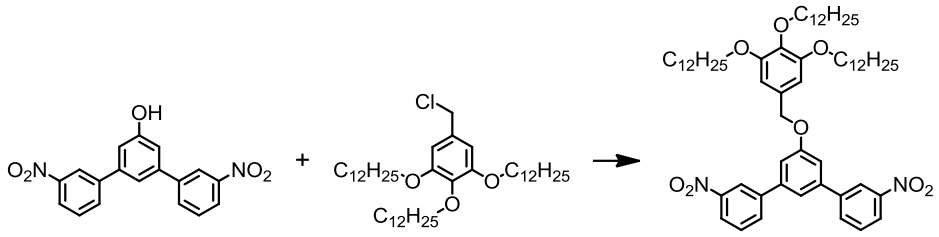

17 **21** **22**

$C_{61}H_{90}N_2O_8$
979.38 g/mol

To a solution of the *m*-terphenyl alcohol **17** (60.0 mg, 0.180 mmol, 1.0 eq.) and the chlorinated benzyl compound **21** (133 mg, 0.200 mmol, 1.1 eq.) in DMF (25 mL) potassium carbonate (245 mg, 1.78 mmol, 10.0 eq.) was added and the resulting orange reaction mixture was stirred at 65 °C for 22 h. The violet reaction mixture was cooled to room temperature and quenched with water (20 mL). After extraction with dichloromethane (3 × 20 mL) the combined organic layers were washed with water (2 × 20 mL), dried over $MgSO_4$ and evaporated to dryness. The crude was purified by column chromatography with silica gel and ethyl acetate:*n*-hexane (1:7). The desired addition product **22** was isolated as a white powder in a yield of 89%.

TLC: R_f = 0.25 (ethyl acetate:*n*-hexane 1:7).

MP: 88-89°C.

^{1}H-NMR (400 MHz, $CDCl_3$): δ = 8.49 (t, $^4J_{HH}$ = 1.5 Hz, 2H), 8.25 (m, 2H), 7.95 (m, 2H), 7.65 (t, $^3J_{HH}$ = 8.0 Hz, 2H), 7.44 (t, $^4J_{HH}$ = 1.5 Hz, 1H), 7.29 (d, $^4J_{HH}$ = 1.5 Hz, 2H), 6.69 (s, 2H), 5.11 (s, 2H), 4.00 (m, 6H), 1.81 (m, 6H), 1.48 (m, 6H), 1.25 (m, 48H), 0.87 (m, 9H) ppm.

^{13}C-NMR (101 MHz, $CDCl_3$): δ = 160.4 (s, 1C), 153.9 (s, 2C), 149.2 (s, 2C), 142.6 (s, 2C), 141.5 (s, 2C), 138.6 (s, 1C), 133.6 (s, 2C), 131.6 (s, 1C), 130.3 (s, 2C), 123.0 (s, 2C), 122.5 (s, 2C), 119.2 (s, 1C), 114.2 (s, 2C), 106.6 (s, 2C), 73.9 (s, 1C), 71.3 (s, 1C), 69.6 (s, 2C), 32.3 (s, 3C), 29.8 (m, 21C), 26.5 (s, 3C), 23.1 (s, 3C), 14.5 (s, 3C) ppm.

IR (ATR, neat, $\tilde{\nu}$/cm^{-1}): 3090 (w), 2916 (s), 2849 (m), 1593 (m), 1522 (s), 1342 (s), 1244 (m), 1196 (s), 1115 (s), 1013 (m), 808 (s).

MS (FAB, m/z): 978.4 (1.4%), 979.4 (1.1%) [M$^+$], 980.2 (0.6%), 643.4 (7.6%), 383.0 (13%), 138.9 (31%), 90.9 (60%), 57.0 (92%), 55.0 (80%), 43.0 (100%).

EA: calculated C 74.81, H 9.26, N 2.86; found C 74.87, H 9.00, N 2.65.

Symmetric alkyloxybenzene functionalized azo macrocycle 2

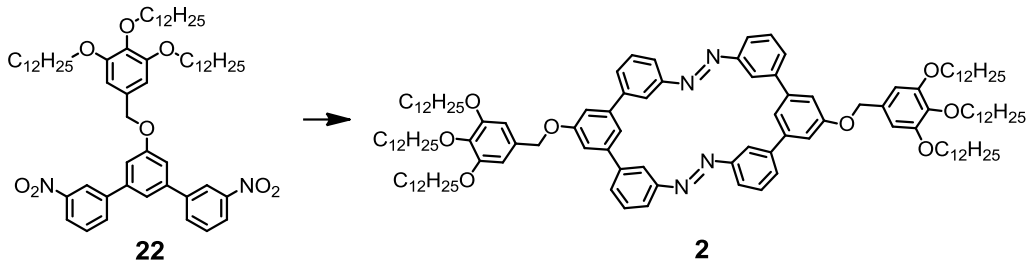

22 **2**

$C_{122}H_{180}N_4O_8$
1830.76 g/mol

To a solution of the nitro functionalized semicycle **22** (58.0 mg, 0.0590 mmol, 2.0 eq.) in dry THF (1000 mL) a 1 M $LiAlH_4$ solution in THF (0.6 mL, 0.601 mmol, 10.2 eq.) was added slowly under argon at room temperature. The reaction mixture was stirred for 2.5 h at room temperature. The black reaction mixture was quenched with water (200 mL). After extraction with toluene (3 × 250 mL) the combined organic layers were washed with brine (200 mL), dried over $MgSO_4$ and evaporated to dryness. The crude was purified by size exclusion column chromatography (SEC) with *Bio-Beads*® S-X Beads and toluene affording macrocycle **2** as an orange solid in a yield of 34%.

TLC: R_f = 0.52 (dichloromethane:*n*-hexane 2:1).

MP: 98-101°C.

^{1}H-NMR (500 MHz, $CDCl_3$): δ = 8.26 (m, 4H), 7.95 (m, 4H), 7.77 (m, 4H), 7.60 (m, 6H), 7.34 (m, 4H), 6.69 (m, 4H), 5.10 (m, 4H), 3.96 (m, 12H), 1.75 (m, 12H), 1.44 (m, 12H), 1.22 (m, 96H), 0.85 (m, 18H) ppm.

^{13}C-NMR (126 MHz, $CDCl_3$, clear determination by HMBC and HMQC): δ = 159.8 (s, Cq, 2C), 153.4 (s, Cq, 4C), 153.2 (s, Cq, 4C), 142.4 (s, Cq, 4C), 142.0 (s, Cq, 4C), 138.1 (s, Cq, 2C), 131.6 (s, Cq, 2C), 130.0 (s, Ct, 4C), 129.7 (s, Ct, 4C), 122.2 (s, Ct, 4C), 121.9 (s, Ct, 4C), 119.0 (s, Ct, 4C), 113.3 (s, Ct, 2C), 106.1 (s, Ct, 4C), 73.5 (s, Cs, 2C), 70.9 (s, Cs, 2C), 69.2 (s, Cs, 4C), 32.0 (s, Cs, 6C), 30.4 (s, Cs, 6C), 29.6 (m, Cs, 36C), 26.1 (s, Cs, 6C), 22.7 (s, Cs, 6C), 14.1 (s, Cp, 6C) ppm.

IR (ATR, neat, $\tilde{\nu}$/cm^{-1}): 3059 (w), 3024 (w), 2920 (s), 2851 (m), 1591 (m), 1504 (w), 1466 (m), 1437 (m), 1334 (m), 1112 (s).

VPO (determined molecular weight, gmol^{-1}): 1740.

UV (λ, nm): 247 (λ_{max}), 321, 436.

GPC (retention time, 0.5 mL/min): 10.80 min, area (100%).

Asymmetric alkyloxybenzene and methoxy functionalized azo macrocycle 4

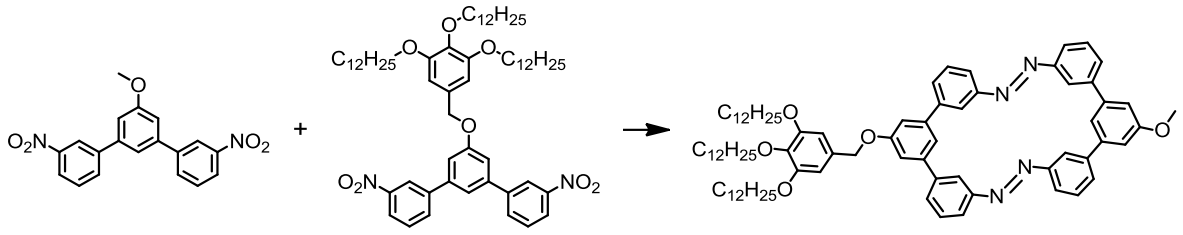

16 **22** **4**

$C_{80}H_{104}N_4O_5$
1201.71 g/mol

To a solution of the semicycle **16** (43.6 mg, 0.125 mmol, 1.0 eq.) and the semicycle **22** (122 mg, 0.125 mmol, 1.0 eq.) in dry THF (1500 mL) a 1 M $LiAlH_4$ solution in THF (1.25 mL, 1.25 mmol, 10.0 eq.) was added slowly over a period of 20 min. After complete addition the reaction mixture was heated to 40 °C and stirred for 5 h. The dark reaction mixture was cooled to room temperature and quenched with water (200 mL). After extraction with dichloromethane (2 × 150 mL) the combined organic layers were washed with brine (200 mL), dried over $MgSO_4$ and evaporated to dryness. The orange crude was purified by size exclusion column chromatography with *Bio-Beads*® S-X Beads and toluene affording macrocycle **4** as an orange solid in a yield of 34%.

TLC: R_f = 0.33 (dichloromethane:*n*-hexane 2:1).

MP: 120-125°C.

^{1}H-NMR (500 MHz, $CDCl_3$): δ = 8.26 (m, 4H), 7.95 (m, 4H), 7.77 (m, 4H), 7.59 (m, 6H), 7.35 (m, 2H), 6.70 (m, 2H), 5.11 (m, 2H), 3.96 (m, 9H), 1.77 (m, 6H), 1.46 (m, 6H), 1.25 (m, 48H), 0.87 (m, 9H) ppm.

^{13}C-NMR (126 MHz, $CDCl_3$, clear determination by HMBC and HMQC): δ = 160.9 (s, Cq, 1C), 160.0 (s, Cq, 1C), 153.8 (s, Cq, 4C), 153.5 (s, Cq, 2C), 142.9 (s, Cq, 4C), 142.4 (s, Cq, 4C), 138.4 (s, Cq, 1C), 132.1 (s, Cq, 1C), 130.3 (s, Ct, 4C), 130.0 (s, Ct, 4C), 122.4 (s, Ct, 4C), 122.3 (s, Ct, 4C), 113.5 (s, Ct, 2C), 112.7 (s, Ct, 4C), 106.7 (s Ct, 2C), 73.9 (s Cs, 1C), 71.2 (s, Cs, 1C), 67.1 (s, Cs, 2C), 56.0 (s, Cq, 1C), 32.4 (s, Cs, 3C), 30.2 (s, Cs, 21C), 26.6 (s, Cs, 3C), 23.1 (s, Cs, 3C), 14.6 (s, Cp, 3C) ppm.

IR (ATR, neat, $\tilde{\nu}$/cm^{-1}): 3063 (w), 2920 (s), 2851 (m), 1591 (m), 1500 (w), 1437 (m), 1337 (m), 1211 (w), 1113 (s).

VPO (determined molecular weight, gmol^{-1}): 1174.

UV (λ, nm): 250 (λ_{max}), 323, 441.

GPC (retention time, 0.5 mL/min): 11.01 min, area (100%).

5'-Methoxy-[1,1':3',1''-terphenyl]-3,3''-diamine (23)

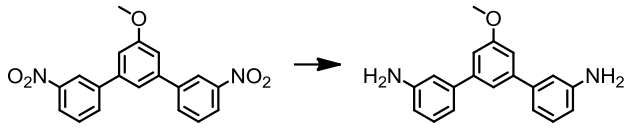

16 **23**

$C_{19}H_{18}N_2O$
290.36 g/mol

The nitro functionalized semicircle **16** (400 mg, 1.14 mmol, 1.0 eq.) was suspended in THF (20 mL). Tin powder (881 mg, 7.42 mmol, 6.5 eq.) and a 37% aq. HCl solution (0.5 mL) were added slowly at room temperature to the reaction mixture and stirred for 4 h. The reaction mixture was quenched with a 1 M aq. NaOH solution (10 mL), stirred at room temperature for 15 min and filtered. The clear reaction mixture was diluted with water (20 mL) and extracted with dichloromethane (3 × 25 mL). The combined organic layers were washed with brine (30 mL), dried over $MgSO_4$ and evaporated to dryness. The crude was purified by column chromatography with silica gel and ethyl acetate:*n*-hexane (1:1). The reduced product **23** was isolated as a colorless solid in a yield of 98%.

TLC: R_f = 0.29 (ethyl acetate:*n*-hexane 1:1).

MP: 171-173°C.

^{1}H-NMR (500 MHz, $CDCl_3$): δ = 7.35 (t, ^4J = 1.5 Hz, 1H), 7.23 (t, ^3J = 7.9 Hz 2H), 7.07 (d, ^4J = 1.5 Hz, 2H), 7.03 (m, 2H), 6.94 (t, ^4J = 1.5 Hz, 2H), 6.69 (dd, ^3J = 7.9, ^4J = 1.5 Hz, 2H), 3.90 (s, 3H), 3.74 (br s, 2H) ppm.

^{13}C-NMR (101 MHz, $CDCl_3$): δ = 160.6 (s, 1C), 147.1 (s, 2C), 143.6 (s, 2C), 142.8 (s, 2C), 130.1 (s, 2C), 119.3 (s, 2C), 118.2 (s, 1C), 114.7 (s, 2C), 114.4 (s, 2C), 112.1 (s, 2C), 55.9 (s, 1C).ppm.

IR (ATR, neat, $\tilde{\nu}$/cm^{-1}): 3285 (br, w), 3082 (w), 2959 (w), 1374 (s), 1274 (m), 1249 (m), 1022 (m), 1041 (m), 834 (m).

MS (EI, m/z): 292.2 (2%), 291.2 (19%), 290.2 (100%) [M^+], 289.1 (2%), 247.1 (8%), 145.1 (10%).

EA: calculated C 78.59, H 6.25, N 9.65; found C 77.4, H 6.58, N 8.82.

1,2,3-Triiodo-5-nitrobenzene (27)

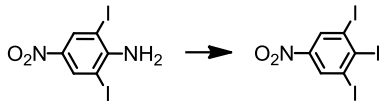

26 **27**

$C_6H_2I_3NO_2$
500.80 g/mol

2,6-Diiodo-4-nitroaniline (**26**) (10.3 g, 25.7 mmol, 1.0 eq.) was dissolved in acetic acid (60 mL) at 15°C, a solution of $NaNO_2$ (2.50 g, 36.2 mmol, 1.4 eq.) in conc. sulfuric acid (15 mL) was added drop wise at room temperature over a period of 10 min. The reaction mixture was stirred at room temperature for 90 min until complete dissolving of the reagents. The yellow reaction mixture was poured onto ice water (200 mL), stirred vigorously, quenched with urea (4.0 g) and filtered. The filtrate was diluted with water (30 mL) and then potassium iodide (6.00 g, 36.2 mmol, 1.4 eq.) in water (30 mL) was added to the suspension. The brown reaction mixture was stirred and heated to 95°C for 2 h. The reaction mixture was cooled to room temperature and quenched with $Na_2S_2O_4$ (5.0 g). The crude was filtered off, dried under high vacuum conditions and recrystallized from methoxyethanol (20 mL) affording the desired iodinated product **27** as brown crystals in a yield of 80%.

TLC: R_f = 0.66 (ethyl acetate:*n*-hexane 1:1).

MP: 166-168°C.

^{1}H-NMR (400 MHz, $CDCl_3$): δ = 8.60 (s, 2H) ppm.

^{13}C-NMR (101 MHz, $CDCl_3$): δ = 147.7 (s, 1C), 133.1 (s, 2C), 131.3 (s, 1C), 107.2 (s, 2C) ppm.

IR (ATR, neat, $\tilde{\nu}$/cm^{-1}): 3082 (w), 3049 (w), 1503 (s), 1498 (s), 1326 (s), 874 (s), 734 (s).

MS (EI, m/z): 500.8 (100%) [M^+], 501.8 (6.7%), 454.9 (15%), 327.9 (15%), 201.0 (23%), 74.0 (30%).

EA: calculated C 14.39, H 0.40, N 2.80; found C 14.41, H 0.42, N 2.85.

1,2,3-Tri(dodec-1-ynyl)-5-nitrobenzene (28)

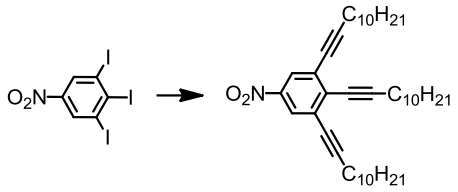

27 **28**

$C_{42}H_{65}NO_2$
615.97 g/mol

Dry triethylamine (60 mL) was degassed for 15 min with argon. 1,2,3-Triiodo-5-nitrobenzene (**27**) (2.00 g, 3.99 mmol, 1.0 eq.), 1-dodecyne (2.85 mL, 13.2 mmol, 3.3 eq.), $Pd(PPh_3)_2Cl_2$ (140 mg, 0.199 mmol, 5 mol-%) and CuI (76.0 mg, 0.399 mmol, 10 mol-%) were added under argon at room temperature. After 180 min at 85°C the black reaction mixture was cooled to room temperature, filtered and washed with water (2 × 30 mL), dried over $MgSO_4$ and evaporated to dryness. The black crude was purified by column chromatography with silica gel and ethyl acetate:*n*-hexane (1:20) affording the desired product **28** as black oil in a yield of 89%.

TLC: R_f = 0.41 (ethyl acetate:*n*-hexane 1:20).

^{1}H-NMR (400 MHz, $CDCl_3$): δ = 8.07 (s, 2H), 2.54 (t, ^3J = 7.0 Hz, 2H), 2.46 (t, ^3J = 7.0 Hz, 4H), 1.63 (m, 6H), 1.48 (m, 6H), 1.27 (m, 36H), 0.87 (t, ^3J = 7.0 Hz, 9H) ppm.

^{13}C-NMR (101 MHz, $CDCl_3$): δ = 146.0 (s, 1C), 134.8 (s, 1C), 128.4 (s, 2C), 125.4 (s, 2C), 104.5 (s, 1C), 97.4 (s, 2C), 78.6 (s, 1C), 78.5 (s, 2C), 32.3 (s, 3C), 30.1-29.0 (m, 18C), 23.1 (s, 3C), 20.1 (s, 3C), 14.5 (s, 3C) ppm.

IR (ATR, neat, $\tilde{\nu}$/cm^{-1}): 3002 (w), 2921 (s), 2853 (m), 1521 (m), 1465 (w), 1347 (m).

MS (EI, m/z): 615.4 (35%) [M^+], 616.3 (16%), 617.3 (0.6%), 585.4 (16%), 530.3 (18%), 474.2 (22%), 446.2 (19%), 404.2 (20%), 390.2 (30%), 378.2 (49%), 83.1 (45%), 69.1 (51%), 55.0 (67%), 43.0 (100%).

EA: calculated C 81.89, H 10.64, N 2.27; found C 81.73, H 10.69, N 1.93.

3,4,5-Tridodecylaniline (29)

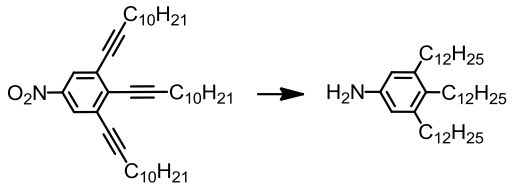

28 **29**

$C_{42}H_{79}N$
598.08 g/mol

The oxidized nitro compound **28** (1.28 g, 2.08 mmol, 1.0 eq.) and palladium on activated carbon (220 mg, 0.208 mmol, 10 mol-%) were suspended in dry ethanol (80 mL) and dry ethyl acetate (20 mL). The reaction mixture was hydrogenated with two hydrogen balloons at room temperature for 28 h while stirring vigorously. The hydrogen balloons were renewed after 16 h. The reaction mixture was filtered over a 3 cm plug of *Celite*® and evaporated to dryness. The crude was purified by column chromatography with silica gel and dichloromethane:*n*-hexane (1:1) affording the reduced product **29** as a pale orange oil in a yield of 59%.

TLC: R_f = 0.32 (dichloromethane:*n*-hexane 1:1).

^{1}H-NMR (250 MHz, $CDCl_3$): δ = 6.38 (s, 2H), 3.43 (br s, 2H), 2.49 (m, 6H), 1.56 (m, 6H), 1.27 (m, 54H), 0.88 (t, ^3J = 6.5 Hz, 9H) ppm.

^{13}C-NMR (101 MHz, $CDCl_3$): δ = 144.0 (s, 1C), 142.4 (s, 1C), 129.5 (s, 2C), 114.5 (s, 2C), 33.7 (s, 3C), 32.3 (s, 3C), 30.1 (m, 24C), 23.1 (s, 3C), 14.5 (s, 3C) ppm.

IR (ATR, neat, $\tilde{\nu}$/cm^{-1}): 3004 (w), 2920 (s), 2852 (m), 1620 (w), 1466 (w), 847 (bw), 631 (m).

MS (EI, m/z): 597.6 (100%) [M^+], 598.6 (42%), 599.6 (9%), 442.4 (60%), 288.2 (9%), 134.1 (12%).

EA: calculated C 84.34, H 13.31, N 2.34; found C 84.36, H 13.12, N 2.26.

2,6-Dibromo-3,4,5-tridodecylaniline (30)

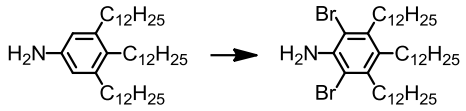

29 **30**

$C_{42}H_{77}Br_2N$
755.88 g/mol

A solution of dry DMF (20 mL) and 3,4,5-tridodecylaniline (**29**) (1.90 g, 3.18 mmol, 1.0 eq.) was cooled to 0°C under argon. *N*-Bromosuccinimide (1.36 g, 7.62 mmol, 2.4 eq.) in dry DMF (20 mL) was added at 0 °C over a period of 20 min. After complete addition the reaction mixture was stirred at room temperature for other 2 h. The dark brown reaction mixture was quenched with water (30 mL) and extracted with TBME (3 × 20 mL). The combined organic layers were dried over $MgSO_4$ and evaporated to dryness. The black crude was purified by column chromatography with silica gel and ethyl acetate:*n*-hexane (1:30) affording the brominated compound **30** as a pale yellow oil in a yield of 70%.

TLC: R_f = 0.44 (ethyl acetate:*n*-hexane 1:30).

^{1}H-NMR (250 MHz, $CDCl_3$): δ = 4.56 (s, 2H), 2.71 (m, 4H), 2.55 (m, 2H), 1.53-1.27 (m, 60H), 0.88 (t, ^3J = 6.5 Hz, 9H) ppm.

^{13}C-NMR (101 MHz, $CDCl_3$): δ= 140.5 (s, 1C), 140.3 (s, 2C), 130.6 (s, 1C), 110.6 (s, 2C), 34.2 (s, 3C), 32.4 (s, 3C), 30.1 (m, 24C), 23.1 (s, 3C), 14.5 (s, 3C) ppm.

IR (ATR, neat, $\tilde{\nu}$/cm^{-1}): 3485 (w), 3387 (w), 2954 (w), 2920 (s), 2852 (m), 1599 (m), 1466 (m), 1430 (w).

MS (EI, m/z): 753.3 (51%), 754.4 (24%), 755.3 (100%) [M^+], 756.3 (45%), 757.3 (56%), 758.3 (23%), 759.3 (5%), 600.2 (6%), 521.3 (7%), 433.0 (7%).

EA: calculated C 66.74, H 10.27, N 1.85; found C 66.78, H 10.23, N 1.70.

1,5-Dibromo-2,3,4-tridodecylbenzene (31)

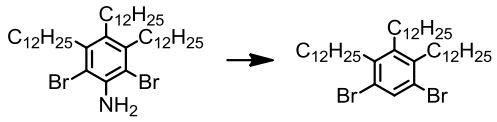

30 **31**

$C_{42}H_{76}Br_2$
740.86 g/mol

The aniline derivative **30** (83.0 mg, 0.110 mmol, 1.0 eq.) was suspended in ethanol (5 mL) and sonicated for 5 min until the reagents were completely dissolved. After adding sulfuric acid (2 mL) and $NaNO_2$ (23.0 mg, 0.331 mmol, 3.0 eq.) the reaction mixture was stirred at 85°C for 4h, cooled down to room temperature and quenched with water (10 mL). The water phase was extracted with dichloromethane (3 × 10 mL) and the combined organic layers were washed with brine (30 mL), dried over $MgSO_4$ and evaporated to dryness. The crude was purified by column chromatography with silica gel and *n*-hexane affording the dibromo compound **31** as a yellow oil in a yield of 95%.

TLC: R_f = 0.58 (*n*-hexane).

^{1}H-NMR (400 MHz, $CDCl_3$): δ = 7.57 (s, 1H), 2.62 (m, 6H), 1.51-1.24 (m, 60H), 0.85 (t, ^3J = 6.5 Hz, 9H) ppm.

^{13}C-NMR (101 MHz, $CDCl_3$): δ = 142.7 (s, 1C), 140.1 (s, 2C), 134.2 (s, 1C), 122.8 (s, 2C), 33.5 (s, 3C), 32.4 (s, 3C), 30.1 (m, 24C), 23.1 (s, 3C), 14.5 (p, 3C) ppm.

MS (EI, m/z): 738.4 (49%), 739.4 (22%), 740.4 (100%) [M^+], 741.4 (44%), 742.4 (55%), 743.4 (23%), 744.4 (5%), 418.1 (15%), 276.9 (33%), 197.0 (10%), 71.1 (14%), 57.1(19%).

EA: calculated C 68.09, H 10.34, N 0.00; found C 68.02, H 10.11, N 0.00.

1,3-(3-Nitrobenzene)-4,5,6-tridodecylbenzene (32)

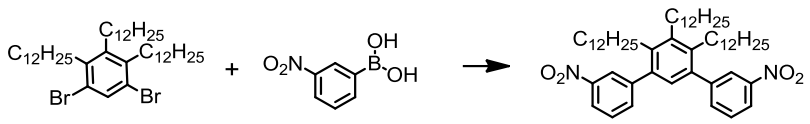

31 **35** **32**

$C_{54}H_{84}N_2O_4$
825.26 g/mol

Conventional conditions: To a solution of the dibromo compound **31** (78.0 mg, 0.105 mmol, 1.0 eq.) in dry toluene (10 mL) and dry ethanol (3 mL), 3-nitrobenzeneboronic acid (**35**) (46.0 mg, 0.274 mmol, 2.6 eq.), $[Pd(PPh_3)_4]$ (10.0 mg, 8.42 µmol, 8.0 mol-%) and K_2CO_3 (116 mg, 0.842 mmol, 8.0 eq.) were added under argon. The reaction mixture was stirred vigorously at 85 °C for 3 h. After cooling to room temperature the reaction mixture was filtered over a 1 cm plug of silica gel and washed with toluene (15 mL) and evaporated to dryness. The dark crude was adsorbed on silica gel and purified by column chromatography with silica gel and toluene:*n*-hexane (1:1) affording the desired addition product **32** as a white solid in a yield of 85%.

Microwave conditions: To a solution of dry toluene (7 mL) and dry ethanol (3 mL), the dibromo compound **31** (78.0 mg, 0.105 mmol, 1.0 eq.), 3-nitrobenzeneboronic acid (**35**) (46.0 mg, 0.274 mmol, 2.6 eq.), $[Pd(PPh_3)_4]$ (10.0 mg, 8.42 µmol, 8.0 mol-%) and K_2CO_3 (116 mg, 0.842 mmol, 8.0 eq.) were added under argon. The reaction mixture was heated to 120°C for 10 min in a microwave. After cooling to room temperature the reaction mixture was filtered over 1 cm plug of silica gel, eluting with toluene and washed with ethanol. The residue was adsorbed on silica gel and chromatographed with silica gel and toluene:*n*-hexane (1:1) affording the desired addition product **32** as white solid in a yield of 96%. With microwave conditions the yield could be improved compared to the yield obtained under conventional conditions.

TLC: R_f = 0.59 (toluene:*n*-hexane 1:1).

MP: 37-39°C.

^{1}H-NMR (400 MHz, $CDCl_3$): δ = 8.20 (m, 4H), 7.64 (d, ^3J = 8.8 Hz, 2H), 7.55 (t, ^3J = 8.8 Hz, 2H), 6.79 (s, 1H), 2.70 (m, 2H), 2.53 (m, 4H), 1.19 (m, 60H), 0.87 (t, ^3J = 6.7 Hz, 9H) ppm.

^{13}C-NMR (101 MHz, $CDCl_3$): δ = 148.3 (s, 2C), 144.6 (s, 2C), 139.4 (s, 2C), 138.1 (s, 1C), 135.9 (s, 2C), 130.1 (s, 2C), 129.3 (s, 2C), 124.7 (s, 2C), 122.2 (s, 2C), 32.3 (s, 3C), 30.0 (m, 27C), 23.1 (s, 3C), 14.5 (s, 3C) ppm.

IR (ATR, neat, $\tilde{\nu}$/cm^{-1}): 3080 (w), 2920 (s), 2851 (m), 1526 (s), 1466 (m), 1346 (m), 1099 (w).

MS (EI, m/z): 824.5 (100%) [M^+], 825.5 (55%), 826.5 (17%), 827.5 (4%), 794.6 (18%), 502.2 (22%), 361.1 (17%), 315.1 (10%).

EA: calculated C 78.59, H 10.26, N 3.39; found C 78.56, H 10.09, N 3.22.

Symmetric triple alkyl functionalized azo macrocycle 3

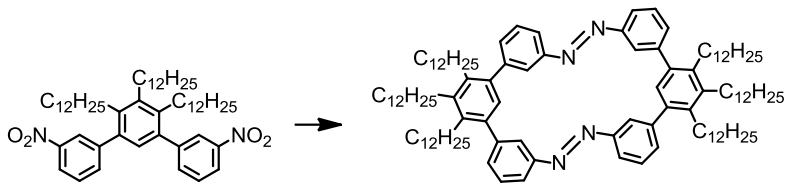

32 **3**

$C_{108}H_{168}N_4$
1522.52 g/mol

To a solution of the semicycle **32** (80.0 mg, 97.0 µmol, 1.0 eq.) in dry THF (1500 mL), a 1 M $LiAlH_4$ solution in THF (0.48 mL, 0.485 mmol, 5.0 eq.) was added slowly under argon at room temperature. The reaction mixture was stirred at 40°C for 3 h and then the black suspension was quenched with water (200 mL). After extraction with dichloromethane (2 × 300 mL) the combined organic layers were

washed with brine (200 mL), dried over $MgSO_4$ and evaporated to dryness. The crude was purified by size exclusion column chromatography with *Bio-Beads*® S-X Beads and toluene affording macrocycle **3** as an orange resin in a yield of 49%.

TLC: R_f = 0.63 (dichloromethane:*n*-hexane 1:2).

MP: 67-69°C.

^{1}H-NMR (400 MHz, $CDCl_3$): δ = 7.91 (m, 4H), 7.85 (m, 4H), 7.49 (m, 4H), 7.44 (m, 4H), 6.96 (s, 2H), 2.71 (m, 4H), 2.60 (m, 8H), 1.57 (m, 12H), 1.41 (m, 12H), 1.26-1.12 (m, 96H), 0.84 (m, 18H) ppm.

^{13}C-NMR (126 MHz, $CDCl_3$, clear determination by HMBC and HMQC): δ = 152.2 (s, Cq, 4C), 143.9 (s, Cq, 4C), 139.2 (s, Cq, 4C), 138.4 (s, Cq, 4C), 135.8 (s, Cq, 2C), 132.1 (s, Ct,4C), 129.7 (s, Ct, 2C), 128.6 (s, Ct, 4C), 123.7 (s, Ct, 4C), 121.5 (s, Ct, 4C), 31.9 (s, Cs, 6C), 31.4 (s, Cs, 6C), 29.7 (m, Cs, 48C), 22.7 (s, Cs, 6C), 14.1 (s, Cp, 6C) ppm.

IR (ATR, neat, $\tilde{\nu}$/cm^{-1}): 3057 (w), 2953 (w), 2920 (s), 2851 (m), 1597 (w), 1458 (m), 1047 (bs).

MS (MALDI-TOF, m/z): 1523.1 (100%) [M^++H], 1431.3 (25%).

VPO (determined molecular weight, gmol^{-1}): 1501.

UV (λ, nm): 213 (λ_{max}), 323, 434.

GPC (retention time, 0.5 mL/min): 10.87 min, area (100%).

4',5',6'-Tridodecyl-[1,1':3',1''-terphenyl]-3,3''-diamine (33)

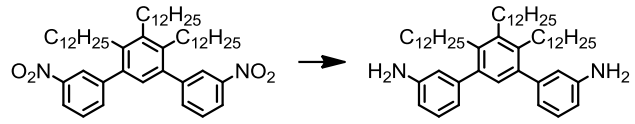

32 **33**

$C_{54}H_{88}N_2$
765.29 g/mol

To a solution of compound **32** (79.0 mg, 96.0 µmol, 1.0 eq) in THF (7 mL) conc. HCl (0.2 mL) and tin powder (74.0 mg, 0.622 mmol, 6.5 eq.) were added. The reaction mixture was stirred at room temperature for 3 h and turned colorless and thereafter a second portion of tin powder (74.0 mg, 0.622 mmol, 6.5 eq.) was added. After stirring for 5 h the colorless reaction mixture was quenched with a 1 M aq. NaOH solution (6 mL) and diluted with water (20 mL). The reaction mixture was extracted with dichloromethane (4 × 30 mL) and the combined organic layers were washed with brine (50 mL), dried over $MgSO_4$ and evaporated to dryness. The crude was purified by column chromatography with silica gel and ethyl acetate:*n*-hexane (1:3) affording the reduced product **33** as a colorless solid in a yield of 73%.

TLC: R_f = 0.63 (ethyl acetate:*n*-hexane 1:3).

MP: 45-47°C.

^{1}H-NMR (400 MHz, $CDCl_3$): δ = 7.13 (t, ^3J = 7.6 Hz, 2H), 6.85 (s, 1H), 6.72 (d, ^3J = 7.6 Hz, 2H), 6.63 (m, 4H), 3.63 (br s, 2H), 2.67 (m, 2H), 2.57 (m, 4H), 1.53-1.14 (m, 60H), 0.90 (t, ^3J = 6.8 Hz, 3H) ppm.

^{13}C-NMR (101 MHz, $CDCl_3$): δ = 146.1 (s, 2C), 144.6 (s, 2C), 140.3 (s, 2C), 139.6 (s, 1C), 138.2 (s, 2C), 129.8 (s, 1C), 128.9 (s, 2C), 120.5 (s, 2C), 116.9 (s, 2C), 113.6 (s, 2C), 32.3- 29.6 (m, 60C), 23.1 (s, 3C), 14.6 (s, 3C) ppm.

IR (ATR, neat, $\tilde{\nu}$ /cm^{-1}): 3383 (br w), 3050 (w), 2916 (s), 2848 (s), 1616 (m), 1583 (w), 1456 (m).

MS (EI, m/z): 763.6 (8%), 764.6 (100%) [M$^+$], 765.6 (59%), 766.6 (9%), 609.5 (9%).

EA: calculated C 83.47, H 11.42, N 3.59; found C 83.45, H 11.18, N 3.43.

6.2.2 Sulfur Functionalized Azo Macrocycles

***Tert*-butyl(3,5-dibromophenyl)sulfane (39)**

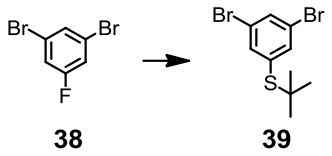

38 **39**

$C_{10}H_{12}Br_2S$
324.08 g/mol

1,3-Dibromo-5-fluorobenzene (**38**) (2.54 g, 10.0 mmol, 1.0 eq.) was dissolved at room temperature under argon in dry DMF (45 mL) and sodium 2-methyl-2-propanethiolate (1.23 g, 11.0 mmol, 1.1 eq.) was added to the reaction mixture. The brown reaction mixture was stirred under argon at room temperature for 2.5 h and then quenched with water (50 mL) and a 5 M aq. HCl solution (2 mL). After stirring for 5 min the reaction mixture was extracted with TBME (3 × 50 mL), the combined organic layers were washed with brine (2 × 50 mL), dried over $MgSO_4$ and evaporated to dryness. After drying under high vacuum conditions the product **39** was isolated as an analytically pure white solid in a yield of 97%.

TLC: R_f = 0.42 (*n*-hexane).

MP: 77-79°C.

^{1}H-NMR (400 MHz, $CDCl_3$): δ = 7.66 (t, ^4J = 1.7 Hz, 1H), 7.61 (d, ^4J = 1.7 Hz, 2H), 1.31 (s, 9H) ppm.

^{13}C-NMR (101 MHz, $CDCl_3$): δ = 138.7 (s, 2C), 137.1 (s, 1C), 134.7 (s, 1C), 122.7 (s, 2C), 47.5 (s, 1C), 31.4 (s, 3C) ppm.

MS (EI, m/z): 323.9 (6%) [M^+], 321.9 (3%), 325.9 (3%), 269.9 (17%), 267.9 (33%), 265.9 (16%), 57.1 (100%).

EA: calculated C 37.06, H 3.73, N 0.0; found C 37.02, H 3.65, N 0.0.

S-(3,5-Dibromophenyl) ethanethioate (40)

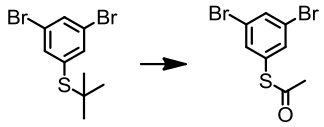

39 **40**

$C_8H_6Br_2OS$
310.01 g/mol

The *tert*-butyl protected sulfur compound **39** (2.79 g, 8.60 mmol, 1.0 eq.) was dissolved in dry toluene (40 mL) and acetyl chloride (9.8 mL, 138 mmol, 16.0 eq.) at room temperature and degassed for 10 min with argon. Boron tribromide (2.15 g, 8.60 mmol, 1.0 eq.) dissolved in dry dichloromethane (8 mL) was added at room temperature over a period of 25 min. After 1 h again boron tribromide (2.15 g, 8.60 mmol, 1.0 eq.) dissolved in dry dichloromethane (8 mL) was added slowly and stirred at room temperature under argon for another 1 h. The reaction mixture was quenched with ice water (50 mL) and extracted with toluene (3 × 50 mL), the combined organic layers were washed with brine (2 × 70 mL), dried over $MgSO_4$ and evaporated to dryness. The brown crude was purified by column chromatography with silica gel and dichloromethane:*n*-hexane (1:2) to give the trans-protected product **40** as a white solid in a yield of 87%.

TLC: R_f = 0.27 (dichloromethane:*n*-hexane 1:2)

MP: 62-63°C

^{1}H-NMR (400 MHz, $CDCl_3$): δ = 7.70 (t, ^4J = 1.7 Hz, 1H), 7.50 (d, ^4J = 1.7 Hz, 2H), 2.44 (s, 3H) ppm.

^{13}C-NMR (101 MHz, $CDCl_3$): δ = 192.5 (s, 1C), 136.0 (s, 2C), 135.4 (s, 1C), 131.7 (s, 1C), 123.4 (s, 2C), 30.7 (s, 1C) ppm.

MS (EI, m/z): 309.8 (7%) [M^+], 307.8 (4%), 311.8 (4%), 267.9 (10%), 63.0 (10%), 43.0 (100%).

EA: calculated C 31.00, H 1.95, N 0.00; found C 30.92, H 1.94, N 0.00.

3,5-Dibromobenzenethiol (41)

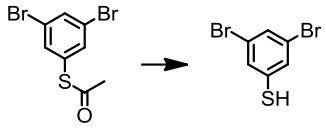

40 **41**

$C_6H_4Br_2S$
267.97 g/mol

The acetyl protected sulfur compound **40** (2.11 g, 6.80 mmol, 1.0 eq.) was dissolved in dry dichloromethane (50 mL) and dry methanol (50 mL) and was degassed for 15 min with argon. The reaction mixture was cooled to 0°C and acetyl chloride (1.94 mL, 27.2 mmol, 4.0 eq.) was added under argon. After 2 h more acetyl chloride (1.94 mL, 27.2 mmol, 4.0 eq.) was added to the colorless reaction mixture and warmed to room temperature. After further 3 h again acetyl chloride (1.45 mL, 20.40 mmol, 3.0 eq.) was added to the reaction mixture and after overall 6 h the reaction mixture was evaporated to dryness and dried under high vacuum conditions. The deprotected product **41** was isolated as an analytically pure yellow powder in quantitative yield.

TLC: R_f = 0.51 (dichloromethane:*n*-hexane 1:2).

MP: 99-102°C.

^{1}H-NMR (400 MHz, $CDCl_3$): δ = 7.44 (t, ^4J = 1.6 Hz, 1H), 7.35 (d, ^4J = 1.6 Hz, 2H), 3.53 (s, 1H) ppm.

^{13}C-NMR (101 MHz, $CDCl_3$): δ = 135.5 (s, 1C), 131.6 (s, 2C), 130.6 (s, 2C), 123.5 (s, 1C) ppm.

MS (EI, m/z): 269.8 (52%), 268.8 (100%) [M^+], 265.8 (50%), 188.9 (47%), 186.9 (46%), 108.0 (53%), 107.0 (11%), 63.0 (19%).

EA: calculated C 26.89, H 1.50, N 0.00; found C 26.12, H 1.50, N 0.00 (instantly disulfide formation).

(2-((3,5-Dibromophenyl)thio)ethyl)trimethylsilane (42)

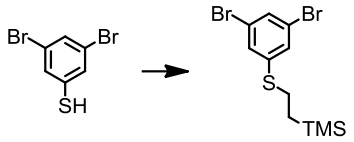

41 **42**

$C_{11}H_{16}Br_2SSi$
368.20 g/mol

The free thiol **41** (2.60 g, 9.70 mmol, 1.0 eq.) was suspended at room temperature under argon in vinyltrimethylsilane (14.0 mL, 86.7 mmol, 8.9 eq.) and di-*tert*-butyl peroxide (709 mg, 4.85 mmol, 0.5 eq.) were added. The reaction mixture was stirred under argon at 65°C for 1.5 h. The light brown mixture was evaporated under argon to dryness and immediately purified by column chromatography with silica gel and cyclohexane. The pre cleaned product was recrystallized from *n*-hexane and the obtained white crystals (disulfide) were filtered off. The filtrate was evaporated to dryness and dried under high vacuum conditions affording the protected product **42** in a yield of 91% as a colorless liquid.

TLC: R_f = 0.47 (cyclohexane).

^{1}H-NMR (400 MHz, $CDCl_3$): δ = 7.42 (t, ^4J = 1.7 Hz, 1H), 7.30 (d, ^4J = 1.7 Hz, 2H), 2.94 (m, 2H), 0.92 (m, 2H), 0.06 (s, 9H) ppm.

^{13}C-NMR (101 MHz, $CDCl_3$): δ = 142.2 (s, 1C), 130.9 (s, 1C), 129.1 (s, 2C), 123.2 (s, 2C), 29.2 (s, 1C), 16.6 (s, 1C), -1.6 (s, 3C) ppm.

MS (EI, m/z): 370.0 (2%), 368.0 (3%) [M^+], 366.0 (1%), 339.9 (2%), 324.9 (6%), 101.1 (14%), 73.1 (100%).

EA: calculated C 35.88, H 4.38, N 0.00; found C 35.84, H 4.41, N 0.00.

(2-((3,3''-Dinitro-[1,1':3',1''-terphenyl]-5'-yl)thio)ethyl)trimethylsilane (43)

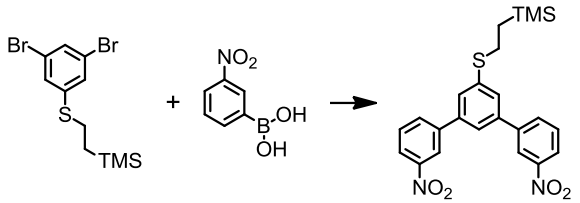

42 **35** **43**

$C_{23}H_{24}N_2O_4SSi$
452.60 g/mol

Conventional conditions: A solution of dry toluene (25 mL), dry ethanol (7 mL), the dibromo compound **42** (663 mg, 1.80 mmol 1.0 eq.) and 3-nitrophenylboronic acid (**35**) (751 mg, 4.50 mmol, 2.5 eq.) was degassed with argon for 10 min and then [$Pd(PPh_3)_4$] (168 mg, 0.14 mmol, 8.0 mol-%) and potassium carbonate (2.01 g, 14.4 mmol, 8.0 eq.) were added under argon at room temperature. The reaction mixture was stirred vigorously at 85°C for 20 h. After cooling to room temperature the reaction mixture was filtered over a 4 cm plug of silica gel, eluting with toluene and washing with ethanol. The residue was adsorbed on silica gel and was purified by column chromatography with silica gel and toluene:*n*-hexane (1:1). The obtained product was not analytically pure and was again purified by column chromatography with silica gel and TBME:*n*-hexane (1:1) to give product **43** as a light yellow solid in a yield of 47%. The mono coupled byproduct was isolated as well in a yield of 41%.

Microwave conditions: A solution of dry toluene (15 mL) and dry ethanol (5 mL), dibromo compound **42** (401 mg, 1.09 mmol 1.0 eq.) and 3-nitrophenylboronic acid (**35**) (500 mg, 3.00 mmol, 2.8 eq.) was degassed with argon for 15 min and then [$Pd(PPh_3)_4$] (102 mg, 87.2 µmol, 8 mol-%) and potassium carbonate (1.22 g, 8.72 mmol, 8.0 eq.) were added under argon. The reaction mixture was heated under microwave conditions to 120°C for 10 min. After cooling to room temperature the reaction mixture was filtered over 4 cm plug of silica gel, eluting with toluene and washing with ethanol. The residue was adsorbed on silica gel and purified by column chromatography with silica gel and TBME:cyclohexane (1:3). The obtained product was not analytically pure and was again purified by column

chromatography with silica gel and TBME:*n*-hexane (1:3) to give the product **43** as a light yellow solid in a yield of 93%. After the same purification steps as for the conventional conditions the desired product was isolated in a significant higher yield. The mono coupled byproduct was still observed, but in a minor amount.

TLC: R_f = 0.58 (TBME:*n*-hexane 1:1).

TLC: R_f = 0.50 (TBME:*n*-hexane 1:3).

TLC: R_f = 0.25 (TBME:cyclohexane 1:3).

TLC: R_f = 0.17 (toluene:*n*-hexane 1:1).

MP: 101-104°C.

^{1}H-NMR (400 MHz, $CDCl_3$): δ = 8.48 (t, ^4J = 2.0 Hz, 2H), 8.26 (ddd, ^3J = 8.2, ^4J = 2.0, ^4J = 1.0 Hz, 2H), 7.96 (ddd, ^3J = 8.2, ^4J = 2.0, ^4J = 1.0 Hz, 2H), 7.67 (t, ^3J = 8.2 Hz, 2H), 7.59 (t, ^4J = 1.6 Hz, 1H), 7.56 (d, ^4J = 1.6 Hz, 2H), 3.10 (m, 2H), 1.02 (m, 2H), 0.08 (s, 9H) ppm.

^{13}C-NMR (101 MHz, $CDCl_3$): δ = 149.2 (s, 2C), 142.4 (s, 2C), 140.8 (s, 2C), 140.5 (s, 1C), 133.6 (s, 2C), 130.4 (s, 2C), 127.4 (s, 2C), 123.8 (s, 1C), 123.1 (s, 2C), 122.5 (s, 2C), 29.9 (s, 1C), 17.3 (s, 1C), -1.3 (s, 3C) ppm.

MS (EI, m/z): 453.1 (1.0%), 452.1 (4.1%) [M^+], 425.1 (14%). 424.1 (48%), 409.1 (7%), 73.0 (100%).

EA: calculated C 61.01, H 5.34, N 6.19; found C 60.63, H 5.45, N 6.22.

Asymmetric sulfur functionalized azo macrocycle 5 with byproduct 1 and 6

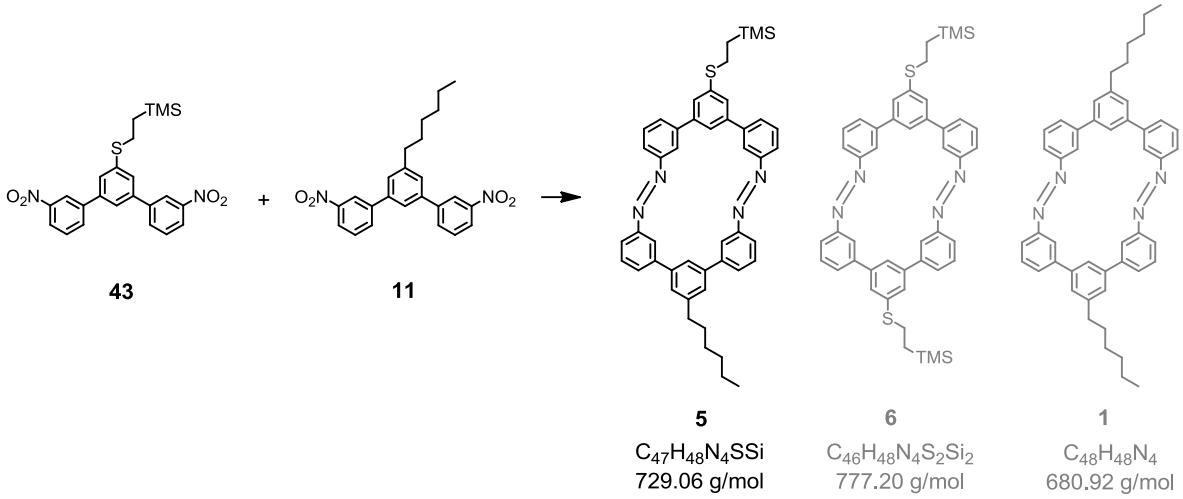

The nitro functionalized semicircle **43** (111 mg, 0.25 mmol, 1.0 eq.) and the nitro functionalized semicircle **11** (99.1 mg, 0.25 mmol, 1.0 eq.) were dissolved in dry THF (1500 mL, dried over K and Na) at room temperature under argon and absolutely aqueous free conditions. A 1 M lithium aluminum hydride solution in THF (2.45 mL, 2.45 mmol, 10.0 eq.) was added over a period of 20 min. The reaction mixture turned yellow, orange and finally black. After complete addition the reaction mixture was heated to 40°C for 2 h. The reaction mixture was then cooled to room temperature, quenched with water (100 mL) and diluted with dichloromethane (300 mL). The organic phase was concentrated and the water phase was extracted with dichloromethane (2 × 50 mL), the combined organic layers were washed with a 5% aq. HCl solution (70 mL) and brine (100 mL), dried over $MgSO_4$ and evaporated to dryness. The oily orange crude was first purified by column chromatography with silica gel and dichloromethane, where the first few orange fractions were collected and evaporated. These isolated fractions were further purified by SEC column chromatography with S-X Beads and toluene. The pre cleaned crude was purified on a preparative TLC plate (0.5 mm silica gel) using dichloromethane:*n*-hexane (1:1) as eluent. After extraction of the first band macrocycle **1** was obtained as orange crystals in a yield of 5%. The second band afforded the asymmetric macrocycle **5** as orange crystals in a yield of 6% and the third band afforded macrocycle **6** as orange solid in a yield of 4%.

TLC (macrocycle **1**): R_f = 0.49 (dichloromethane:*n*-hexane 1:1).

TLC (macrocycle **5**): R_f = 0.42 (dichloromethane:*n*-hexane 1:1).

TLC (macrocycle **6**): R_f = 0.35 (dichloromethane:*n*-hexane 1:1).

*All subsequent analytical data corresponds to macrocycle **5**:*

MP: 131-133°C.

^{1}H-NMR (500 MHz, $CDCl_3$): δ = 8.63 (m, 2H), 8.62 (m, 2H), 8.20 (m, 1H), 8.17 (m, 1H), 8.03 (t, ^3J = 9.0 Hz, 4H), 7.90 (d, ^3J = 7.6 Hz, 2H), 7.87 (d, ^3J = 7.6 Hz, 2H) 7.71-7.62 (m, 6H), 7.58 (m, 2H), 3.11 (m, 2H), 2.80 (t, ^3J = 7.7 Hz, 2H), 1.75 (quin, ^3J = 7.7, 2H), 1.42 (m, 2H), 1.35 (m, 4H), 1.03 (m, 2H), 0.90 (t, ^3J = 6.5 Hz, 3H), 0.08 (s, 9H) ppm.

^{13}C-NMR (126 MHz, $CDCl_3$, clear determination by HMBC and HMQC): δ = 152.9 (s, Cq, 4C), 144.5 (s, Cq, 1C), 141.9 (s, Cq, 2C), 141.5 (s, Cq, 2C), 141.0 (s, Cq, 2C), 140.5 (s, Cq, 2C), 138.5 (s, Cq, 1C), 129.8 (s, Ct, 4C), 129.7 (s, Ct, 2C), 129.3 (s, Ct, 2C), 126.5 (s, Ct, 2C), 126.3 (s, Ct, 2C), 124.1 (s, Ct, 1C), 123.4 (s, Ct, 1C), 123.3 (s, Ct, 2C), 123.1 (s, Ct, 2C), 121.8 (s, Ct, 4C), 36.8 (s, Cs, 1C), 31.8 (s, Cs, 1C), 30.0 (s, Cs, 1C), 29.0 (s, Cs, 1C), 27.4 (m, Cs, 2C), 17.0 (s, Cs, 1C), 14.2 (s, Cp, 1C), -1.7 (s, Cp, 3C) ppm.

UV (λ, nm): 259 (λ_{max}), 318, 438.

GPC (retention time, 1.0 mL/min): 9.01 min, area (99.5%).

MS (MALDI-TOF, m/z): 732.3 (17%), 731.3 (37%), 730.3 (63%), 729.3 (100%) [M-H$^+$], 663.5 (12%).

The analytical data of macrocycle **1** and **6** are shown in the corresponding sections 6.2.1 and 6.2.2, respectively.

Symmetric sulfur functionalized macrocycle 6

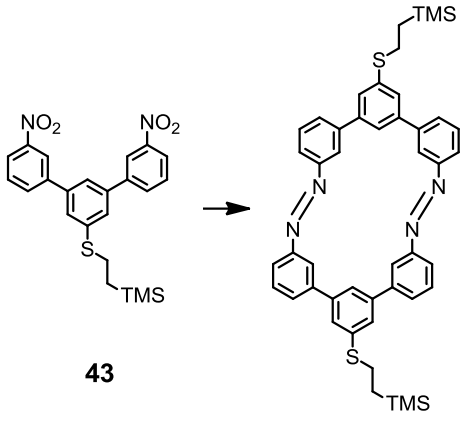

43 **6**

$C_{46}H_{48}N_4S_2Si_2$
777.20 g/mol

The nitro functionalized semicircle **43** (185 mg, 0.409 mmol, 2.0 eq.) was dissolved in dry THF (1000 mL, dried over K and Na) at room temperature under argon and absolutely aqueous free conditions. 1 M lithium aluminum hydride solution (3.27 mL, 3.27 mmol, 16.0 eq.) was added at room temperature over a period of 30 min. The reaction mixture turned yellow, orange and finally black. After complete addition the reaction mixture was heated to 40°C for 2 h. The reaction mixture was cooled to room temperature, quenched with water (200 mL) and diluted with dichloromethane (250 mL). The organic phase was concentrated and the water phase was extracted with dichloromethane (2 × 50 mL), the combined organic layers were washed with a 5% aq. HCl solution (100 mL) and brine (100 mL), dried over $MgSO_4$ and evaporated to dryness. The oily orange crude was first purified by column chromatography with silica gel and dichloromethane, where the first few orange fractions were collected and evaporated. These isolated fractions were further purified on a preparative TLC plate (2.0 mm silica gel) using dichloromethane:*n*-hexane (1:1) as eluent. The broad orange band was extracted with dichloromethane. The pre cleaned crude was now again purified on a preparative TLC plate (0.5 mm silica gel) using dichloromethane:*n*-hexane (1:1) as eluent, affording the desired macrocycle **6** as orange crystals in a yield of 5%.

TLC : R_f = 0.35 (dichloromethane:*n*-hexane 1:1).

MP: 125-128°C.

^{1}H-NMR (500 MHz, $CDCl_3$): δ = 8.61 (m, 4H), 8.16 (m, 2H), 8.04 (d, ^3J = 7.7 Hz, 4H), 7.86 (d, ^3J = 7.7 Hz, 4H), 7.69 (d, ^4J = 1.2 Hz, 4H), 7.66 (t, ^3J = 7.7 Hz, 4H), 3.11 (m, 4H), 1.03 (m, 4H), 0.07 (s, 18H) ppm.

^{13}C-NMR (126 MHz, $CDCl_3$, clear determination by HMBC and HMQC): δ = 152.9 (s, Cq, 4C), 141.9 (s, Cq, 2C), 141.5 (s, Cq, 4C), 138.7 (s, Cq, 2C), 129.9 (s, Ct, 4C), 129.2 (s, Ct, 4C), 126.3 (s, Ct, 4C), 123.6 (s, Ct, 2C), 122.8 (s, Ct, 4C), 122.0 (s, Ct, 4C), 29.8 (s, Cs, 2C), 17.1 (s, Cs, 2C), -1.7 (s, Cp, 6C) ppm.

UV (λ, nm): 251 (λ_{max}), 319, 441.

GPC (retention time, 1.0 mL/min): 8.04 min, area (98.2%).

MS (MALDI-TOF, m/z): 780.3 (10%), 779.3 (35%), 778.3 (57%), 777.3 (100%) [M-H$^+$], 735.8 (45%), 705.5 (18%).

Acetyl protected sulfur functionalized asymmetric macrocycle 7

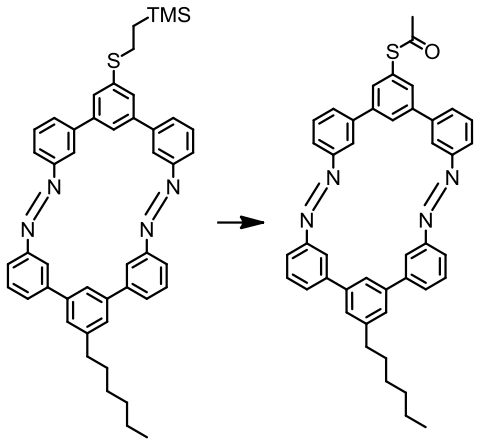

5 **7**

$C_{44}H_{38}N_4OS$
670.86 g/mol

Dry THF (4 mL) was degassed for 10 min with argon and the ethyl-TMS protected macrocycle **5** (6.0 mg, 82.5 µmol, 1.0 eq.) was dissolved at room temperature

under argon. A 1 M tetrabutylammonium fluoride (TBAF) solution in THF (0.21 mL, 0.21 mmol, 25.0 eq.) was added to the reaction mixture, after 1 h 1 M TBAF solution in THF (0.21 mL, 0.21 mmol, 25.0 eq.) was added again and stirred at room temperature for another 1 h. The reaction mixture was then cooled to 0°C and acetyl chloride (0.6 mL) was added. After stirring for 1.5 h the reaction mixture was quenched with water (10 mL) and extracted with dichloromethane (2 × 15 mL), the combined organic layers were washed with brine (20 mL), dried over $MgSO_4$ and evaporated to dryness. The orange crude was purified by column chromatography with silica gel and dichloromethane:cyclohexane (2:1) affording the desired trans-protected macrocycle **7** as an orange solid in a yield of 45%.

TLC : R_f = 0.44 (dichloromethane:cyclohexane 2:1).

MP: 100-102°C.

^{1}H-NMR (500 MHz, $CDCl_3$): δ = 8.61 (m, 4H), 8.41 (m, 1H), 8.20 (m, 1H), 8.03 (dd, ^3J = 8.2, ^4J = 1.8 Hz, 4H), 7.88 (dd, ^3J = 8.2, ^4J = 1.8 Hz, 4H), 7.80 (m, 2H), 7.64 (t, ^3J = 8.2 Hz, 4H), 7.58 (m, 2H), 2.80 (t, ^3J = 7.7 Hz, 2H), 2.51 (s, 3H), 1.75 (quin, ^3J = 7.7 Hz, 2H), 1.25 (m, 6H), 0.90 (t, ^3J = 6.7 Hz, 3H).

^{13}C-NMR (126 MHz, $CDCl_3$, clear determination by HMBC and HMQC): δ = 193.8 (s, Cq, 1C), 152.7 (s, Cq, 4C), 144.2 (s, Cq, 1C), 141.6 (s, Cq, 2C), 141.2 (s, Cq, 2C), 140.5 (s, Cq, 2C), 140.2 (s, Cq, 2C),131.7 (s, Ct, 2C), 131.6 (s, Cq, 1C), 129.7 (s, Ct, 4C), 129.2 (s, Ct, 2C), 129.1 (s, Ct, 2C), 127.0 (s, Ct, 1C), 126.2 (s, Ct, 2C), 123.4 (s, Ct, 1C), 123.0 (s, Ct, 4C), 121.8 (s, Ct, 4C), 36.2 (s, Cs, 1C), 31.6 (s, Cs, 1C), 30.3 (s, Cp, 1C), 29.5 (m, Cs, 3C), 14.1 (s, Cp, 1C)ppm.

UV (λ, nm): 252 (λ_{max}), 320, 443.

GPC (retention time, 1.0 mL/min): 9.95 min, area (99.7%).

MS (MALDI-TOF, m/z): 672.3 (28%), 671.3 (52%), 670.3 (100%) [M^+].

6.3 Platinum Electrode Modification

4-Iodobenzenediazonium tetrafluoroborate (48)

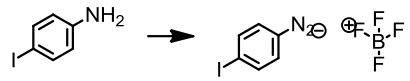

46 **48**

$C_6H_4BF_4IN_2$
317.94 g/mol

4-Iodoaniline (**46**) (1.10 g, 5.00 mmol, 1.0 eq.) and fluoroboric acid (12.5 mL, 100 mmol, 20.0 eq.) were dissolved in water (20 mL) and cooled to 0°C. Sodium nitrite (690 mg, 10.0 mmol, 2.0 eq.) dissolved in water (5 mL) was added and the reaction mixture was stirred at 0°C for 1 h and at room temperature further 2 h. The reaction mixture was cooled to 0°C, the crude was filtered off and washed with a 5% aq. $NaBF_4$ solution (10 mL), cold water (20 mL), cold methanol (20 mL) and dried under high vacuum conditions for 5 h. The crude was recrystallized from *n*-hexane:TBME (9:1) affording the diazonium salt **48** as violet crystals in a yield of 98%.

TLC: R_f = 0.11 (dichloromethane with 5% MeOH).

MP: 140-141°C.

^{1}H-NMR (400 MHz, acetone-d_6): δ = 8.52 (m, 4H) ppm.

^{13}C-NMR (101 MHz, acetone-d_6): δ = 141.5 (s, 2C), 133.4 (s, 2C), 115.4 (s, 1C), 113.0 (s, 1C) ppm.

MS (MALDI-TOF, m/z): 318.9 (100%) $[M-H]^+$.

EA: calculated C 22.68, H 1.27, N 8.81; found C 22.74, H 1.25, N 8.85.

Benzenediazonium tetrafluoroborate (49)

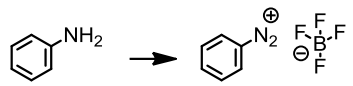

47 **49**

$C_6H_5N_2^+$

105.05 g/mol

Aniline (**47**) (0.46 mL, 5.00 mmol, 1.0 eq.) and fluoroboric acid (12.5 mL, 100 mmol, 20.0 eq.) were dissolved in water (20 mL) and cooled to 0°C. Sodium nitrite (690 mg, 10.0 mmol, 2.0 eq.) dissolved in water (5 mL) was added and the reaction mixture was stirred at 0°C for 1.5 h and at room temperature for further 2 h. The reaction mixture was cooled to 0°C and the crude was filtered off and washed with a 5% aq. $NaBF_4$ solution (15 mL), cold water (20 mL), cold methanol (20 mL) and dried under high vacuum conditions. The crude was recrystallized from *n*-hexane:TBME (10:1) affording the diazonium salt **49** as brown crystals in a yield of 98%.

TLC: R_f = 0.15 (dichloromethane with 5% MeOH).

MP: 102-103°C.

^{1}H-NMR (400 MHz, acetone-d_6): δ = 8.82 (m, 2H), 8.37 (1H, m), 8.07 (2H, m) ppm.

^{13}C-NMR (101 MHz, acetone-d_6): δ = 141.9 (s, 12C), 133.2 (s, 2C), 132.0 (s, 2C), 115.5 (s, 1C) ppm.

MS (FAB, m/z): 105.0 (100%) $[M]^+$, 77.0 (18%).

EA: calculated C 35.87, H 3.01, N 13.94; found C 36.18, H 2.74, N 13.55. (crystallized from H_2O 2:1)

2,2',3,3'-Tetrahydro-5,5'-bithieno[3,4][1,4]dioxine (BiEDOT) (51)

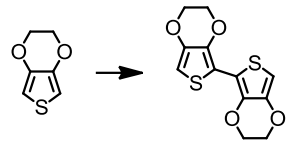

50 **51**

$C_{12}H_{10}O_4S_2$
282.00 g/mol

Ethyldioxythiophene (EDOT) (**50**) (995 mg, 7.00 mmol, 1.0 eq.) was dissolved in dry THF (30 mL) and cooled under an argon atmosphere to -78°C. To the colorless reaction mixture a 1.6 M *n*-BuLi solution in *n*-hexane (4.53 mL, 7.25 mmol, 1.04 eq.) was added drop wise. After stirring at -78°C for 45 min, copper(II)chloride (941 mg, 7.00 mmol, 1.0 eq.) was added to the reaction mixture and stirred at 40°C for further 2 h. The green reaction mixture was quenched with water (50 mL) and the formed precipitate was filtered off and washed with *n*-hexane. The brown crude was absorbed on silica gel and purified by column chromatography with silica gel and dichloromethane. The desired BiEDOT **51** was isolated as white crystals in a yield of 75%.

TLC: R_f = 0.57 (dichloromethane).

MP: 215-218°C.

^{1}H-NMR (400 MHz, $CDCl_3$): δ = 6.27 (s, 2H), 4.31 (m, 4H), 4.24 (m, 4H) ppm.

^{13}C-NMR (101 MHz, $CDCl_3$): δ = 141.6 (s, 2C), 137.4 (s, 2C), 110.3 (s, 2C), 97.9 (s, 2C), 65.4 (s, 2C) 65.0 (s, 2C) ppm.

MS (EI, m/z): 284.0 (11%), 283.0 (15%), 282.0 (100%) $[M]^+$, 226.0 (13%), 185.0 (95%).

EA: calculated C 51.05, H 3.57, N 0.00; found C 51.15, H 3.51, N 0.00.

7-Iodo-2,2',3,3'-tetrahydro-5,5'-bithieno[3,4][1,4]dioxine (52)

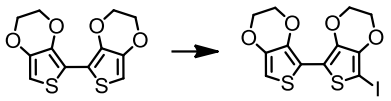

51 **52**

$C_{12}H_9IO_4S_2$
407.90 g/mol

BiEDOT **51** (1.00 g, 3.55 mmol, 1.0 eq.) was dissolved in dry THF (45 mL) and cooled under argon to -78°C. A 1.6 M *n*-BuLi solution in *n*-hexane (2.37 mL, 3.55 mmol, 1.0 eq.) was added drop wise over a period of 5 min to the reaction mixture and stirred at -78°C for 1 h. Iodine (1.01 g, 4.26 mmol, 1.2 eq.) was added at -78°C and stirred at room temperature for 1 h. The reaction mixture was quenched with water (20 mL) and extracted with diethylether (4 × 20 mL). The combined organic layers were washed with a 10% aq. $NaHSO_3$ solution (30 mL), a 10% aq. $NaHCO_3$ solution (30 mL), brine (30 mL) and dried over $MgSO_4$ and evaporated to dryness under an argon atmosphere. The yellowish crude product **52** was used without further purification.

TLC: R_f = 0.47 (dichloromethane).

MS (MALDI-TOF, m/z): 408.7 (100%) $[M]^+$.

Trimethyl((2,2',3,3'-tetrahydro-[5,5'-bithieno[3,4][1,4]dioxin]-7-yl)ethynyl)-silane (15)

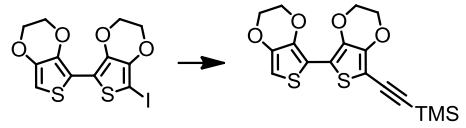

52 **53**

$C_{17}H_{18}O_4S_2Si$
378.04 g/mol

The crude product **52** was dissolved in dry THF (40 mL) and diisopropylamine (10 mL) and degassed for 10 min with argon. [$Pd(PPh_3)_4$] (410 mg, 0.36 mmol, 10 mol-%), copper iodide (135 mg, 0.71 mmol, 20 mol-%) and trimethyl-silylacetylene (502 µL, 3.48 mmol, 1.0 eq.) were added under argon to the reaction mixture and stirred at room temperature for 5 h. The reaction mixture was quenched with water (30 mL) extracted with *tert*-butylmethylether (3 × 20 mL). The combined organic layers were washed with brine (30 mL), dried over $MgSO_4$ and evaporated to dryness. The black crude was adsorbed on silica gel and purified by column chromatography with silica gel in dichloromethane:*n*-hexane (2:1) to give the desired product **53** as a light brown powder in a yield of 66% over two steps.

TLC: R_f = 0.38 (dichloromethane:*n*-hexane 2:1).

MP: 149-151°C.

^{1}H-NMR (400 MHz, $CDCl_3$): δ = 6.29 (s, 1H), 4.32 (m, 6H), 4.24 (m, 2H), 0.24 (s, 9H) ppm.

^{13}C-NMR (101 MHz, $CDCl_3$): δ = 144.6 (s, 1C), 141.6 (s, 1C), 138.3 (s, 1C), 135.9 (s, 1C), 112.1 (s, 1C), 110.0 (s, 1C), 103.3 (s, 1C), 98.9 (s, 1C), 96.5 (s, 1C), 95.5 (s, 1C), 65.5 (s, 1C), 65.4 (s, 1C), 65.1 (s, 1C), 65.0 (s, 1C) ppm.

MS (EI, m/z): 380.1 (16%), 379.0 (25%), 378.0 (100%) $[M]^+$, 281.3 (25%), 185.5 (16%).

EA: calculated C 53.94, H 4.79, N 0.00; found C 53.29, H 4.53, N 0.00.

7-Ethynyl-2,2',3,3'-tetrahydro-5,5'-bithieno[3,4-b][1,4]dioxine (54)

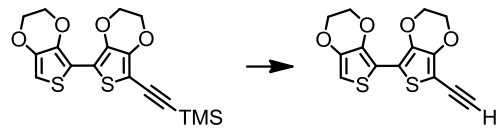

53 **54**

$C_{14}H_{10}O_4S_2$
306.00 g/mol

The TMS protected acetylene **53** (170 mg, 0.45 mmol, 1.0 eq.) was dissolved in MeOH (6 mL) and degassed with argon at room temperature for 10 min. Potassium carbonate (31.1 mg, 0.23 mmol, 0.5 eq.) was added to the reaction mixture and stirred at room temperature for 15 min. The reaction mixture was directly evaporated under an argon atmosphere and immediately purified by column chromatography with silica gel and dichloromethane under an argon atmosphere, affording the desired free acetylene **54** as a red brown solid in a yield of 52%.

TLC: R_f = 0.63 (dichloromethane).

MP: decomp. >60°C.

^{1}H-NMR (400 MHz, $CDCl_3$): δ = 6.30 (s, 1H), 4.33 (m, 6H), 4.25 (m, 2H), 3.56 (s, 1H) ppm.

^{13}C-NMR (101 MHz, $CDCl_3$): δ = 145.4 (s, 1C), 141.6 (s, 1C), 138.4 (s, 1C), 135.9 (s, 1C), 112.3 (s, 1C), 109.8 (s, 1C), 99.1 (s, 1C), 95.0 (s, 1C), 85.4 (s, 1C), 75.2 (s, 1C), 65.6 (s, 1C), 65.5 (s, 1C), 65.2 (s, 1C), 65.0 (s, 1C) ppm.

MS (EI, m/z): 308.0 (11%), 307.0 (17%), 306.0 (100%) $[M]^+$, 250.3 (11%), 209.5 (34%), 185.5 (31%).

EA: calculated C 54.89, H 3.29, N 0.00; found C 53.24, H 3.21, N 0.00.

1,3-Dibromo-5-iodobenzene (56)

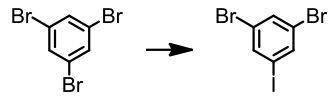

55 **56**

$C_6H_3Br_2I$
359.76 g/mol

1,3,5-Tribromobenzene (**56**) (12.8 g, 40.0 mmol, 1.0 eq.) was dissolved in dry diethylether (300 mL) under an argon atmosphere and cooled to -90°C. A 1.6 M *n*-BuLi solution in *n*-hexane (22.5 mL, 40.8 mmol, 1.02 eq.) was added to the reaction mixture at -90°C over a period of 1 h. The reaction mixture was stirred for 30 min and iodine (10.7 g, 42.0 mmol, 1.05 eq.) dissolved in dry THF (30 mL) was added over a period of 5 min. The reaction mixture was allowed to reach room temperature and stirred under argon for additional 1.5 h. The reaction mixture was then washed with a 10% aq. Na_2SO_3 solution (2 × 50 mL) and brine (100 mL) and dried over $MgSO_4$ and evaporated to dryness. The crude was recrystallized from *n*-hexane to afford the iodinated product **56** as brown needles in a yield of 77%.

TLC: R_f = 0.61 (*n*-hexane).

MP: 126-128°C.

^{1}H-NMR (400 MHz, $CDCl_3$): δ = 7.79 (d, ^4J = 1.7 Hz, 1H), 7.63 (t, ^4J = 1.7 Hz, 1H) ppm.

^{13}C-NMR (101 MHz, $CDCl_3$): δ = 138.9 (s, 2C), 134.1 (s, 1C), 123.8 (s, 2C), 94.9 (s, 1C) ppm.

MS (EI, m/z): 363.8 (47%), 361.8 (100%), 359.8 (50%) $[M]^+$, 236.9 (18%), 234.9 (37%), 232.9 (19%), 154.0 (10%), 75.1 (23%), 74.1 (22%).

EA: calculated C 19.92, H 0.84, N 0.00; found C 19.97, H 0.88, N 0.00.

((3,5-Dibromophenyl)ethynyl)trimethylsilane (19)

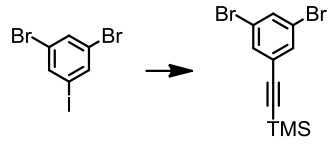

56 **57**

$C_{11}H_{12}Br_2Si$
329.91 g/mol

Dry THF (20 mL) and diisopropylamine (30 mL) were degassed with argon at 0°C for 10 min. 1,3-Dibromo-5-iodobenzene (**56**) (796 mg, 2.20 mmol, 1.0 eq.), trimethylsilylacetylene (0.32 mL, 2.20 mmol, 1.0 eq.), copper iodide (16.8 mg, 88.0 µmol, 4 mol-%,) and $[Pd(PPh_3)_4]$ (51.4 mg, 44.0 µmol, 2 mol-%,) were added to the solution, the reaction mixture was stirred under argon at 0°C for 20 min and then warmed to room temperature and stirred for further 2 h. The light brown reaction mixture was filtered and evaporated to dryness. The brown crude was adsorbed on silica gel and purified by column chromatography with silica gel in *n*-hexane affording the desired protected acetylene **57** as a colorless liquid in a yield of 89%.

TLC: R_f = 0.55 (*n*-hexane).

^{1}H-NMR (400 MHz, $CDCl_3$): δ = 7.61 (t, ^4J = 1.8 Hz, 1H), 7.53 (d, ^4J = 1.8 Hz, 2H), 0.24 (s, 9H) ppm.

^{13}C-NMR (101 MHz, $CDCl_3$): δ = 134.6 (s, 1C), 133.8 (s, 2C), 126.9 (s, 1C), 122.9 (s, 2C), 102.1 (s, 1C), 98.0 (s, 1C), 0.1 (s, 3C) ppm.

MS (EI, m/z): 333.9 (9%), 331.9 (17%), 329.9 (8%) $[M]^+$, 318.9 (52%), 317.9 (15%), 316.9 (100%), 314.9 (48%).

EA: calculated C 39.78, H 3.64, N 0.00; found C 39.73, H 3.63, N 0.00.

1,3-Dibromo-5-ethynylbenzene (20)

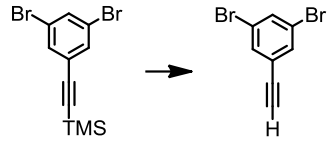

57 **58**

$C_8H_4Br_2$
257.87 g/mol

The TMS protected acetylene **57** (279 mg, 0.84 mmol, 1.0 eq.) was dissolved in MeOH (4 mL) and THF (5 mL) and degassed with argon at room temperature for 10 min, then potassium carbonate (129 mg, 0.92 mmol, 1.1 eq.) was added and the reaction mixture was stirred at room temperature for 30 min. The white reaction mixture was directly adsorbed on silica and quickly purified by column chromatography with silica gel in *n*-hexane to give the desired free acetylene **58** as white crystals in a yield of 99%.

TLC: R_f = 0.52 (*n*-hexane).

MP: 90-92°C.

^{1}H-NMR (400 MHz, $CDCl_3$): δ = 7.65 (t, ^4J = 1.8 Hz, 1H), 7.56 (d, ^4J = 1.8 Hz, 2H), 3.16 (s, 1H) ppm.

^{13}C-NMR (101 MHz, $CDCl_3$): δ = 135.1 (s, 1C), 134.0 (s, 2C), 125.9 (s, 1C), 123.0 (s, 2C), 81.0 (s, 1C), 80.2 (s, 1C) ppm.

MS (EI, m/z): 261.9 (49%), 259.9 (100%), 257.9 (51%) $[M]^+$, 181.0 (18%), 179.0 (18%), 100.0 (23%), 99.0 (21%), 98.0 (13%), 74.0 (20%), 50.0 (12%).

EA: calculated C 36.97, H 1.55, N 0.00; found C 36.59, H 1.59, N 0.00.

Platinum electrode (E0)

E0

The used platinum electrodes were fabricated on a silicon wafer by coating with a 5 nm thick titanium layer followed by a 25 nm thick platinum layer.

4-Iodophenyl functionalized platinum electrode (E5)

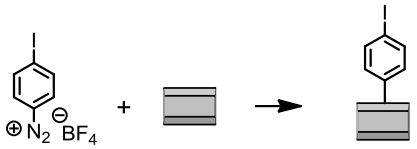

48 **E0** **E5**

An acetonitrile solution of aryl diazonium salts **48** (10 mM) and $TBABF_4$ (100 mM) was degassed with argon at room temperature for 10 min. The platinum electrode **E0** was sonicated in acetone for 5 min and in isopropanol for 10 min and finally cleaned in an ozone/UV cleaner for 15 min. The electrode **E0** was placed in the acetonitrile solution and surface reduction was performed using cyclic voltammetry (CV) with a scan rate of 50 mVs^{-1} for five cycles between +0.15 V and -0.9 V for the electroreduction of the diazonium salt. The electrode was rinsed with copious amount of acetonitrile, acetone and dichloromethane and then sonicated for 5 min in acetone and dried under a stream of argon. Electrode **E5** was completely functionalized with 4-iodophenyl.

Phenyl functionalized platinum electrode (E6)

49 **E0** **E6**

An acetonitrile solution of aryl diazonium salts **48** (10 mM) and $TBABF_4$ (100 mM) was degassed with argon at room temperature for 10 min. The platinum electrode **E0** was sonicated in acetone for 5 min and in isopropanol for 10 min and finally cleaned in an ozone/UV cleaner for 15 min. The electrode **E0** was placed in the acetonitrile solution and surface reduction was performed using cyclic voltammetry (CV) with a scan rate of 50 mVs^{-1} for five cycles between +0.15 V and -0.9 V for the electroreduction of the diazonium salt. The electrode was rinsed with copious amount of acetonitrile, acetone and dichloromethane and then sonicated for 5 min in acetone and dried under a stream of argon. Electrode **E6** was completely functionalized with phenyl.

General procedure for the Sonogashira cross coupling reaction on modified platinum electrode

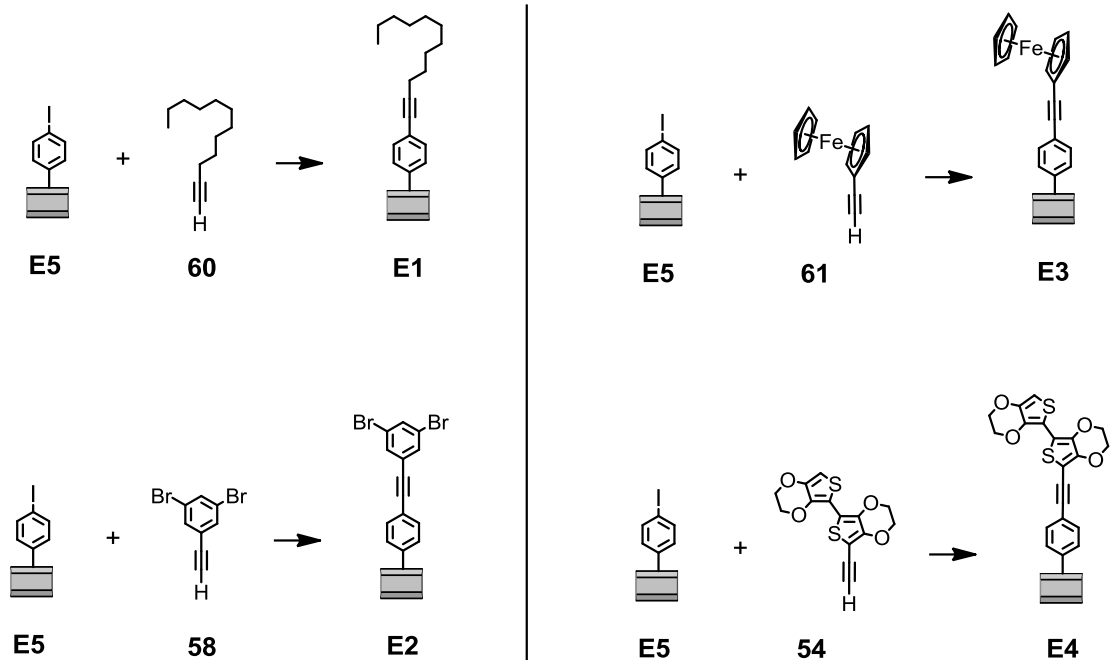

$PdCl_2$ (1.00 mg, 5.64 µmol, 5 mol-%), pyrrolidine (1.00 mL, 12.2 mmol, 20.0 eq.) and water (50 mL) were added to a flask. The modified substrate **E5** was placed in the middle of the flask (avoiding the contact with the stirring bar) under aerobic conditions and the resulting mixture was stirred and heated to 50°C for 5 min. The appropriate acetylene **54**, **58**, **60** or **61** (0.61 mmol, 1.0 eq) was added to the reaction mixture and stirred at 50 °C for 24 h. The substrate was fully rinsed with acetone and dichloromethane and sonicated for 5 min in acetone and dichloromethane, respectively. The resulting substrate was dried with an argon gas stream and stored under ambient conditions.

Azidomethyl-ferrocene (63)

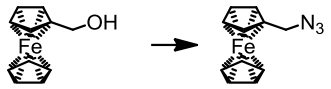

62 **63**

$C_{11}H_{11}FeN_3$
241.03 g/mol

Ferrocenemethanol (**62**) (335 mg, 1.55 mmol, 1.0 eq.) and sodium azide (0.33 mL, 9.30 mmol, 6.0 eq.) were dissolved in glacial acetic acid (20 mL) and stirred at 50°C for 4h. After cooling down to room temperature the reaction mixture was diluted with dichloromethane (100 mL) and stirred for 5 min. The organic layer was separated and washed with a sat. aq. $NaHCO_3$ solution (3 × 50ml), dried over $MgSO_4$ and evaporated to dryness. The dark yellow crude was adsorbed on silica gel and purified by column chromatography with silica gel and ethyl acetate:*n*-hexane (1:20) affording the product **63** as an amorphous dark red solid in a yield of 99%.

TLC: R_f = 0.40 (ethyl acetate:*n*-hexane 1:20).

MP: 37-38°C.

^{1}H-NMR (400 MHz, $CDCl_3$): δ = 4.24 (t, ^3J = 2.1 Hz, 2H), 4.20 (t, ^3J = 2.1 Hz, 2H), 4.16 (m, 5H), 4.12 (s, 2H) ppm.

^{13}C-NMR (101 MHz, $CDCl_3$): δ = 82.5 (s), 69.1 (s), 69.0 (s), 51.3 (s) ppm.

MS (EI, m/z): 242.0 (9%), 241.0 (60%) $[M]^+$, 214.1 (15%), 213.1 (100%), 212.0 (13%), 211.0 (11%), 199.0 (13%), 186.0 (29%), 184.0 (10%), 148.0 (16%), 147.0 (25%), 146.0 (11%), 121.0 (86%), 55.9 (38%).

EA: calculated C 54.80, H 4.60, N 17.43; found C 54.79, H 4.77, N 17.68.

6.4 Switchable Conducting Azo Biphenyl

3,3'-Dimethyl-[1,1'-biphenyl]-4,4'-diaminium chloride (67)

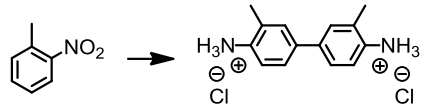

66 **67**

$C_{14}H_{18}Cl_2N_2$
284.08 g/mol

2-Nitrotoluene (**66**) (12.3 mL, 146 mmol, 2.0 eq.) was dissolved in ethanol (20 mL) and heated to 80°C. The oil bath was removed and zinc dust (15.0 g, 229 mmol, 1.6 eq.) was added in portion over a period of 15 min. Then sodium hydroxide (2.90 g, 73.0 mmol, 1.0 eq.) was dissolved in ethanol (20 mL) and water (10 mL) and slowly added to the reaction mixture at room temperature over a period of 30 min. Thereafter another portion of zinc dust (15.0 g, 229 mmol, 1.6 eq.) was slowly added to the reaction mixture. After complete addition of the zinc dust the reaction mixture was heated to 90°C for 2 h. The black suspension was cooled to room temperature and quenched with a 20% aq. HCl solution (300 mL). To dissolve all remaining zinc conc. HCl (100 mL) was added and the resulting white crude product was filtered off and washed with copious amount of cold water. The crude was dried under high vacuum conditions for 24 h affording the product **67** as a white powder in a yield of 88%.

MP: 133-134°C.

^{1}H-NMR (400 MHz, DMSO-d_6): δ = 9.66 (br s, 6H), 7.62 (d, ^4J = 1.3 Hz, 2H), 7.55 (dd, ^3J = 8.2, ^4J = 1.3 Hz, 2H), 7.40 (d, ^4J = 8.2 Hz, 2H), 2.37 (s, 6H) ppm.

^{13}C-NMR (101 MHz, DMSO-d_6): δ = 138.9 (s, 2C), 132.6 (s, 2C), 132.2 (s, 2C), 130.3 (s, 2C), 126.0 (s, 2C), 124.0 (s, 2C), 18.0 (s, 2C) ppm.

MS (EI, m/z): 213.1 (13%), 212.1 (100%) $[M\text{-}2Cl]^+$, 211.1 (11%), 106.1 (8%).

EA: calculated C 58.96, H 6.36, N 9.82; found C 58.86, H 6.47, N 9.85.

4,4'-Dichloro-3,3'-dimethyl-1,1'-biphenyl (68)

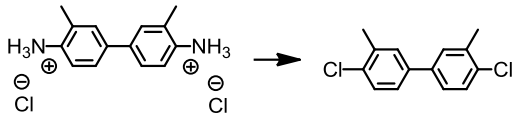

67 **68**

$C_{14}H_{12}Cl_2$
250.03 g/mol

Diaminium chloride **67** (2.50 g, 8.77 mmol, 1.0 eq.) was dissolved in conc. HCl (20 mL) and water (150 mL) and cooled to -10°C. Sodium nitrite (1.27 g, 18.4 mmol, 2.1 eq.) was dissolved in water (40 mL) cooled to 0°C and added to the reaction mixture over a period of 30 min. The yellow reaction mixture was stirred at -5°C for further 30 min.

Copper(I)chloride (4.77 g, 48.2 mmol, 5.5 eq.) was dissolved in a 2.5% HCl solution and heated to 100°C. The previously prepared yellow -5°C cold diazonium salt solution was added over a period of 30 min. The green reaction mixture was stirred at 100°C for 90 min, cooled to room temperature and extracted with TBME (3 × 100 mL). The combined organic layers were washed with a 1M aq. NaOH solution (50 mL) and with brine (50 mL), dired over $MgSO_4$ and evaporated to dryness. The black crude was adsorbed on silica gel and purified by column chromatography with silica gel and *n*-hexane to afford the chlorinated product **68** as a white solid in a yield of 30%. The mono chlorinated product was isolated in a yield of 15%.

TLC: R_f = 0.34 (*n*-hexane).

MP: 57-58°C.

^{1}H-NMR (400 MHz, $CDCl_3$): δ = 7.39 (m, 4H), 7.30 (m, 2H), 2.43 (s, 6H).ppm.

^{13}C-NMR (101 MHz, $CDCl_3$): δ = 139.1 (s, 2C), 136.8 (s, 2C), 134.2 (s, 2C), 129.9 (s, 2C), 129.8 (s, 2C), 126.0 (s, 2C), 20.6 (s, 2C) ppm.

MS (EI, m/z): 254.1 (10%), 253.1 (9%), 252.1 (65%), 251.1 (16%), 250.1 (100%) $[M]^+$, 216.1 (37%), 215.1 (15%), 197.1 (15%), 165.1 (26%), 89.1 (12%).

EA: calculated C 66.95, H 4.82, N 0.00; found C 67.04, H 4.87, N 0.00.

3,3'-Bis(bromomethyl)-4,4'-dichloro-1,1'-biphenyl (69)

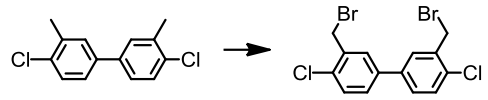

68 **69**

$C_{14}H_{10}Br_2Cl_2$
405.85 g/mol

The dichloro biphenyl **68** (2.75 g, 11.0 mmol, 1.0 eq.) and *N*-bromosuccinimide (NBS) (3.99 g, 22.5 mmol, 2.05 eq.) were dissolved in dry carbon tetrachloride (30 mL) and benzoylperoxide (133 mg, 0.55 mmol, 5 mol-%) was added at room temperature under argon. The reaction mixture was irradiated with visible light (200 W) at such a distance from the reaction flask that reflux was maintained. After 2 h of irradiation the reaction mixture was cooled to 0°C and the white precipitate was filtered off. The white crude was dissolved in dichloromethane (100 mL), washed with water (75 mL) and with brine (50 mL), dried over $MgSO_4$ and evaporated to dryness. After purification by recrystallization from hot dichloromethane the desired brominated product **69** was isolated as a white powder in a yield of 58%.

TLC: R_f = 0.34 (dichloromethane:*n*-hexane 1:5).

MP: 168-170°C.

^{1}H-NMR (400 MHz, $CDCl_3$): δ = 7.61 (d, ^4J = 2.0 Hz, 3H), 7.46 (m, 4H), 4.64 (s, 2H) ppm.

^{13}C-NMR (101 MHz, $CDCl_3$): δ = 139.1 (s, 2C), 136.4 (s, 2C), 134.4 (s, 2C), 131.0 (s, 2C), 130.0 (s, 2C), 128.8 (s, 2C), 30.7 (s, 2C) ppm.

MS (EI, m/z): 411.9 (9%), 410.9 (4%), 409.9 (25%), 408.9 (7%), 407.9 (29%), 405.9 (11%) $[M]^+$, 330.9 (44%), 329.0 (100%), 327.0 (60%), 250.0 (24%), 248.0 (36%), 178.1 (27%), 124.0 (20%), 88.0 (11%).

EA: calculated C 41.12, H 2.46, N 0.00; found C 41.19, H 2.31, N 0.00.

4,4'-Dichloro-3,3'-bis(3-nitrobenzyl)-1,1'-biphenyl (70)

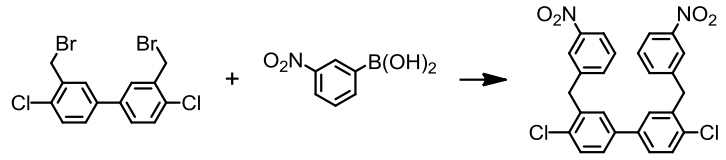

69 **35** **70**

$C_{26}H_{18}Cl_2N_2O_4$
492.06 g/mol

The brominated biphenyl **69** (200 mg, 0.49 mmol, 1.0 eq.), potassium carbonate (404 mg, 2.93 mmol, 6.0 eq.) and boronic acid **35** (295 mg, 1.72 mmol, 3.5 eq.) were dissolved in dry toluene (16 mL) and dry ethanol (4 mL). The reaction mixture was degassed with argon for 10 min and $[Pd(PPh_3)_4]$ (57.0 mg, 49.0 µmol, 10 mol-%) was added. The reaction mixture was heated under microwave conditions to 85°C for 30 min. After cooling down to room temperature the reaction mixture was filtered off and the filtrate was adsorbed on silica gel and purified by column chromatography with silica gel and toluene, affording the desired doubly coupled product **70** as a white powder in a yield of 95%.

TLC: R_f = 0.46 (toluene).

MP: 152-153°C.

^{1}H-NMR (400 MHz, $CDCl_3$): δ = 8.07 (m, 4H), 7.54 (m, ^3J = 8.2 Hz, 2H), 7.46 (m, 4H), 7.39 (d, ^4J = 2.3 Hz, 2H), 7.36 (m, 2H), 4.25 (s, 4H) ppm.

^{13}C-NMR (101 MHz, $CDCl_3$): δ = 148.8 (s, 2C), 141.7 (s, 2C), 139.4 (s, 2C), 137.9 (s, 2C), 135.4 (s, 2C), 134.4 (s, 2C), 130.8 (s, 2C), 130.0 (s, 2C), 129.8 (s, 2C), 127.5 (s, 2C), 124.0 (s, 2C), 122.0 (s, 2C), 39.5 (s, 2C) ppm.

MS (EI, m/z): 496.0 (13%), 495.1 (19%), 494.1 (69%), 493.0 (30%), 492.1 (100%) $[M]^+$, 477.0 (22%), 475.1 (33%), 410 (6%), 327.1 (7%), 239.1 (8%), 164.1(8%).

EA: calculated C 63.30, H 3.68, N 5.68; found C 63.32, H 3.68, N 5.42.

3,3'-((4,4'-Dichloro-[1,1'-biphenyl]-3,3'-diyl)bis(methylene))dianiline (71)

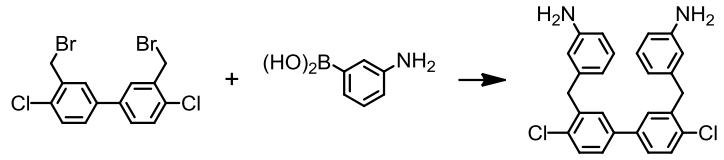

69 **72** **71**

$C_{26}H_{22}Cl_2N_2$
432.12 g/mol

The brominated biphenyl **69** (100 mg, 0.24 mmol, 1.0 eq.), potassium carbonate (202 mg, 1.47 mmol, 6.0 eq.) and boronic acid **72** (113 mg, 0.73 mmol, 3.0 eq.) were dissolved in dry toluene (15 mL) and dry ethanol (4 mL). The reaction mixture was degassed with argon for 15 min and $[Pd(PPh_3)_4]$ (29.0 mg, 24.4 µmol, 10 mol-%) was added. The reaction mixture was heated under microwave conditions to 90°C for 25 min. After cooling down to room temperature the reaction mixture was filtered with toluene over a 1 cm plug of silica gel and washed with ethanol. The crude was adsorbed on silica gel and purified by column chromatography with silica gel and toluene with 5% MeOH, affording the desired doubly coupled product **71** as an instable white powder in a yield of 51%.

TLC: R_f = 0.20 (toluene 5% MeOH).

MP: 113-115°C.

^{1}H-NMR (400 MHz, $CDCl_3$): δ = 7.41 (d, ^3J = 8.2 Hz, 2H), 7.31 (m, 4H), 7.10 (t, ^3J = 7.5 Hz, 2H), 6.64 (d, ^3J = 7.5 Hz, 2H), 6.54 (m, 4H), 4.06 (s, 4H), 3.56 (br s, 4H) ppm.

^{13}C-NMR (101 MHz, $CDCl_3$): δ = 147.0 (s, 2C), 141.0 (s, 2C), 139.5 (s, 2C), 139.2 (s, 2C), 134.1 (s, 2C), 130.3 (s, 2C), 130.0 (s, 2C), 129.8 (s, 2C), 126.6 (s, 2C), 119.7 (s, 2C), 116.0 (s, 2C), 113.7 (s, 2C), 39.6 (s, 2C) ppm.

MS (EI, m/z): 436.1 (11%), 435.1 (18%), 434.1 (67%), 433.1 (30%), 432.1 (100%) $[M]^+$, 397.1 (45%), 361.2 (12%), 304.1 (50%), 269.1 (16%), 181.1 (54%), 172.1 (11%), 106.1 (46%).

3,3'-((4,4'-Dichloro-[1,1'-biphenyl]-3,3'-diyl)bis(methylene))dianiline (71)

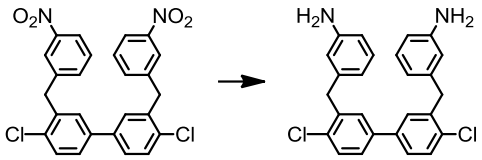

70 **71**

$C_{26}H_{22}Cl_2N_2$
432.12 g/mol

The nitro compound **70** (93.0 mg, 0.19 mmol, 1.0 eq.) was dissolved at room temperature in THF (25 mL) and conc. HCl (0.2 mL) and tin powder (224 mg, 1.89 mmol, 10.0 eq.) were added. The grey suspension was stirred at room temperature for 2 h. The meanwhile colorless reaction mixture was quenched with a 1 M aq. NaOH solution (50 mL, > pH 7) and diluted with water (100 mL). The resulting basic mixture was extracted with dichloromethane (3 × 70 mL). The combined organic layers were washed with brine (150 mL), dried over $MgSO_4$ and evaporated to dryness. The oily crude was purified by column chromatography with silica gel and dichloromethane with 3% MeOH affording the reduced product **71** as an instable white solid in a yield of 45%.

TLC: R_f = 0.51 (dichloromethane 3% MeOH).

MP: 113-115°C.

^{1}H-NMR (400 MHz, $CDCl_3$): δ = 7.41 (d, ^3J = 8.2 Hz, 2H), 7.31 (m, 4H), 7.10 (t, ^3J = 7.5 Hz, 2H), 6.64 (d, ^3J = 7.5 Hz, 2H), 6.54 (m, 4H), 4.06 (s, 4H), 3.56 (br s, 4H) ppm.

^{13}C-NMR (101 MHz, $CDCl_3$): δ = 147.0 (s, 2C), 141.0 (s, 2C), 139.5 (s, 2C), 139.2 (s, 2C), 134.1 (s, 2C), 130.3 (s, 2C), 130.0 (s, 2C), 129.8 (s, 2C), 126.6 (s, 2C), 119.7 (s, 2C), 116.0 (s, 2C), 113.7 (s, 2C), 39.6 (s, 2C) ppm.

MS (EI, m/z): 436.1 (11%), 435.1 (18%), 434.1 (67%), 433.1 (30%), 432.1 (100%) $[M]^+$, 397.1 (45%), 361.2 (12%), 304.1 (50%), 269.1 (16%), 181.1 (54%), 172.1 (11%), 106.1 (46%).

4,4'-Dichloro-3,3'-bis(3-iodobenzyl)-1,1'-biphenyl (73)

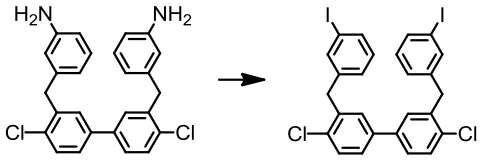

71 **73**

$C_{26}H_{18}Cl_2I_2$
653.89 g /mol

The diamino biphenyl **71** (35.0 mg, 80.8 µmol, 1.0 eq.) was dissolved in conc. HCl (20 mL) and DMF (7 mL) at room temperature. After stirring for 10 min, sodium nitrite (16.7 mg, 242 µmol, 3.0 eq.) dissolved in water (10 mL) was added and the reaction mixture was stirred at 0°C for 20 min.

Copper(I)iodide (62.0 mg, 323 µmol, 4.0 eq.) was dissolved in a 2% aq. HCl solution (30 mL) at 50°C and the 0°C biphenyl solution was added drop wise over a period of 30 min. After complete addition the brown reaction mixture was stirred at 50°C for 1.5 h and then cooled to room temperature. The reaction mixture was extracted with TBME (3 × 50 mL) and the combined organic layers were washed with brine (70 mL), dried over $MgSO_4$ and evaporated to dryness. The crude was purified by column chromatography with silica gel and dichloromethane:*n*-hexane (1:2 → 2:1) affording the iodinated product **73** as a white solid in a yield of 9%. The poor yield can be explained by a chlorine iodine exchange during the reaction.

TLC: R_f = 0.51 (dichloromethane:*n*-hexane 1:2).

MP: 123-124°C.

^{1}H-NMR (400 MHz, $CDCl_3$): δ = 7.43 (d, ^3J = 8.2 Hz, 2H), 7.33 (m, 2H), 7.29 (m, 2H), 7.20 (m, 6H), 7.09 (dd, ^3J = 8.2, ^4J = 1.4 Hz, 2H), 4.12 (s, 4H) ppm.

^{13}C-NMR (101 MHz, $CDCl_3$): δ = 142.1 (s, 2C), 139.3 (s, 2C), 138.2 (s, 2C), 135.9 (s, 2C), 134.7 (s, 2C), 134.2 (s, 2C), 130.5 (s, 2C), 130.2 (s, 2C), 129.3 (s, 2C), 128.5 (s, 2C), 127.4 (s, 2C), 127.0 (s, 2C), 39.4 (s, 2C) ppm.

MS (FAB, m/z): 657.9 (10%), 656.9 (16%), 655.9 (66%), 654.9 (26%), 653.9 (100%) $[M]^+$, 563.9 (59%), 561.9 (60%), 365.1 (27%), 165.2 (45%), 125.0 (17%).

4,4'-Difluoro-3,3'-dimethyl-1,1'-biphenyl (83)

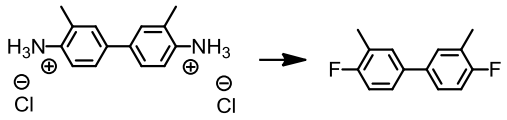

67 **83**

$C_{14}H_{12}F_2$
218.09 g/mol

The protonated biphenyl salt **67** was dissolved in a 1M aq. NaOH solution (100 mL) and extracted with dichloromethane (3 × 50 mL). The combined organic layers were dried over $MgSO_4$ and evaporated to dryness, to afford the basic amine of **67** as a grey solid. The amine of **67** (57.0 mg, 0.27 mmol, 1.0 eq.) and hydrogen fluoride pyridine (1.63 g, 10.7 mmol, 40.0 eq.) were stirred at room temperature until all the amine was dissolved. The reaction mixture was then cooled to -50°C and sodium nitrite (41.0 mg, 0.59 mmol, 2.2 eq.) was added. The orange reaction mixture was stirred at -50°C for 30 min and then at 60°C for 60 min. After cooling down to room temperature the reaction mixture was quenched with water (20 mL) and with a sat. aq. $NaHCO_3$ solution (10 mL), thereafter the reaction mixture was extracted with dichloromethane (5 × 50 mL) and the combined organic layers were washed with a sat. aq. $NaHCO_3$ solution (50 mL) and with brine (50 mL), dried over $MgSO_4$ and evaporated to dryness. The brown crude was purified by column chromatography with silica gel and dichloromethane:*n*-hexane (1:1) affording the desired fluorinated biphenyl **83** as a colorless liquid in a yield of 62%.

TLC: R_f = 0.73 (dichloromethane:*n*-hexane 1:1).

^{1}H-NMR (400 MHz, $CDCl_3$): δ = 7.34 (dd, ^3J = 7.3, ^4J = 2.1 Hz, 2H), 7.30 (m, 4H), 7.05 (d, ^3J = 9.1 Hz, 2H), 2.34 (d, ^4J = 1.8 Hz, 6H) ppm.

^{19}F NMR (376 MHz, $CDCl_3$): δ = -121.40 (m, 2F) ppm.

^{13}C-NMR (101 MHz, $CDCl_3$): δ = 161.3 (d, *J* = 244.9 Hz), 136.7 (d, *J* = 3.6 Hz), 130.5 (d, *J* = 5.3 Hz), 126.2 (d, *J* = 8.1 Hz), 125.4 (d, *J* = 17.5 Hz), 115.6 (d, *J* = 22.5 Hz), 15.09 (d, *J* = 3.4 Hz) ppm.

MS (EI, m/z): 219.1 (15%), 218.1 (100%) $[M]^+$, 203.0 (21%), 202.0 (13%), 201.0.

EA: calculated C 76.05, H 5.54, N 0.00; found C 76.36, H 5.75, N 0.00.

4,4'-Diiodo-3,3'-dimethyl-1,1'-bipheny (80)

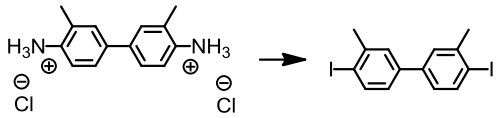

67 **80**

$C_{14}H_{12}I_2$
433.90 g/mol

The biphenyl salt **67** (2.30 g, 8.06 mmol, 1.0 eq.) was dissolved in conc. HCl (20 mL) and water (150 mL) at -15°C. Sodium nitrite (1.56 g, 22.6 mmol, 3.0 eq.) dissolved in water (40 mL) was added over a period of 45 min and the reaction mixture was then stirred at -10°C for 2.5 h.

Potassium iodide (4.90 g, 29.5 mmol, 3.7 eq.) was dissolved in a 2% aq. HCl solution (30 mL) at 100°C and the cooled biphenyl solution (-10°C) was added drop wise over a period of 60 min. After complete addition the brown reaction mixture was stirred at 100°C for 4.5 h and then cooled to room temperature. The reaction mixture was extracted with TBME (3 × 150 mL) and the combined organic layers were washed with brine (100 mL), dried over $MgSO_4$ and evaporated to dryness. The crude was adsorbed on silica gel and purified by column chromatography with silica gel and *n*-hexane affording the iodinated product **80** as a beige solid in a yield of 36%.

TLC: R_f = 0.30 (*n*-hexane).

MP: 115-117°C.

^{1}H-NMR (400 MHz, $CDCl_3$): δ = 7.85 (d, ^3J = 8.2 Hz, 2H), 7.41 (s, 2H), 7.05 (d, ^3J = 8.2 Hz, 2H), 2.49 (s, 6H) ppm.

^{13}C-NMR (101 MHz, $CDCl_3$): δ = 142.3 (s, 2C), 140.7 (s, 2C), 139.8 (s, 2C), 128.6 (s, 2C), 126.3 (s, 2C), 100.6 (s, 2C), 28.6 (s, 2C) ppm.

MS (EI, m/z): 435.0 (15%), 433.9 (100%) $[M]^+$, 165.1 (17%), 89.0 (7%).

EA: calculated C 38.74, H 2.79, N 0.00; found C 38.96, H 2.72, N 0.00.

(*Trans*)-1,2-bis(3-bromophenyl)diazene (78)

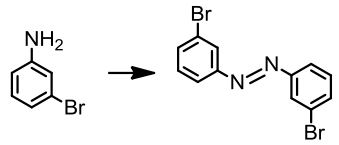

77 **78**

$C_{12}H_8Br_2N_2$
337.91 g/mol

3-Bromaniline (**77**) (1.58 g, 9.19 mmol, 2.0 eq.) and mangan(IV)oxid (activated 5 micron, 85%) (4.70 g, 49.9 mmol, 10.0 eq.) were suspended in dry toluene (30 mL). After addition of molecular sieves 4 Å (4.0 g) the reaction mixture was stirred at room temperature for 4.5 h and at 110°C for 14 h. The reaction mixture was cooled to room temperature and filtered over a 2 cm plug of *Celite*®. The orange crude was adsorbed on silica gel and purified by column chromatography with silica gel and dichloromethane:*n*-hexane (1:1) affording the desired azo compound **78** as a orange powder in a yield of 85%.

TLC: R_f = 0.61 (dichloromethane:*n*-hexane 1:1).

MP: 128-130°C.

^{1}H-NMR (500 MHz, $CDCl_3$): δ = 8.05 (s, 2H), 7.89 (d, ^3J = 7.9 Hz, 2H), 7.62 (d, ^3J = 7.9 Hz, 2H), 7.42 (t, ^3J = 7.9 Hz, 2H) ppm.

^{13}C-NMR (126 MHz, $CDCl_3$): δ = 153.2 (s, 2C), 134.2 (s, 2C), 130.6 (s, 2C), 124.8 (s, 2C), 123.3 (s, 2C), 123.2 (s, 2C) ppm.

MS (EI, m/z): 341.9 (19%), 339.9 (40%), 337.9 (20%) $[M]^+$, 184.9 (47%), 182.9 (47%), 156.9 (99%), 154.9 (100%), 152.0 (17%), 76.0 (46%), 75.0 (31%), 50.0 (17%).

EA: calculated C 42.39, H 2.37, N 8.24; found C 42.43, H 2.34, N 8.18.

(*Trans*)-(diazene-1,2-diylbis(3,1-phenylene))diboronic acid (79)

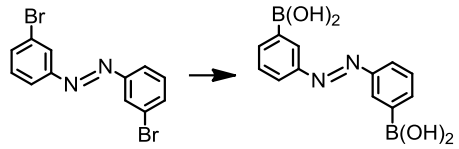

78 **79**

$C_{12}H_{12}B_2N_2O_4$
270.10 g/mol

The dibromo compound **78** (300 mg, 0.88 mmol, 1.0 eq.) was dissolved under argon at -78°C in dry THF (10 mL). A 1.6 M *n*-BuLi solution in hexane (1.9 mL, 3.09 mmol, 3.5 eq.) was added drop wise over a period of 10 min, then triisopropylborat (1.6 mL, 7.06 mmol, 8.0 eq.) was added over a period of 5 min and the reaction mixture was stirred under argon at -78°C for 75 min and at -20°C for 90 min. The black reaction mixture was stirred at room temperature for additional 60 min and was quenched with water (50 mL) and a 20% aq. HCl solution (20 mL). The reaction mixture was extracted with TBME (3 × 50 mL) and the combined organic layers were washed with a 4% aq. HCl solution (50 mL) and with brine (50 mL), dried over $MgSO_4$ and evaporated to dryness. The orange crude was filtered over a 2 cm plug of silica gel with toluene, evaporated to dryness and dried under high vacuum conditions for 24 h affording the extremely instable boronic acid **79** as an orange resin in crude yield of 80%. The boronic acid was immediately used without further purification, but already in the timeframe of the NMR measurements 50% of the product was degenerated.

TLC: R_f = 0.62 (ethyl acetate:*n*-hexane 1:1).

^{1}H-NMR (250 MHz, $CDCl_3$): δ = 8.06 (t, ^4J = 1.9 Hz, 2H), 7.89 (dt, ^3J = 7.9 Hz, ^4J = 1.9 Hz, 2H), 7.62 (dt, ^3J = 7.9 Hz, ^4J = 1.9 Hz, 2H), 7.42 (t, ^3J = 7.9 Hz, 2H), 3.47 (br s, 4H) ppm.

MS (MALDI-TOF, m/z): 271.3 (100%) $[M-H]^+$.

1,2-Di-*m*-tolylhydrazine (92)

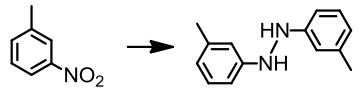

91 **92**

$C_{14}H_{16}N_2$
212.13 g/mol

3-Nitrotoluene (**91**) (6.02 mL, 50.0 mmol, 2.0 eq.) was dissolved in methanol (30 mL) the reaction misture was degassed with argon for 5 min and then aluminium powder (2.73 g, 100 mmol, 4.0 eq.) and potassium hydroxide (16.8 g, 300 mmol, 12.0 eq.) were added in small portions (caution: very exothermic). The reaction mixture turned orange after 30 min and was then diluted with methanol (20 mL). Afterwards more aluminium powder (2.73 g, 100 mmol, 4.0 eq.) and potassium hydroxide (16.8 g, 300 mmol, 12.0 eq.) were added. After refluxing for 60 min the reaction mixture lost its orange color and was then cooled to room temperature and diluted with diethyl ether (50 mL). The reaction mixture was filtered and washed with a 0.1 M aq. HCl solution (3 × 100 mL) and with brine (100 mL), dried over $MgSO_4$ and evaporated to dryness. The crude was purified by column chromatography with silica gel and dichloromethane:*n*-hexane (1:1) affording the desired coupling product **92** as a yellow oil in a yield of 90%.

TLC: R_f = 0.35 (dichloromethane:*n*-hexane 1:1).

^{1}H-NMR (400 MHz, $CDCl_3$): δ = 7.11 (t, ^3J = 8.2 Hz, 2H), 6.68 (m, 6H), 5.54 (br s, 2H), 2.29 (s, 6H) ppm.

^{13}C-NMR (101 MHz, $CDCl_3$): δ = 149.5 (s, 2C), 139.7 (s, 2C), 129.6 (s, 2C), 121.2 (s, 2C), 113.4 (s, 2C), 109.6 (s, 2C), 22.0 (s, 2C) ppm.

MS (EI, m/z): 213.1 (16%), 212.1 (100%) $[M]^+$, 211.1 (15%), 197.1 (17%), 107.1 (20%), 106.1 (59%), 95.1 (22%), 91.1 (33%), 79.1 (29%), 77.0 (23%).

EA: calculated C 79.21, H 7.60, N 13.20; found C 79.21, H 7.74, N 13.08.

4,4-Dimethyl-1,2-di-*m*-tolylpyrazolidine-3,5-dione (93)

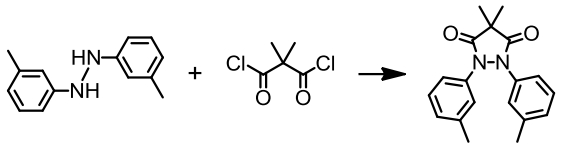

92 **90** **93**

$C_{19}H_{20}N_2O_2$
308.15 g/mol

A solution of dry dichloromethane (15 mL), pyridine (5 mL) and DMAP (11.0 mg, 0.09 mmol, 1.0 mol-%) was cooled under argon to -20°C, then dimethylmalonyl chloride (**90**) (1.47 mL, 10.8 mmol, 1.2 eq.) dissolved in dry dichloromethane (6 mL) was added. The reaction mixture was allowed to reach room temperature and the hydrazine **92** (1.91 g, 9.00 mmol, 1.0 eq.) dissolved in dry dichloromethane (30 mL) was added. The red reaction mixture was stirred under argon at room temperature for 7 h and then washed with a 2M aq. HCl solution (4 × 50 mL), with water (2 × 50 mL), with a 5% aq. $NaHCO_3$ solution (2 × 50 mL) and brine (50 mL). The organic layer was dried over $MgSO_4$ and evaporated to dryness. The oily orange crude was adsorbed on silica gel an purified by column chromatography with silica gel and dichloromethane (0% → 3% MeOH) affording the desired compound **93** as a beige solid in a yield of 95%.

TLC: R_f = 0.33 (dichloromethane).

MP: 74-76°C.

^{1}H-NMR (400 MHz, $CDCl_3$): δ = 7.20 (m, 2H), 7.17 (d, ^3J = 7.8 Hz, 2H), 7.07 (m, 2H), 6.99 (m, 2H), 2.31 (s, 6H), 1.49 (s, 6H) ppm.

^{13}C-NMR (101 MHz, $CDCl_3$): δ = 174.8 (s, 2C), 139.4 (s, 2C), 136.4 (s, 2C), 129.1 (s, 2C), 128.1 (s, 2C), 123.8 (s, 2C), 119.9 (s, 2C), 44.8 (s, 2C), 22.2 (s, 2C), 21.9 (s, 2C) ppm.

MS (EI, m/z): 309.2 (22%), 308.1 (100%) $[M]^+$, 132.1 (11%), 119.1 (23%), 91.1 (51%), 65.1 (7%).

EA: calculated C 74.00, H 6.54, N 9.08; found C 73.79, H 6.55, N 9.04.

1,2-Bis(3-(bromomethyl)phenyl)-4,4-dimethylpyrazolidine-3,5-dione (94)

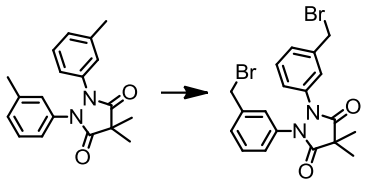

93 **94**

$C_{19}H_{18}Br_2N_2O_2$
463.97 g/mol

The pyrazolidine derivative **93** (2.47 g, 8.00 mmol, 1.0 eq.), NBS (3.10 g, 16.6 mmol, 2.07 eq.) and AIBN (131 mg, 0.80 mmol, 0.1 eq.) were dissolved in dry carbon tetrachloride (110 mL) under argon. The reaction mixture was irradiated with visible light (200 W) at 35°C for 1.5 h and then cooled in a freezer. The precipitate was filtered off and washed with cold carbon tetrachloride (not chloroform, dissolves the precipitate). The collected filtrate was evaporated to dryness and the oily orange crude was purified by column chromatography with silica gel and ethyl acetate:*n*-hexane (1:5). With this column the product was separated from the mono brominated product. To separate the product from the over brominated compound three subsequent column chromatography with silica gel and dichloromethane were necessary to give the desired brominated product **94** in as a white solid in a yield of 35%. After four columns not all over brominated product could be removed and the purity, calculated from ^{1}H-NMR, was 95%.

TLC: R_f = 0.33 (dichloromethane).

MP: 94-96°C.

^{1}H-NMR (500 MHz, $CDCl_3$): δ = 7.39 (s, 2H), 7.30 (m, 2H), 7.22 (m, 4H), 4.40 (s, 4H), 1.51 (s, 6H) ppm.

^{13}C-NMR (126 MHz, $CDCl_3$): δ = 174.2 (s, 2C), 139.0 (s, 2C), 136.2 (s, 2C), 129.5 (s, 2C), 127.3 (s, 2C), 123.0 (s, 2C), 122.0 (s, 2C), 44.4 (s, 2C), 32.4 (s, 2C), 21.8 (s, 2C) ppm.

MS (EI, m/z): 469.0 (10%), 468.0 (50%), 467.0 (29%), 466.0 (100%), 464.9 (28%), 464.0 (50%) $[M]^+$, 387.1 (24%), 385.1 (24%), 171.0 (17%), 169.0 (18%).

4,4'-Dimethoxy-3,3'-dimethyl-1,1'-biphenyl (96)

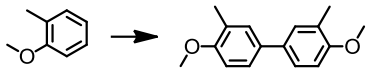

95 **96**

$C_{16}H_{18}O_2$
242.13 g/mol

Molubdenum(V)chloride (14.1 g, 51.6 mmol, 2.1 eq.) was dried under high vacuum conditions for 30 min and was then suspended in dry dichloromethane (250 mL) under argon at 0°C and then 2-methylanisol (**95**) (4.57 mL, 24.6 mmol, 1.5 eq.) was added in small portions over a period of 15 min. The black reaction mixture was stirred under argon at 0°C for 60 min and then quenched with a sat. aq. $NaHCO_3$ solution (250 mL). The reaction mixture was extracted with dichloromethane (4 × 100 mL) and the combined organic layers were washed with brine (150 mL), dried over $MgSO_4$ and evaporated to dryness. The black crude was adsorbed on silica gel and purified by column chromatography with silica gel and dichloromethane:*n*-hexane (1:1) affording the desired coupling product **96** as a white powder in a yield of 69%

TLC: R_f = 0.38 (dichloromethane:*n*-hexane 1:1).

MP: 156-158°C.

^{1}H-NMR (400 MHz, $CDCl_3$): δ = 7.36 (m, 4H), 6.88 (m, 2H), 3.88 (s, 6H), 2.30 (s, 6H) ppm.

^{13}C-NMR (101 MHz, $CDCl_3$): δ = 157.3 (s, 2C), 133.7 (s, 2C), 129.6 (s, 2C), 127.2 (s, 2C), 125.3 (s, 2C), 110.6 (s, 2C), 55.8 (s, 2C), 16.8 (s, 2C) ppm.

MS (EI, m/z): 243.1 (16%), 242.1 (100%) $[M]^+$, 228.1 (14%), 227.1 (90%), 121.0 (7%).

EA: calculated C 79.31, H 7.49, N 0.00; found C 79.17, H 7.56, N 0.00.

3,3'-Bis(bromomethyl)-4,4'-dimethoxy-1,1'-biphenyl (97)

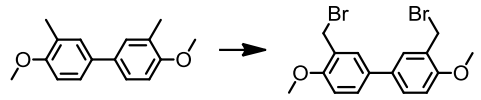

96 **97**

$C_{16}H_{16}Br_2O_2$
397.95 g/mol

The biphenyl **96** (1.90 g, 7.84 mmol, 1.0 eq.) was suspended under argon in dry carbon tetrachloride (45 mL) and NBS (2.80 g, 15.7 mmol, 2.0 eq.) was added in three portions in an interval of 10 min. Meanwhile the reaction mixture was irradiated with visible light (200 W) for 90 min at such a distance from the reaction flask that reflux was maintained. The reaction mixture was cooled to room temperature, diluted with dichloromethane (100 mL) and then quenched with water (100 mL). The reaction mixture was extracted with dichloromethane (2 × 100 mL) and the combined organic layers were washed with brine (100 mL), dried over $MgSO_4$ and evaporated to dryness. The yellow crude was recrystallized from hot TBME to give the desired brominated product **97** as a white powder in a yield of 63%.

TLC: R_f = 0.29 (TBME:*n*-hexane 1:4).

MP: 174-176°C.

^{1}H-NMR (400 MHz, $CDCl_3$): δ = 7.51 (d, ^4J = 2.4 Hz, 2H), 7.46 (dd, ^3J = 8.5 Hz, ^4J = 2.4 Hz, 2H), 6.94 (d, ^3J = 8.5 Hz, 2H), 4.62 (s, 4H), 3.94 (s, 6H) ppm.

^{13}C-NMR (101 MHz, $CDCl_3$): δ = 157.3 (s, 2C), 133.2 (s, 2C), 129.6 (s, 2C), 128.3 (s, 2C), 126.8 (s, 2C), 111.4 (s, 2C), 56.3 (s, 2C), 29.3 (s, 2C) ppm.

MS (EI, m/z): 402.0 (23%), 400.0 (48%) $[M]^+$, 398.0 (24%), 322.1 (20%), 321.1 (99%), 320.1 (21%), 319.1 (100%), 291.1 (17%), 289.1 (18%), 211.2 (22%), 210.2 (49%), 180.1 (25%), 165.2 (25%), 152.1 (19%), 120.1 (29%).

EA: calculated C 48.03, H 4.03, N 0.00; found C 48.24, H 4.04, N 0.00.

(4,4'-Dimethoxy-[1,1'-biphenyl]-3,3'-diyl)bis(methylene) diacetate (98)

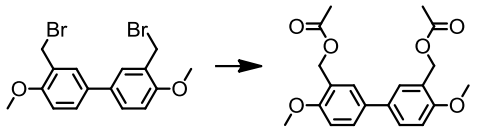

97 **98**

$C_{20}H_{22}O_6$
358.14 g/mol

The dibromo biphenyl **97** (444 mg, 1.11 mmol, 1.0 eq.) and acetic acid potassium salt (440 mg, 4.44 mmol, 4.0 eq,) were suspended in glacial acetic acid (10 mL) and heated to reflux for 2.5 h. The reaction mixture was cooled to room temperature and diluted with dichloromethane (50 mL). The organic layer was separated and washed with a sat. aq. $NaHCO_3$ solution (3 × 20 mL), dried over $MgSO_4$ and evaporated to dryness. The crude was recrystallized from hot TBME to give the acetylated product **98** as a white powder in a yield of 96%.

TLC: R_f = 0.30 (dichloromethane with 0.5% MeOH).

MP: 149-150°C.

^{1}H-NMR (400 MHz, $CDCl_3$): δ = 7.51 (d, ^4J = 2.0 Hz, 2H), 7.48 (dd, ^3J = 8.4, ^4J = 2.2 Hz, 2H), 6.95 (d, ^3J = 8.4 Hz, 2H), 5.22 (s, 4H), 3.88 (s, 6H), 2.12 (s, 6H) ppm.

^{13}C-NMR (101 MHz, $CDCl_3$): δ = 171.4 (s, 2C), 157.2 (s, 2C) 133.5 (s, 2C), 128.8 (s, 2C), 128.2 (s, 2C), 124.9 (s, 2C), 111.3 (s, 2C), 62.2 (s, 2C) 56.1 (s, 2C), 21.5 (s, 2C) ppm.

MS (EI, m/z): 359.1 (20%), 358.1 (100%) $[M]^+$, 299.1 (11%), 269.1 (10%), 255.0 (25%), 241.0 (14%).

EA: calculated C 67.03, H 6.19, N 0.00; found C 66.72, H 6.32, N 0.00.

(4,4'-Dimethoxy-[1,1'-biphenyl]-3,3'-diyl)dimethanol (99)

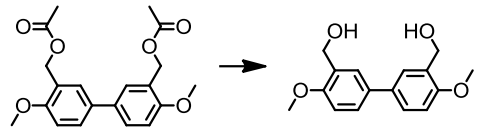

98 **99**

$C_{16}H_{18}O_4$
274.12 g/mol

The diacetate **98** (280 mg, 0.78 mmol, 1.0 eq.) and sodium hydroxide (204 mg, 5.10 mmol, 6.5 eq.) were suspended in water (12 mL) and ethanol (6 mL). The reaction mixture was refluxed for 3 h and then cooled down to room temperature, the ethanol was evaporated and the reaction mixture was neutralized with a few drops of a 3 M aq. HCl solution. The reaction mixture was diluted with water (15 mL) extracted with dichloromethane (5 × 20 mL), the combined organic layer were washed with brine (50 mL), dried over $MgSO_4$ and evaporated to dryness. The yellow crude was adsorbed on silica gel and purified by column chromatography with silica gel and dichloromethane with 2% MeOH to afford the deprotected product **99** as a white powder in a yield of 91%.

TLC: R_f = 0.19 (dichloromethane with 2% MeOH).

MP: 179-181°C.

^{1}H-NMR (400 MHz, $CDCl_3$): δ = 7.47 (m, 4H), 6.93 (d, ^3J = 8.3 Hz, 2H), 4.74 (s, 4H), 3.91 (s, 6H), 2.31 (br s, 2H) ppm.

^{13}C-NMR (101 MHz, $CDCl_3$): δ = 157.1 (s, 2C), 133.7 (s, 2C), 129.7 (s, 2C), 127.7 (s, 2C), 127.4 (s, 2C), 111.0 (s, 2C), 62.7 (s, 2C), 55.9 (s, 2C) ppm.

MS (EI, m/z): 275.1 (34%), 274.1 (100%) $[M]^+$, 213.1 (7%), 201.1 (6%), 186.1 (10%), 168.0 (7%).

EA: calculated C 70.06, H 6.61, N 0.00; found C 69.86, H 6.66, N 0.00.

2-Methoxyphenyl acetate (101)

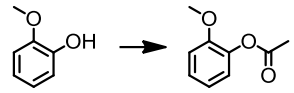

100 **101**

$C_9H_{10}O_3$
166.06 g/mol

2-Methoxyphenol (**100**) (4.97 g, 40.0 mmol, 1.0 eq.) and pyridine (7.44 mL, 92.0 mmol, 2.3 eq.) were dissolved in dry dichloromethane (50 mL), cooled to 0°C and degassed with argon for 10 min. Acetyl chloride (3.43 mL, 48.0 mmol, 1.2 eq.) was added at 0°C under argon over a period of 10 min and then stirred at room temperature for 1h. The yellow reaction mixture was poured into a 1M aq. H_3PO_3 solution (50 mL) and stirred for 5 min at room temperature, the organic layer was separated and the water phase was extracted with dichloromethane (2 × 50 mL). The combined organic layer were washed with brine (50 mL), dried over $MgSO_4$ and evaporated to dryness to afford the product **101** in a yield of 99%. The obtained light yellow oil was analytically pure and was used without further purification.

TLC: R_f = 0.54 (diethyl ether:*n*-hexane 1:1).

^{1}H-NMR (400 MHz, $CDCl_3$): δ = 7.20 (td, ^3J = 8.4 Hz, ^4J = 1.6 Hz, 1H), 7.04 (dd, ^3J = 8.4 Hz, ^4J = 1.6 Hz, 1H), 6.96 (m, 2H), 3.83 (s, 3H), 2.32 (s, 3H) ppm.

^{13}C-NMR (101 MHz, $CDCl_3$): δ = 169.5 (s, 1C), 151.5 (s, 1C), 140.1 (s, 1C), 127.3 (s, 1C), 123.2 (s, 1C), 121.1 (s, 1C), 112.8 (s, 1C), 56.2 (s, 1C), 21.1 (s, 2C) ppm.

MS (EI, m/z): 166.1 (7%) $[M]^+$, 124.0 (100%), 109.0 (56%), 81.0 (10%), 43.0 (13%).

EA: calculated C 65.05, H 6.07, N 0.00; found C 65.23, H 6.17, N 0.00.

5-Iodo-2-methoxyphenyl acetate (102)

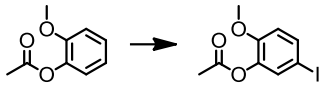

101 **102**

$C_9H_9IO_3$
291.96 g/mol

2-Methoxyphenyl acetate (**101**) (6.65 g, 40.0 mmol, 1.0 eq.) was dissolved under argon at 0°C in dichloromethane (50 mL). Iodine monochloride (2.45 mL, 7.79 g, 48.0 mmol, 1.2 eq.) dissolved in dry dichloromethane (50 mL) was added drop wise over a period of 70 min. The reaction mixture was slowly allowed to reach room temperature and stirred under argon for 18 h. The dark violet reaction mixture was poured into a sat. aq. $Na_2S_2O_3$ solution (200 mL) and stirred at room temperature for 5 min and was then extracted with dichloromethane (2 × 150 mL), the combined organic layer were washed with brine (150 mL), dried over $MgSO_4$ and evaporated to dryness. The yellow crude was purified by column chromatography with silica gel and toluene. The iodinated product **102** was isolated after drying under high vacuum conditions as a white powder in a yield of 93%.

TLC: R_f = 0.22 (toluene).

MP: 77-79°C.

^{1}H-NMR (400 MHz, $CDCl_3$): δ = 7.49 (dd, ^3J = 8.6 Hz, ^4J = 2.1 Hz, 1H), 7.33 (d, ^4J = 2.1 Hz, 1H), 6.72 (d, ^3J = 8.6 Hz, 1H), 3.80 (s, 3H), 2.30 (s, 3H) ppm.

^{13}C-NMR (101 MHz, $CDCl_3$): δ = 169.0 (s, 1C), 151.8 (s, 1C), 140.9 (s, 1C), 136.1 (s, 1C), 132.0 (s, 1C), 114.7 (s, 1C), 81.7 (s, 1C), 56.4 (s, 1C), 21.0 (s, 1C) ppm.

MS (EI, m/z): 292.0 (13%) $[M]^+$, 250.0 (100%), 234.9 (33%), 206.9 (9%), 79.0 (8%), 43.0 (10%).

EA: calculated C 37.01, H 3.11, N 0.00; found C 37.28, H 2.82, N 0.00.

5-Iodo-2-methoxyphenol (103)

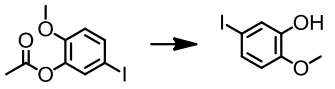

102 **103**

$C_7H_7IO_2$
249.95 g/mol

5-Iodo-2-methoxyphenyl acetate (**102**) (3.50 g, 12.0 mmol, 1.0 eq.) was dissolved under argon at room temperature in THF (15 mL), methanol (15 mL) and water (5 mL). Lithium hydroxide (1.17 g, 48.0 mmol, 4.0 eq.) was added in one portion to the reaction mixture, which was then stirred at room temperature for 20 h and further lithium hydroxide (1.17 g, 48.0 mmol, 4.0 eq.) was added. The reaction mixture was poured into a cold 1M aq. HCl solution (50 mL) and stirred for 10 min. This mixture was extracted with TBME (3 × 50 mL) and the combined organic layer were washed with brine (100 mL), dried over $MgSO_4$ and evaporated to dryness. The light yellow crude was recrystallized from hot *n*-hexane with a few drops of TBME, affording the deprotected alcohol **103** as white crystals in a yield of 87%.

TLC: R_f = 0.41 (TBME:*n*-hexane 1:1).

MP: 87-88°C.

^{1}H-NMR (400 MHz, $CDCl_3$): δ = 7.23 (d, ^4J = 2.1 Hz, 1H), 7.16 (dd, ^3J = 8.4 Hz, ^4J = 2.1 Hz, 1H), 6.60 (d, ^3J = 8.4 Hz, 1H), 5.59 (s, 1H), 3.86 (s, 3H) ppm.

^{13}C-NMR (101 MHz, $CDCl_3$): δ = 147.1 (s, 1C), 147.0 (s, 1C), 129.5 (s, 1C), 123.8 (s, 1C), 112.9 (s, 1C), 83.4 (s, 1C), 56.4 (s, 1C) ppm.

MS (EI, m/z): 251.0 (7%), 250.0 (100%) $[M]^+$, 235.0 %1%), 207.0 (17%), 52.1 (8%).

EA: calculated C 33.63, H 2.82, N 0.00; found C 33.94, H 2.74, N 0.00.

4-Iodo-2-isopropoxy-1-methoxybenzene (104)

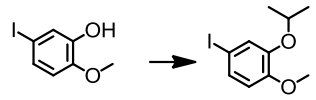

103 **104**

$C_{10}H_{13}IO_2$
292.00 g/mol

The alcohol **103** (2.30 g, 9.20 mmol, 1.0 eq.), 2-brompropane (1.48 mL, 15.6 mmol, 1.7 eq.) and potassium carbonate (2.16 g, 15.6 mmol, 1.7 eq.) were dissolved in ethanol (20 mL) and heated to reflux for 18 h. The reaction mixture was cooled to room temperature and the white precipitate was filtered off. The filtrate was evaporated to dryness and recrystallized from hot methanol to afford the protected alcohol **104** as a white powder in a yield of 94%.

TLC: R_f = 0.47 (dichloromethane:*n*-hexane 1:1).

MP: 59-61°C.

^{1}H-NMR (400 MHz, $CDCl_3$): δ = 7.21 (dd, ^3J = 8.4 Hz, ^4J = 2.1 Hz, 1H), 7.16 (d, ^4J = 2.1 Hz, 1H), 6.62 (d, ^3J = 8.4 Hz, 1H), 4.49 (hept, ^3J = 6.1 Hz, 1H), 3.82 (s, 3H), 1.36 (d, ^3J = 6.1 Hz, 6H) ppm.

^{13}C-NMR (101 MHz, $CDCl_3$): δ = 151.0 (s, 1C), 148.7 (s, 1C), 130.5 (s, 1C), 125.0 (s, 1C), 114.3 (s, 1C), 82.7 (s, 1C), 72.2 (s, 1C), 56.4 (s, 1C), 22.4 (s, 2C) ppm.

MS (EI, m/z): 293.0 (3%), 292.0 (30%) $[M]^+$, 250.0 (100%), 235.0 (53%), 207.0 (7%).

EA: calculated C 41.12, H 4.49, N 0.00; found C 41.25, H 4.40, N 0.00.

3,3'-Diisopropoxy-4,4'-dimethoxy-1,1'-biphenyl (105)

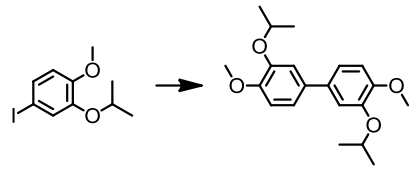

104 **105**

$C_{20}H_{26}O_4$
330.18 g/mol

The iodinated compound **104** (1.66 g, 5.68 mmol, 2.0 eq.) and copper powder (1.55 g, 24.1 mmol, 8.5 eq.) were mixed without solvent and slowly heated to 250°C. After the exothermic reaction was subsided the reaction mixture was stirred at 260°C for 90 min and cooled down to room temperature. The black crude was dissolved in dichloromethane (200 mL) and after filtration, in order to remove the copper, the filtrate was evaporated to dryness. The brown crude was adsorbed on silica gel and purified by column chromatography with silica gel and dichloromethane. The obtained yellow solid was recrystallized from hot methanol to afford the coupled product **105** as a white powder in a yield of 78% after drying under high vacuum conditions.

TLC: R_f = 0.38 (dichloromethane).

MP: 93-95°C.

^{1}H-NMR (400 MHz, $CDCl_3$): δ = 7.09 (m, 4H), 6.93 (m, 2H), 4.59 (hept, ^3J = 6.1 Hz, 2H), 3.89 (s, 6H), 1.40 (d, ^3J = 6.1 Hz, 12H) ppm.

^{13}C-NMR (101 MHz, $CDCl_3$): δ = 150.2 (s, Cq, 2C), 147.8 (s, Cq, 2C), 134.5 (s, Cq, 2C), 120.0 (s, Ct, 2C), 115.7 (s, Ct, 2C), 112.7 (s, Ct, 2C), 72.1 (s, Ct, 2C), 56.5 (s, Cp, 2C), 22.6 (s, Cp, 4C) ppm.

MS (EI, m/z): 331.2 (12%), 330.2 (62%) $[M]^+$, 247.1 (13%), 246.1 (100%), 231.1 (31%), 203.1 (16%).

EA: calculated C 72.70, H 7.93, N 0.00; found C 72.70, H 7.94, N 0.00.

4,4'-Dimethoxy-[1,1'-biphenyl]-3,3'-diol (106)

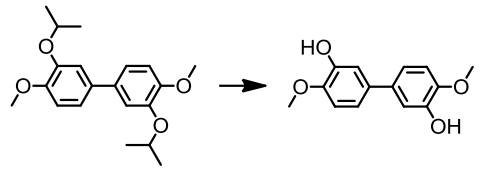

105 **106**

$C_{14}H_{14}O_4$
246.09 g/mol

The protected biphenyl **105** (195 mg, 0.59 mmol, 1.0 eq.) was dissolved under argon at room temperature in dry dichloromethane (6 mL), then iron(III) chloride (300 mg, 1.85 mmol, 3.1 eq.) was added and the resulting mixture was stirred at room temperature for 18 h. The dark green reaction mixture was poured into methanol (5 mL), diluted with dichloromethane (100 mL) and washed with water (50 mL) and with brine (50 mL), dried over $MgSO_4$ and evaporated to dryness. The dark crude was adsorbed on silica gel and purified by column chromatography with silica gel and dichloromethane with 1% MeOH. The obtained violet solid was recrystallized from hot ethanol to afford the deprotected methoxy biphenyl **106** as a white solid in a yield of 79% after drying under high vacuum conditions.

TLC: R_f = 0.42 (dichloromethane with 1% MeOH).

MP: 164-166°C.

^{1}H-NMR (250 MHz, $CDCl_3$): δ = 7.14 (d, ^4J = 2.2 Hz, 2H), 7.04 (dd, ^3J = 8.3 Hz, ^4J = 2.2 Hz, 2H), 6.89 (d, ^3J = 8.3 Hz, 2H), 5.62 (s, 2H), 3.92 (s, 6H) ppm.

^{13}C-NMR (101 MHz, acetone-d_6): δ = 147.2 (s, Cq, 2C), 147.1 (s, Cq, 2C), 134.6 (s, Cq, 2C), 117.9 (s, Ct, 2C), 113.7 (s, Ct, 2C), 112.3 (s, Ct, 2C), 56.9 (s, Cp, 2C) ppm.

MS (EI, m/z): 247.1 (15%), 246.1 (100%) $[M]^+$, 232.1 (12%), 231.1 (84%), 203.1 (41%), 188.1 (16%), 160.1 (11%).

EA: calculated C 64.17, H 6.06, N 0.00; found C 63.92, H 5.76, N 0.00 (product crystallized with one water molecule).

3,3'-Dimethoxy-1,1'-biphenyl (109)

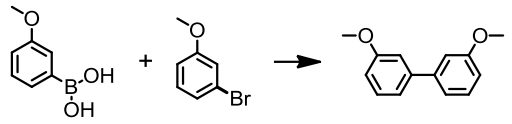

107 **108** **109**

$C_{14}H_{14}O_2$
214.10 g/mol

Dry toluene (30 mL) and dry ethanol (10 mL) were degassed with argon at room temperature for 15 min. Then 3-methoxyphenylboronic acid (**107**) (456 mg, 3.00 mmol, 1.0 eq.), 3-bromanisole (**108**) (567 mg, 3.00 mmol, 1.0 eq.), $[Pd(PPh_3)_4]$ (175 mg, 0.15 mmol, 5 mol-%) and potassium carbonate (1.26 g, 9.00 mmol, 3.0 eq.) were added. The reaction mixture was stirred under argon at 85°C for 4 h. After cooling down to room temperature, the reaction mixture was filtered over a 3 cm plug of silica gel. The crude was evaporated and adsorbed on silica gel and after purification by column chromatography with silica gel and dichloromethane:*n*-hexane (1:2 → 1:1) the coupling product **109** was isolated as a colorless oil in a yield of 94%.

TLC: R_f = 0.36 (dichloromethane:*n*-hexane 1:2).

^{1}H-NMR (400 MHz, $CDCl_3$): δ = 7.36 (t, ^3J = 8.1 Hz, 2H), 7.19 (dt, ^3J = 8.1 Hz, ^4J = 2.5 Hz, 2H), 7.13 (t, ^4J = 2.5 Hz, 2H), 6.91 (dd, ^3J = 8.1 Hz, ^4J = 2.5 Hz, 2H), 3.87 (s, 3H) ppm.

^{13}C-NMR (101 MHz, $CDCl_3$): δ = 160.3 (s, Cq, 2C), 143.1 (s, Cq, 2C), 130.1 (s, Ct, 2C), 120.1 (s, Ct, 2C), 113.4 (s, Ct, 2C), 113.2 (s, Ct, 2C), 55.7 (s, Cp, 2C) ppm.

MS (EI, m/z): 215.1 (14%), 214.1 (100%) $[M]^+$, 171.1 (17%), 141.1 (6%), 128.1 (11%), 115.1 (5%).

EA: calculated C 78.48, H 6.59, N 0.00; found C 78.55, H 6.85, N 0.00.

1,1'-Biphenyl-3,3'-diol (110)

109 **110**

$C_{12}H_{10}O_2$
186.07 g/mol

The methoxy biphenyl **109** (557 mg, 2.60 mmol, 1.0 eq.) was dissolved under argon at 0°C in dry dichloromethane (20 mL). A 1 M boron tribromide solution in dichloromethane (9.10 mL, 9.10 mmol, 3.5 eq.) was added drop wise over a period of 20 min and the reaction mixture was stirred under argon at 0°C for 3 h. The brown reaction mixture was quenched with water (10 mL) and a 1 M aq. NaOH solution (5 mL). The organic layer was separated, dried over $MgSO_4$ and evaporated to dryness. The brown crude was recrystallized from hot dichloromethane to afford the free alcohol **110** as a white solid in a yield of 90%.

TLC: R_f = 0.33 (dichloromethane with 5% MeOH).

MP: 127-129°C.

^{1}H-NMR (400 MHz, DMSO-d_6): δ = 9.50 (s, 2H), 7.23 (t, ^3J = 7.9 Hz, 2H), 7.00 (d, ^3J = 7.9 Hz, 2H), 6.95 (t, ^4J = 2.0 Hz, 2H), 6.75 (dd, ^3J = 7.9 Hz, ^4J = 2.0 Hz, 2H) ppm.

^{13}C-NMR (101 MHz, DMSO-d_6): δ = 158.6 (s, Cq, 2C), 142.6 (s, Cq, 2C), 130.7 (s, Ct, 2C), 118.2 (s, Ct, 2C), 115.2 (s, Ct, 2C), 114.2 (s, Ct, 2C) ppm.

MS (EI, m/z): 187.1 (12%), 186.1 (100%) $[M]^+$, 157.1 (10%), 128.0 (8%).

EA: calculated C 77.40, H 5.41, N 0.00; found C 77.30, H 5.48, N 0.00.

_S_,_S_'-((4,4'-dimethoxy-[1,1'-biphenyl]-3,3'-diyl)bis(methylene)) diethanethioate (111)

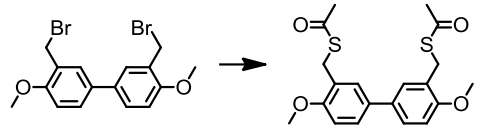

97 **111**

$C_{20}H_{22}O_4S_2$
390.10 g/mol

The biphenyl **97** (240 mg, 0.60 mmol, 1.0 eq.) and potassium thioacetate (224 mg, 1.92 mmol, 3.2 eq.) were dissolved at room temperature in dry DMF (10 mL) and stirred for 2 h. The reaction mixture was evaporated. The remaining crude was dissolved in dichloromethane (50 mL) and washed with water (3 × 30 mL) and with brine (30 mL), dried over $MgSO_4$ and evaporated to dryness. The crude was purified by column chromatography with silica gel and dichloromethane to afford the addition product **111** as a white powder in a yield of 81%.

TLC: R_f = 0.38 (dichloromethane).

MP: 183-185°C.

^{1}H-NMR (400 MHz, $CDCl_3$): δ = 7.49 (d, ^4J = 2.3 Hz, 2H), 7.40 (dd, ^3J = 8.5 Hz, ^4J = 2.3 Hz, 2H), 6.89 (d, ^3J = 8.5 Hz, 2H), 4.18 (s, 4H), 3.87 (s, 6H), 2.33 (s, 6H) ppm.

^{13}C-NMR (101 MHz, $CDCl_3$): δ = 196.1 (s, 2C), 157.0 (s, 2C), 133.5 (s, 2C), 129.3 (s, 2C), 127.3 (s, 2C), 126.5 (s, 2C), 111.2 (s, 2C), 56.1 (s, 2C), 30.8 (s, 2C), 29.0 (s, 2C) ppm.

MS (EI, m/z): 392.1 (12%), 391.1 (23%), 390.1 (100%) $[M]^+$, 316.1 (16%), 315.1 (78%), 285.1 (16%), 271.1 (16%), 211.1 (11%), 210.1 (14%), 165.1 (9%).

EA: calculated C 61.21, H 5.68, N 0.00; found C 61.03, H 5.56, N 0.00.

(4,4'-Dimethoxy-[1,1'-biphenyl]-3,3'-diyl)dimethanethiol (112)

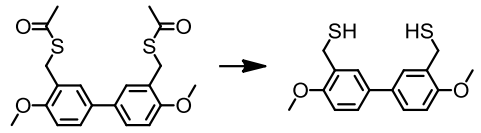

111 **112**

$C_{16}H_{18}O_2S_2$
306.07 g/mol

The protected sulfur **111** (170 mg, 0.44 mmol, 1.0 eq.) was dissolved under argon in dichloromethane (10 mL) and methanol (15 mL) and was degassed with argon at room temperature for 10 min. The reaction mixture was cooled to 0°C and acetyl chloride (0.25 mL, 3.48 mmol, 8.0 eq.) was added drop wise and the reaction mixture was then heated slowly to 35°C and stirred for 5 h. The reaction mixture was then evaporated to dryness (under argon) to give the deprotected sulfur **112** as a white powder in a yield of 94%. The product was used as obtained, for the cyclization reaction, without further purification, due to its strong tendency to form disulfides.

TLC: R_f = 0.84 (dichloromethane).

MP: 99-101°C.

^{1}H-NMR (400 MHz, $CDCl_3$): δ = 7.43 (d, ^4J = 2.3 Hz, 2H), 7.40 (dd, ^3J = 8.4 Hz, ^4J = 2.3 Hz, 2H), 6.92 (d, ^3J = 8.4 Hz, 2H), 3.91 (s, 6H), 3.78 (d, ^3J = 7.9 Hz, 4H), 1.99 (t, ^3J = 7.9 Hz, 2H) ppm.

MS (EI, m/z): 308.1 (11%), 307.1 (19%), 306.1 (100%) $[M]^+$, 274.1 (16%), 273.1 (82%), 243.1 (31%), 210.1 (12%), 120.1 (18%).

4,4'-Dimethoxy-3,3'-bis(3-nitrobenzyl)-1,1'-biphenyl (116)

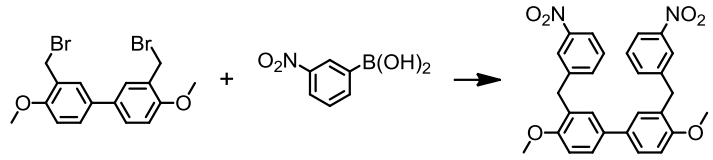

97 **35** **116**

$C_{28}H_{24}N_2O_6$
484.16 g/mol

The bromide **97** (400 mg, 1.00 mmol, 1.0 eq.), potassium carbonate (827 mg, 6.00 mmol, 6.0 eq.) and the boronic acid **35** (584 mg, 3.50 mmol, 3.5 eq.) were dissolved in dry toluene (20 mL) and ethanol (5 mL), the resulting mixture was degassed at room temperature with argon for 15 min. After the addition of $[Pd(PPh_3)_4]$ (58 mg, 50 µmol, 5 mol-%) the reaction mixture was heated under microwave conditions to 85°C for 50 min. The reaction mixture was cooled to room temperature, filtered over a 1 cm plug of silica gel and washed with ethanol. The crude was adsorbed on silica gel and purified by column chromatography with silica gel and toluene affording the desired coupling product **116** as a yellow powder in a yield of 91%.

TLC: R_f = 0.42 (toluene).

MP: 171-173°C.

^{1}H-NMR (400 MHz, $CDCl_3$): δ = 8.12 (t, ^4J = 2.1 Hz, 2H), 8.03 (dd, ^3J = 8.1 Hz, ^4J = 2.1 Hz, 2H), 7.56 (d, ^3J = 8.1 Hz, 2H), 7.42 (t, ^3J = 8.1 Hz, 2H), 7.38 (dd, ^3J = 8.1 Hz, ^4J = 2.1 Hz, 2H), 7.28 (d, ^4J = 2.1 Hz, 2H), 6.93 (d, ^3J = 8.1 Hz, 2H), 4.09 (s, 4H), 3.84 (s, 6H) ppm.

^{13}C-NMR (101 MHz, $CDCl_3$): δ = 156.9 (s, 2C), 148.7 (s, 2C), 143.5 (s, 2C), 135.5 (s, 2C), 133.8 (s, 2C), 129.5 (s, 2C), 129.3 (s, 2C), 128.7 (s, 2C), 126.8 (s, 2C), 124.1 (s, 2C), 121.5 (s, 2C), 111.4 (s, 2C), 55.9 (s, 2C), 36.5 (s, 2C) ppm.

MS (EI, m/z): 486.1 (6%), 485.1 (31%), 484.2 (100%) $[M]^+$, 469.1 (5%), 333.1 (4%).

EA: calculated C 69.41, H 4.99, N 5.78; found C 69.44, H 5.06, N 5.59.

3,3'-Bis(3-nitrobenzyl)-[1,1'-biphenyl]-4,4'-diol (117)

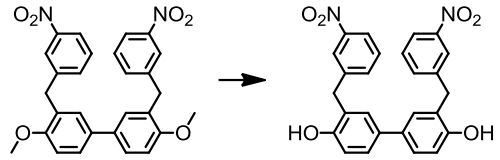

116 **117**

$C_{26}H_{20}N_2O_6$
456.13 g/mol

The methoxy biphenyl **116** (105 mg, 0.22 mmol, 1.0 eq.) was dissolved under argon in dry dichloromethane (15 mL) and cooled to -78°C. A 1 M boron tribromide solution in dichloromethane (0.91 mL, 0.91 mmol, 4.2 eq.) was added slowly to the reaction mixture over a period of 15 min. The reaction mixture was allowed to reach room temperature and was stirred under argon for 4 h and then it was poured into ice water (50 mL) and stirred for 5 min. The resulting mixture was extracted with dichloromethane (4 × 50 mL) and the combined organic layers were washed with a 10% aq. $NaHSO_3$ solution (100 mL), with a 5% aq. HCl solution (100 mL), with water (50 mL) and with brine (50 mL), dried over $MgSO_4$ and evaporated to dryness. The brown crude was adsorbed on silica gel and purified by flash column chromatography with silica gel and dichloromethane with 5% MeOH. The instable deprotected diol **117** was isolated after drying under high vacuum conditions as an amorphous brown solid in a yield of 91% and was directly used in the next step. Even storage under argon and -20°C yielded in decomposition of the product.

TLC: R_f = 0.31 (dichloromethane with 5% MeOH).

MP: 61-62°C.

^{1}H-NMR (400 MHz, $CDCl_3$): δ = 8.14 (t, ^4J = 1.3 Hz, 2H), 8.04 (dd, ^3J = 7.9 Hz, ^4J = 1.3 Hz, 2H), 7.60 (d, ^3J = 7.9 Hz, 2H), 7.42 (t, ^3J = 7.9 Hz, 2H), 7.27 (m, 4H), 6.81 d, ^3J = 7.9 Hz, 2H), 5.14 (br s, 2H), 4.12 (s, 4H) ppm.

MS (EI, m/z): 458.1 (5%), 457.1 (29%), 456.1 (100%) $[M]^+$, 439.1 (5%), 392.1 (4%), 362.2 (5%).

.

3,3'-Bis(3-nitrobenzyl)-[1,1'-biphenyl]-4,4'-diyl bis(trifluoromethanesulfonate) (118)

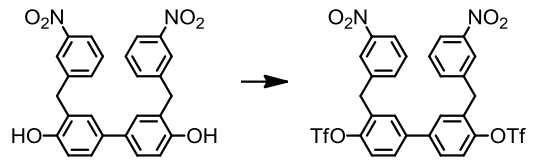

117 **118**

$C_{28}H_{18}F_6N_2O_{10}S_2$
720.03 g/mol

The diol **117** (1.28 g, 2.80 mmol, 1.0 eq.) was dried under high vacuum conditions for 1 h and then dissolved under argon in dry pyridine (35 mL). The reaction mixture was cooled down to 0°C and Tf_2O (1.86 mL, 11.2 mmol, 4.0 eq.) was added over a period of 1h. The yellow reaction mixture was allowed to reach room temperature and was stirred for 1 h. Afterwards the reaction mixture poured into a sat. aq. $NaHCO_3$ solution (200 mL) and stirred for 5 min. The resulting mixture was extracted with dichloromethane (4 × 75 mL) and the combined organic layers were washed with water (50 mL) and brine (50 mL), dried over $MgSO_4$ and evaporated to dryness. The dark crude was purified by column chromatography with silica gel and dichloromethane affording the product **118** as a white solid in a yield of 75%.

TLC: R_f = 0.24 (dichloromethane).

MP: 143-144°C.

^{1}H-NMR (400 MHz, $CDCl_3$): δ = 8.12 (dt, ^3J = 8.3 Hz, ^4J = 2.2 Hz, 2H), 8.04 (s, 2H), 7.53 (m, 4H), 7.47 (dd, ^3J = 8.3 Hz, ^4J = 2.2 Hz, 2H), 7.40 (d, ^3J = 8.3 Hz, 2H), 7.30 (d, ^4J = 2.2 Hz, 2H), 4.23 (s, 4H) ppm.

^{19}F-NMR (376 MHz, $CDCl_3$): δ = -74.7 (s, 6F) ppm.

^{13}C-NMR (101 MHz, $CDCl_3$): δ = 149.0 (s, 2C), 148.1 (s, 2C), 140.4 (d, J = 20.9 Hz, 2C), 135.5 (s, 2C), 133.5 (s, 2C), 130.2 (s, 2C), 128.2 (s, 2C), 124.1 (s, 2C), 122.8 (s, 2C), 122.5 (s, 2C), 121.5 (s, 2C), 120.4 (s, 2C), 117.4 (d, J = 234.5 Hz, 2C), 36.1 (s, 2C) ppm.

MS (EI, m/z): 720.1 (13%), 720.0 (57%) $[M]^+$, 587.9 (34%), 586.9 (100%).

EA: calculated C 46.37, H 2.52, N 3.89; found C 46.05., H 2.54, N 4.15.

3,3'-((4,4'-Dimethoxy-[1,1'-biphenyl]-3,3'-diyl)bis(methylene))dianiline (122)

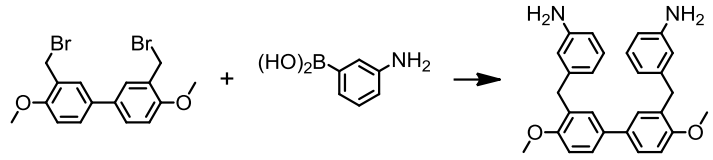

97 **72** **122**

$C_{28}H_{28}N_2O_2$
424.22 g/mol

The bromide **97** (80.0 mg, 199 µmol, 1.0 eq.), potassium carbonate (166 mg, 1.99 mmol, 6.0 eq.) and the boronic acid **35** (102 mg, 657 µmol, 3.3 eq.) were dissolved in dry toluene (10 mL) and ethanol (5 mL), the resulting mixture was degassed at room temperature with argon for 15 min. After the addition of $[Pd(PPh_3)_4]$ (11.5 mg, 9.85 µmol, 5 mol-%) the reaction mixture was heated under microwave conditions to 85°C for 45 min. The reaction mixture was cooled to room temperature, filtered over a 1 cm plug of *Celite*® and washed with ethanol. The crude was adsorbed on silica gel and purified by column chromatography with silica gel and dichloromethane with 1.5% MeOH affording the desired coupling product **122** as a beige solid in a yield of 92%. The product turned out to be very instable and was stored under argon at -20°C.

TLC: R_f = 0.30 (dichloromethane with 2% MeOH).

MP: 39-41°C.

^{1}H-NMR (400 MHz, $CDCl_3$): δ = 7.38 (dd, ^3J = 8.4 Hz, ^4J = 2.4 Hz, 2H), 7.31 (d, ^4J = 2.4 Hz, 2H), 7.10 (t, ^3J = 8.4 Hz, 2H), 6.92 (d, ^3J = 8.4 Hz, 2H), 6.71 (dt, ^3J = 8.4 Hz, ^4J = 2.4 Hz, 2H), 6.57 (t, ^4J = 2.4 Hz, 2H), 6.53 (dd, ^3J = 8.4 Hz, ^4J = 2.4 Hz, 2H), 3.97 (s, 4H), 3.85 (s, 6H), 3.57 (br s, 4H) ppm.

^{13}C-NMR (101 MHz, $CDCl_3$): δ = 157.0 (s, 2C), 146.8 (s, 2C), 142.7 (s, 2C), 133.8 (s, 2C), 130.2 (s, 2C), 129.6 (s, 2C), 129.5 (s, 2C), 126.0 (s, 2C), 119.9 (s, 2C), 116.2 (s, 2C), 113.3 (s, 2C), 111.2 (s, 2C), 56.0 (s, 2C), 36.3 (s, 2C) ppm.

MS (EI, m/z): 426.3 (5%), 425.2 (32%), 424.2 (100%) $[M]^+$,106.1 (23%).

3,3'-Bis(3-aminobenzyl)-[1,1'-biphenyl]-4,4'-diyl-bis-(trifluoromethane-sulfonate) (123)

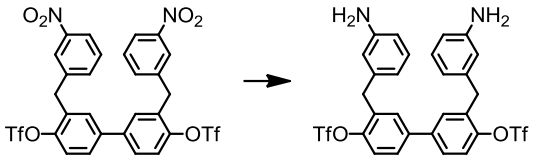

118 **123**

$C_{28}H_{22}F_6N_2O_6S_2$
660.08 g/mol

The nitro biphenyl **118** (530 mg, 0.74 mmol, 1.0 eq.) and palladium on activated carbon (78 mg, 73.6 µmol, 10 mol-%) were suspended in dry dichloromethane (50 mL) and ethanol (10 mL). The reaction mixture was hydrogenated with three hydrogen balloons at room temperature for 17 h while stirring vigorously. The hydrogen balloons were renewed after 5 h. The reaction mixture was filtered over a 3 cm plug of *Celite*® and evaporated to dryness. The crude was purified by column chromatography with silica gel and dichloromethane (containing 1.5% NEt_3 and 1% MeOH), affording the reduced product **123** after drying under high vacuum conditions as a pale yellow oil in a yield of 98%. The product was very instable even when storing under argon at -20°C.

TLC: R_f = 0.33 (dichloromethane with 1.5% NEt_3 and 1% MeOH).

^{1}H-NMR (400 MHz, $CDCl_3$): δ = 7.36 (dd, ^3J = 8.3 Hz, ^4J = 2.1 Hz, 2H), 7.32 (s, 2H), 7.29 (d, ^4J = 2.1 Hz, 2H), 7.10 (t, ^3J = 8.3 Hz, 2H), 6.59 (m, 4H), 6.52 (t, ^4J = 2.1 Hz, 2H), 4.00 (s, 4H) ppm.

^{19}F-NMR (376 MHz, $CDCl_3$): δ = -74.8 (s, 6F) ppm.

^{13}C-NMR (101 MHz, $CDCl_3$): δ = 148.1 (s, 2C), 146.7 (s, 2C), 140.1 (d, J = 20.5 Hz, 2C), 129.8 (s, 2C), 135.0 (s, 2C), 131.02 (s, 2C), 127.2 (s, 2C), 122.2 (s, 2C), 120.6 (s, 2C), 120.1 (s, 2C), 116.3 (s, 2C), 114.2 (s, 2C), 112.4 (d, J = 233.7 Hz, 2C), 36.2 (s, 2C) ppm.

MS (EI, m/z): 663.1 (3%), 662.1 (14%), 661.2 (31%), 660.1 (100%) $[M]^+$, 527.2 (18%), 512.2 (13%), 394.2 (78%), 393.2 (95%), 197.1 (26%), 196.1 (17%), 106.1 (21%).

Biphenyl urea macrocycle 124

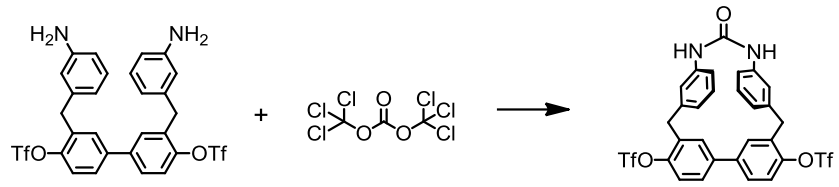

123 **89** **124**

$C_{29}H_{20}F_6N_2O_7S_2$
686.06 g/mol

The diamino compound **123** (170 mg, 257 µmol, 1.0 eq.) and DMAP (34.0 mg, 283 µmol. 1.1 eq.) were dissolved under argon at room temperature in dry dichloromethane (200 mL). Bis(trichloromethyl)carbonat **89** (23.0 mg, 77.0 µmol, 0.3 eq.) dissolved in dry dichloromethane (5 mL) was added drop wise over a period of 30 min to the reaction mixture. The resulting mixture was stirred for 18 h and was then diluted with dichloromethane (50 mL) and quenched with water (50 mL), to be sure that all triphosgene has been quenched the reaction mixture was stirred at room temperature for 30 min. The organic phase was separated and washed with a 1 M aq. NaOH solution (70 mL), with water (50 mL) and with brine (50 mL), dried over $MgSO_4$ and evaporated to dryness. The crude was adsorbed on silica gel and purified by column chromatography with ethyl acetate:*n*-hexane (1:1, containing 5% NEt_3) affording the cyclized product **124** after drying under high vacuum conditions as a beige solid in a yield of 10%.

TLC: R_f = 0.29 (ethyl acetate:*n*-hexane 1:1, containing 5% NEt_3).

MP: 57-59°C

^{1}H-NMR (400 MHz, $CDCl_3$): δ = 7.60 (d, ^3J = 8.0 Hz, 2H), 7.38 (m, 6H), 7.17 (d, ^4J = 2.0 Hz, 2H), 7.08 (d, ^3J = 8.0 Hz, 2H), 6.91 (t, ^4J = 2.0 Hz, 2H), 6.41 (s, 2H), 4.11 (s, 4H) ppm.

^{19}F-NMR (376 MHz, $CDCl_3$): δ = -74.6 (s, 6F) ppm.

^{13}C-NMR (101 MHz, $CDCl_3$): δ = 228.5 (s, 1C), 154.0 (s, 2C), 147.8 (s, 2C), 140.5 (s, 2C), 138.4 (s, 2C), 134.0 (s, 2C), 131.2 (s, 2C), 131.0 (s, 2C), 127.4 (s, 2C), 127.0 (s, 2C), 122.6 (s, 2C), 120.6 (s, 2C) ppm. The carbons which coupled with fluorine were not observed, due to the low intensities.

MS (EI, m/z): 689.0 (3%), 688.0 (14%), 687.0 (33%), 686.0 (100%) $[M]^+$, 555.1 (3%), 554.1 (10%), 553.0 (30%), 539.0 (6%), 538.1 (20%), 422.1 (4%), 421.1 (20%), 420.1 (64%), 405.1 (12%), 403.1 (13%), 210.1 (10%), 132.0 (5%), 106.1 (10%).

EA: calculated C 51.65, H 3.73, N 6.14; found C 51.69, H 3.63, N 4.04. The impurities derive from the eluent during the column chromatography (0.55% ethyl acetate and 0.25% NEt_3).[318] Even under high vacuum conditions it was not possible to remove the solvents.

Biphenyl azo macrocycle 126

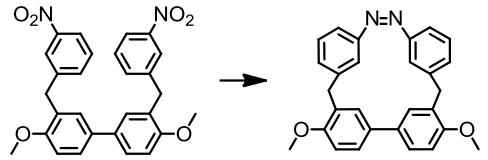

116 **125**

$C_{28}H_{24}N_2O_2$
420.18 g/mol

The nitro compound **116** (113 mg, 0.23 mmol, 1.0 eq.) was dissolved under argon at room temperature in dry THF (1000 mL, dried over K, Na). A 1 M lithium aluminium hydride solution in THF (1.4 mL, 1.40 mmol, 6.0 eq.) was added drop wise over a period of 20 min. The resulting mixture was stirred under argon at room temperature for 1 h and then at 40°C for 16 h. The reaction mixture was cooled down to room temperature, quenched with water (200 mL), diluted with dichloromethane (300 mL) and extracted with dichloromethane (2 × 100 mL). The combined organic layers were washed with brine (150 mL), dried over $MgSO_4$ and evaporated to dryness. The dark yellow crude was purified by a sequence of preparative TLCs. (First: 2.0 mm silica gel and dichloromethane; second: 0.5 mm silica gel and dichloromethane:cyclohexane 2:1; third: 0.5 mm silica gel and dichloromethane:*n*-hexane 2:1; fourth: 0.5 mm silica gel and TBME:cyclohexane 1:3). The desired cyclized azo compound **125** was isolated as a dark yellow solid in a *cis*/*trans* mixture in a yield of 2%.

TLC (Isomer A): R_f = 0.72 (dichloromethane).

MP: 141-142°C.

^{1}H-NMR (Isomer A, 500 MHz, $CDCl_3$): δ = 7.60 (d, ^3J = 8.3 Hz, 2H), 7.51 (s, 2H), 7.38 (t, ^3J = 8.3 Hz, 2H), 7.35 (m, 2H), 7.21 (m, 4H), 6.83 (m, 2H), 4.12 (s, 4H), 3.84 (s, 6H) ppm.

^{1}H-NMR (Isomer B, 500 MHz, $CDCl_3$): δ = 7.31 (dd, ^3J = 8.4 Hz, ^4J = 2.1 Hz, 2H), 7.22 (m, 2H), 6.99 (d, ^3J = 8.4 Hz, 2H), 6.86 (t, ^3J = 8.4 Hz, 2H), 6.83 (m, 2H), 6.74 (d, ^3J = 8.4 Hz, 2H), 6.61 (d, ^4J = 2.1 Hz, 2H), 3.97 (s, 4H), 3.88 (s, 6H) ppm.

^{13}C-NMR (Isomer A, 126 MHz, $CDCl_3$, clear determination by HMBC and HMQC): δ = 156.8 (s, Cq, 2C), 156.2 (s, Cq, 2C), 141.8 (s, Cq, 2C), 129.0 (s, Ct, 2C), 128.9 (s, Ct, 2C), 128.6 (s, Cq, 2C), 128.5 (s, Ct, 2C), 123.7 (s, Ct, 2C), 119.9 (s, Cq, 2C), 119.7 (s, Ct, 2C), 118.2 (s, Ct, 2C), 110.3 (s, Ct, 2C), 55.8 (s, Cp, 2C), 34.3 (s, Cs, 2C) ppm.

^{13}C-NMR (Isomer B, 126 MHz, $CDCl_3$, clear determination by HMBC and HMQC): δ = 156.6 (s, Cq, 2C), 155.2 (s, Cq, 2C), 140.7 (s, Cq, 2C), 130.6 (s, Ct, 2C), 129.4 (s, Ct, 2C), 128.9 (s, Ct, 2C), 128.6 (s, Cq, 2C), 128.5 (s, Ct, 2C), 128.4 (s, Cq, 2C), 126.9 (s, Ct, 2C), 118.4 (s, Ct, 2C), 118.2 (s, Ct, 2C), 55.9 (s, Cp, 2C), 33.2 (s, Cs, 2C) ppm.

UV (λ, nm): 230 (λ_{max}), 321, 465.

GPC (retention time, 0.5 mL/min): 34.6 min, area (99.2%).

MS (MALDI-TOF, m/z): 422.2 (37%), 421.2 (80%), 420.2 (100%) $[M]^+$.

7 Abbreviations

µ	micro
Ac	acetyl
AFM	atomic force microscopy
AIBN	2,2-azobis(2-methylpropionitrile)
aq.	aqueous
BiEDOT	2,2’-bis(3,4-ethylenedioxythiophene)
BINAP	2,2'-bis(diphenylphosphino)-1,1'-binaphthyl
Boc	*tert*-butyloxycarbonyl
br	broad
brine	saturated aqueous NaCl solution
BuLi	butyl lithium
CA	contact angle
CMOS	complementary metal oxide semiconductor
conc	concentrated
COSY	correlation spectroscopy
Cp	primary carbon
Cq	quaternary carbon
Cs	secondary carbon
Ct	tertiary carbon
CV	cyclovoltammetry
d	duplet
dba	dibenzylideneacetone
DCM	dichloromethane
decomp.	decomposition
DIEA	diisopropylethylamine
DIPA	diisopropylamine
DMAP	4-dimethylaminopyridine
DMF	*N,N*-dimethylformamide
DMI	*N,N*-dimethyl imidazolidinone
DMSO	dimethylsulfoxide
dppf	diphenylphosphinoferrocene
EA	elemental analysis

EDOT	ethyldioxythiophene
EI	electron impact
eq.	equivalent
ESI	electron spray ionization
Et	ethyl
EtOAc	ethyl acetate
EtOH	ethanol
FAB	fast atom bombardment
Fc	ferrocene
FTIR	fourier transform infrared spectroscopy
GPC	gel permeation chromatography
h	hours
hept	heptet
HMBC	heteronuclear multiple bond coherence
HMQC	heteronuclear multiple quantum coherence
HOPG	highly oriented pyrolytic graphite
HOPG	highly-ordered-pyrolytic-graphite
HPLC	high performance liquid chromatography
hv	light
IR	infrared spectroscopy
K	kelvin
LB	Langmuir-Blodgett films
LC	liquid chromatography
LDA	lithium diisopropylamine
m	multiplet
M	molar
m	milli
m/z	mass per charge
MALDI	matrix-assisted laser desorption ionization
Me	methyl
MeOH	methanol
min	minute
mL	milliliter
MP	melting point

MS	mass spectrometry
MW	microwave
n	nano
NaO^{t}bu	sodium *tert* butoxide
NBS	*N*-bromosuccinimide
n-BuLi	*n*-buthyl lithium
NMR	nuclear magnetic resonance
NOESY	nuclear Overhauser effect spectroscopy
OP	oligophenylene
OPE	oligo(phenylene ethynylene)
OPV	oligo(phenylene vinylene)
OTf	triflate
PG	protection group
Ph	phenyl
ppm	parts per million
Prep	preparative
PSS	photostationary state
py	pyridine
q	quartet
quant.	quantitative
R_f	retention factor
RM	reaction mixture
RT	room temperature
s	singlet
SAM	self assembled monolayers
sat	saturated
SEC	size exclusion chromatography
SECM	scanning electrochemical microscopy
SEM	scanning electron microscopy
SERS	surface-enhanced Raman scattering
sext	sextet
STM	scanning tunneling microscopy
STS	scanning tunneling spectroscopy
t	triplet

$TBABF_4$	terbutylammonium tetrafluoroborate
TBAF	tetra-n-butylammonium fluoride
TBAOH	tetrabutylammonium hydroxid
TBME	tert-butyl methyl ether
^{t}Bu	*tert*-butyl
Tf_2O	trifluoromethanesulfonic anhydride
TFA	trifluoroacetic acid
THF	tetrahydrofuran
TIPS	tri-*iso*-propylsilyl
TLC	thin layer chromatography
TMEDA	*N,N,N′,N′*-tetramethylenediamine
TMS	trimethylsilyl
TMS	tetramethylsilane
TOCSY	totally correlated spectroscopy
TOF	time of flight
triphosgene	bis(trichloromethyl) carbonate
Trt	trityl
UV	ultra violet
UV/Vis	ultraviolet and visible
v/v	volume per volume
vdW	van der Waals
Vis	visible
VPO	vapor pressure osmometry
W	watt
XPS	X-ray photoelectron spectroscopy
ε	extinction coefficient
Φ	quantum yield

8 Appendix

8.1 Contributions and Collaborations

All molecules were synthesized and characterized by Marcel Müri. The discussed measurements were performed and analyzed be Marcel Müri except: All UV/Vis investigations in section 2 Azo Macrocycles and section 4 Switchable Conducting Azo Biphenyls were performed by Dr. Klaus C. Schuermann (in the group of Prof. Dr. Luisa De Cola). The CV measurements in section 3 Platinum Electrode Modification with the corresponding calculations of consumed electrons were partially performed by Dr. Yann Leroux. The XPS and AFM measurements in section 3 Platinum Electrode Modification were done in collaboration with the IBM Research Center in Rüschlikon by Dr. Bernd Gotsmann (in the group of Dr. Heike Riel).

8.2 Further Synthetic Achievements

Within this PhD thesis some further target compounds were synthesized and characterized, but not further discussed. These compounds are listed in **Figure 76**.

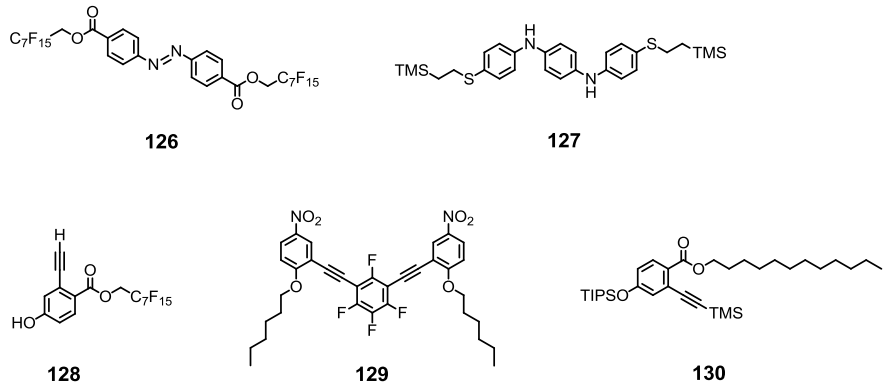

Figure 76 Synthesized and characterized but not discussed target structures **126**-**130**.

The details of the synthesis and characterization of the fluorinated azobenzene **126** can be found in the papers which were done in collaboration with the group of Prof. Dr. Markus Arndt in Vienna.[319][320]

The details of the VPO measurements of shape persistent macrocycles comprising perfluorinated benzene units can be found in the corresponding paper.[321]

8.3 Spectra of Target structures

In the following the NMR spectra of the described target macrocycles **1**-**7**, of the biphenyl macrocycle **125** and of the key intermediate **116** are shown.

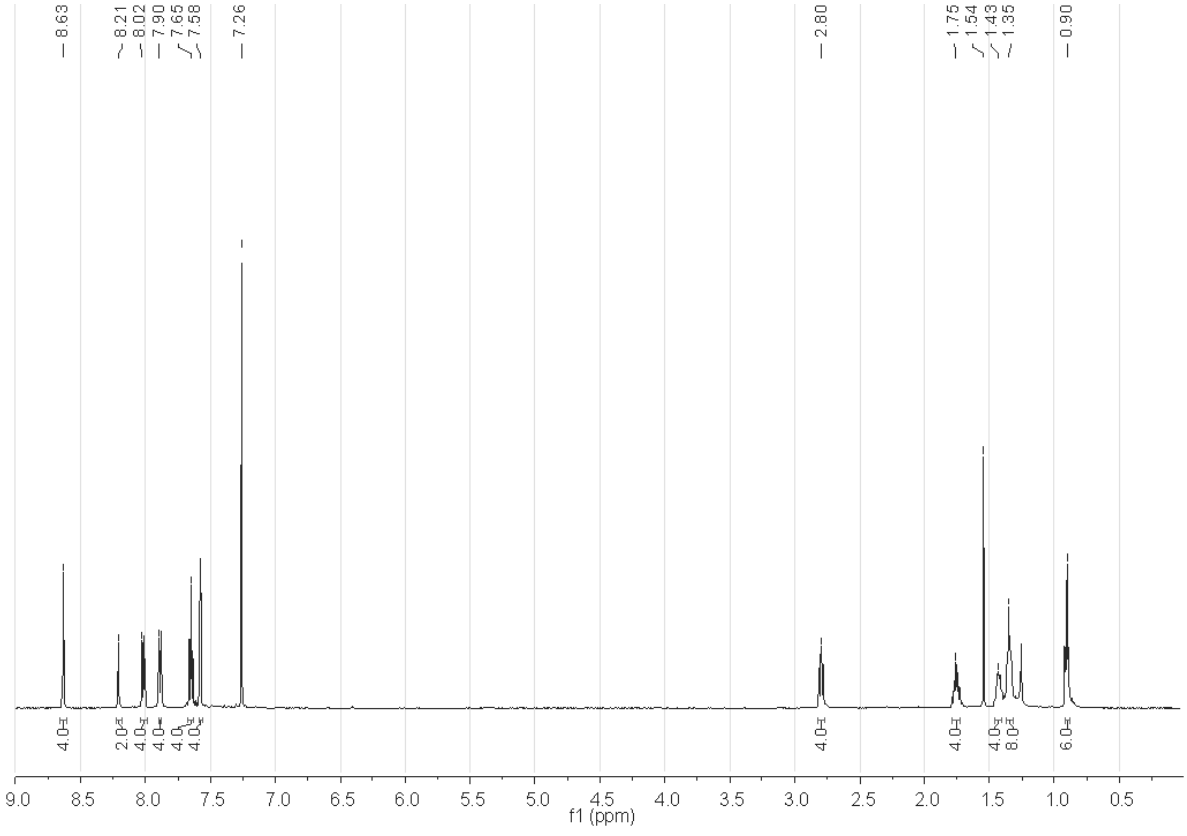

Figure 77 ^{1}H-NMR spectrum of target macrocycle **1**. Measured at RT in $CDCl_3$ with 128 scans and 400 MHz.

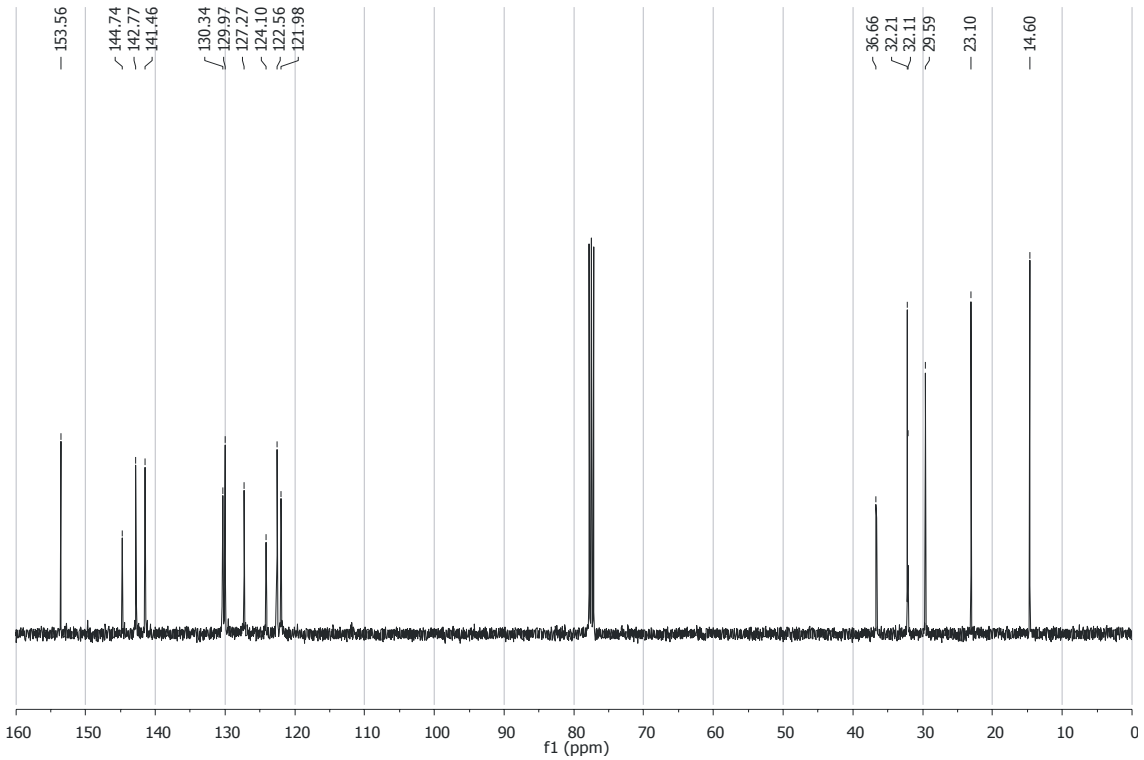

Figure 78 ^{13}C-NMR spectrum of target macrocycle **1**. Measured at RT in $CDCl_3$ with 512 scans and 101 MHz.

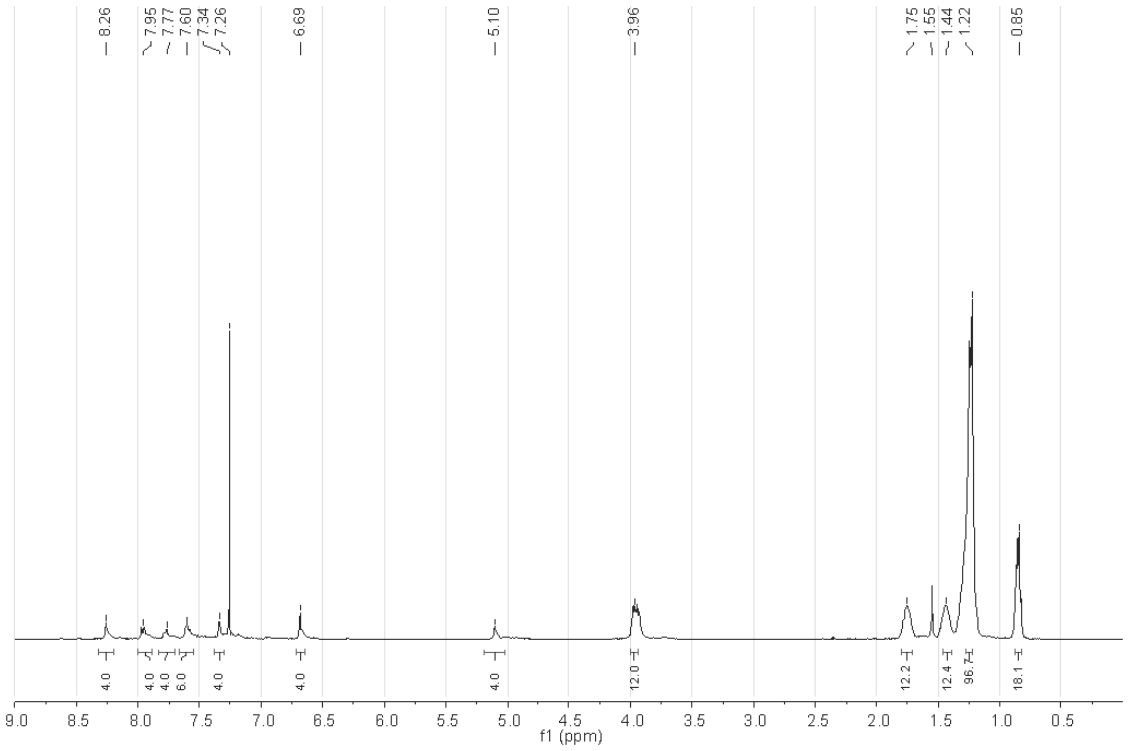

Figure 79 ^{1}H-NMR spectrum of target macrocycle **2**. Measured at RT in $CDCl_3$ with 128 scans and 400 MHz.

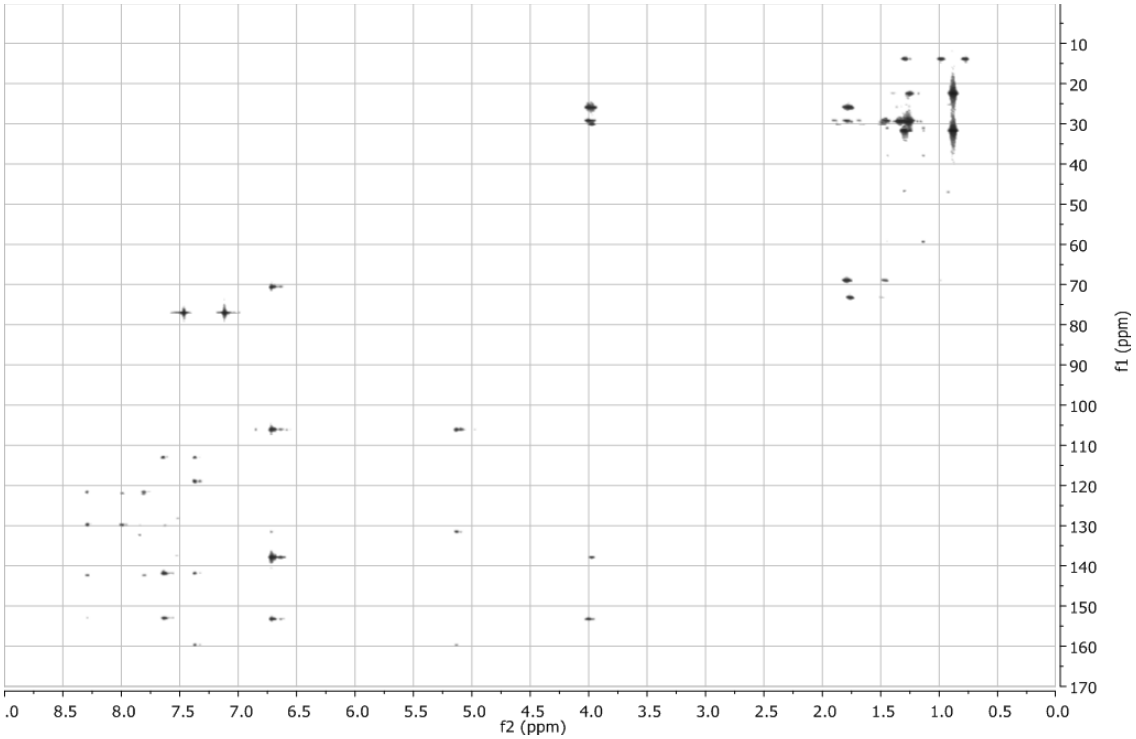

Figure 80 HMBC spectrum of target macrocycle **2**. Measured at RT in $CDCl_3$.

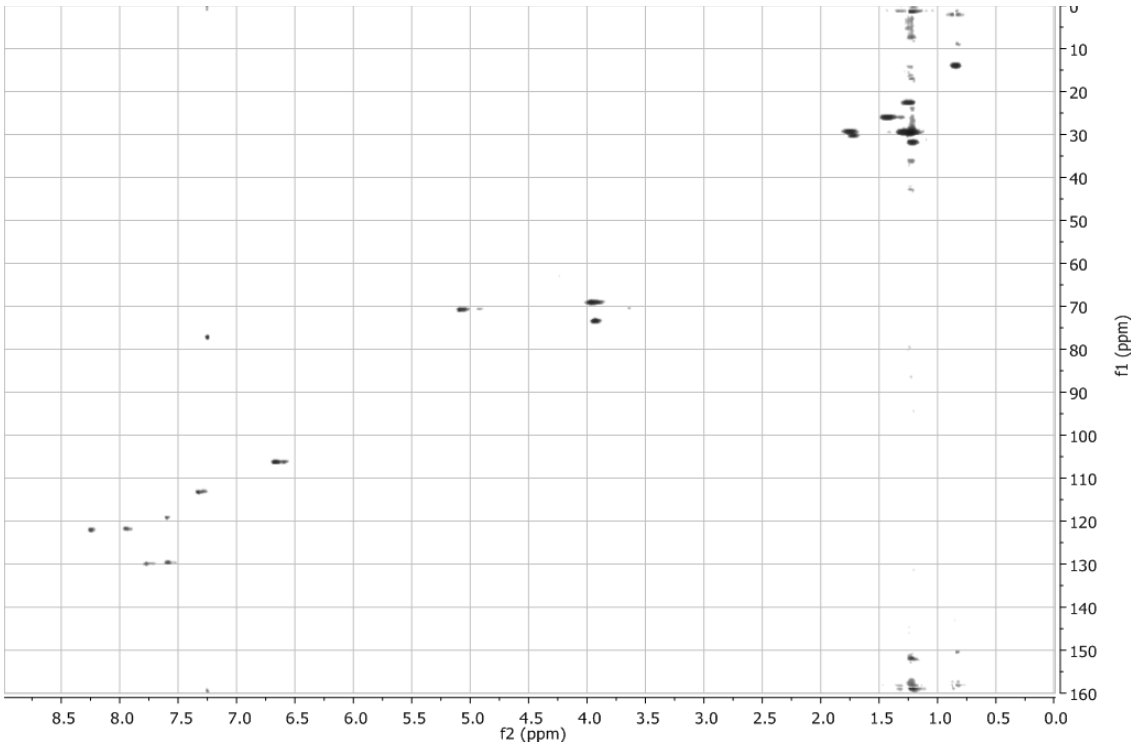

Figure 81 HMQC spectrum of target macrocycle **2**. Measured at RT in $CDCl_3$.

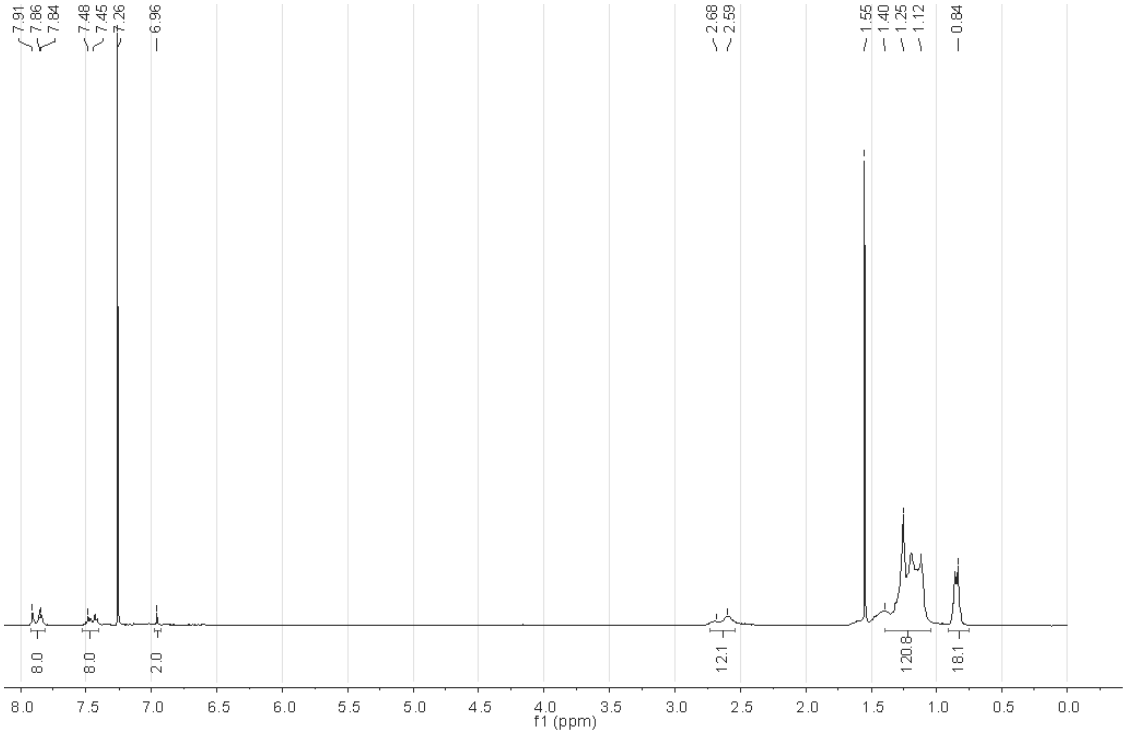

Figure 82 ^{1}H-NMR spectrum of target macrocycle **3**. Measured at RT in $CDCl_3$ with 128 scans and 400 MHz.

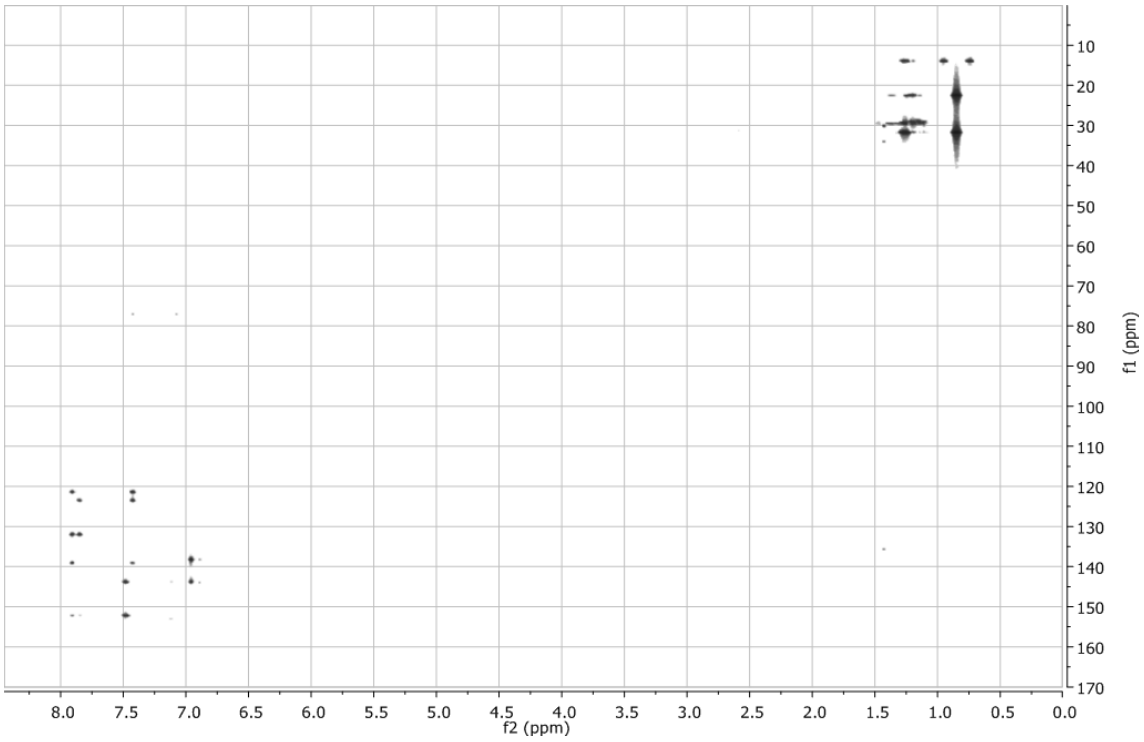

Figure 83 HMBC spectrum of target macrocycle **3**. Measured at RT in $CDCl_3$.

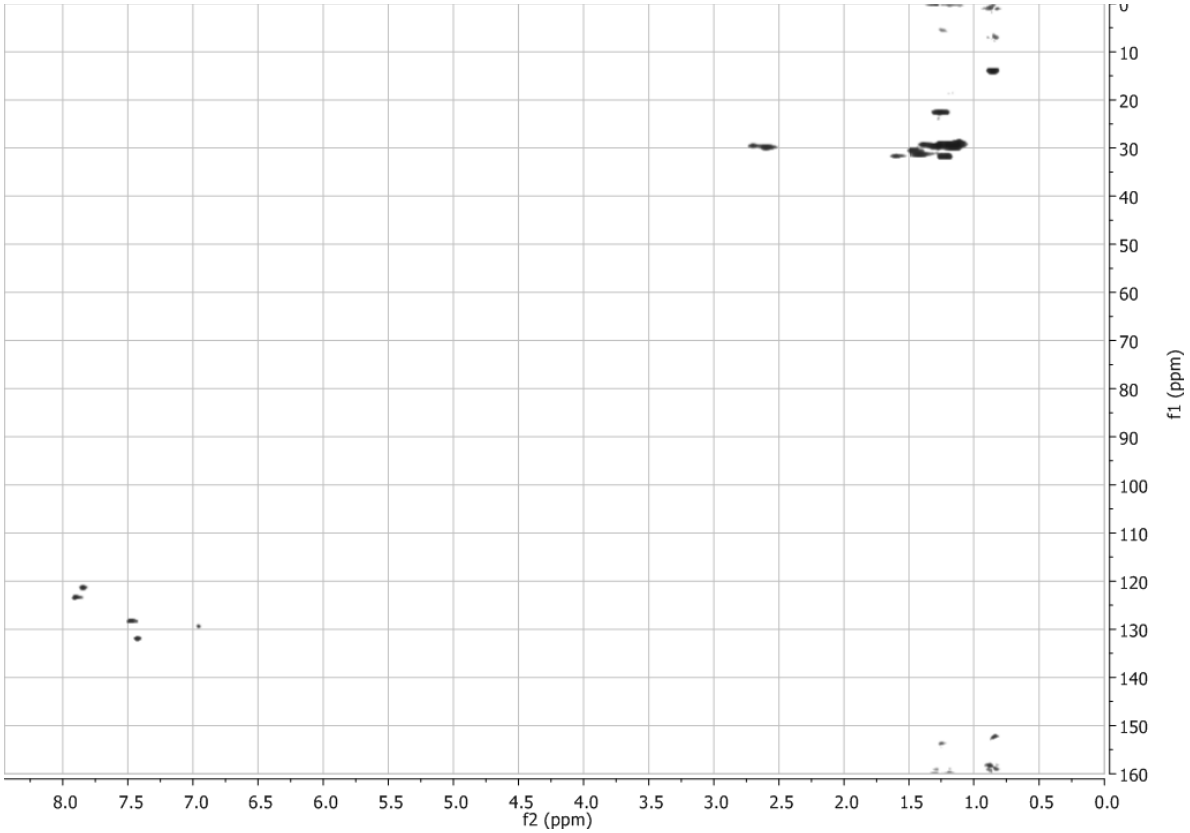

Figure 84 HMQC spectrum of target macrocycle **3**. Measured at RT in $CDCl_3$.

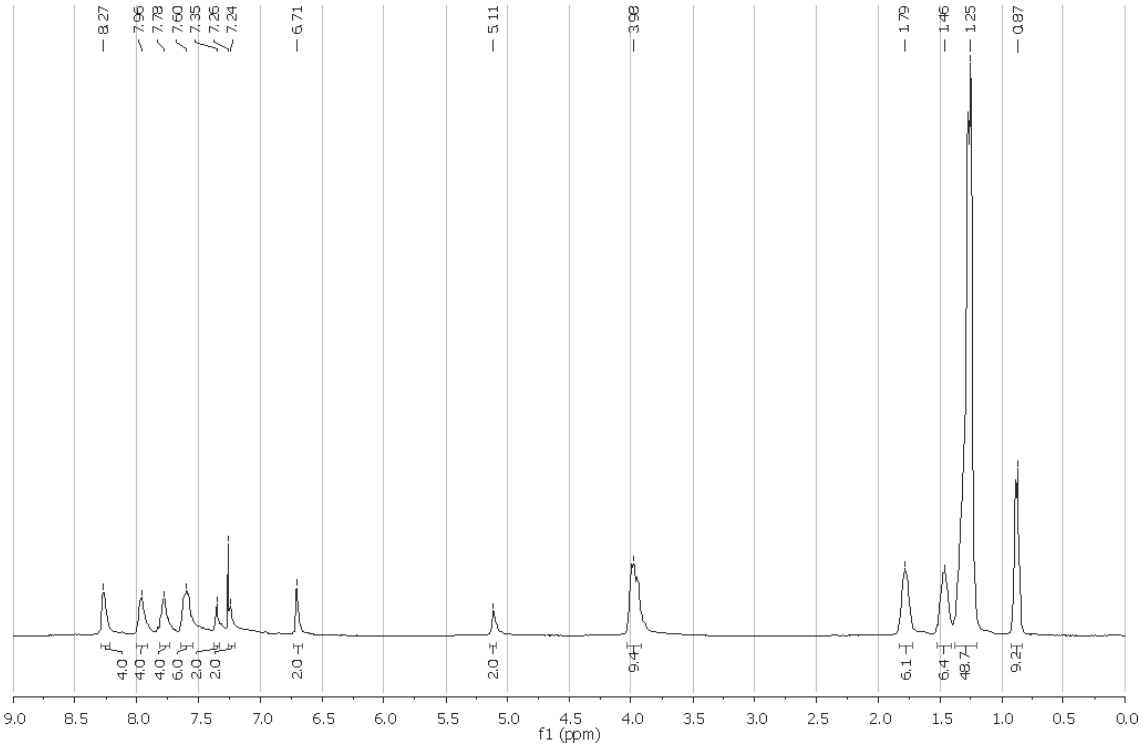

Figure 85 ^{1}H-NMR spectrum of target macrocycle **4**. Measured at RT in $CDCl_3$ with 128 scans and 400 MHz.

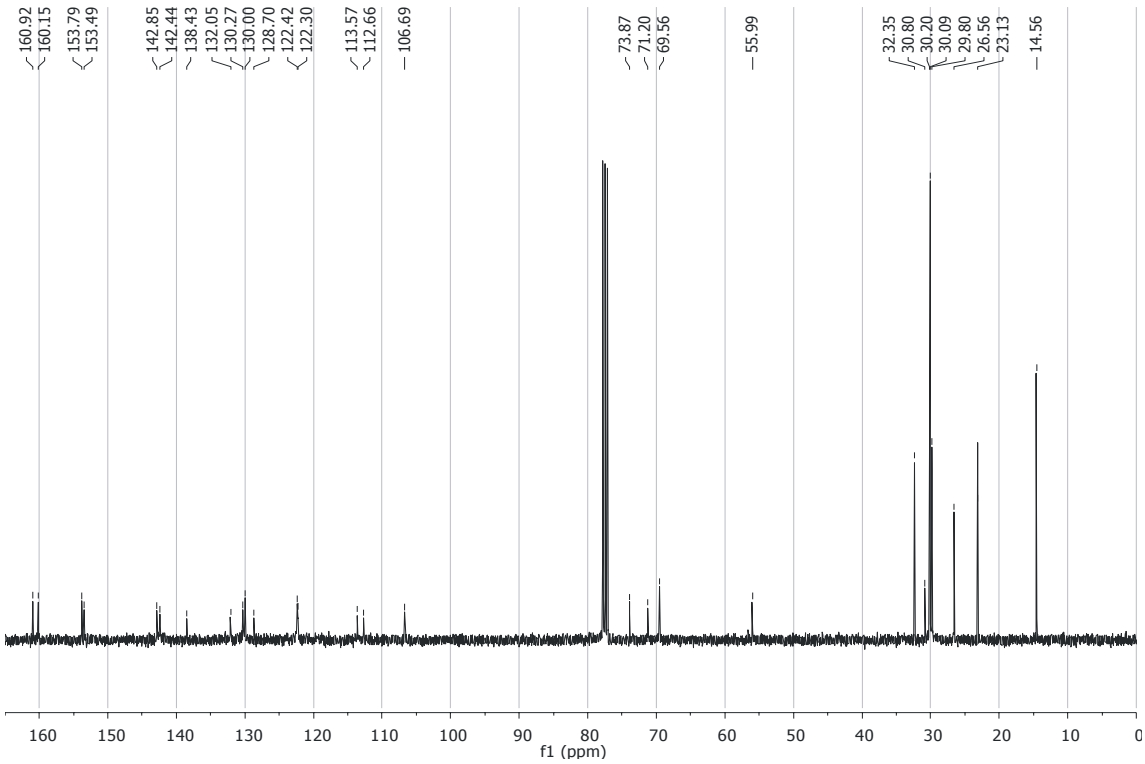

Figure 86 ^{13}C-NMR spectrum of target macrocycle **4**. Measured at RT in $CDCl_3$ with 512 scans and 101 MHz.

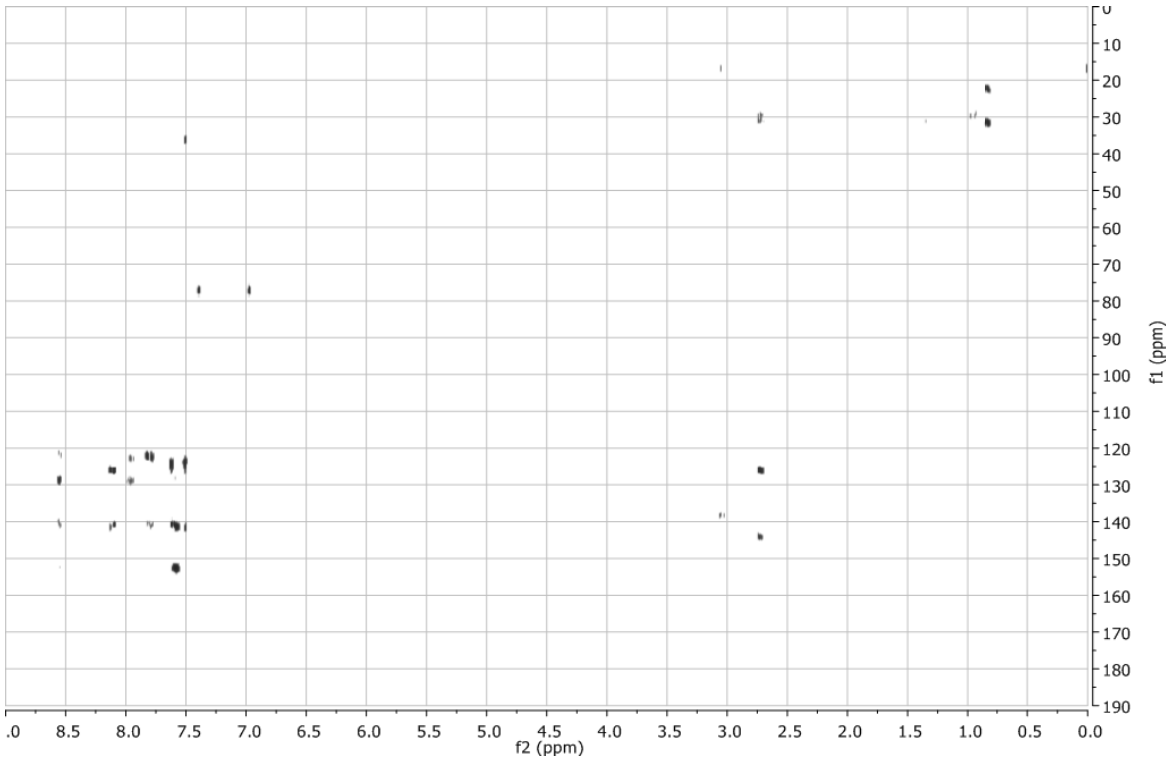

Figure 87 HMBC spectrum of target macrocycle **5**. Measured at RT in $CDCl_3$.

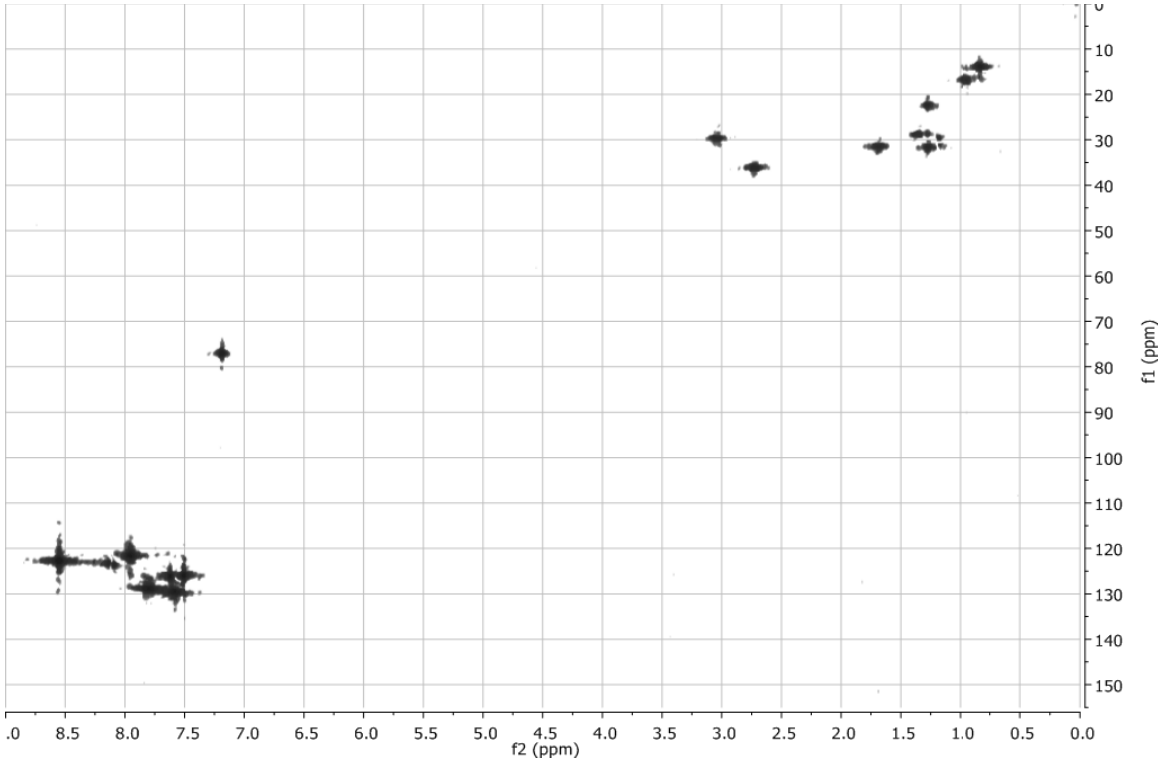

Figure 88 HMQC spectrum of target macrocycle **5**. Measured at RT in $CDCl_3$.

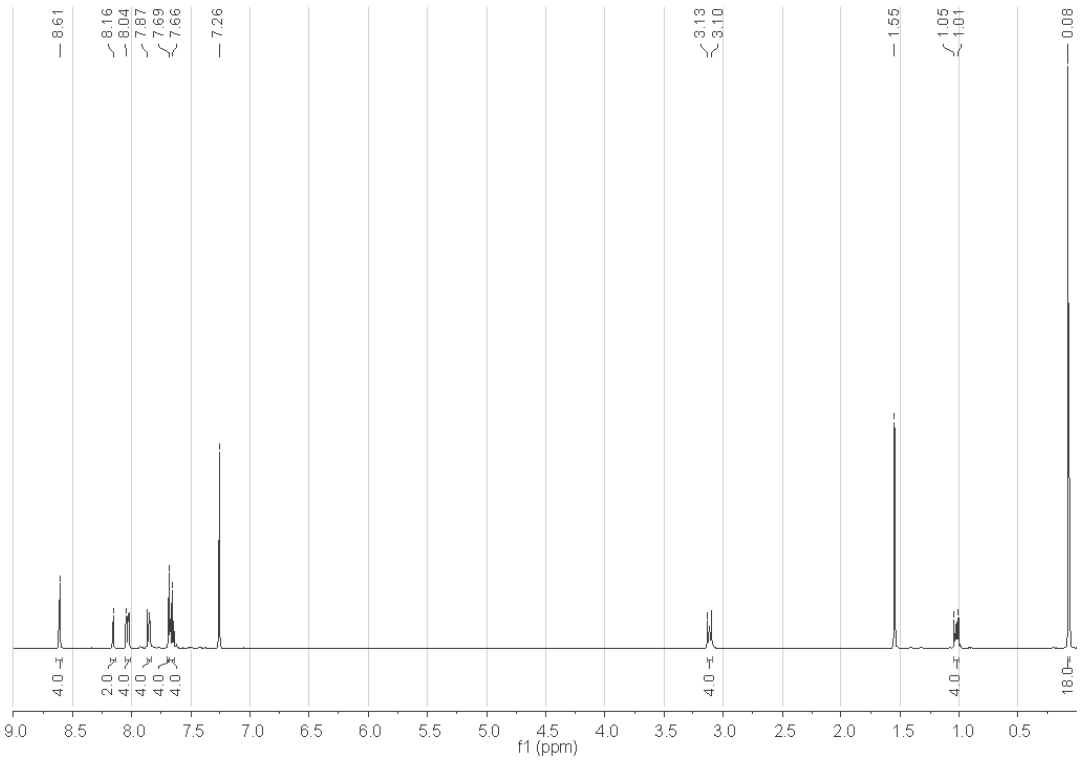

Figure 89 ^{1}H-NMR spectrum of target macrocycle **6**. Measured at RT in $CDCl_3$ with 128 scans and 500 MHz.

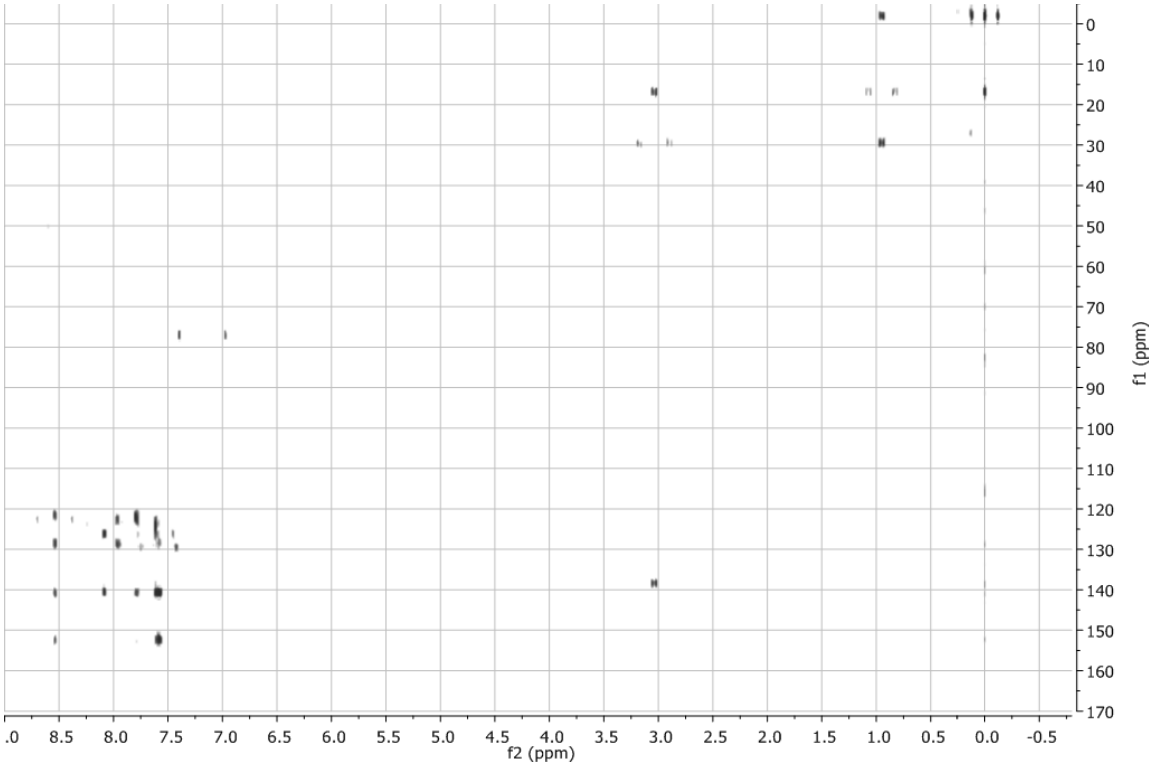

Figure 90 HMBC spectrum of target macrocycle **6**. Measured at RT in $CDCl_3$.

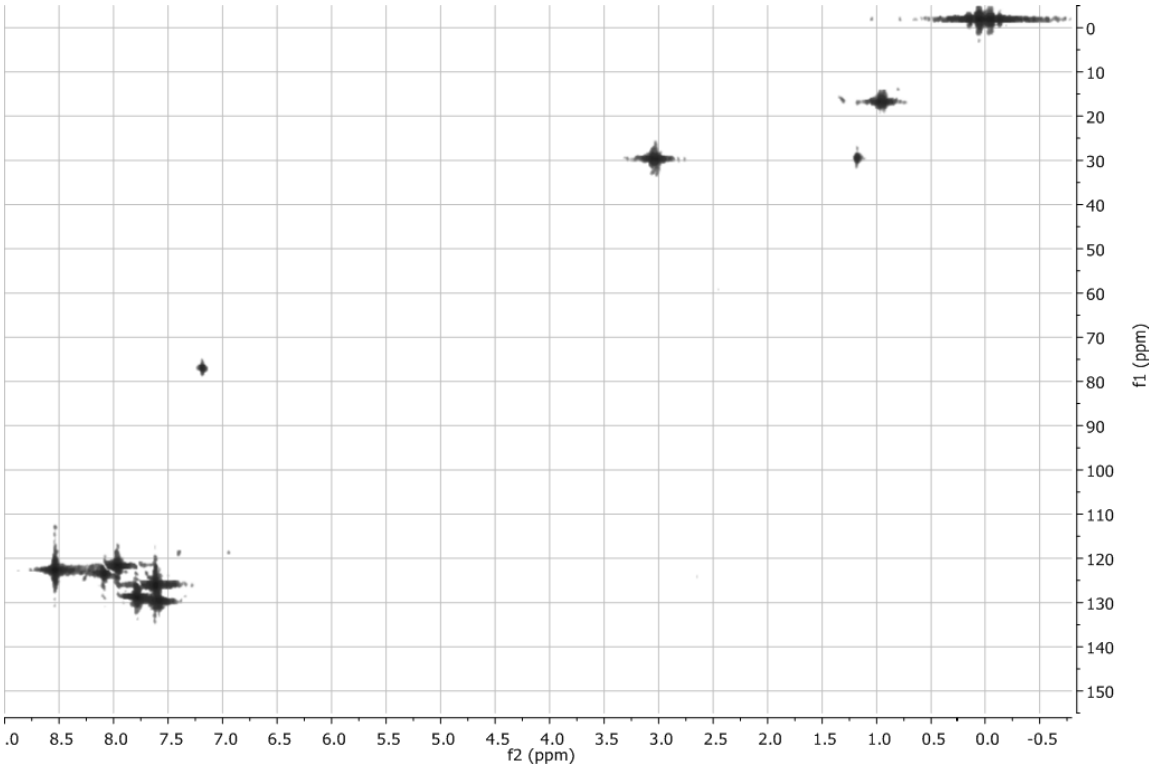

Figure 91 HMQC spectrum of target macrocycle **6**. Measured at RT in $CDCl_3$.

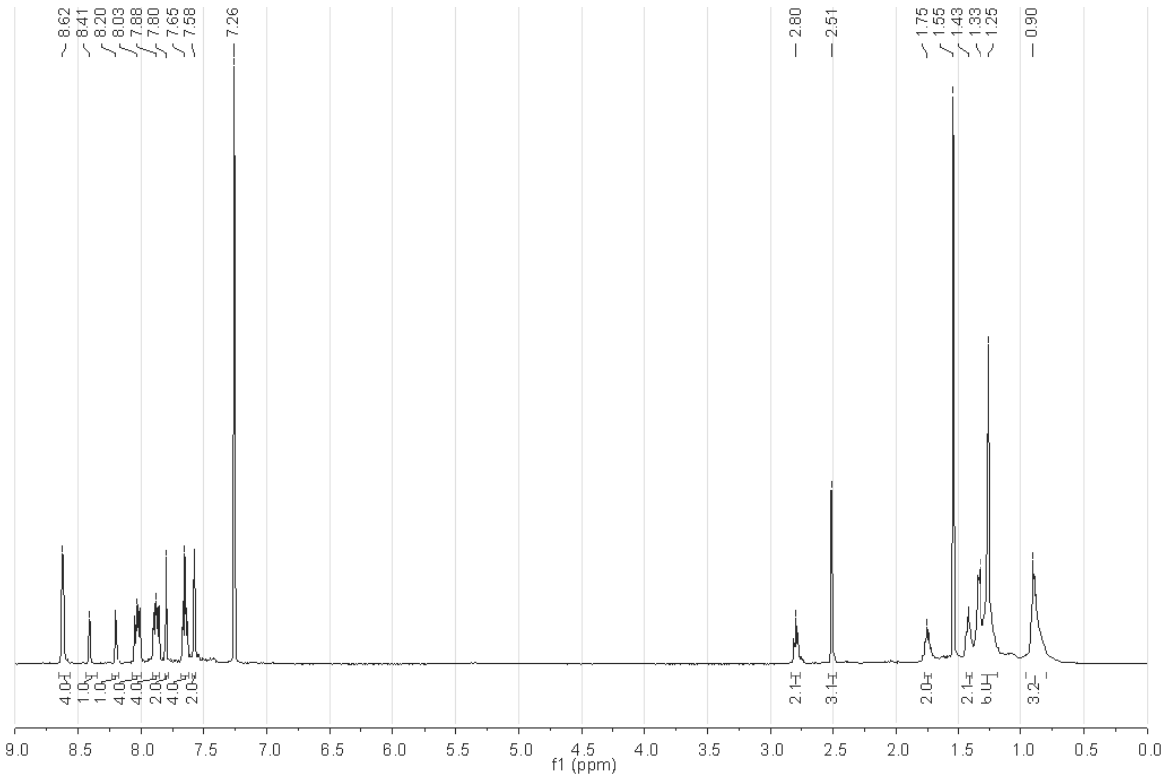

Figure 92 ^{1}H-NMR spectrum of target macrocycle **7**. Measured at RT in $CDCl_3$ with 128 scans and 500 MHz.

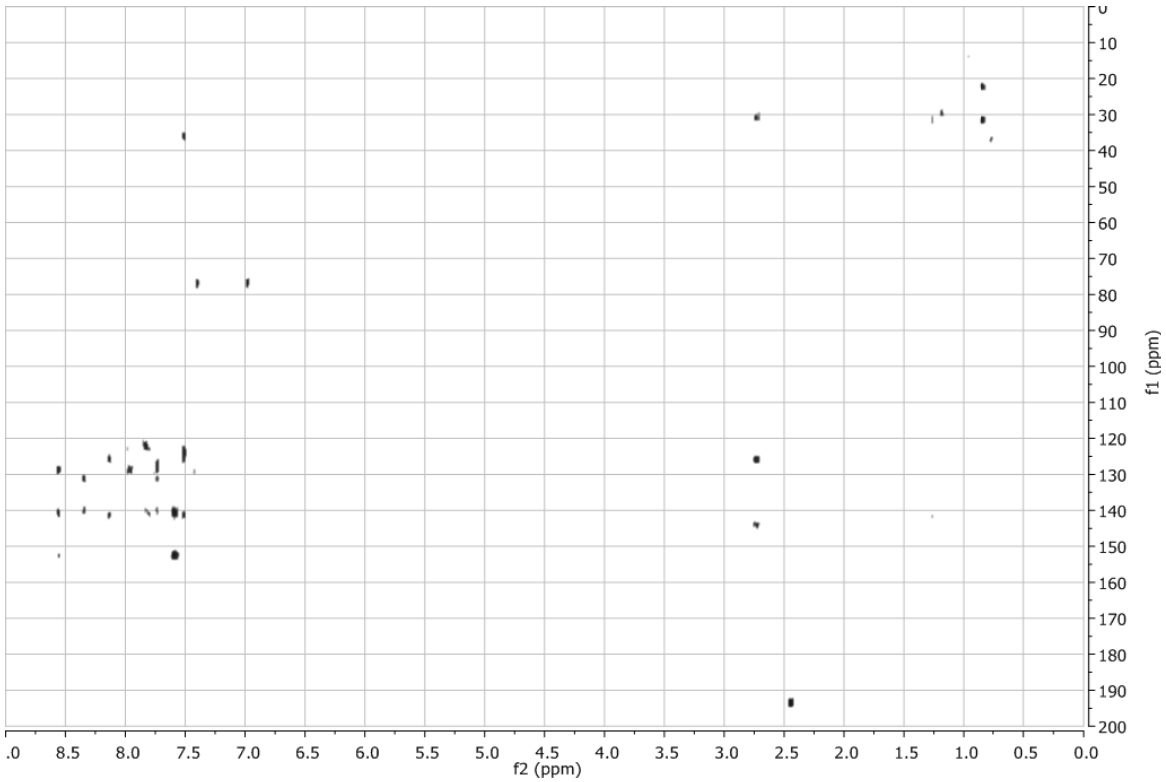

Figure 93 HMBC spectrum of target macrocycle **7**. Measured at RT in $CDCl_3$.

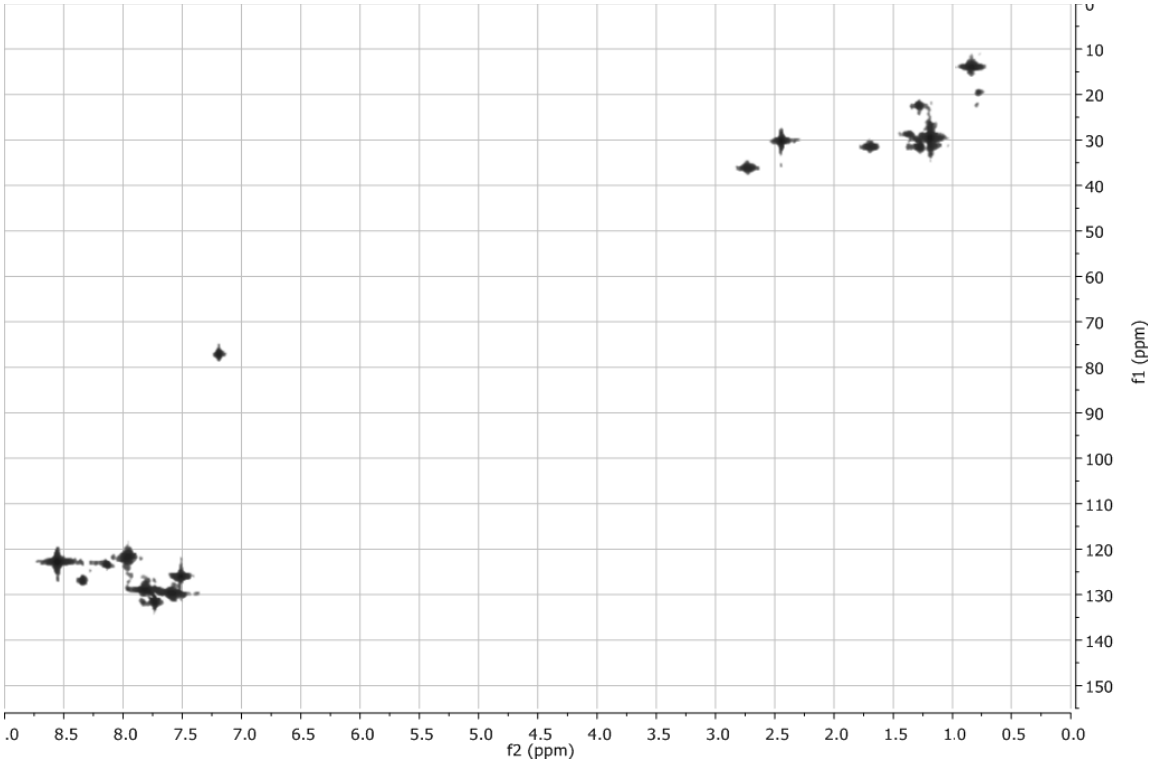

Figure 94 HMQC spectrum of target macrocycle **7**. Measured at RT in $CDCl_3$.

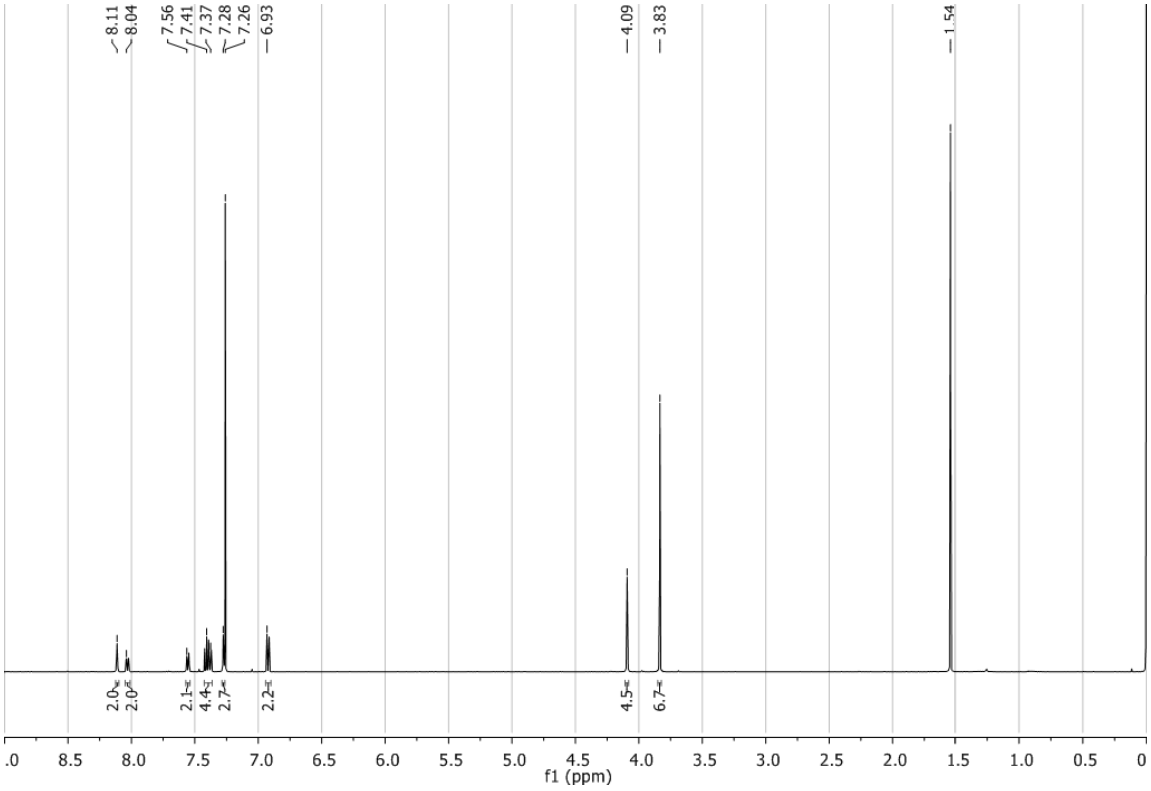

Figure 95 ^{1}H-NMR spectrum of key intermediate **116**. Measured at RT in $CDCl_3$ with 128 scans and 500 MHz.

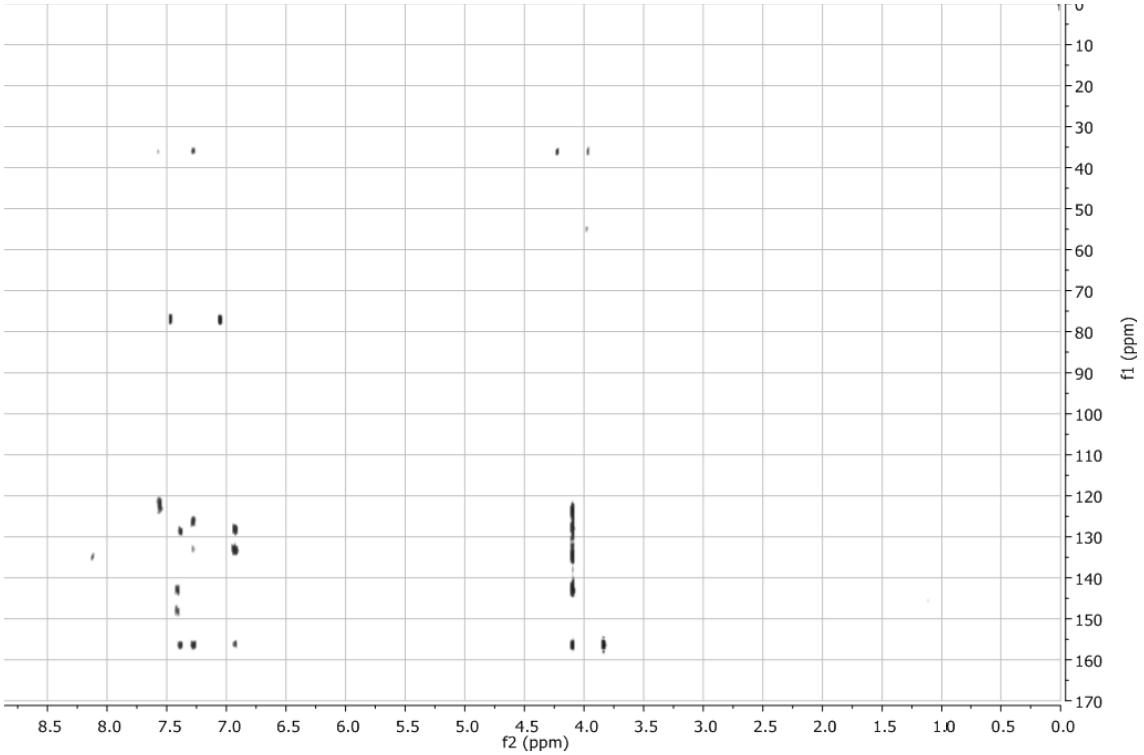

Figure 96 HMBC spectrum of key intermediate **116**. Measured at RT in $CDCl_3$.

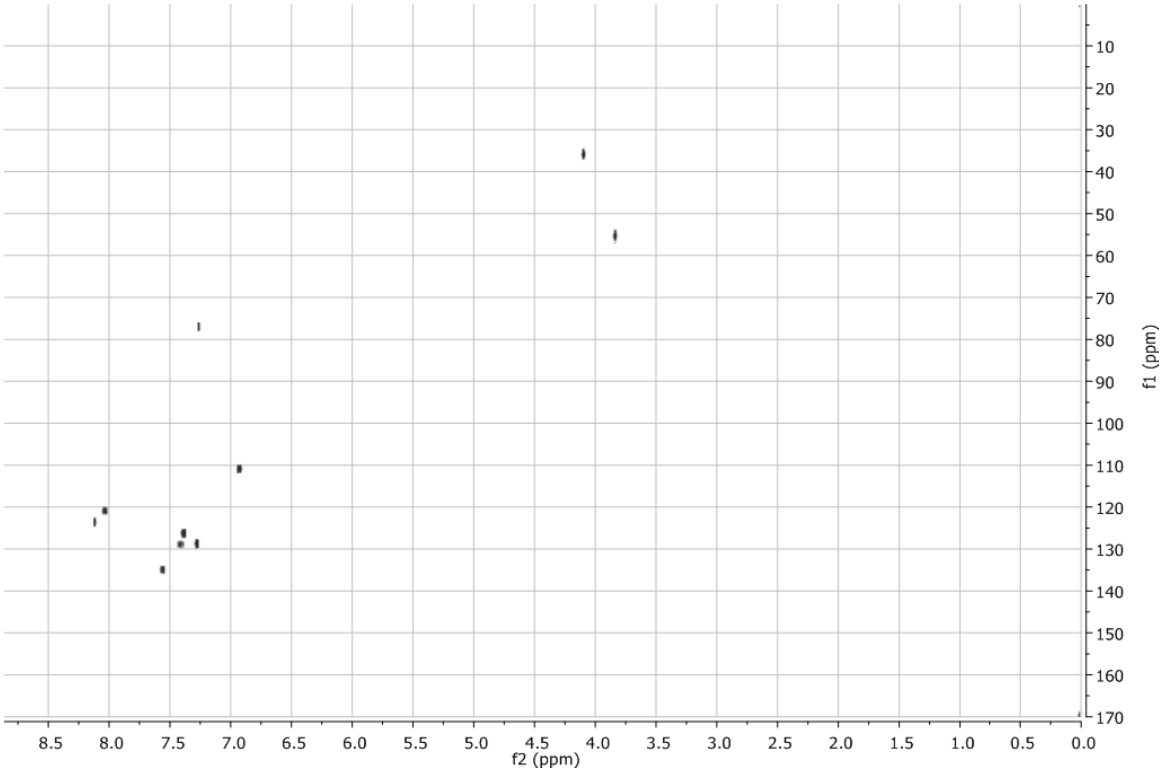

Figure 97 HMQC spectrum of key intermediate **116**. Measured at RT in $CDCl_3$.

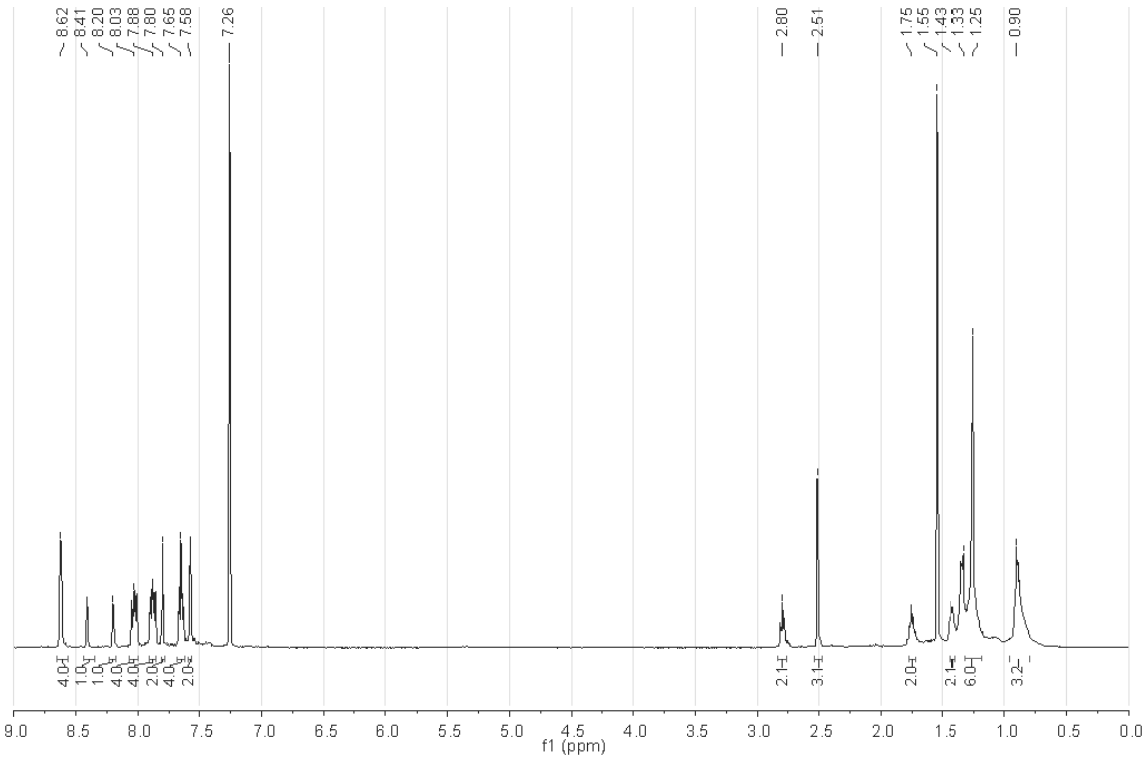

Figure 98 ^{1}H-NMR spectrum of biphenyl macrocycle **125**. Measured at RT in $CDCl_3$ with 128 scans and 500 MHz.

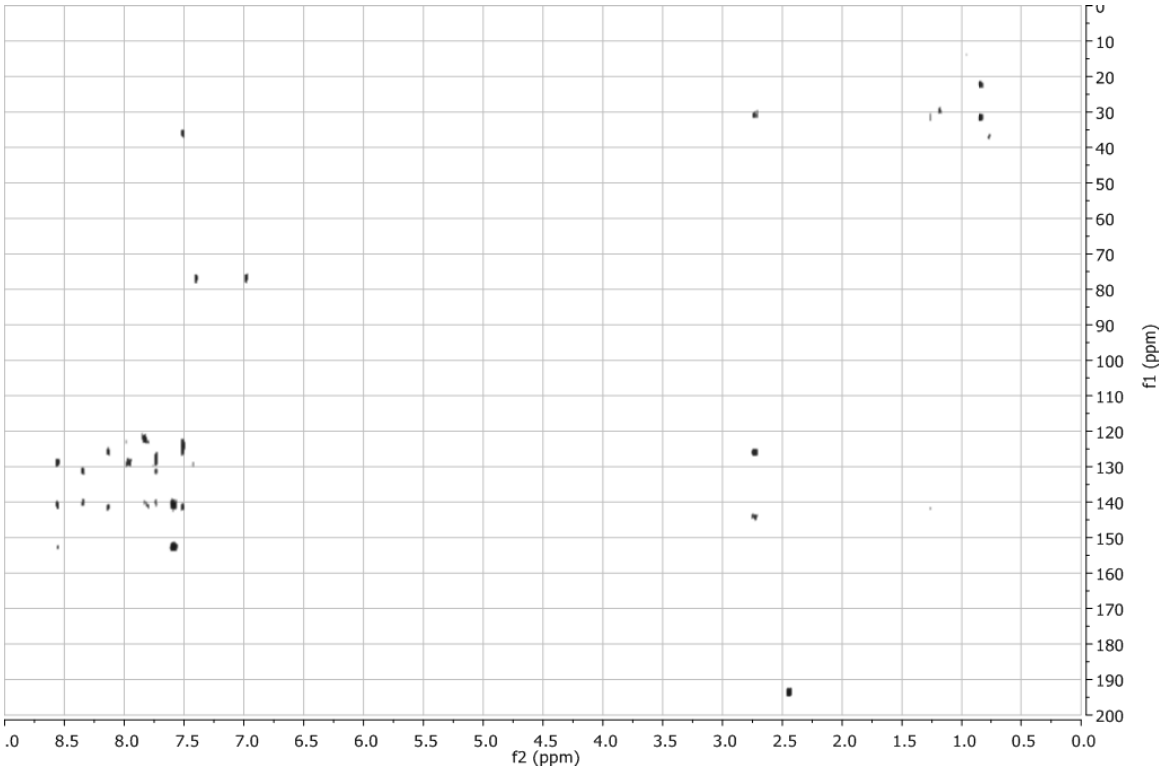

Figure 99 HMBC spectrum of biphenyl macrocycle **125**. Measured at RT in $CDCl_3$.

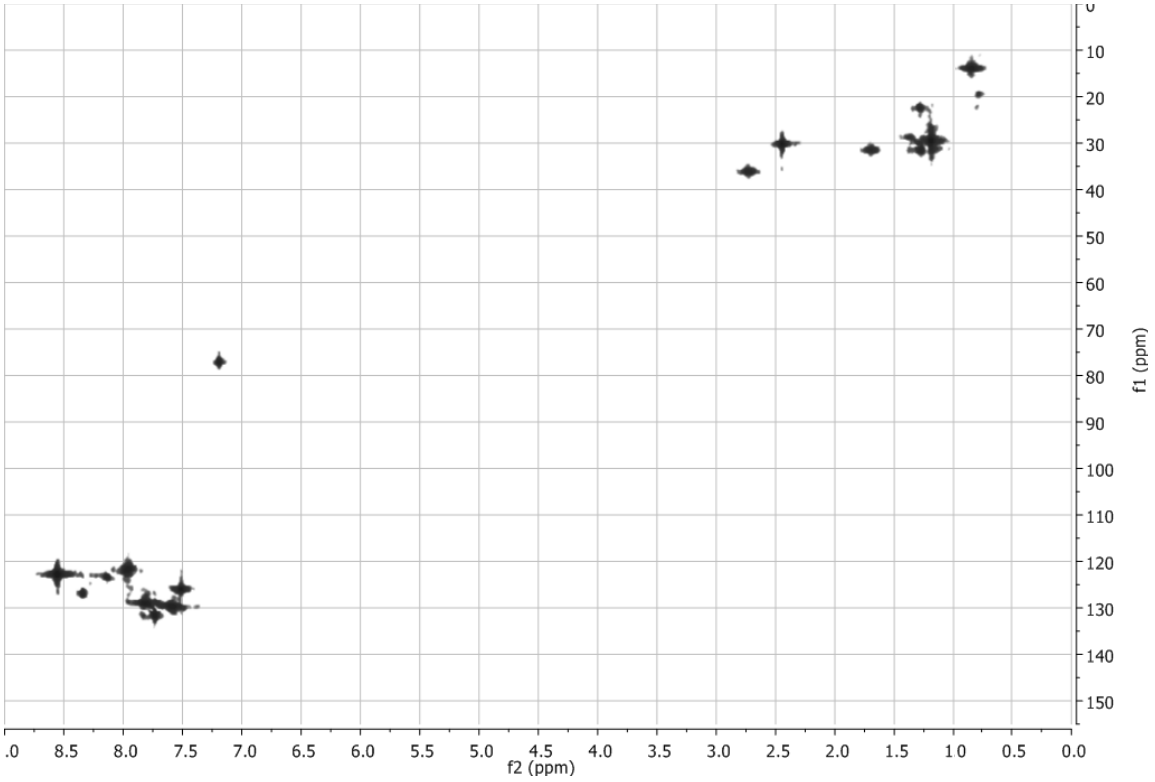

Figure 100 HMQC spectrum of biphenyl macrocycle **125**. Measured at RT in $CDCl_3$.

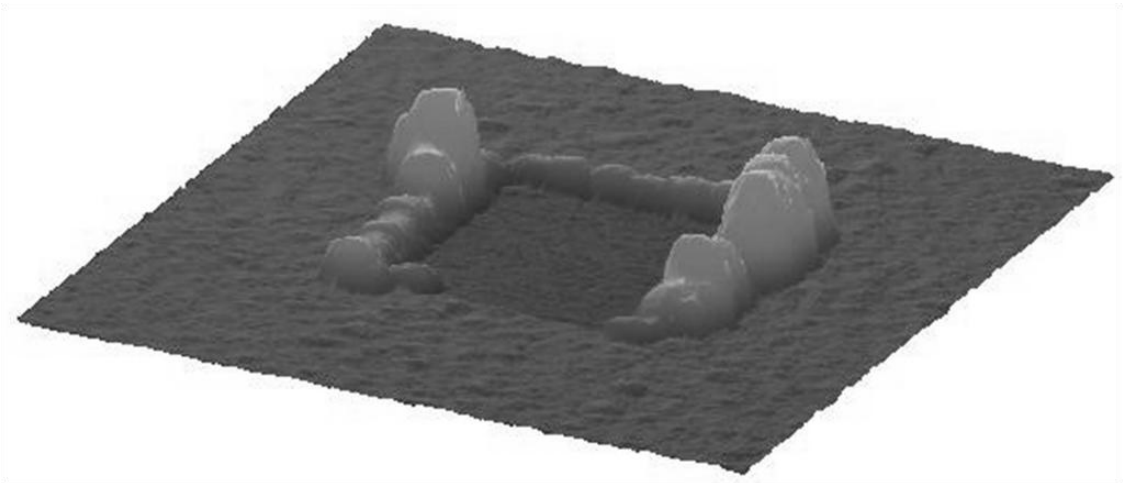

Figure 101 3D AFM picture of the scratched 500 × 500 nm square of electrode **E1** to determine the layer thickness.

9 Bibliography

[1] E. Frey, *ChemPhysChem* **2002**, *3*, 270-279.
[2] C. Renner, L. Moroder, *ChemBioChem* **2006**, *7*, 868-878.
[3] V. Balzani, A. Credi, M. Venturi, *Molecular Devices and Machines - A Journey into the Nanoworld*, Wiley-vch, Weinheim, **2003**.
[4] V. Balzani, A. Credi, F. Marchioni, J. F. Stoddart, *Chemical communications (Cambridge, England)* **2001**, 1860-1.
[5] G. Schmid, H. Brune, H. Ernst, A. Grundwald, W. Grünwald, H. Hofmann, H. Krug, P. Janich, M. Mayor, W. Rathgeber, u. a., *Nanotechnology*, Springer-verlag, Berlin - Heidelberg, **2006**.
[6] H. Zollinger, *Diazo Chemistry I. Aromatic and Heteroaromatic Compounds*, Vch, New York, **1994**.
[7] E. Mitscherlich, *Annalen der Pharmazie* **1834**, 311-314.
[8] A. Hantzsch, *Berichte der Deutschen Chemischen Gesellschaft* **1895**, *28*, 1734-1758.
[9] E. Bamberger, *Berichte der Deutschen Chemischen Gesellschaft* **1895**, *28*, 444-449.
[10] H. Zollinger, *Color Chemistry - Synthesis, Properties and Applications of Organic Dyes and Pigments*, Verlag Helvetica Chimica Acta, Zürich, **2003**.
[11] F. Würthner, J. Rebek Jr., *Angewandte Chemie International Edition in English* **1995**, *34*, 446-448.
[12] F. Würthner, J. Rebek Jr., *Angewandte Chemie* **1995**, *107*, 503-505.
[13] N. Tamaoki, S. Song, M. Moriyama, H. Matsuda, *Advanced Materials* **2000**, *12*, 94-97.
[14] N. Tamaoki, *Advanced Materials (Weinheim, Germany)* **2001**, *13*, 1135-1147.
[15] M. Z. Alam, T. Yoshioka, T. Ogata, T. Nonaka, S. Kurihara, *Chemistry - A European Journal* **2007**, *13*, 2641-2647.
[16] V. Ferri, M. Elbing, G. Pace, M. D. Dickey, M. Zharnikov, P. Samori, M. Mayor, M. A. Rampi, *Angewandte Chemie, International Edition* **2008**, *47*, 3407-3409.
[17] J. M. Mativetsky, G. Pace, M. Elbing, M. A. Rampi, M. Mayor, P. Samorì, *Journal of the American Chemical Society* **2008**, *130*, 9192-9193.
[18] M. Baroncini, S. Silvi, M. Venturi, A. Credi, *Chem. Eur. J.* **2010**, *16*, 11580-11587.
[19] J. Liu, Y. He, X. Wang, *Langmuir* **2009**, *25*, 5974-5979.
[20] G. Liu, T. Böcking, J. J. Gooding, *Journal of Electroanalytical Chemistry* **2007**, *600*, 335-344.
[21] M. A. Karimi Zarchi, M. Karimi, *Journal of Applied Polymer Science* **2011**, *120*, 538-543.
[22] „IUPAC“, can be found under http://www.iupac.org/, **o. J.**
[23] E. Merino, *Chem. Soc. Rev.* **2011**, DOI 10.1039/c0cs00183j.
[24] T. Laue, A. Plagens, *Namens- Und Schlagwort Reaktionen in Der Organischen Chemie*, B. G. Teubner, Stuttgart, **1998**.
[25] Autorenkollektiv, *Organikum*, Wiley-vch, Weinheim, **2001**.

[26] E. Haselbach, *Helvetica Chimica Acta* **1970**, *53*, 1526-43.
[27] B. Ortiz, P. Villanueva, F. Walls, *Journal of Organic Chemistry* **1972**, *37*, 2748-2750.
[28] M. Hedayatullah, J. P. Dechatre, L. Denivelle, *Tetrahedron Letters* **1975**, 2039-2042.
[29] E. Tauer, R. Machinek, *Liebigs Annalen* **1996**, 1213-1216.
[30] M. Elbing, Funktionale Molekulare Bausteine, **2004**.
[31] A. Archut, F. Vögtle, L. De Cola, G. C. Azzellini, V. Balzani, P. S. Ramanujam, R. H. Berg, *Chemistry - A European Journal* **1998**, *4*, 699-706.
[32] K. H. Schündehütte, *Methoden Der Organischen Chemie*, Thieme, Stuttgart, **1965**.
[33] M. H. Davey, V. Y. Lee, R. D. Miller, T. J. Marks, *The Journal of Organic Chemistry* **1999**, *64*, 4976-4979.
[34] Y. Ogata, Y. Takagi, *Journal of the American Chemical Society* **1958**, *80*, 3591-3595.
[35] Y.-K. Lim, K.-S. Lee, C.-G. Cho, *Organic Letters* **2003**, *5*, 979-982.
[36] F. Paul, J. Patt, J. F. Hartwig, *Journal of the American Chemical Society* **1994**, *116*, 5969-5970.
[37] A. S. Guram, S. L. Buchwald, *Journal of the American Chemical Society* **1994**, *116*, 7901-7902.
[38] H.-M. Kang, H.-Y. Kim, J.-W. Jung, C.-G. Cho, *The Journal of organic chemistry* **2007**, *72*, 679-82.
[39] H.-M. Kang, Y.-K. Lim, I.-J. Shin, H.-Y. Kim, C.-G. Cho, *Organic letters* **2006**, *8*, 2047-50.
[40] H. Rau, *Photochromism - Azo Compounds*, **2003**.
[41] G. S. Hartley, *Nature (London, United Kingdom)* **1937**, *140*, 281.
[42] G. M. Wyman, *Chemical Reviews* **1955**, *55*, 625-657.
[43] W. R. Brode, J. H. Gould, G. M. Wyman, *Journal of the American Chemical Society* **1952**, *74*, 4641-6.
[44] D. L. Ross, J. Blanc, *Photochromism*, Wiley, New York, **1971**.
[45] H. Rau, *Angewandte Chemie* **1973**, *85*, 248-258.
[46] H. Rau, *Angewandte Chemie International Edition in English* **1973**, *12*, 224-235.
[47] H. Rau, E. Lueddecke, *Journal of the American Chemical Society* **1982**, *104*, 1616-20.
[48] H. Rau, in *Photoreactive Organic Thin Films*, Academic Press, San Diego, **2002**, S. 3-47.
[49] B. L. Feringa, *Molecular Switches*, Wiley-vch, Weinheim, **2001**.
[50] C. Dugave, L. Demange, *Chemical Reviews* **2003**, *103*, 2475-2532.
[51] E. R. Kay, D. A. Leigh, F. Zerbetto, *Angewandte Chemie International Edition* **2007**, *46*, 72-191.
[52] H. Basch, T. Zoz, *The Chemistry of the Hydrazo, Azo and Azoxy Groups*, John Wiley, Berlin Heidelberg New York, **1997**.
[53] A. W. Adamson, A. Vogler, H. Kunkely, R. Wachter, *Journal of the American Chemical Society* **1978**, *100*, 1298-1300.
[54] T. Nägele, R. Hoche, W. Zinth, J. Wachtveitl, *Chemical Physics Letters* **1997**, *272*, 489-495.
[55] D. Y. Curtin, E. J. Grubbs, C. G. McCarty, *Journal of the American*

Chemical Society **1966**, *88*, 2775-2786.
[56] T. Asano, T. Okada, *The Journal of Organic Chemistry* **1984**, *49*, 4387-4391.
[57] T. Asano, T. Yano, T. Okada, *Journal of the American Chemical Society* **1982**, *104*, 4900-4904.
[58] N. J. Bunce, G. Ferguson, C. L. Forber, G. J. Stachnyk, *The Journal of Organic Chemistry* **1987**, *52*, 394-398.
[59] H. Kessler, D. Leibfritz, *Tetrahedron Letters* **1970**, *11*, 1423-1426.
[60] H. Rau, E. Lueddecke, *Journal of the American Chemical Society* **1982**, *104*, 1616-1620.
[61] N. Tamaoki, K. Ogata, K. Koseki, T. Yamaoka, *Tetrahedron* **1990**, *46*, 5931-5942.
[62] N. Tamaoki, T. Yamaoka, *Journal of the Chemical Society, Perkin Transactions 2* **1991**, 873-8.
[63] N. Tamaoki, K. Koseki, T. Yamaoka, *Tetrahedron Letters* **1990**, *31*, 3309-12.
[64] E. Wei-Guang Diau, *The Journal of Physical Chemistry A* **2004**, *108*, 950-956.
[65] R. Hagen, T. Bieringer, *Advanced Materials (Weinheim, Germany)* **2001**, *13*, 1805-1810.
[66] K. Ichimura, *Chemical Reviews (Washington, D. C.)* **2000**, *100*, 1847-1873.
[67] O. Pieroni, A. Fissi, N. Angelini, F. Lenci, *Accounts of chemical research* **2001**, *34*, 9-17.
[68] D. A. Leigh, J. K. Y. Wong, F. Dehez, F. Zerbetto, *Nature (London, United Kingdom)* **2003**, *424*, 174-179.
[69] V. Balzani, F. Scandola, *Supramolecular Photochemistry*, Horwood, Chichester, **1991**.
[70] S. Ljunggren, G. Wettermark, *Acta Chemica Scandinavica (1947-1973)* **1971**, *25*, 1599-606.
[71] T. Kameo, T. Hirashima, O. Manabe, H. Hiyama, *Kogyo Kagaku Zasshi* **1969**, *72*, 1327-31.
[72] D. L. Beveridge, H. H. Jaffe, *Journal of the American Chemical Society* **1966**, *88*, 1948-53.
[73] M. V. Peters, R. S. Stoll, A. Kuehn, S. Hecht, *Angewandte Chemie International Edition* **2008**, *47*, 5968-5972, S5968/1-S5968/32.
[74] A. Khan, C. Kaiser, S. Hecht, *Angewandte Chemie International Edition* **2006**, *45*, 1878-1881.
[75] Y. Shirai, T. Sasaki, J. M. Guerrero, B.-C. Yu, P. Hodge, J. M. Tour, *ACS Nano* **2008**, *2*, 97-106.
[76] N. T. Yasuo Norikane, *European Journal of Organic Chemistry* **2006**, *2006*, 1296-1302.
[77] D. Röttger, H. Rau, *Journal of Photochemistry and Photobiology A: Chemistry* **1996**, *101*, 205-214.
[78] E. Luboch, R. Bilewicz, M. Kowalczyk, E. Wagner-Wysiecka, J. F. Biernat, in *Advances in Supramolecular Chemistry*, Cerberus Press, **o. J.**, S. 71-162.
[79] K. G. Yager, C. J. Barrett, *Polymeric Nanostructures and Their Applications* **2007**, *2*, 243-280.

[80] G. Wen, D. Zhang, Y. Huang, R. Zhao, L. Zhu, Z. Shuai, D. Zhu, *The Journal of Organic Chemistry* **2007**, *72*, 6247-6250.
[81] N. Landraud, J. Peretti, F. Chaput, G. Lampel, J. P. Boilot, K. Lahlil, V. I. Safarov, *Applied Physics Letters* **2001**, *79*, 4562-4564.
[82] B. Darracq, F. Chaput, K. Lahlil, Y. Levy, J.-P. Boilot, *Advanced Materials (Weinheim, Germany)* **1998**, *10*, 1133-1136.
[83] U. Funke, H.-F. Grützmacher, *Tetrahedron* **1987**, *43*, 3787-3795.
[84] Y. Norikane, R. Katoh, N. Tamaoki, *Chemical Communications (Cambridge, United Kingdom)* **2008**, 1898-1900.
[85] S. Guo, L. Konopny, R. Popovitz-Biro, H. Cohen, H. Porteanu, E. Lifshitz, M. Lahav, *Journal of the American Chemical Society* **1999**, *121*, 9589-9598.
[86] D. G. Kurth, P. Lehmann, M. Schutte, *Proceedings of the National Academy of Sciences of the United States of America* **2000**, *97*, 5704-5707.
[87] A. Semenov, J. P. Spatz, M. Moller, J.-M. Lehn, B. Sell, D. Schubert, C. H. Weidl, U. S. Schubert, *Angewandte Chemie, International Edition* **1999**, *38*, 2547-2550.
[88] A. P. Bisson, F. J. Carver, D. S. Eggleston, R. C. Haltiwanger, C. A. Hunter, D. L. Livingstone, J. F. McCabe, C. Rotger, A. E. Rowan, *Journal of the American Chemical Society* **2000**, *122*, 8856-8868.
[89] G. R. Desiraju, *Angewandte Chemie, International Edition in English* **1995**, *34*, 2311-27.
[90] G. Gottarelli, S. Masiero, E. Mezzina, S. Pieraccini, J. P. Rabe, P. Samori, G. P. Spada, *Chemistry--A European Journal* **2000**, *6*, 3242-3248.
[91] J. H. K. K. Hirschberg, L. Brunsveld, A. Ramzi, J. A. J. M. Vekemans, R. P. Sijbesma, E. W. Meijer, *Nature (London)* **2000**, *407*, 167-170.
[92] H. Engelkamp, S. Middelbeek, R. J. M. Nolte, *Science (Washington, D. C.)* **1999**, *284*, 785-788.
[93] J. P. Rabe, S. Buchholz, *Science (Washington, DC, United States)* **1991**, *253*, 424-7.
[94] G. Binning, H. Rohrer, C. Gerber, E. Weibel, *Physical Review Letters* **1982**, *49*, 57-61.
[95] L. Askadskaya, C. Boeffel, J. P. Rabe, *Berichte der Bunsen-Gesellschaft* **1993**, *97*, 517-21.
[96] S. Ito, M. Wehmeier, J. D. Brand, C. Kubel, R. Epsch, J. P. Rabe, K. Mullen, *Chemistry--A European Journal* **2000**, *6*, 4327-4342.
[97] V. S. Iyer, K. Yoshimura, V. Enkelmann, R. Epsch, J. P. Rabe, K. Mullen, *Angewandte Chemie, International Edition* **1998**, *37*, 2696-2699.
[98] A. Stabel, P. Herwig, K. Muellen, J. P. Rabe, *Angewandte Chemie, International Edition in English* **1995**, *34*, 1609-11.
[99] P. Samori, F. Jackel, O. Unsal, A. Godt, J. P. Rabe, *ChemPhysChem* **2001**, *2*, 461-464.
[100] P. Samori, A. Fechtenkoetter, F. Jaeckel, T. Boehme, K. Muellen, J. P. Rabe, *Journal of the American Chemical Society* **2001**, *123*, 11462-11467.
[101] P. Samori, X. Yin, N. Tchebotareva, Z. Wang, T. Pakula, F. Jaeckel, M. D. Watson, A. Venturini, K. Muellen, J. P. Rabe, *Journal of the American Chemical Society* **2004**, *126*, 3567-3575.
[102] I. Widmer, U. Hubler, M. Stohr, L. Merz, H. J. Guntherodt, B. A. Hermann,

P. Samori, J. P. Rabe, P. B. Rheiner, G. Greiveldinger, u. a., *Helvetica Chimica Acta* **2002**, *85*, 4255-4263.
[103] D. Mössinger, J. Hornung, S. Lei, S. De Feyter, S. Höger, *Angewandte Chemie International Edition* **2007**, *46*, 6802-6806.
[104] A. Ziegler, W. Mamdouh, A. Ver Heyen, M. Surin, H. Uji-i, M. M. S. Abdel-Mottaleb, F. C. De Schryver, S. De Feyter, R. Lazzaroni, S. Höger, *Chemistry of Materials* **2005**, *17*, 5670-5683.
[105] S. Höger, K. Bonrad, A. Mourran, U. Beginn, M. Möller, *Journal of the American Chemical Society* **2001**, *123*, 5651-5659.
[106] M. Fischer, G. Lieser, A. Rapp, I. Schnell, W. Mamdouh, S. De Feyter, F. C. De Schryver, S. Höger, *Journal of the American Chemical Society* **2004**, *126*, 214-222.
[107] L. Venkataraman, *Physics* **2008**, *1*, 5.
[108] R. L. McCreery, A. J. Bergren, *Advanced Materials* **2009**, *21*, 4303-4322.
[109] J. M. Seminario, C. E. De La Cruz, P. A. Derosa, *Journal of the American Chemical Society* **2001**, *123*, 5616-5617.
[110] J. M. Seminario, A. G. Zacarias, J. M. Tour, *Journal of the American Chemical Society* **1999**, *121*, 411-416.
[111] R. M. Tovar, K. P. Johnson, K. Ashline, J. M. Seminario, *International Journal of Quantum Chemistry* **2008**, *108*, 1546-1554.
[112] D. Vonlanthen, Biphenyl-Cyclophanes: The Molecular Control over the Conductivity of Single-Molecule Junctions, Basel, **2010**.
[113] F. Chen, X. Li, J. Hihath, Z. Huang, N. Tao, *Journal of the American Chemical Society* **2006**, *128*, 15874-15881.
[114] E. Barendrecht, *Journal of Applied Electrochemistry* **1990**, *20*, 175-185.
[115] N. M. Markovic, P. N. Ross, *Surface Science Reports* **2002**, *45*, 117-229.
[116] R. F. Lane, A. T. Hubbard, *The Journal of Physical Chemistry* **1973**, *77*, 1401-1410.
[117] C. Fave, Y. Leroux, Trippé, H. Randriamahazaka, V. Noel, J.-C. Lacroix, *Journal of the American Chemical Society* **2007**, *129*, 1890-1891.
[118] J. M. Buriak, *Chemical Reviews* **2002**, *102*, 1271-1308.
[119] F. Hauquier, J. Ghilane, B. Fabre, P. Hapiot, *Journal of the American Chemical Society* **2008**, *130*, 2748-2749.
[120] B. Fabre, *Accounts of Chemical Research* **2010**, *43*, 1509-1518.
[121] D. Vuillaume, *Condensed Matter* **2010**, *1*, 1-12.
[122] D. Vuillaume, *Molecular Electronics Based on Self-assembled Monolayers*, University Press, Oxford, **2008**.
[123] L. Touahir, P. Allongue, D. Aureau, R. Boukherroub, J.-N. Chazalviel, E. Galopin, A. C. Gouget-Laemmel, C. H. de Villeneuve, A. Moraillon, J. Niedziólka-Jönsson, u. a., *Bioelectrochemistry* **2010**, *80*, 17-25.
[124] J. ter Maat, R. Regeling, M. Yang, M. N. Mullings, S. F. Bent, H. Zuilhof, *Langmuir* **2009**, *25*, 11592-11597.
[125] C. Xue, G. Arumugam, K. Palaniappan, S. A. Hackney, H. Liu, J. Liu, *Chemical Communications* **2005**, 1055.
[126] M. Lu, T. He, J. M. Tour, *Chemistry of Materials* **2008**, *20*, 7352-7355.
[127] M. A. C. Campos, J. M. J. Paulusse, H. Zuilhof, *Chemical Communications* **2010**, *46*, 5512.
[128] M. Janin, J. Ghilane, H. Randriamahazaka, J.-C. Lacroix, *Electrochemistry Communications* **2009**, *11*, 647-650.

[129] O. I. Covaci, B. Bucur, M. P. Bucur, G. L. Radu, *Microchimica Acta* **2010**, *169*, 335-343.
[130] D. Bélanger, J. Pinson, *Chem. Soc. Rev.* **2011**, DOI 10.1039/c0cs00149j.
[131] A. Ulman, *Chemical Reviews* **1996**, *96*, 1533-1554.
[132] H. Qi, S. Sharma, Z. Li, G. L. Snider, A. O. Orlov, C. S. Lent, T. P. Fehlner, *Journal of the American Chemical Society* **2003**, *125*, 15250-15259.
[133] M. Delamar, R. Hitmi, J. Pinson, J. M. Saveant, *Journal of the American Chemical Society* **1992**, *114*, 5883-5884.
[134] C. Saby, B. Ortiz, G. Y. Champagne, D. Bélanger, *Langmuir* **1997**, *13*, 6805-6813.
[135] Y.-C. Liu, R. L. McCreery, *Analytical Chemistry* **1997**, *69*, 2091-2097.
[136] N. Weibel, S. Grunder, M. Mayor, *Organic & Biomolecular Chemistry* **2007**, 2343-2353.
[137] C. Combellas, D.-en Jiang, F. Kanoufi, J. Pinson, F. I. Podvorica, *Langmuir* **2009**, *25*, 286-293.
[138] C. Combellas, F. Kanoufi, J. Pinson, F. I. Podvorica, *Journal of the American Chemical Society* **2008**, *130*, 8576-8577.
[139] A. Adenier, E. Cabet-Deliry, A. Chaussé, S. Griveau, F. Mercier, J. Pinson, C. Vautrin-Ul, *Chemistry of Materials* **2005**, *17*, 491-501.
[140] S. Baranton, D. Bélanger, *The Journal of Physical Chemistry B* **2005**, *109*, 24401-24410.
[141] C. A. Dyke, J. M. Tour, *Journal of the American Chemical Society* **2003**, *125*, 1156-1157.
[142] Y. Goto, H. Sato, S. Shinkai, K. Sada, *Journal of the American Chemical Society* **2008**, *130*, 14354-14355.
[143] Y. R. Leroux, H. Fei, J.-M. Noël, C. Roux, P. Hapiot, *Journal of the American Chemical Society* **2010**, *132*, 14039-14041.
[144] M. R. Lockett, J. C. Carlisle, D. V. Le, L. M. Smith, *Langmuir* **2009**, *25*, 5120-5126.
[145] M. R. Lockett, L. M. Smith, *Langmuir* **2009**, *25*, 3340-3343.
[146] R. Chinchilla, C. Nájera, *Chemical Reviews* **2007**, *107*, 874-922.
[147] B. Liang, M. Dai, J. Chen, Z. Yang, *The Journal of Organic Chemistry* **2005**, *70*, 391-393.
[148] K. Sonogashira, Y. Tohda, N. Hagihara, *Tetrahedron Letters* **1975**, *16*, 4467-4470.
[149] A. de Meijere, F. Diederich, Editors, *Metal-Catalyzed Cross-Coupling Reactions, Second, Completely Revised and Enlarged Edition: Volume 1*, Wiley-vhc, **2004**.
[150] R. Singh, G. Just, *The Journal of Organic Chemistry* **1989**, *54*, 4453-4457.
[151] W. B. Austin, N. Bilow, W. J. Kelleghan, K. S. Y. Lau, *The Journal of Organic Chemistry* **1981**, *46*, 2280-2286.
[152] M. Qu, Y. Zhang, J. He, X. Cao, J. Zhang, *Applied Surface Science* **2008**, *255*, 2608-2612.
[153] A. Aviram, M. A. Ratner, *Chemical Physics Letters* **1974**, *29*, 277-283.
[154] A. Nitzan, M. A. Ratner, *Science* **2003**, *300*, 1384 -1389.
[155] R. L. Carroll, C. B. Gorman, *Angewandte Chemie International Edition* **2002**, *41*, 4378-4400.
[156] N. J. Tao, *Nature Nanotechnology* **2006**, *1*, 173-181.

[157] D. Vonlanthen, A. Mishchenko, M. Elbing, M. Neuburger, T. Wandlowski, M. Mayor, *Angewandte Chemie International Edition* **2009**, *48*, 8886-8890.
[158] E. Lörtscher, M. Elbing, M. Tschudy, C. von Hänisch, H. B. Weber, M. Mayor, H. Riel, *ChemPhysChem* **2008**, *9*, 2252-2258.
[159] M. Mayor, H. B. Weber, J. Reichert, M. Elbing, C. von Hänisch, D. Beckmann, M. Fischer, *Angewandte Chemie International Edition* **2003**, *42*, 5834-5838.
[160] Z. Li, I. Pobelov, B. Han, T. Wandlowski, A. Błaszczyk, M. Mayor, *Nanotechnology* **2007**, *18*, 044018.
[161] J. Wang, G. Cooper, D. Tulumello, A. P. Hitchcock, *The Journal of Physical Chemistry A* **2005**, *109*, 10886-10896.
[162] S. Ando, T. Hironaka, H. Kurosu, I. Ando, *Magnetic Resonance in Chemistry* **2000**, *38*, 241-250.
[163] W. Haiss, C. Wang, R. Jitchati, I. Grace, S. Martín, A. S. Batsanov, S. J. Higgins, M. R. Bryce, C. J. Lambert, P. S. Jensen, u. a., *Journal of Physics: Condensed Matter* **2008**, *20*, 374119.
[164] H. Kondo, J. Nara, H. Kino, T. Ohno, *The Journal of Chemical Physics* **2008**, *128*, 064701.
[165] F. Pauly, J. K. Viljas, J. C. Cuevas, *Physical Review B* **2008**, *78*, 035315.
[166] J. Zhang, M. Nieuwenhuyzen, J. P. H. Charmant, S. L. James, *Chem. Commun.* **2004**, 2808.
[167] J. R. Farrell, C. A. Mirkin, L. M. Liable-Sands, A. L. Rheingold, *Journal of the American Chemical Society* **1998**, *120*, 11834-11835.
[168] B. Nohra, Y. Yao, C. Lescop, R. Réau, *Angewandte Chemie International Edition* **2007**, *46*, 8242-8245.
[169] J. F. Kang, S. Liao, R. Jordan, A. Ulman, *Journal of the American Chemical Society* **1998**, *120*, 9662-9667.
[170] A. Mazzanti, L. Lunazzi, M. Minzoni, J. E. Anderson, *The Journal of Organic Chemistry* **2006**, *71*, 5474-5481.
[171] F. Leroux, *ChemBioChem* **2004**, *5*, 644-649.
[172] K. Müllen, W. Heinz, F. Klärner, W. R. Roth, I. Kindermann, O. Adamczak, M. Wette, J. Lex, *Chemische Berichte* **1990**, *123*, 2349-2371.
[173] H.-S. Im, E. R. Bernstein, *J. Chem. Phys.* **1988**, *88*, 7337.
[174] S. Woitellier, J. P. Launay, C. Joachim, *Chemical Physics* **1989**, *131*, 481-488.
[175] F. Pauly, J. K. Viljas, J. C. Cuevas, G. Schön, *Physical Review B* **2008**, *77*, 155312.
[176] L. Venkataraman, J. E. Klare, C. Nuckolls, M. S. Hybertsen, M. L. Steigerwald, *Nature (London, U. K.)* **2006**, *442*, 904-907.
[177] A. Mishchenko, L. A. Zotti, D. Vonlanthen, M. Bürkle, F. Pauly, J. C. Cuevas, M. Mayor, T. Wandlowski, *Journal of the American Chemical Society* **2011**, *133*, 184-187.
[178] D. Vonlanthen, J. Rotzler, M. Neuburger, M. Mayor, *European Journal of Organic Chemistry* **2010**, *2010*, 120-133.
[179] A. Mishchenko, D. Vonlanthen, V. Meded, M. Bürkle, C. Li, I. V. Pobelov, A. Bagrets, J. K. Viljas, F. Pauly, F. Evers, u. a., *Nano Letters* **2010**, *10*, 156-163.
[180] M. Müri, K. C. Schuermann, L. D. Cola, M. Mayor, *European Journal of Organic Chemistry* **2009**, 2562-2575.

[181] S. A. Nagamani, Y. Norikane, N. Tamaoki, *The Journal of Organic Chemistry* **2005**, *70*, 9304-9313.
[182] Y. Norikane, K. Kitamoto, N. Tamaoki, *The Journal of organic chemistry* **2003**, *68*, 8291-304.
[183] T. Schmitz-Hubsch, F. Sellam, R. Staub, M. Torker, T. Fritz, C. Kubel, K. Mullen, K. Leo, *Surface Science* **2000**, *445*, 358-367.
[184] D. Borissov, A. Ziegler, S. Höger, W. Freyland, *Langmuir* **2004**, *20*, 2781-2784.
[185] Y.-K. Lim, K.-S. Lee, C.-G. Cho, *Organic Letters* **2003**, *5*, 979-982.
[186] Y.-K. Lim, J.-W. Jung, H. Lee, C.-G. Cho, *The Journal of Organic Chemistry* **2004**, *69*, 5778-5781.
[187] W. Adam, O. Krebs, *Chemical Reviews* **2003**, *103*, 4131-4146.
[188] H. Yamamoto, M. Kawasaki, *Bulltin of the Chemical Society of Japan* **2007**, *4*, 595-607.
[189] D. Zhao, M. Johansson, J. E. Bäckvall, *European Journal of Organic Chemistry* **2007**, *2007*, 4431–4436.
[190] L. Shu, M. Mayor, *Chemical Communications (Cambridge, United Kingdom)* **2006**, 4134-4136.
[191] K. C. Nicolaou, P. G. Bulger, D. Sarlah, *Angewandte Chemie, International Edition* **2005**, *44*, 4442-4489.
[192] N. Miyaura, A. Suzuki, *Chemical Reviews (Washington, D. C.)* **1995**, *95*, 2457-83.
[193] N. Miyaura, K. Yamada, A. Suzuki, *Tetrahedron Letters* **1979**, *20*, 3437-3440.
[194] N. Miyaura, A. Suzuki, *Journal of the Chemical Society, Chemical Communications* **1979**, *19*, 666-667.
[195] Y. Teki, S. Miyamoto, M. Nakatsuji, Y. Miura, *Journal of the American Chemical Society* **2001**, *123*, 294-305.
[196] S. Hoeger, K. Bonrad, A. Mourran, U. Beginn, M. Moeller, *Journal of the American Chemical Society* **2001**, *123*, 5651-5659.
[197] S. Hoger, K. Bonrad, L. Karcher, A.-D. Meckenstock, *The Journal of Organic Chemistry* **2000**, *65*, 1588-1589.
[198] G.-B. Pan, X.-H. Cheng, S. Hoeger, W. Freyland, *Journal of the American Chemical Society* **2006**, *128*, 4218-4219.
[199] S. Tisserand, R. Baati, M. Nicolas, C. Mioskowski, *Journal of Organic Chemistry* **2004**, *69*, 8982-8983.
[200] M. Crozet, L. Zink, V. Remuat, C. Curti, P. Vanelle, *Synthesis* **2009**, *18*, 3150-3156.
[201] M. Larhed, A. Hallberg, *The Journal of Organic Chemistry* **1996**, *61*, 9582-9584.
[202] H. Hayashi, K. Kamata, J. Abe, H. Yoshida, S. Asaoka, T. Iyoda, *Transactions of the Materials Research Society of Japan* **2003**, *28*, 569-572.
[203] M. J. Jones, *Organic Chemistry*, W. W. Norton & Company, New York, **2000**.
[204] F. A. Carey, R. J. Sundberg, *Organische Chemie*, Wiley-vhc, Weinheim, **1995**.
[205] C. Niemann, C. E. Redemann, *Journal of the American Chemical Society* **1941**, *63*, 1549-52.

[206] F. Wurthner, Z. Chen, V. Dehm, V. Stepanenko, *Chemical communications (Cambridge, England)* **2006**, 1188-90.
[207] R. Brückner, *Reaktionsmechanismen - Organische Raktionen, Stereochemie, Moderne Synthesemethoden*, Spektrum Akademischer Verlag, Heidelberg Berlin, **2003**.
[208] G. Pace, V. Ferri, C. Grave, M. Elbing, C. Von H\änisch, M. Zharnikov, M. Mayor, M. A. Rampi, P. Samorì, *Proceedings of the National Academy of Sciences* **2007**, *104*, 9937.
[209] S. Wang, R. C. Advincula, *Organic Letters* **2001**, *3*, 3831-3834.
[210] B. Priewisch, K. Rueck-Braun, *Journal of Organic Chemistry* **2005**, *70*, 2350-2352.
[211] S. Wang, R. C. Advincula, *Organic Letters* **2001**, *3*, 3831-3834.
[212] R. Welti, Y. Abel, V. Gramlich, F. Diederich, *Helvetica Chimica Acta* **2003**, *86*, 548-562.
[213] S. Berger, S. Braun, *200 and More NMR Experiments*, Wiley-vch, Weinheim, **2004**.
[214] E. Pretsch, P. Bühlmann, M. Badertscher, *Spektroskopische Daten Zur Strukturaufklärung Organischer Verbindungen*, Springer, Berlin, **o. J.**
[215] G. Zimmermann, L. Y. Chow, U. I. Paik, *Journal of the American Chemical Society* **1958**, *80*, 3528.
[216] M. Elbing, A. Błaszczyk, C. von Hänisch, M. Mayor, V. Ferri, C. Grave, M. A. Rampi, G. Pace, P. Samorì, A. Shaporenko, u. a., *Advanced Functional Materials* **2008**, *18*, 2972-2983.
[217] S. Wu, M. T. Gonzalez, R. Huber, S. Grunder, M. Mayor, C. Schonenberger, M. Calame, *Nature Nanotechnology* **2008**, *3*, 569-574.
[218] R. Huber, M. T. González, S. Wu, M. Langer, S. Grunder, V. Horhoiu, M. Mayor, M. R. Bryce, C. Wang, R. Jitchati, u. a., *Journal of the American Chemical Society* **2008**, *130*, 1080-1084.
[219] S. G. Newman, V. Aureggi, C. S. Bryan, M. Lautens, *Chemical Communications* **2009**, 5236.
[220] S. Grunder, R. Huber, S. Wu, C. Schönenberger, M. Calame, M. Mayor, *European Journal of Organic Chemistry* **2010**, *2010*, 833-845.
[221] S. Grunder, R. Huber, V. Horhoiu, M. T. González, C. Schönenberger, M. Calame, M. Mayor, *The Journal of Organic Chemistry* **2007**, *72*, 8337-8344.
[222] S. Grunder, New Functional Molecules in Molecular Junctions, University of Basel, **2009**.
[223] C. J. Yu, Y. Chong, J. F. Kayyem, M. Gozin, *The Journal of Organic Chemistry* **1999**, *64*, 2070-2079.
[224] D. A. Schlueter, *Functional Molecular Nanostructures*, Springer Verlag Gmbh, Berlin, **2005**.
[225] F. Alonso, I. P. Beletskaya, M. Yus, *Tetrahedron* **2008**, *64*, 3047–3101.
[226] M. Tanaka, T. Sawaguchi, Y. Sato, K. Yoshioka, O. Niwa, *Langmuir* **2011**, *27*, 170-178.
[227] B. Sciacca, S. D. Alvarez, F. Geobaldo, M. J. Sailor, *Dalton Transactions* **2010**, *39*, 10847.
[228] G. Qin, C. Santos, W. Zhang, Y. Li, A. Kumar, U. J. Erasquin, K. Liu, P. Muradov, B. W. Trautner, C. Cai, *Journal of the American Chemical Society* **2010**, *132*, 16432-16441.

[229] A. P. Bonifas, R. L. McCreery, *Nature Nanotechnology* **2010**, *5*, 612-617.
[230] J. Pinson, F. Podvorica, *Chemical Society Reviews* **2005**, *34*, 429-439.
[231] D. D. M. Wayner, R. A. Wolkow, *Journal of the Chemical Society, Perkin Transactions 2* **2002**, 23-34.
[232] G. G. Condorelli, C. Tudisco, A. Motta, A. Di Mauro, F. Lupo, A. Gulino, I. L. Fragalà, *European Journal of Inorganic Chemistry* **2010**, *2010*, 4121-4129.
[233] S. Fellah, R. Boukherroub, F. Ozanam, J.-N. Chazalviel, *Langmuir* **2004**, *20*, 6359-6364.
[234] J.-C. Lin, J.-H. Kim, J. A. Kellar, M. C. Hersam, S. T. Nguyen, M. J. Bedzyk, *Langmuir* **2010**, *26*, 3771-3773.
[235] P. Allongue, M. Delamar, B. Desbat, O. Fagebaume, R. Hitmi, J. Pinson, J.-M. Savéant, *Journal of the American Chemical Society* **1997**, *119*, 201-207.
[236] J. Pinson, F. Podvorica, *Chemical Society Reviews* **2005**, *34*, 429.
[237] M. Chahma, R. Hicks, *Canadian Journal of Chemistry* **2004**, *82*, 1629-1633.
[238] Y.-C. Liu, R. L. McCreery, *Journal of the American Chemical Society* **1995**, *117*, 11254-11259.
[239] F. Anariba, S. H. DuVall, R. L. McCreery, *Analytical Chemistry* **2003**, *75*, 3837-3844.
[240] R. Tadmor, *Langmuir* **2004**, *20*, 7659-7664.
[241] C. D. Wagner, L. E. Davis, M. V. Zeller, R. H. Taylor, R. H. Raymond, L. H. Gale, *Surface and Interface Analysis* **1981**, *3*, 211-225.
[242] J. H. Scofield, *Journal of Electron Spectroscopy and Related Phenomena* **1976**, *8*, 129-137.
[243] G. A. Sotzing, J. R. Reynolds, P. J. Steel, *Advanced Materials* **1997**, *9*, 795–798.
[244] V. Lemau de Talancé, M. Hissler, L.-Z. Zhang, T. Kárpáti, L. Nyulászi, D. Caras-Quintero, P. Bäuerle, R. Réau, *Chemical Communications* **2008**, 2200.
[245] P. Siemsen, R. C. Livingston, F. Diederich, *Angewandte Chemie International Edition* **2000**, *39*, 2632-2657.
[246] S. Takahashi, Y. Kuroyama, K. Sonogashira, N. Hagihara, *Synthesis* **1980**, *1980*, 627-630.
[247] O. Navarro, H. Kaur, P. Mahjoor, S. P. Nolan, *The Journal of Organic Chemistry* **2004**, *69*, 3173-3180.
[248] M. S. Viciu, G. A. Grasa, S. P. Nolan, *Organometallics* **2001**, *20*, 3607-3612.
[249] R. S. Nicholson, I. Shain, *Analytical Chemistry* **1964**, *36*, 706-723.
[250] G. K. Rowe, M. T. Carter, J. N. Richardson, R. W. Murray, *Langmuir* **1995**, *11*, 1797-1806.
[251] M. J. Honeychurch, *Langmuir* **1998**, *14*, 6291-6296.
[252] C. E. D. Chidsey, C. R. Bertozzi, T. M. Putvinski, A. M. Mujsce, *Journal of the American Chemical Society* **1990**, *112*, 4301-4306.
[253] R. L. Carroll, C. B. Gorman, *Angewandte Chemie International Edition* **2002**, *41*, 4378-4400.
[254] J. R. Heath, M. A. Ratner, *Physics Today* **2003**, *56*, 43.
[255] J. M. Seminario, *Nature Materials* **2005**, *4*, 111-113.

[256] O. Hod, R. Baer, E. Rabani, *Journal of Physics: Condensed Matter* **2008**, *20*, 383201.
[257] S. Saha, J. F. Stoddart, *Chemical Society Reviews* **2007**, *36*, 77.
[258] C. Joachim, M. A. Ratner, *Proceedings of the National Academy of Sciences of the United States of America* **2005**, *102*, 8801 -8808.
[259] H. Shirakawa, E. J. Louis, A. G. MacDiarmid, C. K. Chiang, A. J. Heeger, *Journal of the Chemical Society, Chemical Communications* **1977**, 578.
[260] C. K. Chiang, C. R. Fincher, Y. W. Park, A. J. Heeger, H. Shirakawa, E. J. Louis, S. C. Gau, A. G. MacDiarmid, *Physical Review Letters* **1977**, *39*, 1098.
[261] P. J. Low, M. A. J. Paterson, D. S. Yufit, J. A. K. Howard, J. C. Cherryman, D. R. Tackley, R. Brook, B. Brown, *Journal of Materials Chemistry* **2005**, *15*, 2304.
[262] H. Naarmann, *Electrically Conducting Polymers*, Wiley-vch, Weinheim, **2002**.
[263] H. Klauk, *Organic Electronics*, Wiley-vch, Weinheim, **2006**.
[264] S. Günes, H. Neugebauer, N. S. Sariciftci, *Chemical Reviews* **2007**, *107*, 1324-1338.
[265] N. Robertson, *Angewandte Chemie International Edition* **2006**, *45*, 2338-2345.
[266] A. P. Kulkarni, C. J. Tonzola, A. Babel, S. A. Jenekhe, *Chemistry of Materials* **2004**, *16*, 4556-4573.
[267] A. Helms, D. Heiler, G. McLendon, *Journal of the American Chemical Society* **1991**, *113*, 4325-4327.
[268] M. A. Reed, C. Zhou, C. J. Muller, T. P. Burgin, J. M. Tour, *Science* **1997**, *278*, 252-254.
[269] C. Kergueris, J.-P. Bourgoin, S. Palacin, D. Esteve, C. Urbina, M. Magoga, C. Joachim, *Physical Review B* **1999**, *59*, 12505.
[270] R. H. M. Smit, Y. Noat, C. Untiedt, N. D. Lang, M. C. van Hemert, J. M. van Ruitenbeek, *Nature* **2002**, *419*, 906-909.
[271] J. Reichert, R. Ochs, D. Beckmann, H. B. Weber, M. Mayor, H. v Löhneysen, *Physical Review Letters* **2002**, *88*, 176804.
[272] M. Mayor, C. von Hänisch, H. B. Weber, J. Reichert, D. Beckmann, *Angewandte Chemie International Edition* **2002**, *41*, 1183-1186.
[273] M. Elbing, R. Ochs, M. Koentopp, M. Fischer, C. von Hänisch, F. Weigend, F. Evers, H. B. Weber, M. Mayor, *Proceedings of the National Academy of Sciences of the United States of America* **2005**, *102*, 8815 - 8820.
[274] **o. J.**, Calculated with Chem3D.
[275] D. S. Surry, S. L. Buchwald, *Angewandte Chemie International Edition* **2008**, *47*, 6338-6361.
[276] J. F. Hartwig, *Angewandte Chemie International Edition* **1998**, *37*, 2046-2067.
[277] R. F. Heck, J. P. Nolley, *The Journal of Organic Chemistry* **1972**, *37*, 2320-2322.
[278] I. P. Beletskaya, A. V. Cheprakov, *Chemical Reviews* **2000**, *100*, 3009-3066.
[279] J. K. Stille, *Angewandte Chemie International Edition in English* **1986**, *25*, 508-524.

[280] H. H. Hodgson, *Chemical Reviews* **1947**, *40*, 251-277.
[281] H. H. Hodgson, J. Walker, *Journal of the Chemical Society* **1933**, 1620.
[282] T. Sandmeyer, *Berichte der Deutschen Chemischen Gesellschaft* **1884**, *17*, 1633-1635.
[283] R. Appel, *Angewandte Chemie International Edition in English* **1975**, *14*, 801-811.
[284] P. E. Fanta, *Synthesis* **1974**, *1974*, 9-21.
[285] Y.-H. Lai, *Synthesis* **1981**, *1981*, 585-604.
[286] A. Shaporenko, M. Elbing, A. Błaszczyk, C. von Hänisch, M. Mayor, M. Zharnikov, *The Journal of Physical Chemistry B* **2006**, *110*, 4307-4317.
[287] W. WENNER, *The Journal of Organic Chemistry* **1952**, *17*, 523-528.
[288] K. Fuji, T. Yamada, E. Fujita, *Organic Magnetic Resonance* **1981**, *17*, 250-253.
[289] M. P. Doyle, B. Siegfried, J. F. Dellaria, *The Journal of Organic Chemistry* **1977**, *42*, 2426-2431.
[290] G.-J. M. Gruter, O. S. Akkerman, F. Bickelhaupt, *The Journal of Organic Chemistry* **1994**, *59*, 4473-4481.
[291] C. G. Blettner, W. A. König, W. Stenzel, T. Schotten, *The Journal of Organic Chemistry* **1999**, *64*, 3885-3890.
[292] H. Lucas, E. R. Kennedy, *Organic Synthesis* **1933**, *19*, 100-102.
[293] J. H. Lee, B. S. Lee, H. Shin, D. H. Nam, D. Y. Chi, *Synlett* **2006**, *1*, 65-68.
[294] A. Zarei, A. Hajipour, L. Khazdooz, *Synthesis* **2009**, *2009*, 941-944.
[295] Z. Wang, R. T. Skerlj, G. J. Bridger, *Tetrahedron Letters* **1999**, *40*, 3543-3546.
[296] F. Y. Kwong, A. Klapars, S. L. Buchwald, *Organic Letters* **2002**, *4*, 581-584.
[297] A. M. Gilbert, A. Failli, J. Shumsky, Y. Yang, A. Severin, G. Singh, W. Hu, D. Keeney, P. J. Petersen, A. H. Katz, *Journal of Medicinal Chemistry* **2006**, *49*, 6027-6036.
[298] C. Raimondo, F. Reinders, U. Soydaner, M. Mayor, P. Samorì, *Chemical Communications* **2010**, *46*, 1147.
[299] A. R. Katritzky, J. Wu, S. V. Verin, *Synthesis* **1995**, *26*, 651-653.
[300] P. G. Wuts, T. W. Greene, *Protective Groups in Organic Synthesis*, Wiley, Hoboken, New Jersey, USA, **2007**.
[301] J. M. Khurana, S. Singh, *Journal of the Chemical Society, Perkin Transactions 1* **1999**, 1893-1896.
[302] H.-F. Grützmacher, J. Schmiegel, *Chemische Berichte* **1989**, *122*, 1929-1933.
[303] T. Peterle, A. Leifert, J. Timper, A. Sologubenko, U. Simon, M. Mayor, *Chemical Communications* **2008**, 3438.
[304] T. Peterle, P. Ringler, M. Mayor, *Advanced Functional Materials* **2009**, *19*, 3497-3506.
[305] D. Mirk, B. Wibbeling, R. Fröhlich, S. R. Waldvogel, *Synlett* **2004**, 1970-1974.
[306] K. Yamamoto, T. Harada, Y. Okamoto, H. Chikamatsu, M. Nakazaki, Y. Kai, T. Nakao, M. Tanaka, S. Harada, N. Kasai, *Journal of the American Chemical Society* **1988**, *110*, 3578-3584.
[307] A. Czech, B. P. Czech, R. A. Bartsch, C. A. Chang, V. O. Ochaya, *The Journal of Organic Chemistry* **1988**, *53*, 5-9.

[308] B. P. Czech, R. A. Bartsch, *Journal of Organic Chemistry* **1984**, *49*, 4076-8.
[309] J. D. Lambert, J. E. Rice, J. Hong, Z. Hou, C. S. Yang, *Bioorganic & Medicinal Chemistry Letters* **2005**, *15*, 873-876.
[310] K. S. Feldman, *The Journal of Organic Chemistry* **1997**, *62*, 4983-4990.
[311] R. J. Bushby, Z. Lu, *Synthesis* **2001**, *2001*, 0763-0767.
[312] J. N. Moorthy, P. Venkatakrishnan, S. Samanta, *Organic & Biomolecular Chemistry* **2007**, *5*, 1354.
[313] M. Hussain, V. Ahmed, B. Hill, Z. Ahmed, S. D. Taylor, *Bioorganic & Medicinal Chemistry* **2008**, *16*, 6764-6777.
[314] J. Schmiegel, U. Funke, A. Mix, H.-F. Grützmacher, *Chemische Berichte* **1990**, *123*, 1397-1401.
[315] R. A. Falconer, I. Jablonkai, I. Toth, *Tetrahedron Letters* **1999**, *40*, 8663-8666.
[316] S. George, A. Nangia, *Acta Crystallographica Section E Structure Reports Online* **2003**, *59*, o901-o902.
[317] S. Boz, M. Stöhr, U. Soydaner, M. Mayor, *Angewandte Chemie International Edition* **2009**, *48*, 3179-3183.
[318] U. Jordis, M. Knapp, P. G. Potvin, „JASPER v2.0 - JavaScript Percentage Elemental Results Calculator“, can be found under http://www.chem.yorku.ca/profs/potvin/Jasper/jasper2.htm, **2011**.
[319] S. Gerlich, L. Hackermuller, K. Hornberger, A. Stibor, H. Ulbricht, M. Gring, F. Goldfarb, T. Savas, M. Muri, M. Mayor, u. a., *Nature Physics* **2007**, *3*, 711-715.
[320] M. Gring, S. Gerlich, S. Eibenberger, S. Nimmrichter, T. Berrada, M. Arndt, H. Ulbricht, K. Hornberger, M. Müri, M. Mayor, u. a., *Physical Review A* **2010**, *81*, 031604.
[321] L. Shu, M. Müri, R. Krupke, M. Mayor, *Organic & Biomolecular Chemistry* **2009**, *7*, 1081.

Curriculum Vitae

PERSONAL INFORMATION

Name	Marcel Müri
Date/Place of birth	June 11th, 1981, Olten, Switzerland
Nationality	Swiss

EDUCATION

12/2009 – 06/2011	**PhD** work at the University of Basel, Switzerland, Department of Chemistry. *"Shape Switchable Azo Macrocycles"* Supervisor: Prof. Marcel Mayor, Dr. Heike Riel
04/2005 – 09/2006	**Master of Science** (MSc) in Chemistry, University of Basel, Switzerland. *"Polymorphable Macrocycles & Labelled Azobenzene."* Supervisor: Prof. Marcel Mayor
10/2001 – 03/2005	**Bachelor of Science** (BSc) in Chemistry, University of Basel, Switzerland.
08/1996 – 01/2001	**Maturity Certificate** in Mathematics and Natural Science, Kantonsschule Hardwald Olten, Switzerland.

PUBLICATIONS

Modular Functionalization of Electrodes by Cross Coupling Reaction at their Surfaces; Marcel Müri, Bernd Gotsmann, Yann Leroux, Marius Trouwborst, Emanuel Lörtscher, Heike Riel, Marcel Mayor*, Adv. Fuct. Mater* **2011**, 10.1002/adfm.201100642.

Influence of conformational molecular dynamics on matter wave interferometry; Michael Gring, Stefan Gerlich, Sandra Eibenberger, Stefan Nimmrichter, Tarik Berrada, Markus Arndt, Hendrik Ulbricht, Klaus Hornberger, Marcel Müri, Marcel Mayor, Marcus Böckmann, Nikos L. Doltsinis; *Phys. Rev. A* **2010**, *81*, 031604(R).

Shape-Switchable Azo-Macrocycles; Marcel Müri, Klaus C. Schuermann, Luisa De Cola, Marcel Mayor; *Eur. J. Org. Chem.*, **2009**, *15*, 2562-2575.

Shape-persistent macrocycles comprising perfluorinated benzene subunits: synthesis, aggregation behaviour and unexpected μ-rod formation; Lijin Shu, Marcel Müri, Ralph Krupke, Marcel Mayor; *Org. Biomol. Chem.*, **2009**, *7*, 1081-1092.

A Kapitza-Dirac-Talbot-Lau interferometer for highly polarizable molecules; Stefan Gerlich, Lucia Hackermüller, Klaus Hornberger, Alexander Stibor, Hendrik Ulbricht, Michael Gring, Fabienne Goldfarb, Tim Savas, Marcel Müri, Marcel Mayor, Markus Arndt; *Nature Physics*, **2007**, *3*, 711-715.

Application of a contactless conductivity detector to the determination of inorganic ions in ion chromatography; Pavel Kuban, Marcel A. Mueri, Peter C. Hauser; *Analyst*, **2004**, *129*, 82-86.

SCHOLARSHIP

PhD – Thesis related to Industry in the Field of Supramolecular Materials – Nanoscience from NRP 47, *SNF and CTI*